Transcriptional responses of tumor cell lines to interferon-alpha

Inauguraldissertation

zur
Erlangung der Würde eines Doktors der Philosophie
vorgelegt der
Philosophisch-Naturwissenschaftlichen Fakultät
der Universität Basel

von

Fredy Siegrist

aus Menziken (AG)

Basel, 2013

Genehmigt von der Philosophisch-Naturwissenschaftlichen Fakultät

auf Antrag von
Prof. Dr. Markus Rüegg
Fakultätsverantwortlicher

Prof. Dr. Ulrich Certa
Dissertationsleiter

Prof. Dr. Primo Schär
Korreferent

Basel, den 29.03.2011

Prof. Dr. Martin Spiess
Dekan

Attribution-Noncommercial-No Derivative Works 2.5 Switzerland

You are free:

to Share — to copy, distribute and transmit the work

Under the following conditions:

Attribution. You must attribute the work in the manner specified by the author or licensor (but not in any way that suggests that they endorse you or your use of the work).

Noncommercial. You may not use this work for commercial purposes.

No Derivative Works. You may not alter, transform, or build upon this work.

- For any reuse or distribution, you must make clear to others the license terms of this work. The best way to do this is with a link to this web page.
- Any of the above conditions can be waived if you get permission from the copyright holder.
- Nothing in this license impairs or restricts the author's moral rights.

Your fair dealing and other rights are in no way affected by the above.

This is a human-readable summary of the Legal Code (the full license) available in German:
http://creativecommons.org/licenses/by-nc-nd/2.5/ch/legalcode.de

Disclaimer:
The Commons Deed is not a license. It is simply a handy reference for understanding the Legal Code (the full license) — it is a human-readable expression of some of its key terms. Think of it as the user-friendly interface to the Legal Code beneath. This Deed itself has no legal value, and its contents do not appear in the actual license. Creative Commons is not a law firm and does not provide legal services. Distributing of, displaying of, or linking to this Commons Deed does not create an attorney-client relationship.

Quelle: http://creativecommons.org/licenses/by-nc-nd/2.5/ch/deed.en Datum: 3.4.2009

Transcriptional responses of tumor cell lines to interferon-alpha

"La perfection de l'invention confine ainsi à l'absence d'invention."

Antoine de Saint-Exupery - Terre des Hommes, *Deux cent quarante-septième édition: III. L'Avion, p. 60 [Paris] (Gallimard 1946)*

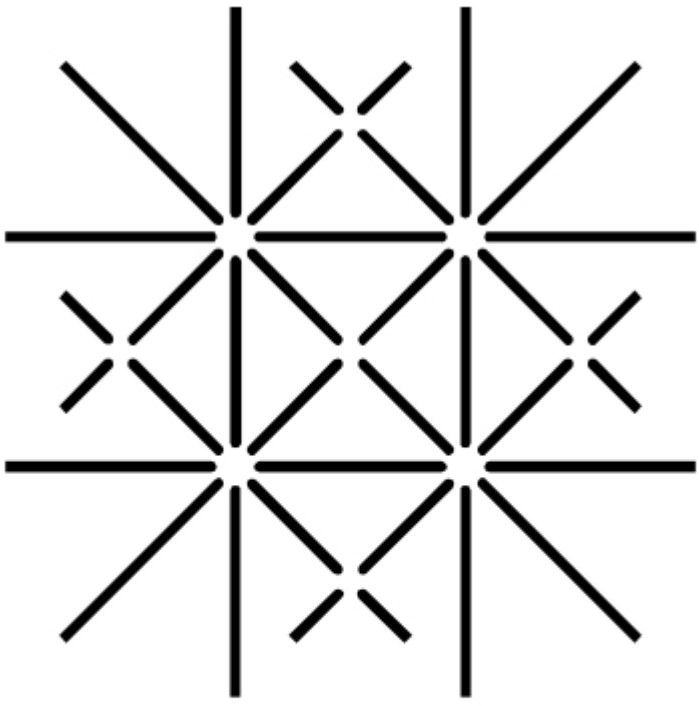

UNI
BASEL

PHILOSOPHISCH-
NATURWISSENSCHAFTLICHE
FAKULTÄT

Table of Contents

Illustration Index

Drawings Index

Tables Index

Summary

Interferon is an antiviral and antiproliferative cytokine therapeutically applied to treat hepatitis infection and cancer expansion. The beneficial effects of interferon-alpha are dependent on efficient signaling by activation of defined JAK-STAT pathway and the induction of interferon stimulation genes. These genes are translated to proteins with antiviral, antiproliferative, anti-tumor and apoptotic properties. Induction of gene expression is consolidated by binding of interferon activated transcription factors to interferon-specific elements in the promoter of such genes. This interaction is dependent on the accessibility of the chromosomal region given by an open chromatin structure. Some interferon-induced proteins are negatively regulating the signal transduction to avoid overreactions such as triggering senescence and to restore responsiveness to a next round of cytokine stimulation. The response to interferon was characterized using whole-genome gene-expression microarrays. Interferon induced proteins were characterized for their antiproliferative effects by measuring growth in cell culture. These proteins were tagged fluorescently to localize them to cell compartments. Suppressor of cytokine signaling proteins were overexpressed in cancer cell lines and their effect on gene expression was described by genome-wide micro-array analyzes. The epigenetic state in tumor samples was determined, the effect of interferon-alpha on DNA mehtylation was described for one gene and the epigenetic changes documented in embryonic cells defective in a gene involved in DNA damage repair. Our results document antiproliferative action for the interferon-stimulated genes *IFI44* and *IFITM3*. Induction of gene expression can be blocked by overexpression of SOCS1 proteins in cancer cell lines. The epigenetic DNA methylation status is altered in tumor cells and methylation of unique CpG sites can dynamically change during cytokine treatment and may involve a DNA demethylation factor. The interferon-alpha response of cancer cell lines depends on the expression, the inducibility and the epigenetic state of interferon-stimulated genes. The genes studied here are effective in blocking proliferation or signal transduction in interferon-alpha sensitive cell lines. Screening of clinical samples for the expression of these genes or their proteins or determination of the DNA methylation status therein is promising in customization of drug therapy for personalized healthcare.

List of abbreviations

Abbreviation	Description
ADC	antibody-drug conjugates
aza	5-aza-2'-deoxycytidine
BED	browser extensible data
BiFC	bimolecular fluorescence complementation
C/EBP (-β)	CCAAT/enhancer-binding protein (-beta)
CHC	chronic hepatitis C
CHF	change factors
CIMP	CpG island methylator phenotype
CISH	cytokine-inducible SH2-containing protein (human)
CpG	catosine-guanine dinucleotide
CRC	colorectal cancer
DAC	deoxyazacytidine (see aza)
DI	DNA index
DM1	cytotoxic agent DM1 (antimicrotubule agent)
EMSA	electrophoretic mobility shift assay
FDA	Food and Drug Administration
fdr	false discovery rate
GAS	gamma activated sequences
HCC	hepatocellular carcimona
HCV	hepatitis C virus
HER(2)	human epidermal growth factor receptor (2 [gene symbol: ERBB2])
HIV	human immunodeficiency virus
HLA (-C)	human leukocyte antigen (C)
IFI	interferon induced
IFITM	interferon induced transmembrane (protein / gene)
IFN (α/β/γ/λ)	interferon (alpha / beta / gamma / lambda)
IFNAR1 / IFNAR2	interferon type I receptor 1 / 2
IL	Interleukin
IRF	interferon response factor
IRS (1)	insulin receptor substrate (1)
ISG	interferon stimulated genes
ISGF3 (γ / G)	interferon stimulated gene factor (3 gamma: [gene symbol: IRF9])
ISRE	interferon stimulated response element
Jak	Janus kinases
KIR	kinase inhibitory region
lfc	log factor change
miRNA	micro RNAs
MLH1	mutL (methyl-directed mismatch repair protein) homolog 1
MT2A	metallothionein 2 a (protein / gene)
NS	non-structural (viral protein / gene)
p-value	probability value (for the given statistical test)
p53	tumor protein 53 (gene symbol: TP53)
PBMC	peripheral blood mononuclear cell
PCA	principal component analysis
PCP	proliferation control protein
Pegasys	pegylated interferon (trade mark)
PIAS	protein inhibitors of activated STATs

Abbreviation	Description
PPAR (γ)	peroxisome proliferator-activated receptor (gamma)
PRC	polymerase chain reaction
qMSP	quantitative methylation specific PCR
qPCR	quantitative PCR
RBV	ribavirin
SH2	Src homology domain 2
SH2 domain	phospho-tyrosine recognition site
SHP	Src homology domain 2-containing protein tyrosine phosphatase
SOC	standard-of-care
SOCS	suppressors of cytokine signaling
STAT	signal transducer and activator of transcription
STAT-C	specifically targeted antiviral therapy for HCV
TDG	thymine-DNA glycosylase
TGF(β)	transforming growth factor (beta-1)
Tkip	tyrosine kinase inhibitor peptide
TLR	Toll-like receptor
TSA	trichostatin A
Tyk	tyrosine kinases
UCSC	University of California Santa Cruz
VST	variance-stabilizing transformation
wt	wild type
YFP (eYFP)	yellow fluorescent protein (enhanced YFP)

General introduction

Interferon-alpha

'INTERFERON is the name that was given to a substance produced by the interaction of inactivated influenza virus with cells[1].'
(Isaacs *et al.* 1958) on [1] (Isaacs *et al.* 1957).

Interferons are originally defined as proteins secreted by virus-infected cells that inhibit viral replication in infected and uninfected cells (Isaacs and Lindenmann 1957). The name of the protein originates from its activity to “interfere” with viral infections. Later on, interferon (IFN) showed more than antiviral activity, it can inhibit cellular growth; it has effects on the immune system and on apoptosis (Stark *et al.* 1998). Thus, IFN can be used for antiviral and antitumor applications. Almost every cell in the body has the capacity to induce IFNs, but the type of IFN produced by different cells varies. Therefore, IFNs were classified in two subgroups, type I (leucocyte [α] and fibroblast [β] interferon)(Havell *et al.* 1975) and type II IFN (immune interferon [γ])(Stewart 1980). A third subgroup, type III IFN (antiviral interferons [λ]) has been defined some years later (Kotenko *et al.* 2003). Interferon alpha (IFNα) family consists of proteins coded by 17 non-allelic genes in a single region of the human genome on chromosome 9 together with a single gene for interferon beta (IFNβ) (Owerbach *et al.* 1981; Shows *et al.* 1982; Weissmann *et al.* 1982; Díaz *et al.* 1994).

IFNs are able to induce the expression of a variety of interferon-stimulated genes (ISG). Several types of IFN and transcription factors can induce many of them. Some messenger RNAs (mRNA) are known since more than a quarter century to be regulated by IFNα signaling (Stark *et al.* 1984). These mRNA include the genes coded by the clones 1-8 (IFITM2), 9-27 (IFITM1), 6-16 (IFI6), 6-26 (TMSB4X), 10Q (unknown), 2A (HLA-C) and MTII (MT2A, coding for the metallothionein 2 protein); being 1-8 the most abundant IFN-induced mRNA (Friedman *et al.* 1984). Signaling is propagated by activation of cytokine receptors, kinases and transcriptional activators mainly through transient phosphorylation of these molecules. There are plenty of genes induced and they act through different mechanisms to protect the body from viruses and to control cellular growth. The mechanism of action of ISGs is manifold, they are involved in RNA editing and degradation, block of protein synthesis, protein modifications such as polyubiquitation resulting in protein degradation, induction of cytokines and cross talk with signaling pathways, antiviral, antitumor, antiangiogenic and apoptotic actions (Borden *et al.* 2007). The antiproliferative action of IFNα involves control of cell cycle checkpoints (Roos *et al.* 1984). The mechanism how IFNα is able to induce cell-cycle arrest or apoptosis is mediated by induction of tumor protein 53 (p53) signaling for example (Thyrell *et al.* 2002). However, p53 is not required for IFN mediated induction of apoptosis (Herzer *et al.* 2009).

JAK-STAT signaling

Many cytokines, more than 38 if we count type I IFN as a single one, signal through a discrete number of Janus kinases (Jaks) to phosphorylate seven signal transducer and activator of transcription (STAT) phospho-tyrosine recognition site (SH2 domain) containing proteins (Schindler *et al.* 2007). IFNα and IFNβ signal transduction is initiated by binding of the cytokine to and consequently dimerizing of interferon type I receptors

(IFNAR1 and IFNAR2). The cell-surface interaction induces conformational changes down to the cytosolic part of the receptors, attracts receptor associated tyrosine kinases (Tyk): Jak1 and Tyk2, which get rapidly auto-phosphorylated (Platanias *et al.* 1994). This activation of Jaks leads to tyrosine-phosphorylation of the receptors and subsequent recruitment of various signaling proteins, including STATs (Schindler *et al.* 1992). After IFNα driven JAK1 / Tyk2 activation, primarily STAT1 and STAT2 are recruited from the cytosol to the membrane where they get phosphorylated, too (Fu *et al.* 1992). Once activated, the STATs dimerize and relocate to the cytosol. IFNα signaling cascade primarily promotes STAT2 binding to the co-factor IRF9 (ISGF3γ or p48) and they form together with STAT1 the interferon stimulated gene factor 3 (ISGF3) (Fu *et al.* 1990). This complex translocates to the nucleus where it can bind interferon stimulated response elements (ISRE) and consequently initiate the transcription of IFN type I specific genes (Darnell *et al.* 1994; Darnell 1997; Stark *et al.* 1998; Caraglia *et al.* 2005). Beside this prototypical transcription factor, STAT1 homodimers are formed as well and consequently initiate transcription of IFN (gamma) stimulated genes through the binding to gamma-activated sequences (GAS). Additionally, STAT1-IRF9 complexes, STAT3-STAT1 and rarely occurring dimers such as STAT2 homodimers may be formed (Bluyssen *et al.* 1996; Wesoly *et al.* 2007). Subsequently, phosphorylated as well as unphosphoryated STAT proteins shuttle rapidly in and out the nucleus (Xu *et al.* 2004; Meyer *et al.* 2004; Meyer *et al.* 2007). STAT molecules are non-tyrosine phosphorylated in absence of cytokine stimulus. Nevertheless, they can assemble into dimers and higher order complexes and may have some activity in the nucleus (Ndubuisi *et al.* 1999; Haan *et al.* 2000). Interestingly, these IFN-unstimulated and unphosphorylated STAT1 molecules are also bound to DNA and may alter gene expression in a different manner (Robertson *et al.* 2007). This allows IFN signaling to control gene expression in addition to the short-lived JAK-STAT phosphorylation. Unphosphorylated STAT1 accumulates after IFN stimulus and maintains or increases the expression of certain ISG (Yang *et al.* 2008; Cheon *et al.* 2009). However, this accumulation is a very dynamic process and not static. Shuttling of transcription factors typically occurs without tyrosine phosphorylation of STAT1 (Meyer and Vinkemeier 2007). Interestingly, nuclear transition of unphosphorylated STAT2 is dependent on its constitutive association with IRF9 (Banninger *et al.* 2004). The ability of IFNs and other cytokines to induce STAT molecules in any number of ratios explains why the IFN response varies dependent on IFN subtype and cellular conditions. STAT1 primarily promotes growth arrest, apoptosis and antitumor immunity downstream of type I and II IFNs. By contrast, STAT3 mediates activity of cytokines generally associated with systemic acute phase and cancer-promoting inflammation (Jarnicki *et al.* 2010). In addition to IFN signaling through STATs, there is signaling through IFN receptor dimerization without activation of STATs. Therefore, cells with mutations in crucial tyrosines for IFN type 1 signaling are able to induce IRF9 independently of STAT phosphorylation and for example linked to IRF1 and C/EBP-β signaling (Rani *et al.* 2010).

ISRE and GAS

The sequence composition of IFN response elements is defined by a set of promoter sequences of ISG that show similarities to other IFN response factor binding sites that have been analyzed biochemically (Brierley *et al.* 2007). A list of such sequences is shown in table 1. The data of high confident ISRE and GAS sequences was merged from published lists (Tsukahara *et al.* 2006; Robertson *et al.* 2007; Montgomery *et al.* 2006). In addition, IFITM ISRE sequences were added, which we have identified as potential ISRE sequences due to evolutionary conservation (Siegrist *et al.* 2011). In table 1 the STAT1 regulatory elements are split into GAS and ISRE sequences but the ISRE subgroups are

refined by counting the distance of the first 'TTT' (3T) nucleotide stretch to the 'C' after the second 3Ts instead of looking at 3Ts only (Robertson *et al.* 2007). To get a better overview of the sequence characteristics of ISRE and GAS elements, nucleic acid occurrence is plotted for all the GAS elements and all ISRE elements including these subgroups. This grouping then points out the importance of a 'TTTC' element repetition with a spacer of two or three nucleotides in size between them (Illustration 1 and 2).

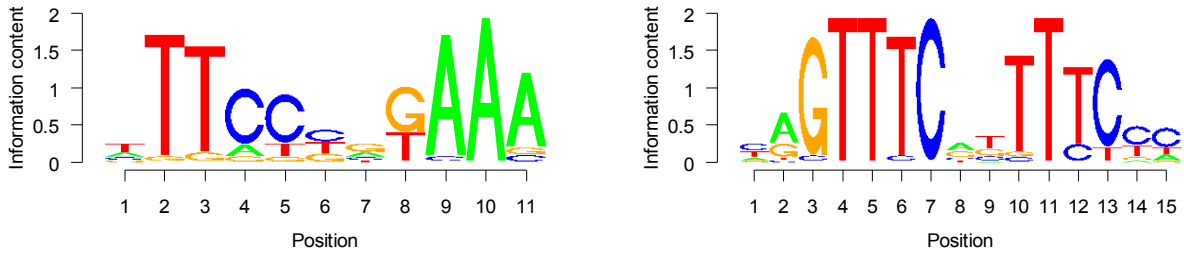

Illustration 1: Nucleotide frequency in all GAS (left) and ISRE sequences (right).

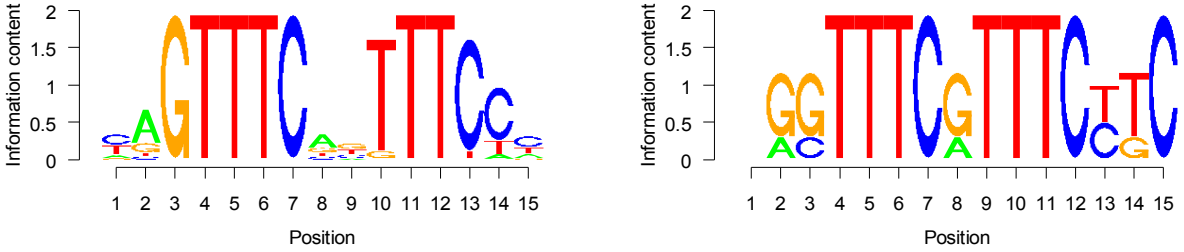

Illustration 2: Nucleotide frequency in ISRE_3 sequences (left) and Nucleotide frequency in ISRE_2 sequences (right).

The use of large scale and genome wide microarray expression data for a more comprehensive definition of ISRE sequences has been recently described (Hertzog *et al.* 2011). New definitions will replace these biased and rigid consensus sequences that are still part of transcription factor binding site databases. However, we should keep in mind that the consensus sequence defined for a database, TransFac for example, is based on a small number of highly induced genes after stimulation of type I IFN signaling. Promoter sequences of lower affinity binding sites to the ISRE transcription complex seem to be as well sensitive to IFN signaling if other transcription factors are abundant.

Gene Symbol	Group	Organism	Sequence	Reference
GBP1	GAS	Human	ATTACTCTAAA	(Lew *et al.* 1991)
CSF1	GAS	Human	TTTCCCATAAA	(Tsuchimoto *et al.* 2004)
FCGR1A	GAS	Human	TTTCCCAGAAA	(Pearse *et al.* 1993)
FOS	GAS	Human	GTTCCCGTCAA	(Eilers *et al.* 1994)
SERPINA3	GAS	Human	ATTACCAGAAA	(Kordula *et al.* 1998)
SERPINA3	GAS	Human	AGTCCGAGAAC	(Kordula *et al.* 1998)
WARS	GAS	Human	ATTCTCAGAAA	(Seegert *et al.* 1994)
CIITA	GAS	Human	CTTCTGATAAA	(Muhlethaler-Mottet *et al.* 1998)
MVP	GAS	Human	CTGCCGGGAAG	(Steiner *et al.* 2006)
NOS2A	GAS	Human	TTTACTGGAAA	(Gao *et al.* 1997)
NOS2A	GAS	Human	GTTCTGGGAAA	(Gao *et al.* 1997)
CCL2	GAS	Human	GTTCCTGGAAA	(Guyer *et al.* 1995)
ICAM1	GAS	Human	TTTCCTTGAAA	(Tessitore *et al.* 1998)
ICAM1	GAS	Human	TTTCCGGGAAA	(Tessitore *et al.* 1998)
CD40	GAS	Human	CTTCCTTGAAA	(Nguyen *et al.* 2000)
CD86	GAS	Human	TTTGGTCTAAA	(Li *et al.* 2000)
CD86	GAS	Human	CTTGCTTTAAA	(Li *et al.* 2000)
IL6ST	GAS	Human	ATTCCCGTAAC	(O'Brien *et al.* 1997)
IRF1	GAS	Human	TTTCCCCGAAA	(Sims *et al.* 1993)
HLA-E	GAS	Human	TTGCTGGGAAA	(Gustafson *et al.* 1996)
TAP1	GAS	Human	TTTAGGGGAAA	(Chatterjee-Kishore *et al.* 1998)
IDO1	GAS	Human	TTTCCTGTAAA	(Chon *et al.* 1996)
IRF1	GAS	Mouse	TTTCCCCGAAA	(Coccia *et al.* 1999)
LY6E	GAS	Mouse	ATTCCTGTAAG	(Khan *et al.* 1993)
IRF8	GAS	Mouse	TTTCTCGGAAA	(Kanno *et al.* 1993)
FOS67	GAS	Human	TTTCCCGTAAA	(Eilers *et al.* 1994)
ADAR	ISRE_2	Human	CGCTTTCGTTTCCTC	(George *et al.* 1999)
OAS1	ISRE_2	Human	TGGTTTCGTTTCCTC	(Rutherford *et al.* 1988)
MX1	ISRE_2	Human	AGGTTTCGTTTCTGC	(Ronni *et al.* 1998)
MX1	ISRE_2	Human	GAGTTTCATTTCTTC	(Ronni *et al.* 1998)
ISG15	ISRE_3	Human	CAGTTTCGGTTTCCC	(Levy *et al.* 1988)
IFI6	ISRE_3	Human	CAGTTTCATTTTCCC	(Porter *et al.* 1988)
IFI6	ISRE_3	Human	GAGTTTCATTTTCCC	(Porter *et al.* 1988)
IFIT2	ISRE_3	Human	TAGTTTCACTTTCCC	(Levy *et al.* 1988)
IFIT1	ISRE_3	Human	TAGTTTCACTTTCCC	(Grandvaux *et al.* 2002)
IFITM1	ISRE_3	Human	AAGTTTCTATTTCCT	(Reid *et al.* 1989)
IFITM3	ISRE_3	Human	TAGTTTCGGTTTCTC	(Lewin *et al.* 1991)
IFITM3	ISRE_3	Human	CAGTTTCCTTTTCCT	(Lewin *et al.* 1991)
ISG20	ISRE_3	Human	CTGTTTCAGTTTCTA	(Gongora *et al.* 2000)
EIF2AK2	ISRE_3	Human	CAGTTTCGTTTTCCC	(Ward *et al.* 2002)
CXCL10	ISRE_3	Human	AGGTTTCACTTTCCA	(Cheng *et al.* 1998)
HLA-E	ISRE_3	Human	CAGTTTCCCGTTCCT	(Gustafson and Ginder 1996)
CFB	ISRE_3	Human	CAGTTTCTGTTTCCT	(Huang *et al.* 2001)
IDO1	ISRE_3	Human	TGGTTTCAGTTTTCC	(Konan *et al.* 1996)
IDO1	ISRE_3	Human	TGGTTTCATTTTCTA	(Konan and Taylor 1996)
IFITM1	ISRE_3	Human	TCGTTTCAGTTTCAG	(Siegrist *et al.* 2011)
IFITM2	ISRE_p	Human	CAGTTTCCTCTTCGA	(Siegrist *et al.* 2011)
IFITM2	ISRE_p	Human	TAGTTCCGTTTTCTC	(Siegrist *et al.* 2011)

Table 1: High confident ISRE and GAS motifs

Therapeutic use of interferon-alpha

Interestingly, it was not the initially described antiviral action that led to the licensing of IFNα, the first recombinant cytokine, for the treatment of a malignancy but its antitumor activity. In 1986, IFNα2a (Hoffman-La Roche) and IFNα2b (Schering-Plough) got the approval in the USA for the treatment of Hairy Cell Leukemia. Other approved antitumor applications exist for AIDS-related Kaposi's Sarcoma, Chronic Myelogenous Leukemia, Malignant Melanoma and Follicular Lymphoma (Bekisz *et al.* 2010). The idea that HCV infected patients might benefit from IFNα was based on the observation that hepatitis often cause a chronic infection leading to cirrhosis and hepatocellular carcinoma (HCC) (Blumberg 1977). The following idea was to administer IFNα in CHC patients as cancer prevention and only secondary as antiviral therapy. In the beginning, low dose of IFNα showed a partial effect on cancer occurrence and had limited antiviral effect. Then, high dose IFNα therapy confirmed beneficial effects in the treatment of hepatitis after affordable, recombinant IFNα became available for therapeutic application (Hoofnagle *et al.* 1988).

HCV treatment

Combination therapy with antivirals and a new formulation of IFNα have proven to be more effective than IFNα alone. The recommended therapy for chronic hepatitis C (CHC) and standard-of-care (SOC) medication for hepatitis C virus (HCV) infections in general was for more than a decade pegylated interferon-alpha-2a (Pegasys) in combination with ribavirin (RBV), a weak antiviral medication (Glue *et al.* 2000; Borden *et al.* 2007). Moreover, Pegasys is used to treat other type of chronic hepatitis (B and D) infection and HIV-HCV co-infections (Poynard *et al.* 2003; Flamm 2003). There is no cure for hepatitis B but medication can suppress the virus for a long time period. Patients may achieve HCV eradication but in some cases there is recurrence of viral infection. Another problem is that some patients with hepatitis C benefit from the treatment and others do not. This may be due to cellular factors such as STAT3, CD81, DICER, TP53, ISGF3G all of them important for viral replication *in vitro* (Randall *et al.* 2007). Diagnostic factors such as virus genotype or insulin resistance have an independent effect on the treatment response (Persico *et al.* 2007; Moucari *et al.* 2008; Petta *et al.* 2008).
Another factor that correlates with insulin resistance and differs between HCV genotypes are genes of the family of suppressor of cytokine signaling (SOCS) (Persico *et al.* 2009; Vanni *et al.* 2009). Recent results indicate a correlation of SOCS3 expression and outcome of IFN therapy in HCV patients (Miyaaki *et al.* 2009; Kim *et al.* 2009b). Properties of the virus itself may also differ in patients and several viral mechanisms may interfere with IFNα signaling in infected cells. HCV protein mediates upregulation of protein phosphatase 2A resulting in STAT hypomethylation (Duong *et al.* 2004). HCV core protein also regulates SOCS3 and causes a blockage of IFNα-induced ISGF3G formation and proteasome-dependent degradation of STAT1 (Bode *et al.* 2003; Lin *et al.* 2005).

Melanoma treatment

IFNα therapy has been first approved for other cancer treatment and shows also a beneficial effect as adjuvant therapy of stage II to III melanomas after physical removal of the tumor (Kirkwood *et al.* 1996; Pehamberger *et al.* 1998; Kirkwood *et al.* 2000). IFNs are stimulants of the immune system and can induce antitumor effects. They have some antiangiogenic properties and antiproliferative effect on fast growing cancer cells. Meta-analysis of several clinical trials with IFNα treatment in melanoma patients with limited statistical significance demonstrates an increase in relapse-free survival (Garbe *et al.*

2010). However, only a small percentage of patients benefit from IFNα treatment. The molecular basis for this is not clear. SOCS proteins are also involved in the resistance of IFN in melanoma cells after several passages *in vitro* (Fojtova *et al.* 2007). This indicates that tumor cells change their responsiveness to IFNα during the treatment period and counteract the antiproliferative effect of IFNα by upregulation of suppressors of IFN signaling.

Limits of therapeutic use of interferon-alpha

There are some disadvantages of IFNα therapy, despite the ability to erase HCV or reduction below the detection level in some patients. A major disadvantage is the resistance that often already exist in patients, in contrast to specific antiviral agents for example peptidase and polymerase inhibitors. This may be due to preexisting viral evasion of ISGs (Short 2009; Bonjardim *et al.* 2009). In other cases, host factors limit the action of IFNα in infected cells or immune cells (Del Campo *et al.* 2009).
HCV can be cleared in almost all IFNα rapid responder patients, but there is no effective treatment for HCV in resistant patients. Therefore, it is important to understand the molecular mechanism underlying the resistance to IFNα therapy to establish personalized healthcare and a more effective therapy. The limited efficacy in eliminating the infection with SOC therapy and its relative toxicity inspired many researcher and pharmaceutical companies to invest in new and improved therapeutics (Shimakami *et al.* 2009).
In contrast to HCV therapy, the question whether patients benefit from IFNα in melanoma treatment remains controversial. The application is very limited and only few patients may really benefit and toxicity is a concerning issue, especially after surgery to eliminate the cancer.

Improvements: pegylated interferon and new formulations

The future of HCV therapy will focus on new strategies including new IFN formulations (Albuferon, oral IFNs), the use of IFN type III (peg-IFNλ) or a RBV prodrug (taribavirin). Other strategies aim for agents that target cellular (host) factors such as cyclophilin inhibitors with the potential to avoid the development of HCV mutational resistance and “specifically targeted antiviral therapy for HCV” (STAT-C). The list of STAT-C drugs includes NS3/4 protease inhibitors (R7227), NS5B polymerase inhibitors for example a nucleoside analogue of cytidine (R7128), internal ribosomal entry site inhibitors and interfering RNAs. Moreover, inhibitors of HCV assembly, HCV release and inhibitors of HCV entry are under development. (Mallet *et al.* 2010; Flisiak *et al.* 2010). In the next years, research focus lies on the use of triple therapy with a combination of Pegasys, RBV and one of these new STAT-C drugs (Flisiak and Parfieniuk 2010). They are very effective and also trials with combination of R7227 and R7128 without IFN and RBV are ongoing and preliminary results confirm greater than additive activity (Bartels *et al.* 2008). Another approach is to enhance endogenous viral defense by boosting SOC with ritonavir. Ritonavir is an inhibitor of cytochrome P450-3A4, a liver enzyme that normally metabolizes protease inhibitors and was originally developed as inhibitor of HIV protease (Merry *et al.* 1997).

Gene-expression analysis

There are at least 8 different microarray formats and they use different technology and have specific advantages and weakness (Ahmed 2006). The Illumina beadarray technology, a cost effective, flexible has become available in our lab to examine whole genome expression. Illumina Sentrix beadarray technology is a direct hybridization based

approach to detect fluorescent-labeled copy RNA on DNA probes linked to glass beads randomly distributed on glass slides. Similarly, small non-coding RNA such as micro-RNAs (miRNA) can be processed, labeled with a generic nucleic acid code and hybridized to beadarrays used for general purpose. A similar technology is applied for the detection of single nucleotide polymorphisms, copy number variations and DNA CpG methylation ratio in genetic material of samples.

Bioinformatic and statistic challenges

The flexibility of Illumina gene expression arrays is not only an optional property, but the use of only one gene specific DNA sequence for most of the genes makes a greater flexibility necessary. Therefore, probes that do not behave optimally can be exchanged with annually updates of the bead pool. As a result, DNA probe sequences are continuously changing and this can be very challenging when signals form different bead versions are compared. The use of probe IDs that correspond to the DNA sequence of the given probe makes it easier for a better annotation to the newest genome assembly (Du *et al.* 2007). The use of open source software such as R/Bioconductor and customizable methods can be used to find the optimal procedure for analyzing microarray data (Du *et al.* 2008). These methods include normalization methods to reduce or adjust signal intensities among or within strips. A simple method to stabilize the variance bias for some probes is to apply the logarithmic function to the signals. The results often get optimized when the log transformation is replaced by variance stabilizing transformation (VST) that converts high signals on a logarithmic scale and low values in a more linear way (Lin *et al.* 2008). To reduce different signal intensities among the samples a simple and fast method is to apply quantile normalization. This has usually little influence on single probe intensities because the high number of probes used for Illumina beadarrays limits strong manipulation of intensity data. However, there is no appropriate method for an absolute estimate of mRNA abundance. In addition, the sigmoid intensity shape, demonstrated when RNA is spiked in, indicates that fold changes are dependent on the signal intensity and that methods as quantitative PCR (qPCR) or transcriptomic deep sequencing are more adequate to estimate ratios across genes. In comparison with Affymetrix gene expression arrays, the background for Illumina beadarrays is not estimated on several probes for one gene but on the intensity of all probes on the chip. This results in high intensity values for not detected probes. Thus, a background subtraction or a filter for low intensity probes is necessary to avoid positive results for not expressed genes. An optimal method is VST or adjustments in the test statistics to keep high probability candidate probes with low expression signal in the test set without applying a exclusion filter on probes with low intensity values. It is also useful to adjust the resulting p-values for the multiple testing for these thousands of probes. To avoid problems for the bioinformatic processing of the gene expression data, a proper study design is absolutely essential. Replicates should be evenly distributed among the strips and the chips used. The processing of the biological material for example the *in vitro* transcription is also biased and therefore amplification of mRNA should be minimized.

Transformations and normalizations

There are many different ways to pre-process microarray data and combination of different transformations, normalizations and adjustments may be ideal for a study to be analyzed (Schmid *et al.* 2010). Many methods for the analysis of Illumina beadarrays have been developed on advanced methods used for Affymetrix gene chips. The main use of Illumina gene expression arrays here is the identification of genes with different expression under conditions with or without IFNα treatment. For a better illustration how Illumina gene

expression values behave with different processing, we used the data from knock-out animals. This data from mouse cells with deletions in the given gene illustrates differences in the data transformation and normalization of intensities (Illustration 3).

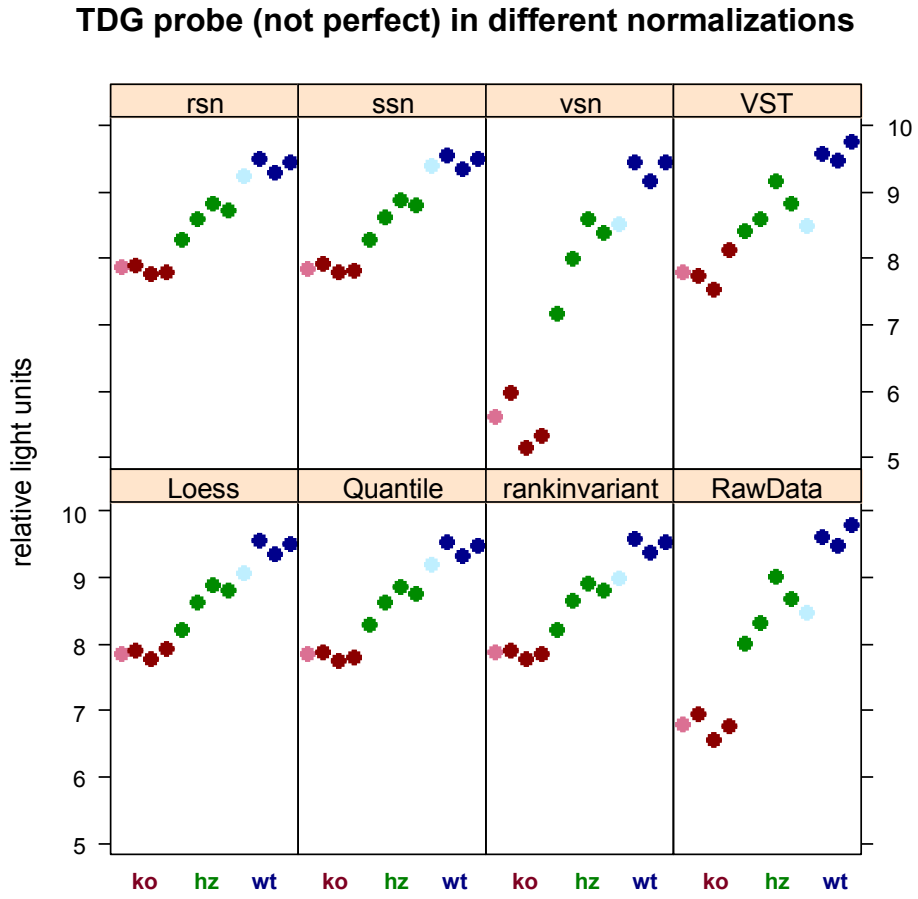

Illustration 3: Comparison of normalization from knock-out, heterozygote and wild-type (wt) mouse embryonic cells. The expression data of the probe for TDG (matching to the deleted sequence of the knock-out mice) was transformed by a simple log2 transformation (RawData) or the variance stabilizing transformation (VST). After VST, Robust Spline Normalization (rsn), Simple Scaling Normalization (ssn), Quantile or Loess normalization was applied. The last method used for variance stabilization and normalization (vsn) is based on another approach (Huber et al. 2002). Values in light color were detected as outliers.

As expected, most of the transformations result in a normalization of the knocked-out gene to a background value. The heterozygous cells have expression values between knock-out and wt cells and the normalization for the outlying data from one wt cell (indicated in light blue) bring the value for the *Tdg* gene in the range of the other wt cells. A look at the literature indicates that several possibilities to improve normalization for every new Illumina beadarray type are reported from the labs. Illumina whole genome 6 sample arrays contain two strips, for example. One strip with probes for well expressed RefSeq genes and a second one for expressed sequence tags, hypothetical genes and genes from other sources. It has been recommended to normalize each of the strips separately to reduced influences of non-RefSeq genes and for better comparison to RefSeq arrays (Shi *et al.* 2009).

Moderate t-test and false discovery rate correction of p-values

Advanced normalization methods may be useful in special cases to look deeper in to the samples than just to detect differential expression of some genes. Some of the methods can be useful for most of the microarrays available on the market. A list of differentially expressed genes with less than 5% false positives for example can be generated using a moderate t-test and application of false discovery rate (fdr) correction of the resulting p-value (Smyth *et al.* 2003). Moderate t-statistics take the absolute (fold) change in to account and p-value adjustment reduces the chances for reporting false positives to a meaningful cut-off (Illustration 4). The comparison between limma moderated t-test and equal variance t-test for samples generated from *Tdg* heterozygous or knockout fibroblasts shows as an example the effect of these adjustments (Cortázar *et al.* 2011).

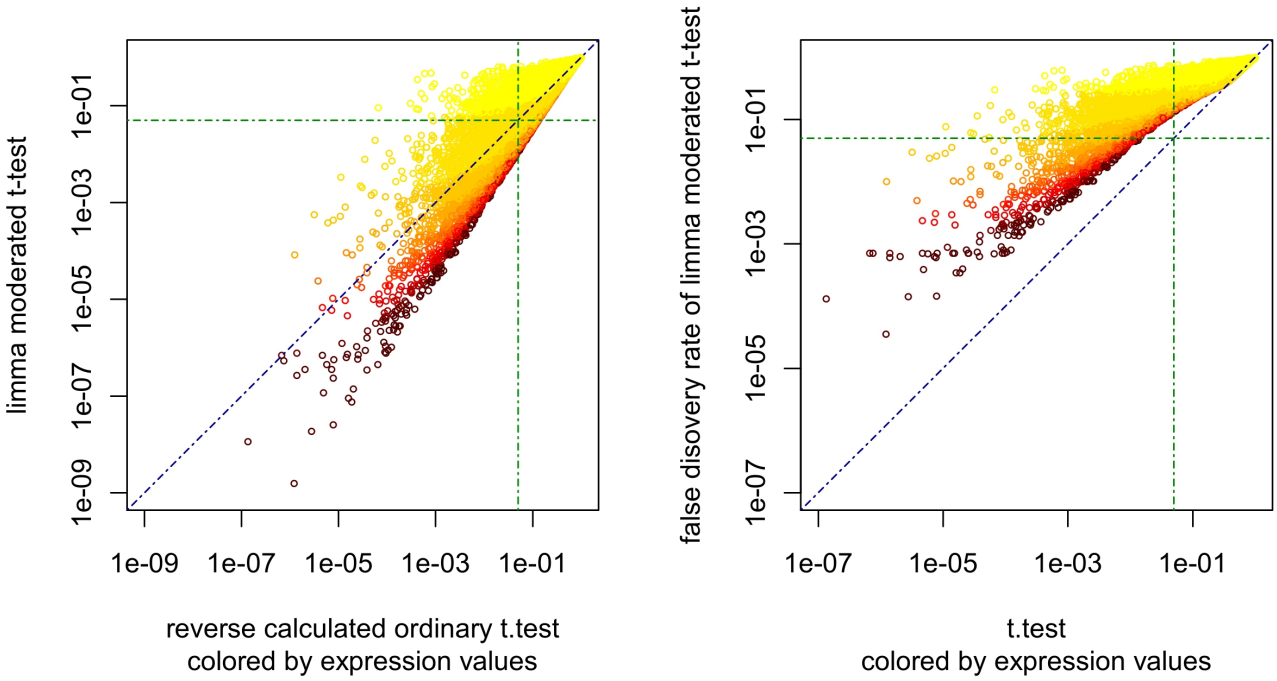

Illustration 4: Comparison of t-test used for microarray analysis. Data taken from Affymetrix gene expression data set (Gene Omnibus Series GSE20693). Left: Ordinary p-values from t-test statistic are compared to p-values of moderated t-test limma statistics and colored by absolute fold changes (yellow indicates small change and red indicates big differences in expression levels). Right: Effect of false discovery rate adjustment to the moderated t-test shown on the left, the values on x-axis show t-test statistics.

Benefits of in-house and public databases & visualization in genome browser

The processing of micro-array data with open source programs enables fast and simple transformation of the results to genome browsers such as the USCS genome browser (Fujita *et al.* 2011) for better visualization and easy browsing of genes or chromosome locations. Once transformed to the BED14 format, custom tracks such as a panel of ten cancer cell lines treated with IFNα can be used to merge information on IFN response to annotations of the genome (Illustration 5).

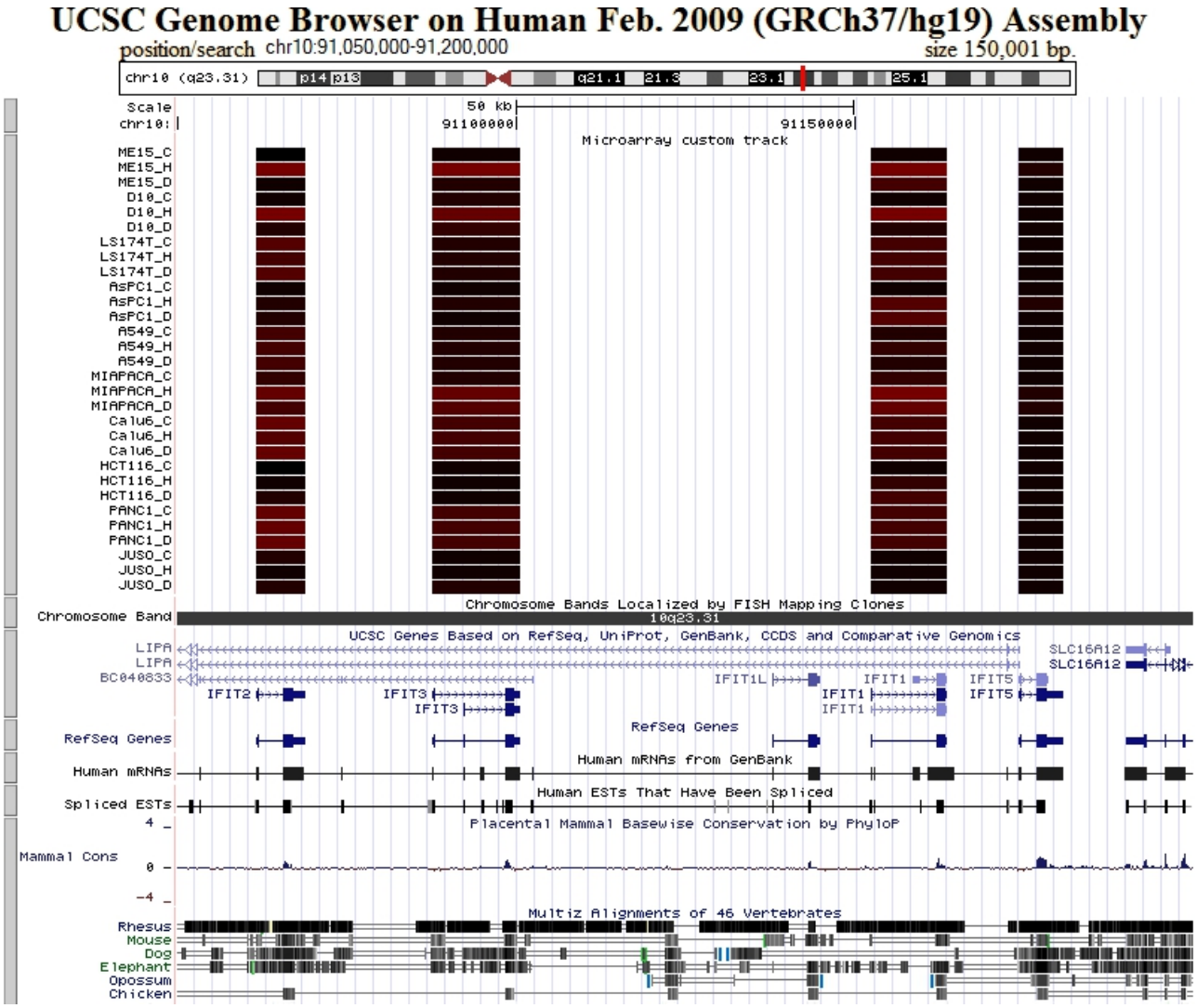

Illustration 5: Data integration to the USCS genome browser taken from the data-set GSE21158 (Siegrist et al. 2011). Identification label of 10 cancer cell lines is indicated in the first column with treatment label: C (control, no IFNα, medium changed 24 hours before cell harvest), H (4 hours IFNα), D (24 hours IFNα). The color of the bars on the chromosomal location of the gene indicates the intensities of IFIT genes with undetectable levels in black and high expression levels in red (on a log scale).

Introduction to the Chapters

Chapter 1 - Characterization of IFNα transcriptional responses in cancer cell lines

A hallmark of cellular resistance to type I IFNs is the lack of antiproliferative responses. Earlier results in our lab have shown that co-stimulation with IFNα and transforming growth factor beta-1 (TGFβ) potentates antiproliferative activity in a sensitive (ME-15) and resistant (D10) human melanoma cell line (Foser *et al.* 2006). IFNα therapy can be beneficial in the treatment of a diversity of cancer types partially due to stimulation of the immune system. Many cell types and some of the cancer cells have IFNARs and respond to IFNα. However, IFNα signals are different from tissue to tissue and do not always translate to a reduction in cellular growth or inhibit replication in cancer cells (table 2). Differences of growth inhibition in ME-15 and D10 cells are reported to be 21 % and 9 %, respectively (Pansky *et al.* 2000). These growth response rates are not stable over multiple passages of the cell lines. D10 cells acquired a more pronounced resistance to the growth-inhibitory action of IFNα during cultivation in our labs for example. This is partially due to massive rearrangements in the genome such as chromosomal crossover, duplications and deletion of entire parts of their genome. Cell-lines have been genotyped to generate a genomic fingerprint of the clones used in different laboratories and some of them acquired substantial rearrangements in the genome (unpublished data).

Cell line	Origin / morphology	Response on Chip	Response apoptotic IFNα	Response IFNα and TGFβ	Response TGFβ	Response IFNα
ME-15	Endothelian	+++	+	+++	++	++
D10	Endothelian	+++	+	+++	++	+
AsPC-1	Pancreas	+++	++	+++	++	++
MIA PACA 2	Pancreas / epithelial	++	+++	+	-	+
HCT 116	Colon / epithelial	++	+	-	-	-
LS 174T	Colon / epithelial	+	+++	-	-	-
JUSO	Endothelian	+	N/D	+	+	-
Calu-6	Prob. Lung	-	N/D	+	+	-
PANC-1	Pancreas / epithelial	-	N/D	+	+	-
A549	Lung / epithelial	-	N/D	+	+	-

Table 2: Panel of ten cancer cells lines cultivated for different purposes. Overview of gene expression responses and growth related responses to cytokines involved in cancer growth. Apoptotic response was estimated based on microscopic inspection of cell cultures treated with 10000 U / ml of IFNα. Stefan Foser, F. Hoffman-La Roche Ltd., Basel, kindly provided experimental data of growth-inhibition by IFNα and TGFβ. Experimental setup has been described (Foser et al. 2006).

DNA index in cultivated cancer cell lines

The acquired resistance to IFNα in D10 cells could be a result of higher rearrangement in the chromosome of D10 cells compared with ME-15 cells. The amplification rate is usually higher in cultivated cancer cells than the deletion rate. Thus the ratio of total DNA content of a cancer cell lines compared with healthy donor peripheral blood mononuclear cells (PBMC) was measured to estimate the 'chromosomal age' of these immortal cells. ME-15

and D10 melanoma cell lines were tested for their DNA content in the presence of IFNα and in control cells. Assignment of the cell cycle phase to IFNα-treated sensitive melanoma cells was less clear than for control cells (Illustration 6). However, no significant accumulation of cells in a specific cell cycle was observed. The DNA index (DI) of both ME-15 and D10 cell lines was 1.3. Therefore we can conclude that both cell lines have accumulated during carcinogenesis, immortalization and passaging an increase in DNA content of about 30%. The DNA accumulation is composed of an increase in chromosome number of about 47-49 chromosomes for D10 and 45-59 chromosomes for ME-15 (Pansky *et al.* 2000). On the other hand, duplications in the chromosomes and recombination of them attribute for the rest of the excess DNA.

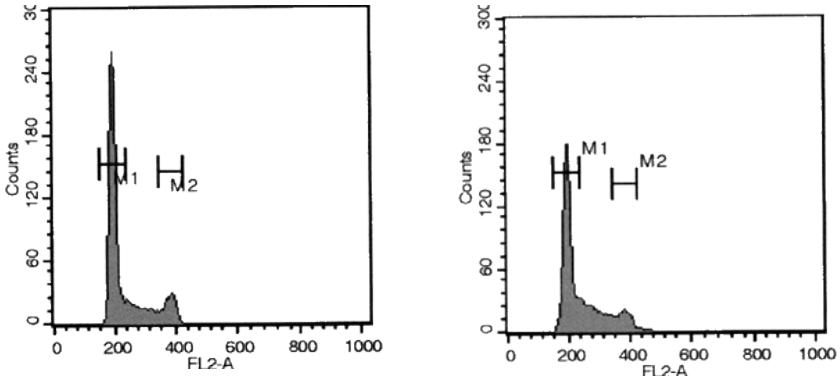

Illustration 6: Cell cycle inhibition of melonama cell lines (ME-15) treated with Pegasys. Control cells day 2 (right) and pegylated- IFNα (1000 U / ml) treated cells day 2 (left). No significant block of cell cycle observable.

Characterization of IFNα signaling in cancer cell lines

Gene induction by small concentration of IFNα (100 U/ml) was analyzed in human cancer cell lines with differences in sensitivity to IFNα and TGFβ. The cell lines are separated according to their tissue of origin by expressing specific mRNAs (Illustration 7). The response to IFNα can be validated by filtering for primary and secondary response genes (Certa *et al.* 2003). Interferon induced 3 and 6 (*IFI3 / IFI6*) can be used for example as representatives of these two subgroups of stimulated genes (Hallen *et al.* 2007).

For some genes the mode of action has not been well characterized. Among them, genes like *IFI44* and *IFITM3* have highly changed expression levels in presence of IFNα (Siegrist *et al.* 2010). Some of the cells lines (Calu-6, PANC-1, A549) had no significant induction of classical ISGs what explains their resistance to growth control. Another panel of cancer cell lines (HCT 116, LS 174T, JUSO) are proficient in inducing ISGs to some extend but this does not translate in a block of proliferation. Therefore, the most promising cell lines to study antiproliferative function of ISG are ME-15, D10, AsPC-1 and MIA PACA 2 because they have most of the ISGs induced and IFNα affects their cell proliferation rate.

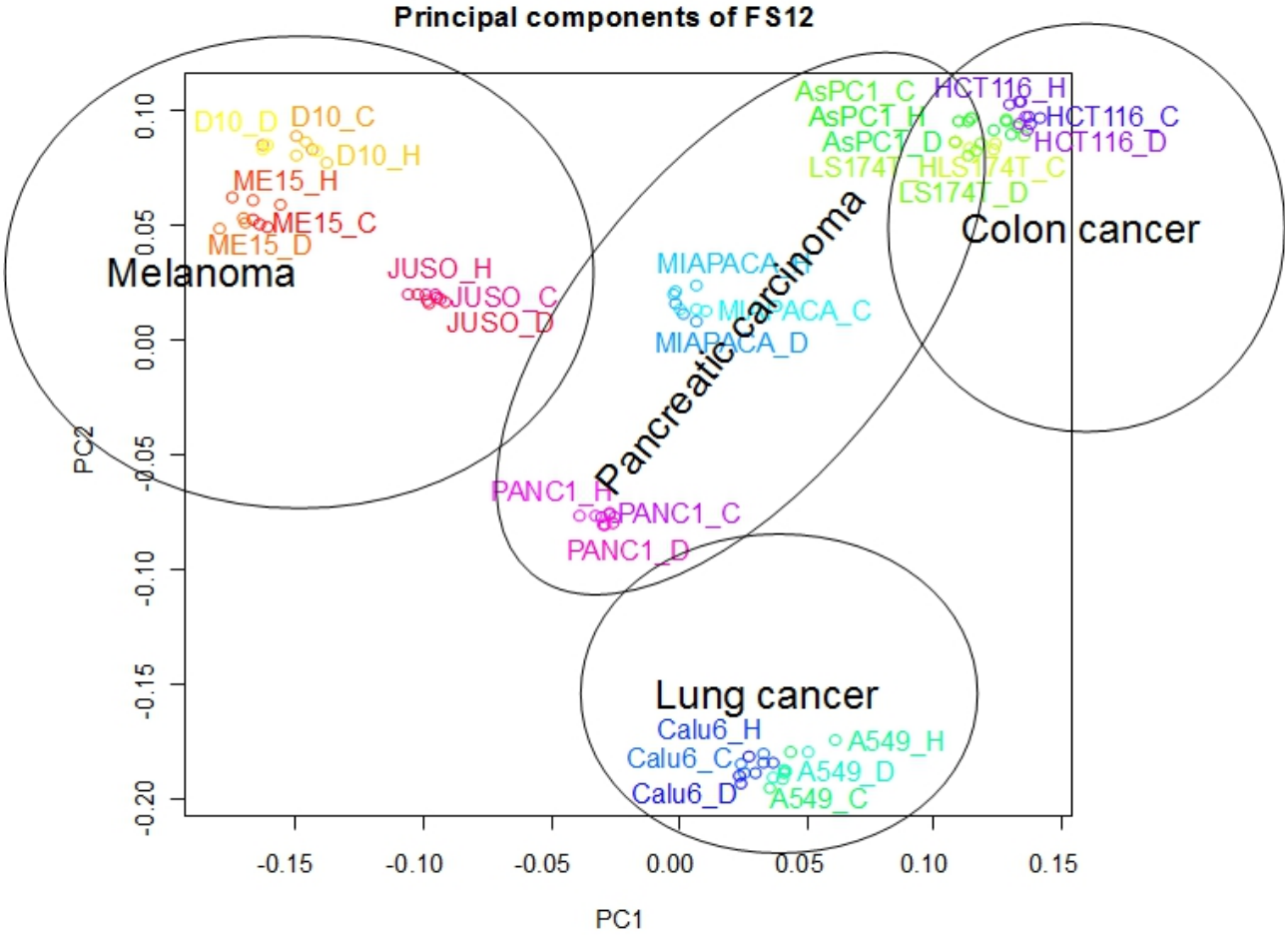

Illustration 7: Principal components analysis of 10 cancer cell lines. RNA of 10 untreated cell lines (C) was collected or from cells treated with IFNα (100 U / ml) and 4 (H) and 24 hours (D) and analyzed on Illumina RefSeq8 gene-expression arrays.

IFNα inducible microRNA profiles

There is a newly discovered group of non-protein coding genes that is also regulated by IFNα stimulation of cancer cell lines (Pedersen *et al.* 2007). These microRNAs (miRNA) are positive and negative regulators of eukaryotic gene expression that modulate transcript abundance by specific binding to sequence motifs located prevalently in the 3' untranslated regions (3'-UTR) of target mRNA. IFNα induces a large set of protein-coding genes mediating antiproliferative and antiviral responses. The small number of identified miRNA and their small size of 19-22 nucleotides request fundamental changes in the detection technology and analysis. Here we used global microarray-based miRNA detection platform to identify miRNA genes that are induced by IFNα in HCC- or melanoma-derived human tumor cell lines. Despite the enormous differences in expression levels between these models, we were able to identify miRNAs that are upregulated by IFNα in both lines, suggesting the possibility that interferon-regulated microRNAs (IRmiRs) are involved in the transcriptional repression of mRNA relevant to cytokine responses (GSE16421).

IFITM3 expression and signal translation

For many years it has been known that the antiproliferative activity of IFNα can be effectively transferred to untreated recipient cells (Lloyd *et al.* 1983). We have shown that

one of the differences between an IFNα antiproliferative sensitive (ME-15) and an insensitive (D10) cell line is the expression of *IFITM3* at the unstimulated status in insensitive cell line (Brem *et al.* 2003). Thus, if a cancer cell becomes insensitive to the antiproliferative effect of *IFITM3* its cellular levels are no longer a handicap and these cells are likely have deregulated protein levels. A recent report shows the antiproliferative function of *IFITM1*, a closely related family member of *IFITM3* lacking the N-terminal sequence (Yang *et al.* 2007). IFITM proteins are also localized in cellular structures that appear as dots in the microscope and can be found associated to exosomes (Brem *et al.* 2003). Therefore, they have the potential to transfer the antiproliferative signals to immune cells for example, what could explain the different evolution of these genes in man and mouse. We have detected this protein in the supernatant of expressing cells and that the addition of IFITM3 antibodies to the medium has a proproliferative effect on the generators (unpublished data that reproduced the initial observation from Stefan Foser, F. Hoffman-La Roche Ltd., Basel). IFITM family member are supposed to act as proliferation control proteins crossing the boundaries of a single cell. The cultivation of cells that do express IFITM with fluorescent-labeled recipient cells is therefore a potential method to analyze the effect in cell culture (Illustration 8).

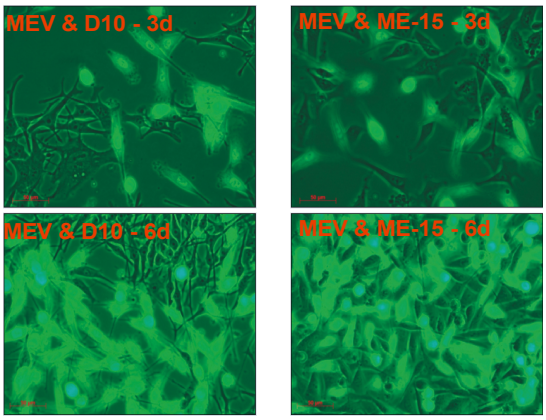

Illustration 8: Snapshots of cocultures of IFN sensitive ME-15 cell line and the melanoma cell line D10 not showing a growth response to IFN.

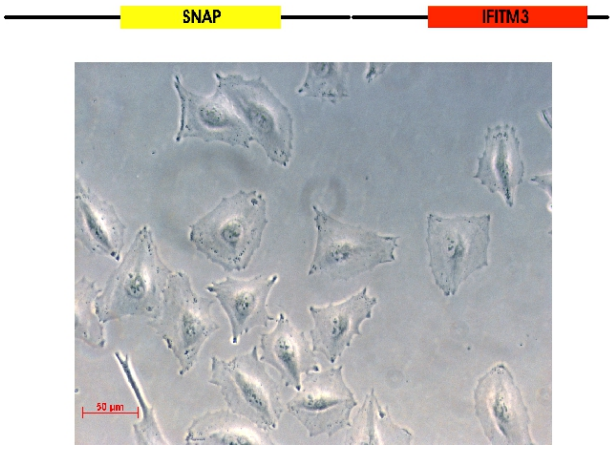

Illustration 9: Overexpression of IFITM3 can induce senescence-like morphology: Melanoma cells (ME-15) were transfected with a SNAP-tag IFITM3 vector construct. The picture shows an extreme case of slow growing cell lines (clone SUE) before singularization.

In addition the generation of IFITM expressing cells could result in a well-defined cancer cell line that has acquired resistance to IFNα. The cells infected with the plasmid are resistant against the selection antibiotic and are halted in proliferation and take flat shape of senescent cells (Illustration 9). This morphology has been described already for IFN treated cells (Pammer *et al.* 2006). However, some cells recover from the antiproliferative pressure of the IFITM3 by blocking expression of IFITM3 proteins. Some rare cell clones do proliferate and maintain the expression of small amounts of IFITM3 proteins. In contrast to our expectations, the cell lines analyzed (SUEG, SUEL and USDG) are normally responding to the antiproliferative effect of IFNα (Illustration 10). This result indicates that expression of IFITM3 is no indication for resistance to IFNα, but does not rule out the possibility that inhibition of *IFITM3* transcription in cancer cells indicate sensitivity to IFNα.

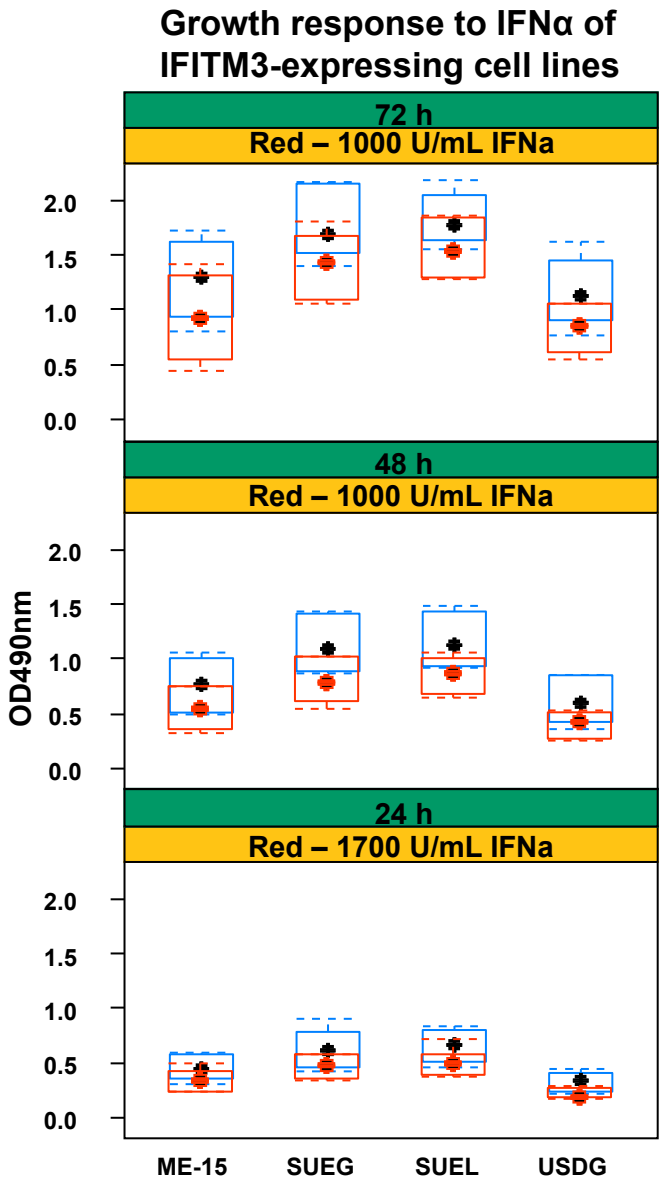

Illustration 10: Growth response to IFNα of IFITM3-expressing cell lines

Chapter 2 -Characterization of IFNα transcriptional responses in cancer cell lines overexpressing suppressor genes

Negative regulation of JAK-STAT signaling

A rapid onset of the IFNα signaling cascade and subsequent decay of JAK-STAT signaling is characteristic for this pathway and important for optimal regulation of transcriptional responses. Kinases, phosphatases and other enzymes can be recruited to the membrane rapidly after cytokine stimulation to inhibit signaling through the same pathway or in crosstalk with other pathways. The most direct way to interfere in kinase dependent signaling is deactivation by dephosphorylation of the crucial proteins. The phosphatase involved in IFN signaling is SHP2 and acts by inhibiting IFN-induced JAK-STAT signaling (You *et al.* 1999). PIAS proteins are another class of IFNα inhibitory proteins (Shuai 2000). They promote the sumoylation of STAT1 (Ungureanu *et al.* 2003; Rogers *et al.* 2003; Ungureanu *et al.* 2005). The last class of JAK-STAT inhibitory proteins has been described recently (Yoshimura *et al.* 1995; Endo *et al.* 1997; Masuhara *et al.* 1997; Minamoto *et al.* 1997). Eight proteins with high similarity in amino acid structure form the family of suppressors of cytokine singaling (SOCS) proteins (See Illustration 11).

Suppressor of cytokine signaling

A plethora of cytokines induces SOCS1 and SOCS3 and the induction is dependent on different STAT molecules for example STAT6 (Albanesi *et al.* 2007). SOCS1 is induced by IFNα and several other cytokines, growth factors and pathogen associated patterns (Dickensheets *et al.* 1999; Wang *et al.* 2000). The IFNα mediated induction is dependent on the functionality of STAT2 and an active ISRE is present in the *SOCS1* promoter region (Zhao *et al.* 2007). IFNα increases all small SOCS proteins tested (CISH, SOCS1-3) in T

Name	Structure	Factors that induce expression	Critical role in cytokine signaling
CIS1/CISH		EPO, IL2, IL3, IL6, IL9, INFα, TNFα, GH, prolactin, EPO, TSLP	GH, prolactin, IL2, IL3, EPO
JAB/SSI1/SOCS1		IL2, IL3, IL4, IL6, IL7, IL9, IL13, LIF, IFNγ, IFNα/β, TNFα,GH, prolactin, EPO, TPO, TSLP, G-/GM/M-CSF, TPO, LPS, CpG	IL2, IL4, IL6, IL7, IL12, IL15, IFNα/β, IFNγ, LIF, TNFα, EPO, TPO, TSLP, GH, prolactin, insulin, leptin, LPS, CpG
CIS2/SOCS2		GH, IL6, LIF, IGF1, IFNγ, IFNα, prolactin, insulin, CTNF, cadiotropin, TSH	GH, IGF1, IL6
CIS3/SSI3/SOCS3		IL1, IL2, IL3, IL4, IL6, IL9, IL10, IL11, IL13, GH, prolactin, EPO, GM-CSF, LIF, IFNα, IFNγ, leptin, IL10, LPS, insulin, CTNF, LPS, CpG	GCSF, IL2, IL4, IL6, IL9, IL11, IL23, IFNγ, IFNα/β, LIF, leptin, prolactin, insulin, EPO
CIS7/SOCS4	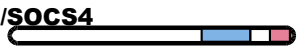		
CIS6/SOCS5	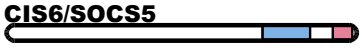	IL6, IL4	IL4, IL6
CIS4/SOCS6	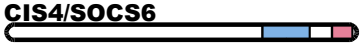		insulin
CIS5/NAP4/SOCS7	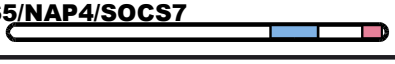		insulin

Illustration 11: SOCS protein inducing factors and signaling pathways controlled by negative feedback. Modified from (Yoshimura et al. 2005) and other reviews.

cells, this indicates a more general effect of IFNα on SOCS expression in haemopoietic cells compared to epithelial cells (Brender *et al.* 2001). Among the eight SOCS proteins that may be able to interfere in IFN signaling, genetic evidence from knockout mice show a direct target receptor regulatory role only for SOCS1 and SOCS3 (Illustration 12 A) (Alexander *et al.* 2004; Yoshimura *et al.* 2007). The inhibitory interaction of SOCS is partially kinase-independent by a steric block of the activated IFNAR and requires functional SH2 and SOCS box domain in the case of SOCS1 (Fenner *et al.* 2006; Gingras *et al.* 2004; Walsh *et al.* 2006). The primary mode of action is SOCS1 interaction with a critical phospho-tyrosine residue within the JAK2 catalytic loop (Endo *et al.* 1997) (Illustration 12 B). The interaction may be through a specific domain in SOCS1 and SOCS3, the kinase inhibitory region (KIR) or by the phospho-tyrosine binding domain SH2 in dependence of the N-terminal domain. The kinase inhibitory regions of SOCS1 and SOCS3 are able to block kinase activity of JAKs by acting as pseudo-substrate (Yasukawa *et al.* 1999; Sasaki *et al.* 1999). This domain may also bind to the autophosphorylation loop of Jaks (Waiboci *et al.* 2007; Flowers *et al.* 2004). Furthermore, structural modeling indicates that a block of kinase activity can operate simultaneously with restriction of target protein access to the catalytic cleft (Giordanetto *et al.* 2003). A direct and persistent way to inhibit IFNα activated JAK-STAT signaling by SOCS proteins is the recognition of tyrosine-phosphorylated sites of the signaling proteins involved by the SH2 domain and poly-ubiquitination through the SOCS-box (Illustration 12 C). This results in the degradation of JAK-STAT proteins and consequently reduces the amplitude of ISG expression. There is evidence for an association of SOCS3 with JAK1 and SOCS1 mediated ubiquitination and degradation of Tyk2 (Qing *et al.* 2005; Nguyen *et al.* 2006). In addition to SOCS1-IFNAR, receptor-kinase interactions are blocked dependent on SH2-phospho-tyrosine recognition during inhibition of IFNα by SOCS3 (Illustration 12 D) (Vlotides *et al.* 2004; Pauli *et al.* 2008).

SOCS dependent ubiquitination and proteasomal activity is involved in the regulation of JAK-STAT pathways for several other cytokines (Kim *et al.* 1996; Yu *et al.* 1997; Boyle *et al.* 2009; Lang *et al.* 2003). These mechanistic studies are crucial to understand SOCS3-dependent IFNα signaling suppression and cross-talks of negative feedback-loops in

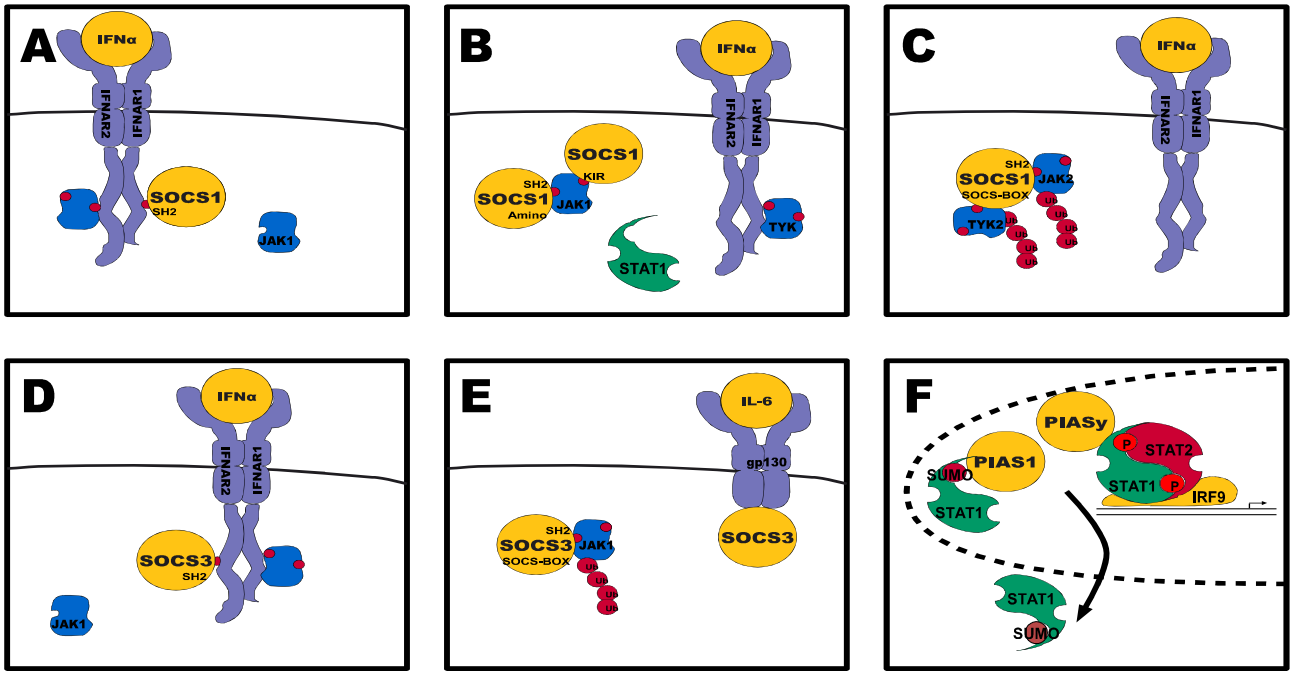

Illustration 12: Mechanism of JAK-STAT pathway regulation by SOCS1, SOCS3 and PIAS.

different signaling pathways (Illustration 12 E). There is no reported function for nuclear SOCS proteins in IFN signaling although SOCS1 molecules can locate to the nucleus and have a nuclear-import signal (Ben-Yair *et al.* 2002; Baetz *et al.* 2008; Koelsche *et al.* 2009). In contrast, PIAS proteins act primary on activated STAT proteins in the nucleus (Illustration 12 F) (Liu *et al.* 1998; Liao *et al.* 2000; Ungureanu *et al.* 2003; Rogers *et al.* 2003).

As summarized in Illustration 11, there is support for an important role of other SOCS molecules in the regulation of IFNα signals. However, imbalances in *SOCS2* levels have a strong effect on growth hormone signaling and both knockout as well as overexpression correlates with abnormal growth (Favre *et al.* 1999). Interestingly, SOCS2 overexpression blocks the inhibitory action of SOCS1, SOCS3 and CISH. Thus, SOCS2 may also regulate IFNα-dependent signaling pathways (Shen *et al.* 2000). This requires an intact SOCS-box and suggests that SOCS2 is involved in the ubiquitination of SOCS1 and SOCS3 (Rico-Bautista *et al.* 2006). We have analyzed the induction of *SOCS4* over a period of 72 hours by qPCR. *SOCS4* mRNA signals were elevated after incubation of ME-15 cells with IFNα compared to untreated cells before treatment but no protein could be detected in the cells to confirm this result (unpublished data). To our knowledge, there is no study on overexpressed SOCS1, SOCS3 and SOCS4 proteins in suppression of IFNα signaling and a report of nuclear functions of SOCS proteins in JAK-STAT signaling.

SOCS proteins may be targeted to control JAK-STAT signaling in cancer cells or to enhance responses to IFNα therapy. The therapeutic effect of IFNα is due to ISG induction in infected / cancer cells or immune cells. Therefore, the analysis of gene expression in response to IFNα treatment of cancer cell lines has the potential to conclude from the expression pattern of cells with elevated SOCS levels what the potential of a new class of IFNα combination therapy with SOCS inhibitors may be. Recent reports on miRNA induction by IFNα and miRNAs that target SOCS mRNA are indicating a feedback-loop for the negative regulators in cytokine signaling (Pedersen *et al.* 2007; Pichiorri *et al.* 2008; Sun *et al.* 2008; Hu *et al.* 2009; Lu *et al.* 2009; Androulidaki *et al.* 2009; Hu *et al.* 2010; Pogribny *et al.* 2010; Jiang *et al.* 2010b; Wang *et al.* 2010). Deregulation of miRNA

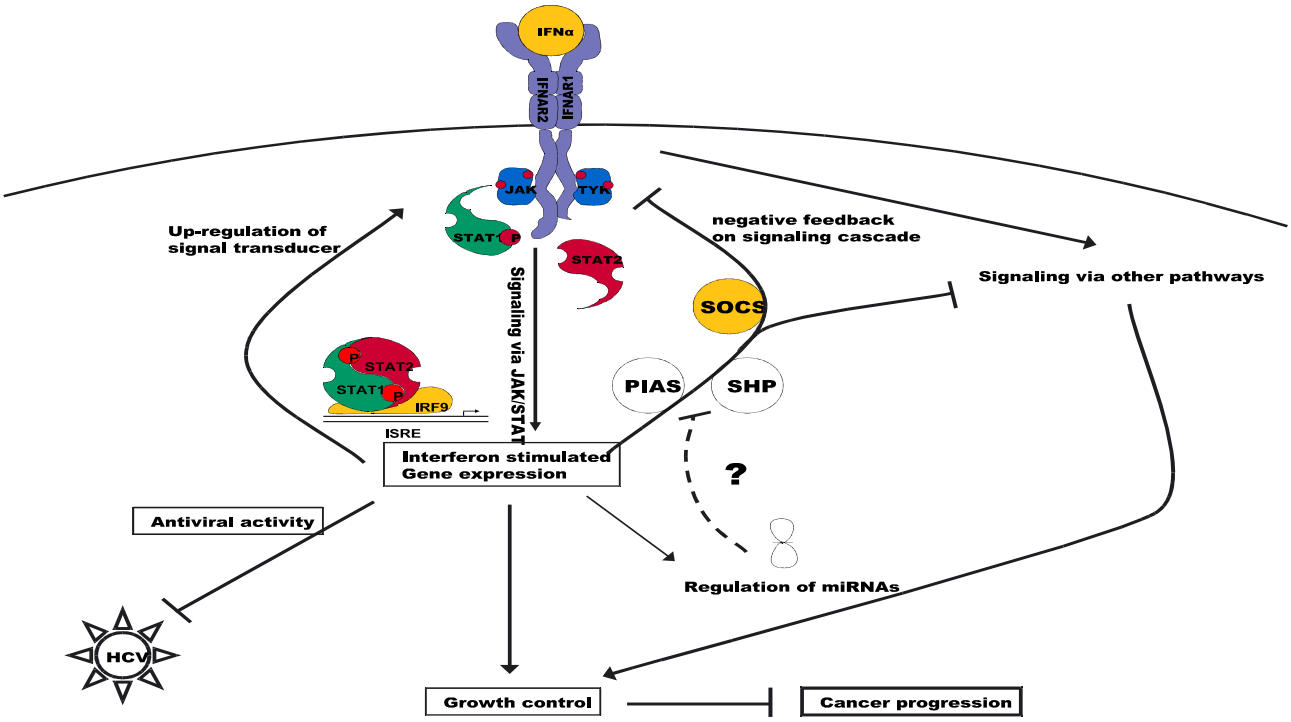

Drawing 1: Model: Therapeutic regulation of SOCS proteins.

involved in this pathway could play a role in IFNα resistance and may be measured systematically in the blood of patients. We have therefore analyzed the potential role of IFNα-induced miRNA in the regulation of SOCS mRNA translation.

Interferon-dependent gene expression profiling in SOCS expressing cell lines

To clarify the impact of SOCS proteins on IFNα induced gene expression in the melanoma (ME-15) and HCC (HuH-7) cell lines, we have generated SOCS overexpressing cell lines and characterized their IFNα-induced gene expression profile. This data refines the reports on cytokine suppression mechanisms in our cell culture model system. The analysis of cytokine signal-suppression in a similar cellular context as *in vivo* with HCV infection and cancer is important for the understanding of resistance to the therapy. SOCS proteins act in a classical negative feedback-loop against the action of IFNs and many other cytokines (Fujimoto *et al.* 2003). SOCS1 and SOCS3 inhibit the expression of IFNα inducible antiviral proteins (Vlotides *et al.* 2004). In contrast to SOCS1 and SOCS3, the importance of SOCS4 is not known. Limited by the assay set-up, sample triplicates, two time-points, two cell lines and controls for every sample, we decided to analyze cell lines expressing three different SOCS proteins and the parental cancer cell lines. The RNA extraction procedure adapted for the recovery of small RNAs allows the use of RNA extracts for gene expression and miRNA expression beadarrays. The miRNA expression profile in our cancer cell lines may resolve whether the same JAK-STAT pathway induces both miRNA and the classical ISGs.

Chapter 3 - Epigenetic alterations in colon cancer, cell lines treated with IFNα and knock-out phenotype of a DNA damage response gene involved in epigenetic stability in vivo

Interferon stimulated genes and DNA methylation in cancer

Epigenetic silencing of tumor suppressor genes is contributing to carcinogenesis and malign-transformation of cancer cells. CpG islands in the promoter region of the *SOCS1* gene get frequently methylated during carcinogenesis and promoter hyper-methylation correlates with protein levels in many cancer types such as HCC (Miyoshi *et al.* 2004; Nomoto *et al.* 2007; Okochi *et al.* 2003; Chu *et al.* 2010). Other ISG are also deregulated in cancer, but for *IFITM3* for example, there is no well-defined CpG island the promoter region. However, when the definition for CpG island is relaxed some CpGs are found in the proximity of *IFITM3*. Silencing of IFITM genes promotes migration and growth in cancer cells and is associated with aberrant DNA methylation of the *IFITM3* promoter. Methyl-specific qPCR correlated DNA methylation in that region to the CpG island methylator phenotype (CIMP) defined in colorectal cancer (CRC) tissues (unpublished data from Stefan Weis, University of Basel). Further, *SOCS1*, *SOCS2* and *SOCS3* CpG mehtylation occurred over all probes in the CIMP CRC sample and only some SOCS probes in the non-CIMP sample were methylated. For this small sample size screen, *SOCS2* promoter mehtylation showed better correlation to mutL homolog 1(*MLH1*) methylation than *SOCS1* (unpublished data). This finding documents the complexity in classifying CRC samples as CIMP+ or CIMP- phenotype. Hyper-methylation of *SOCS1* in CIMP is well known and *SOCS1* promoter methylation is part of the new CIMP definition set (Weisenberger *et al.* 2006; Ogino *et al.* 2007a; Ogino *et al.* 2007b). This data set can be used for better determination of CIMP+ and CIMP- status than the original set of sequences (Teodoridis *et al.* 2008). Promoters of genes from this CIMP set, such as *SOCS1*, are found also in

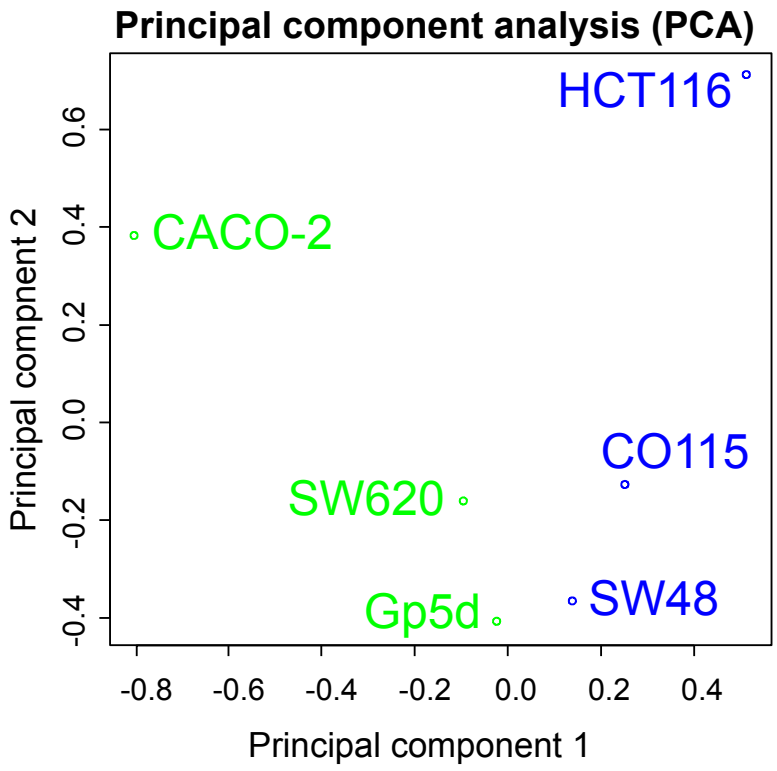

Illustration 13: Principal component analysis of CRC cell lines

breast cancer (Van der Auwera *et al.* 2010). Therefore, clinical samples may be used to find a link from SOCS or IFITM expression and promoter methylation to therapeutic response to chemotherapy, for example using recombinant IFNα.
The use of gene expression arrays to screen changes in mRNA levels of genes that are methylated in CIMP samples may be limited by the low expression of these genes in control tissue. A preliminary screen of six CRC cell lines could in fact separate the CIMP (*MHL1* methylated) from non-CIMP cancer cell lines (Illustration 13). Several genes are lower expressed in cancer cell lines and can be analyzed further by quantitative methylation specific PCR (qMSP). A gene that was highly expressed in non-CIMP colon cancer cell lines was intestinal trefoil factor family 3 (*TFF3*): This is a JAK-STAT induced gene and has been implicated with proliferation and migration in cancer (Jiang *et al.* 2010a). Therefore, the direct analysis of promoter methylation of such genes is in the focus of current research and shed light on the association of DNA methylation and prognostic implications in cancer patients. Hypermethylator (CIMP) and micro-satellite instability phenotype in CRC are critical indicators for clinical outcome (Kim *et al.* 2009a; Issa 2008; Boland *et al.* 2010).
Beadarrays covering most of the cancer related genes are available to analyze methylation specific differences in patient specimens or in cell culture. Therefore, we have initiated a project to integrate transcriptome and epigenome analyzes in CRC samples. Early detection in ademomas before a cancer becomes malignant could improve benefits for the patients. Systematic analysis of the methylation fingerprint of CRC cancers may be used to sub-group patients, update CIMP methylation site diagnosis panel and provide an opportunity for personalized healthcare. Today, detection markers for early diagnosis of cancer risk in adenoma do not cover a large group of patients. Therefore, we are interested in finding a panel of candidate biomarkers by combination of different micro-array technologies to address this task.
Adenomas are thought to generally precede a CRC stage and were screened in 32 adenomas from 28 patients on Affymetrix Chips (GSE8671) (Sabates-Bellver *et al.* 2007). A key feature of in this study was remodeling of the Wnt pathway, which is also affected by the *IFITM* family proteins (Lickert *et al.* 2005; Siegrist *et al.* 2011). To identify candidate gene regions undergoing aberrant methylation at early stages of CRC, integration of different types of microarray data is reasonable. Gene expression profiles in colorectal adenomas and normal mucosa, gene expression analysis of CRC cell lines treated with demethylating agents and beadarray assisted comparison of DNA methylation in normal and CRC samples can generate a list of candidate genes for early detection of CRC malign-transformation.
We have observed specific methylation pattern of *IFITM* genes in CIMP patients and some of the CpGs may be important for IFITM deregulation in cancer in general. CpG sites in the promoter of IFITM genes may be therefore dynamically regulated and factors that promote gene induction from repressed genes in cancer cells may have a general influence on them. *IFITM3* mRNA is not expressed in ME-15 cell but it is inducible by IFNα. Therefore, cytokine stimulation may contribute to dynamic DNA promoter methylation dependent on cellular factors.
IFNα regulates DNA damage repair pathways as well and nuclear SOCS1 plays a regulatory role in that (Calabrese *et al.* 2009). Thymine-DNA glycosylase (*TDG*) is involved in excision of mismatch GT nucleotides in the DNA repair mechanism of cells (Cortázar *et al.* 2007; Kunz *et al.* 2009). TDG may act as modifier in dynamic DNA methylation alterations as proposed for IFNα induced dynamic regulation of DNA methylation. Gene expression experiments in *TDG* knock-out animals promise to generate lists of genes that are regulated by mismatch-directed DNA glycosylase.

Results

Chapter 1
Characterization of IFNα transcriptional responses in cancer cell lines

See Annex page 1A1-1A24 *Review (author)*
The Small Interferon-Induced Transmembrane Genes and Proteins (Siegrist *et al.* 2011)

See Annex page 1B1-1B10 *Research article (microarray analyzes)*
Antiproliferative Activity of the Human IFN-α-Inducible Protein IFI44 (Hallen *et al.* 2007)

See Annex page 1C1-1C7 *Meeting poster presentation (author)*
Phylogenetic analysis of interferon inducible transmembrane gene family and functional aspects of IFITM3 (Siegrist *et al.* 2009a)

See Annex page 1D1-1D11 *Research article (main author)*
MicroRNA Expression Profiling by Bead Array Technology in Human Tumor Cell Lines Treated with Interferon-Alpha-2a (Siegrist *et al.* 2009b)

Chapter 2
Characterization of IFNα transcriptional responses in cancer cell lines overexpressing suppressor genes

See Annex page 2A1-2A8 *Meeting poster presentation and proceedings article (author)*
Micro RNA induction by Interferon alpha and their potential role to interfere in the negative feedback pathway (Siegrist *et al.* 2008b)
Micro RNA induction by interferon alpha and a potential role to interfere with SOCS (Siegrist *et al.* 2008a)

See Annex page 2B1-2B9 *Meeting poster presentation (author)*
Suppression of interferon alpha mediated gene expression by SOCS1 and SOCS3

See Annex page 2C1-2C37 *Research manuscript (author)*
Suppression of interferon-alpha-induced gene expression by SOCS1 and SOCS3 *to be submitted to International Journal of Interferon, Cytokine and Mediator Research*

Chapter 3
Epigenetic alterations in colon cancer, cell lines treated with IFNα and knock-out phenotype of a DNA damage response gene involved in epigenetic stability *in vivo*

See Annex page 3A1-3A8 *Meeting poster abstract (co-author)*
Integrating transcriptome and epigenome analyses to identify DNA methylation changes associated with colorectal carcinogenesis

See Annex page 3B1-3B14 *Research article (project support & supplementary data)*
Interferon-alpha induces reversible DNA demethylation of the IFITM3 core promoter in human melanoma cells (Scott *et al.* 2011)

See Annex page 3C1-3C17 *Research article (microarray analyzes)*
Embryonic Lethal Phenotype Reveals a Function of TDG in Maintaining Epigenetic Stability (Cortázar *et al.* 2011)

Conclusion and Outlook

Chapter 1
Characterization of IFNα transcriptional responses in cancer cell lines

IFNα provides cellular defense mechanisms against cancer and viral infections and are used as drugs to improve health after tumor-surgery or together with antiviral formulations to fight viral infections. Many questions remain unanswered and more basic research is needed to understand the functional interaction of the ISGs to fully realize the potential of IFNα.

We have assessed cell type specific differences in gene expression of several cell lines used in basic research laboratories. Cytokine treatment of cells showed indirectly JAK-STAT pathway activation. These results can be used to select the optimal cell line for a functional study of proteins or drugs. Small double strand RNAs can induce interferon production, one of the side effects that may appear when recombinant small interfering RNA is used, for example. Obviously, a cell culture model must be responsive to IFNα for the evaluation of both IFNα pathway activation and target mRNA silencing on the transcriptome level. Further, pericellular proteins, for example IFITM3, can be detected in cell culture supernatant and may indicate excessive IFNα signaling in treatment-naive individuals.

We have further characterized functional aspects of ISG, such as IFI44, the IFITM gene family and SOCS genes. This may help understand the specific cellular and clinical effects in response to IFNα. However, our results of ISG functionality are based on *in vitro* experiments only and have to be confirmed in a clinical setting. Further, the development of advanced methods for RNA preparation, to conserve the small RNA part for example, the evaluation of different *in vitro* transcription procedures and most of all the adaptation and development of bioinformatic and statistic methods for alternative microarray analysis could improve the scientific value of the results. Pioneer work in the analysis of miRNA and DNA methylation beadarray data introduced new prospects in the research for unappreciated aspects of cytokine signaling for example. Some of the technologies may disappear in the near future and be replaced by more sophisticated methods like next generation sequencing. We could show that microarray based detection of miRNA is useful to detect change in expression levels but is limited to estimate the expression ratio of miRNAs in the same sample. The bias towards certain small RNAs is as well an issue when using a deep sequencing approach to quantify miRNA levels and is not entirely comparable with qPCR. However, the expression ratios of miRNA sequencing and qPCR quantification methods are highly correlated (Linsen *et al.* 2009).

Chapter 2
Characterization of IFNα transcriptional responses in cancer cell lines overexpressing suppressor genes

We have assessed the role of SOCS proteins in repressing the functionality of IFNα signals in different cancer cell lines and concluded that SOCS1 is able to repress transcriptional response in cancer cell lines of different origin. However, transcripts of genes that are not dependent on JAK activation are less affected by the silencing. Among them are STAT1 and IRF9, well known players of the JAK-STAT pathway. SOCS3 expressing cell lines did not show such an overmastering effect and may play a minor role in the translation of the IFNα signal to the antiproliferative effect in cancer cell lines. However, SOCS3 may limit antitumor action of IFNα in stimulation of immune effector cells

and in tumor-antigen presentation. Our results from SOCS overexpressing cancer cell lines extend our knowledge of the molecular causes of resistance to IFNα in HCV and cancer. The bias of SOCS proteins for a specific kinase may be dependent on the extracellular mediator or the cell type. This aspect is crucial for normalizing JAK activation in cancer cells in therapy with SOCS mimics. SOCS3 interacts with Tyk2 to silence TLR3 signaling for example (Zeng *et al.* 2008). Moreover, SOCS1 can bind JAK2 and subsequently initiate ubiquitination and degradation of the kinase in IL6 signaling (Ali *et al.* 2003). These are two examples that further reveal details of the functionality of SOCS-box mediated kinase degradation in general. Research on SOCS proteins will help to understand how SOCS deregulation promotes cellular growth in carcinogenesis and may help to design small molecules to restore growth control. On the one hand, mutations occur in *SOCS1* genes with defective JAK2-degradation activity and this can be restored by insertion of wt *SOCS1* in vitro (Melzner *et al.* 2005). On the other hand, in tumor cells with genetically based constitutive activation of JAK2 or SOCS1 mediated degradation can limit aberrant signaling (Kamizono *et al.* 2001; Frantsve *et al.* 2001; Haan *et al.* 2009). This indicates that hyper-methylation of SOCS1 promoter can induce lost of growth control in cancer cells with aberrant DNA methylation and SOCS mimics may be used in therapy.
All HuH-7 SOCS expressing cell-lines lost CD81 expression and cannot be used for HCV in vitro models because CD81 is a required co-receptor for HCV entry (Bartosch *et al.* 2003; Cormier *et al.* 2004; Zhang *et al.* 2004). Moreover, CD81 is a tetraspanin protein that promotes HCV entry via its interaction with the viral E2 protein and can be associated with IFITM-proteins (Takahashi *et al.* 1990; Bradbury *et al.* 1992; Deblandre *et al.* 1995). Therefore, it is unlikely that the SOCS-modified HuH-7 cell lines can be used for experiments to address suppression of antiviral activity of IFNα Since this effect has not been observed in ME-15 cells, it must be a cell type specific response to either the selection procedure applied (Geneticin or response to singularization of the cells) or to a common genetic feature introduced by the plasmid containing either SOCS1, SOCS3 or the IFN non-responsive SOCS4 in HuH-7 cells. But this connectivity among ISGs shows how important the use of genome-wide gene expression experiments is to understand consequences of genetic mutations that occur during the cultivation of cell lines.
25 years after the introduction of IFNα in the clinics, the mechanism of resistance to IFNα remains a secret. Our project was initiated to describe a link between resistance in cell lines and SOCS proteins. Resistant cell lines with high SOCS expression could be used for screening drug libraries to find SOCS inhibitors that may prolong IFN treatment efficiency and thus reduces dosing interval in patients. However, we did not find high expression of SOCS mRNA in cell lines tested here. The generation of SOCS expressing cell lines enabled closer investigation of their transciptome profiles in response to IFNα treatment. However, concerns about the safety profile of SOCS inhibitors should be first clarified before entering drug development. The deletion of the negative feedback regulator SOCS3 enables excessive STAT3 activation and is associated with increased tumor numbers for example (Rigby *et al.* 2007). Potent SOCS1 antagonists have been described several years ago, for example a JAK2 peptide phosphorylated at Tyr1007 (Waiboci *et al.* 2007). This small molecule exerts broad antiviral activities, synergizes with the IFNγ mimic IFNγ(95-132) at the level of transcription and enhances cellular and humoral immune response (Ahmed *et al.* 2010; Frey *et al.* 2009). Additionally, it shows also inhibitory function against SOCS3 when overexpressed and enhances IFNγ activity (Ahmed *et al.* 2010).

The opposite approach, to treat IFNα resistant HCV infected patients with activated IFNα cascade before treatment or cancer patients with constitutive JAK activation, SOCS agonist may be used to control JAK-STAT signaling. Peptides mimicking SOCS1, tyrosine

kinase inhibitor peptide Tkip or the kinase inhibitory region of SOCS1 (SOCS1-KIR) could be used as inhibitors of JAK2 activation (Waiboci *et al.* 2007). The main difference of the two peptides is that Tkip does inhibit JAK2 autophosphorylation and IFNγ-induced STAT1α phosphorylation, whereas SOCS1-KIR only inhibits STAT1α activation (Waiboci *et al.* 2007).
The use of SOCS targeting drugs is probably limited to a certain subgroup of patients and factors determining the responsibility are needed. In our *in vitro* model, induction of SOCS3 protein expression had no significant effect on gene expression levels arguing for IFNα sensibility in melanoma cells regardless of both the SOCS3 expression and the status of STAT3 activation in the cells.
SOCS1 and *SOCS3* mRNA expression levels are reduced in the HCC region of HCV infected patients and result in hyper-activated STAT3 (Ogata *et al.* 2006). This may be due to *SOCS3* promoter methylation and is true for numerous cancer types including HCC (Weber *et al.* 2005; Niwa *et al.* 2005; He *et al.* 2004). However, reduction in *SOCS* expression levels can also occur without promoter methylation (Yoshida *et al.* 2004). The hyper-activation of JAK-STAT pathway is repressing pro-apoptotic genes and SOCS mimics may overcome resistance to apoptosis in cancer such as HCC (Jarnicki *et al.* 2010). However, application of SOCS mimics may only find application in patients where the IFN response is studied thoroughly since general application could interfere with the constitutive 'weak' IFN signaling which is crucial for a strong response to the cytokine (Taniguchi *et al.* 2001).
In addition to systemic administration of SOCS inhibitors, to stimulate both antiviral or antitumor action of affected cells and cells of the immune system, development of antibody-drug conjugates (ADC) may deliver the inhibitors specifically to cancer cells for example with a HER2 positive phenotype. The first ADC from Roche submitted to the FDA is a similar conjugate: trastuzumab-DM1 is in clinical development; here HER2-antibodies are linked to a chemotherapeutic to increase specific anticancer activity (Lewis Phillips *et al.* 2008; Niculescu-Duvaz 2010). A crucial step in the development of SOCS targeting therapies is in my opinion the monitoring of SOCS levels in patients undergoing a IFNα therapy.

Chapter 3
Epigenetic alterations in colon cancer, cell lines treated with IFNα and knock-out phenotype of a DNA damage response gene involved in epigenetic stability *in vivo*

We have shown different localization of SOCS1 and SOCS3 proteins. Overexpressed SOCS1 is predominantly distributed in the nucleus of IFNα naive cells. However, there is no indication of JAK-STAT modulation by nuclear SOCS1. Recently, the function of nuclear SOCS1 has been linked to IFNα-induced senescence and depends on the formation of SOCS1-p53-ATM complexes (Calabrese *et al.* 2009). The nuclear function can be triggered by ATM DNA damage repair and results in stabilization of activated p53 transcription factor and a prolonged cell cycle arrest. Clarification of the mechanisms that mediate SOCS1 nuclear localization and recruitment to DNA damage sites would be crucial to determine how SOCS1 mediates its tumor suppressor activity. An open question is if mutant SOCS1 proteins that do not localize to the nucleus are potent to inhibit cytokine signaling. Mutants could be generated by mutation of the nuclear localization signal or by insertion of a nuclear export signal.
The interaction of SOCS1 with the DNA damage pathway links this protein to epigenetic activities. Collectively we have found indications that the loss of a gene (Tdg) involved in

DNA damage repair can induce remarkable epigenetic changes in embryonic cells. Furthermore, cell lines treated with cytokines dynamically modify the percentage of DNA mehtylation at unique CpG sites in the promoter of *IFITM3*. This result has to be confirmed for other ISGs and the mechanism of demethylation and the proteins involved in this process have yet to be identified. CpG sites in the promoter sequence of *IFITM3* undergo aberrant methylation in CRC cancer specimens and *SOCS1* CpG island methylation ratio is taken as one factor to classify CRC patients. Therefore, it would be interesting to screen clinical samples for IFNα sensitivity, especially from patients in a therapy with drugs that restore the normal, demethylated state of the *SOCS1* promoter. Arsenic trioxide (A_2O_3) may be used as adjuvant therapeutics in multiple myeloma cells for example by counteracting hypermethylation (Wang *et al.* 2008). In addition, SOCS3 CpG promoter methylation status may be involved in the response rate and overall survival of cancer patients treated with therapeutic CD33 antibodies (Mylotarg®) and the outcome depends on the age of the patients (Middeldorf *et al.* 2010). This suggests that an age related cancer-selective change in CpG methylation patterns of SOCS and tumor suppressor proteins influences the survival of patients. Therefore we suggest to screen cancer patients for their CpG methylation pattern to correlate response rate and overall survival to cancer specific SOCS expression. The costs of such experiments will be marginal compared to the costs resulted from the Mylotarg® withdrawal for example, when combination of CD33 antibodies to chemotherapy resulted in higher death rates and no benefit for the study cohort (SWOG S0106). SOCS screenings may provide an advance in personalized healthcare by reducing risks and raise the benefits from anti-cancer medicines. Therefore, large prospective studies on *SOCS1* and *SOCS3* hypermethylation on response and outcome of anticancer drugs are warranted.
Personally, I recommend publishing raw data generated by microarray assays or deep sequencing in one of the public databases. This allows reusing clinical data and to perform meta-analyzes. This allows further analyzes of clinical trials that lack statistical power to generate valuable data for ongoing research. Further, the data can be validated, used as confirmation of the own data or used to generate new hypotheses in basic research.

References

Ahmed CMI, Dabelic R, Martin JP, Jager LD, Haider SM, Johnson HM. 2010 Jul. Enhancement of antiviral immunity by small molecule antagonist of suppressor of cytokine signaling. J. Immunol. 185(2): 1103-1113.

Ahmed FE. 2006 Jul. Microarray RNA transcriptional profiling: part I. Platforms, experimental design and standardization. Expert Rev. Mol. Diagn. 6(4): 535-550.

Albanesi C, Fairchild HR, Madonna S, Scarponi C, De Pità O, Leung DYM, Howell MD. 2007 Jul. IL-4 and IL-13 negatively regulate TNF-alpha- and IFN-gamma-induced beta-defensin expression through STAT-6, suppressor of cytokine signaling (SOCS)-1, and SOCS-3. J. Immunol. 179(2): 984-992.

Alexander WS, Hilton DJ. 2004. The role of suppressors of cytokine signaling (SOCS) proteins in regulation of the immune response. Annu. Rev. Immunol. 22: 503-529.

Ali S, Nouhi Z, Chughtai N, Ali S. 2003 Dec. SHP-2 regulates SOCS-1-mediated Janus kinase-2 ubiquitination/degradation downstream of the prolactin receptor. J. Biol. Chem. 278(52): 52021-52031.

Androulidaki A, Iliopoulos D, Arranz A, Doxaki C, Schworer S, Zacharioudaki V, Margioris AN, Tsichlis PN, Tsatsanis C. 2009 Aug. The kinase Akt1 controls macrophage response to lipopolysaccharide by regulating microRNAs. Immunity 31(2): 220-231.

Baetz A, Koelsche C, Strebovsky J, Heeg K, Dalpke AH. 2008 Dec. Identification of a nuclear localization signal in suppressor of cytokine signaling 1. FASEB J. 22(12): 4296-4305.

Banninger G, Reich NC. 2004 Sep. STAT2 nuclear trafficking. J. Biol. Chem. 279(38): 39199-39206.

Bartels DJ, Zhou Y, Zhang EZ, Marcial M, Byrn RA, Pfeiffer T, Tigges AM, Adiwijaya BS, Lin C, Kwong AD, Kieffer TL. 2008 Sep. Natural prevalence of hepatitis C virus variants with decreased sensitivity to NS3.4A protease inhibitors in treatment-naive subjects. J. Infect. Dis. 198(6): 800-807.

Bartosch B, Vitelli A, Granier C, Goujon C, Dubuisson J, Pascale S, Scarselli E, Cortese R, Nicosia A, Cosset F. 2003 Oct. Cell entry of hepatitis C virus requires a set of co-receptors that include the CD81 tetraspanin and the SR-B1 scavenger receptor. J. Biol. Chem. 278(43): 41624-41630.

Bekisz J, Baron S, Balinsky C, Morrow A, Zoon KC. 2010 Mar. Antiproliferative Properties of Type I and Type II Interferon. Pharmaceuticals (Basel) 3(4): 994-1015.

Ben-Yair L, Slaaby R, Herman A, Cohen Y, Biener E, Moran N, Yoshimura A, Whittaker J, De Meyts P, Herman B, Gertler A. 2002 Aug. Preparation and expression of biologically active prolactin and growth hormone receptors and suppressor of cytokine signaling proteins 1, 2, 3, and 6 tagged with cyan and yellow fluorescent proteins. Protein Expr. Purif. 25(3): 456-464.

Blumberg BS. 1977 Jul. Australia antigen and the biology of hepatitis B. Science 197(4298): 17-25.

Bluyssen AR, Durbin JE, Levy DE. 1996 Jun. ISGF3 gamma p48, a specificity switch for interferon activated transcription factors. Cytokine Growth Factor Rev. 7(1): 11-17.

Bode JG, Ludwig S, Ehrhardt C, Albrecht U, Erhardt A, Schaper F, Heinrich PC, Häussinger D. 2003 Mar. IFN-alpha antagonistic activity of HCV core protein involves induction of suppressor of cytokine signaling-3. FASEB J. 17(3): 488-490.

Boland CR, Goel A. 2010 Jun. Microsatellite instability in colorectal cancer. Gastroenterology 138(6): 2073-2087.e3.

Bonjardim CA, Ferreira PCP, Kroon EG. 2009 Jan. Interferons: signaling, antiviral and viral evasion. Immunol. Lett. 122(1): 1-11.

Borden EC, Sen GC, Uze G, Silverman RH, Ransohoff RM, Foster GR, Stark GR. 2007

Dec. Interferons at age 50: past, current and future impact on biomedicine. Nat Rev Drug Discov 6(12): 975-990.
Boyle K, Zhang J, Nicholson SE, Trounson E, Babon JJ, McManus EJ, Nicola NA, Robb L. 2009 Mar. Deletion of the SOCS box of suppressor of cytokine signaling 3 (SOCS3) in embryonic stem cells reveals SOCS box-dependent regulation of JAK but not STAT phosphorylation. Cell. Signal. 21(3): 394-404.
Bradbury LE, Kansas GS, Levy S, Evans RL, Tedder TF. 1992 Nov. The CD19/CD21 signal transducing complex of human B lymphocytes includes the target of antiproliferative antibody-1 and Leu-13 molecules. J. Immunol. 149(9): 2841-2850.
Brem R, Oraszlan-Szovik K, Foser S, Bohrmann B, Certa U. 2003 Jun. Inhibition of proliferation by 1-8U in interferon-alpha-responsive and non-responsive cell lines. Cell. Mol. Life Sci. 60(6): 1235-1248.
Brender C, Nielsen M, Röpke C, Nissen MH, Svejgaard A, Billestrup N, Geisler C, Ødum N. 2001. Interferon-alpha induces transient suppressors of cytokine signalling expression in human T cells. Exp. Clin. Immunogenet. 18(2): 80-85.
Brierley I, Pennell S, Gilbert RJC. 2007 Aug. Viral RNA pseudoknots: versatile motifs in gene expression and replication. Nat. Rev. Microbiol. 5(8): 598-610.
Calabrese V, Mallette FA, Deschênes-Simard X, Ramanathan S, Gagnon J, Moores A, Ilangumaran S, Ferbeyre G. 2009 Dec. SOCS1 links cytokine signaling to p53 and senescence. Mol. Cell 36(5): 754-767.
Caraglia M, Marra M, Pelaia G, Maselli R, Caputi M, Marsico SA, Abbruzzese A. 2005 Feb. Alpha-interferon and its effects on signal transduction pathways. J. Cell. Physiol. 202(2): 323-335.
Certa U, Wilhelm-Seiler M, Foser S, Broger C, Neeb M. 2003 Oct. Expression modes of interferon-alpha inducible genes in sensitive and resistant human melanoma cells stimulated with regular and pegylated interferon-alpha. Gene 315: 79-86.
Chatterjee-Kishore M, Kishore R, Hicklin DJ, Marincola FM, Ferrone S. 1998 Jun. Different requirements for signal transducer and activator of transcription 1alpha and interferon regulatory factor 1 in the regulation of low molecular mass polypeptide 2 and transporter associated with antigen processing 1 gene expression. J. Biol. Chem. 273(26): 16177-16183.
Cheng G, Nazar AS, Shin HS, Vanguri P, Shin ML. 1998 Nov. IP-10 gene transcription by virus in astrocytes requires cooperation of ISRE with adjacent kappaB site but not IRF-1 or viral transcription. J. Interferon Cytokine Res. 18(11): 987-997.
Cheon H, Stark GR. 2009 Jun. Unphosphorylated STAT1 prolongs the expression of interferon-induced immune regulatory genes. Proc. Natl. Acad. Sci. U.S.A. 106(23): 9373-9378.
Chon SY, Hassanain HH, Gupta SL. 1996 Jul. Cooperative role of interferon regulatory factor 1 and p91 (STAT1) response elements in interferon-gamma-inducible expression of human indoleamine 2,3-dioxygenase gene. J. Biol. Chem. 271(29): 17247-17252.
Chu P, Yeh C, Hsu NC, Chang Y, Chang J, Yeh K. 2010. Epigenetic alteration of the SOCS1 gene in hepatocellular carcinoma. Swiss Med Wkly 140: w13065.
Coccia EM, Passini N, Battistini A, Pini C, Sinigaglia F, Rogge L. 1999 Mar. Interleukin-12 induces expression of interferon regulatory factor-1 via signal transducer and activator of transcription-4 in human T helper type 1 cells. J. Biol. Chem. 274(10): 6698-6703.
Cormier EG, Tsamis F, Kajumo F, Durso RJ, Gardner JP, Dragic T. 2004 May. CD81 is an entry coreceptor for hepatitis C virus. Proc. Natl. Acad. Sci. U.S.A. 101(19): 7270-7274.
Cortázar D, Kunz C, Saito Y, Steinacher R, Schär P. 2007 Apr. The enigmatic thymine DNA glycosylase. DNA Repair (Amst.) 6(4): 489-504.
Cortázar D, Kunz C, Selfridge J, Lettieri T, Saito Y, MacDougall E, Wirz A, Schuermann D,

Jacobs AL, Siegrist F, Steinacher R, Jiricny J, Bird A, Schär P. 2011 Feb. Embryonic lethal phenotype reveals a function of TDG in maintaining epigenetic stability. Nature 470(7334): 419-423.
Darnell JEJ. 1997 Sep. STATs and gene regulation. Science 277(5332): 1630-1635.
Darnell JEJ, Kerr IM, Stark GR. 1994 Jun. Jak-STAT pathways and transcriptional activation in response to IFNs and other extracellular signaling proteins. Science 264(5164): 1415-1421.
Deblandre GA, Marinx OP, Evans SS, Majjaj S, Leo O, Caput D, Huez GA, Wathelet MG. 1995 Oct. Expression cloning of an interferon-inducible 17-kDa membrane protein implicated in the control of cell growth. J. Biol. Chem. 270(40): 23860-23866.
Del Campo JA, Romero-Gómez M. 2009 Oct. Steatosis and insulin resistance in hepatitis C: a way out for the virus? World J. Gastroenterol. 15(40): 5014-5019.
Díaz MO, Pomykala HM, Bohlander SK, Maltepe E, Malik K, Brownstein B, Olopade OI. 1994 Aug. Structure of the human type-I interferon gene cluster determined from a YAC clone contig. Genomics 22(3): 540-552.
Dickensheets HL, Venkataraman C, Schindler U, Donnelly RP. 1999 Sep. Interferons inhibit activation of STAT6 by interleukin 4 in human monocytes by inducing SOCS-1 gene expression. Proc. Natl. Acad. Sci. U.S.A. 96(19): 10800-10805.
Du P, Kibbe WA, Lin SM. 2007. nuID: a universal naming scheme of oligonucleotides for illumina, affymetrix, and other microarrays. Biol. Direct 2: 16.
Du P, Kibbe WA, Lin SM. 2008 Jul. lumi: a pipeline for processing Illumina microarray. Bioinformatics 24(13): 1547-1548.
Duong FHT, Filipowicz M, Tripodi M, La Monica N, Heim MH. 2004 Jan. Hepatitis C virus inhibits interferon signaling through up-regulation of protein phosphatase 2A. Gastroenterology 126(1): 263-277.
Eilers A, Baccarini M, Horn F, Hipskind RA, Schindler C, Decker T. 1994 Feb. A factor induced by differentiation signals in cells of the macrophage lineage binds to the gamma interferon activation site. Mol. Cell. Biol. 14(2): 1364-1373.
Endo TA, Masuhara M, Yokouchi M, Suzuki R, Sakamoto H, Mitsui K, Matsumoto A, Tanimura S, Ohtsubo M, Misawa H, Miyazaki T, Leonor N, Taniguchi T, Fujita T, Kanakura Y, Komiya S, Yoshimura A. 1997 Jun. A new protein containing an SH2 domain that inhibits JAK kinases. Nature 387(6636): 921-924.
Favre H, Benhamou A, Finidori J, Kelly PA, Edery M. 1999 Jun. Dual effects of suppressor of cytokine signaling (SOCS-2) on growth hormone signal transduction. FEBS Lett. 453(1-2): 63-66.
Fenner JE, Starr R, Cornish AL, Zhang J, Metcalf D, Schreiber RD, Sheehan K, Hilton DJ, Alexander WS, Hertzog PJ. 2006 Jan. Suppressor of cytokine signaling 1 regulates the immune response to infection by a unique inhibition of type I interferon activity. Nat. Immunol. 7(1): 33-39.
Flamm SL. 2003 May. Chronic hepatitis C virus infection. JAMA 289(18): 2413-2417.
Flisiak R, Parfieniuk A. 2010 Jan. Investigational drugs for hepatitis C. Expert Opin Investig Drugs 19(1): 63-75.
Flowers LO, Johnson HM, Mujtaba MG, Ellis MR, Haider SMI, Subramaniam PS. 2004 Jun. Characterization of a peptide inhibitor of Janus kinase 2 that mimics suppressor of cytokine signaling 1 function. J. Immunol. 172(12): 7510-7518.
Fojtova M, Boudny V, Kovarik A, Lauerova L, Adamkova L, Souckova K, Jarkovsky J, Kovarik J. 2007 Jul. Development of IFN-gamma resistance is associated with attenuation of SOCS genes induction and constitutive expression of SOCS 3 in melanoma cells. Br. J. Cancer 97(2): 231-237.
Foser S, Redwanz I, Ebeling M, Heizmann CW, Certa U. 2006 Oct. Interferon-alpha and

transforming growth factor-beta co-induce growth inhibition of human tumor cells. Cell. Mol. Life Sci. 63(19-20): 2387-2396.
Frantsve J, Schwaller J, Sternberg DW, Kutok J, Gilliland DG. 2001 May. Socs-1 inhibits TEL-JAK2-mediated transformation of hematopoietic cells through inhibition of JAK2 kinase activity and induction of proteasome-mediated degradation. Mol. Cell. Biol. 21(10): 3547-3557.
Frey KG, Ahmed CMI, Dabelic R, Jager LD, Noon-Song EN, Haider SM, Johnson HM, Bigley NJ. 2009 Jul. HSV-1-induced SOCS-1 expression in keratinocytes: use of a SOCS-1 antagonist to block a novel mechanism of viral immune evasion. J. Immunol. 183(2): 1253-1262.
Friedman RL, Manly SP, McMahon M, Kerr IM, Stark GR. 1984 Oct. Transcriptional and posttranscriptional regulation of interferon-induced gene expression in human cells. Cell 38(3): 745-755.
Fu XY, Kessler DS, Veals SA, Levy DE, Darnell JEJ. 1990 Nov. ISGF3, the transcriptional activator induced by interferon alpha, consists of multiple interacting polypeptide chains. Proc. Natl. Acad. Sci. U.S.A. 87(21): 8555-8559.
Fu XY, Schindler C, Improta T, Aebersold R, Darnell JEJ. 1992 Aug. The proteins of ISGF-3, the interferon alpha-induced transcriptional activator, define a gene family involved in signal transduction. Proc. Natl. Acad. Sci. U.S.A. 89(16): 7840-7843.
Fujimoto M, Naka T. 2003 Dec. Regulation of cytokine signaling by SOCS family molecules. Trends Immunol. 24(12): 659-666.
Fujita PA, Rhead B, Zweig AS, Hinrichs AS, Karolchik D, Cline MS, Goldman M, Barber GP, Clawson H, Coelho A, Diekhans M, Dreszer TR, Giardine BM, Harte RA, Hillman-Jackson J, Hsu F, Kirkup V, Kuhn RM, Learned K, Li CH, Meyer LR, Pohl A, Raney BJ, Rosenbloom KR, Smith KE, Haussler D, Kent WJ. 2011 Jan. The UCSC Genome Browser database: update 2011. Nucleic Acids Res. 39: D876-82.
Gao J, Morrison DC, Parmely TJ, Russell SW, Murphy WJ. 1997 Jan. An interferon-gamma-activated site (GAS) is necessary for full expression of the mouse iNOS gene in response to interferon-gamma and lipopolysaccharide. J. Biol. Chem. 272(2): 1226-1230.
Garbe C, Peris K, Hauschild A, Saiag P, Middleton M, Spatz A, Grob J, Malvehy J, Newton-Bishop J, Stratigos A, Pehamberger H, Eggermont A. 2010 Jan. Diagnosis and treatment of melanoma: European consensus-based interdisciplinary guideline. Eur J Cancer 46(2): 270-283.
George CX, Samuel CE. 1999 Mar. Characterization of the 5'-flanking region of the human RNA-specific adenosine deaminase ADAR1 gene and identification of an interferon-inducible ADAR1 promoter. Gene 229(1-2): 203-213.
Gingras S, Parganas E, de Pauw A, Ihle JN, Murray PJ. 2004 Dec. Re-examination of the role of suppressor of cytokine signaling 1 (SOCS1) in the regulation of toll-like receptor signaling. J. Biol. Chem. 279(52): 54702-54707.
Giordanetto F, Kroemer RT. 2003 Feb. A three-dimensional model of Suppressor Of Cytokine Signalling 1 (SOCS-1). Protein Eng. 16(2): 115-124.
Glue P, Fang JW, Rouzier-Panis R, Raffanel C, Sabo R, Gupta SK, Salfi M, Jacobs S. 2000 Nov. Pegylated interferon-alpha2b: pharmacokinetics, pharmacodynamics, safety, and preliminary efficacy data. Hepatitis C Intervention Therapy Group. Clin. Pharmacol. Ther. 68(5): 556-567.
Gongora C, Degols G, Espert L, Hua TD, Mechti N. 2000 Jun. A unique ISRE, in the TATA-less human Isg20 promoter, confers IRF-1-mediated responsiveness to both interferon type I and type II. Nucleic Acids Res. 28(12): 2333-2341.
Grandvaux N, Servant MJ, tenOever B, Sen GC, Balachandran S, Barber GN, Lin R, Hiscott J. 2002 Jun. Transcriptional profiling of interferon regulatory factor 3 target genes:

direct involvement in the regulation of interferon-stimulated genes. J. Virol. 76(11): 5532-5539.
Gustafson KS, Ginder GD. 1996 Aug. Interferon-gamma induction of the human leukocyte antigen-E gene is mediated through binding of a complex containing STAT1alpha to a distinct interferon-gamma-responsive element. J. Biol. Chem. 271(33): 20035-20046.
Guyer NB, Severns CW, Wong P, Feghali CA, Wright TM. 1995 Oct. IFN-gamma induces a p91/Stat1 alpha-related transcription factor with distinct activation and binding properties. J. Immunol. 155(7): 3472-3480.
Haan S, Kortylewski M, Behrmann I, Müller-Esterl W, Heinrich PC, Schaper F. 2000 Feb. Cytoplasmic STAT proteins associate prior to activation. Biochem. J. 345 Pt 3: 417-421.
Haan S, Wüller S, Kaczor J, Rolvering C, Nöcker T, Behrmann I, Haan C. 2009 Aug. SOCS-mediated downregulation of mutant Jak2 (V617F, T875N and K539L) counteracts cytokine-independent signaling. Oncogene 28(34): 3069-3080.
Hallen LC, Burki Y, Ebeling M, Broger C, Siegrist F, Oroszlan-Szovik K, Bohrmann B, Certa U, Foser S. 2007 Aug. Antiproliferative activity of the human IFN-alpha-inducible protein IFI44. J. Interferon Cytokine Res. 27(8): 675-680.
Havell EA, Berman B, Ogburn CA, Berg K, Paucker K, Vilcek J. 1975 Jun. Two antigenically distinct species of human interferon. Proc. Natl. Acad. Sci. U.S.A. 72(6): 2185-2187.
He B, You L, Xu Z, Mazieres J, Lee AY, Jablons DM. 2004 May. Activity of the suppressor of cytokine signaling-3 promoter in human non-small-cell lung cancer. Clin Lung Cancer 5(6): 366-370.
Hertzog P, Forster S, Samarajiwa S. 2011 Jan. Systems biology of interferon responses. J. Interferon Cytokine Res. 31(1): 5-11.
Herzer K, Hofmann TG, Teufel A, Schimanski CC, Moehler M, Kanzler S, Schulze-Bergkamen H, Galle PR. 2009 Feb. IFN-alpha-induced apoptosis in hepatocellular carcinoma involves promyelocytic leukemia protein and TRAIL independently of p53. Cancer Res. 69(3): 855-862.
Hoofnagle JH, Peters M, Mullen KD, Jones DB, Rustgi V, Di Bisceglie A, Hallahan C, Park Y, Meschievitz C, Jones EA. 1988 Nov. Randomized, controlled trial of recombinant human alpha-interferon in patients with chronic hepatitis B. Gastroenterology 95(5): 1318-1325.
Hu G, Zhou R, Liu J, Gong A, Chen X. 2010 Jul. MicroRNA-98 and let-7 regulate expression of suppressor of cytokine signaling 4 in biliary epithelial cells in response to Cryptosporidium parvum infection. J. Infect. Dis. 202(1): 125-135.
Hu G, Zhou R, Liu J, Gong A, Eischeid AN, Dittman JW, Chen X. 2009 Aug. MicroRNA-98 and let-7 confer cholangiocyte expression of cytokine-inducible Src homology 2-containing protein in response to microbial challenge. J. Immunol. 183(3): 1617-1624.
Huang Y, Krein PM, Winston BW. 2001 Dec. Characterization of IFN-gamma regulation of the complement factor B gene in macrophages. Eur. J. Immunol. 31(12): 3676-3686.
Huber W, von Heydebreck A, Sültmann H, Poustka A, Vingron M. 2002. Variance stabilization applied to microarray data calibration and to the quantification of differential expression. Bioinformatics 18 Suppl 1: S96-104.
Isaacs A, Burke DC. 1958 Oct. Mode of action of interferon. Nature 182(4642): 1073-1074.
Isaacs A, Lindenmann J. 1957 Sep. Virus interference. I. The interferon. Proc. R. Soc. Lond., B, Biol. Sci. 147(927): 258-267.
Issa J. 2008 Oct. Colon cancer: it's CIN or CIMP. Clin. Cancer Res. 14(19): 5939-5940.
Jarnicki A, Putoczki T, Ernst M. 2010. Stat3: linking inflammation to epithelial cancer - more than a "gut" feeling? Cell Div 5: 14.
Jiang G, Zhong X, Cui Y, Liu W, Tai S, Wang Z, Shi Y, Zhao S, Li C. 2010a Dec. IL-

6/STAT3/TFF3 signaling regulates human biliary epithelial cell migration and wound healing in vitro. Mol. Biol. Rep. 37(8): 3813-3818.
Jiang S, Zhang H, Lu M, He X, Li Y, Gu H, Liu M, Wang E. 2010b Apr. MicroRNA-155 functions as an OncomiR in breast cancer by targeting the suppressor of cytokine signaling 1 gene. Cancer Res. 70(8): 3119-3127.
Kamizono S, Hanada T, Yasukawa H, Minoguchi S, Kato R, Minoguchi M, Hattori K, Hatakeyama S, Yada M, Morita S, Kitamura T, Kato H, Nakayama Ki, Yoshimura A. 2001 Apr. The SOCS box of SOCS-1 accelerates ubiquitin-dependent proteolysis of TEL-JAK2. J. Biol. Chem. 276(16): 12530-12538.
Kanno Y, Kozak CA, Schindler C, Driggers PH, Ennist DL, Gleason SL, Darnell JEJ, Ozato K. 1993 Jul. The genomic structure of the murine ICSBP gene reveals the presence of the gamma interferon-responsive element, to which an ISGF3 alpha subunit (or similar) molecule binds. Mol. Cell. Biol. 13(7): 3951-3963.
Khan KD, Shuai K, Lindwall G, Maher SE, Darnell JEJ, Bothwell AL. 1993 Jul. Induction of the Ly-6A/E gene by interferon alpha/beta and gamma requires a DNA element to which a tyrosine-phosphorylated 91-kDa protein binds. Proc. Natl. Acad. Sci. U.S.A. 90(14): 6806-6810.
Kim JH, Shin SH, Kwon HJ, Cho NY, Kang GH. 2009a Dec. Prognostic implications of CpG island hypermethylator phenotype in colorectal cancers. Virchows Arch. 455(6): 485-494.
Kim K, Lin W, Tai AW, Shao R, Weinberg E, De Sa Borges CB, Bhan AK, Zheng H, Kamegaya Y, Chung RT. 2009b Apr. Hepatic SOCS3 expression is strongly associated with non-response to therapy and race in HCV and HCV/HIV infection. J. Hepatol. 50(4): 705-711.
Kim TK, Maniatis T. 1996 Sep. Regulation of interferon-gamma-activated STAT1 by the ubiquitin-proteasome pathway. Science 273(5282): 1717-1719.
Kirkwood JM, Ibrahim JG, Sondak VK, Richards J, Flaherty LE, Ernstoff MS, Smith TJ, Rao U, Steele M, Blum RH. 2000 Jun. High- and low-dose interferon alfa-2b in high-risk melanoma: first analysis of intergroup trial E1690/S9111/C9190. J. Clin. Oncol. 18(12): 2444-2458.
Kirkwood JM, Strawderman MH, Ernstoff MS, Smith TJ, Borden EC, Blum RH. 1996 Jan. Interferon alfa-2b adjuvant therapy of high-risk resected cutaneous melanoma: the Eastern Cooperative Oncology Group Trial EST 1684. J. Clin. Oncol. 14(1): 7-17.
Koelsche C, Strebovsky J, Baetz A, Dalpke AH. 2009 Aug. Structural and functional analysis of a nuclear localization signal in SOCS1. Mol. Immunol. 46(13): 2474-2480.
Konan KV, Taylor MW. 1996 Aug. Importance of the two interferon-stimulated response element (ISRE) sequences in the regulation of the human indoleamine 2,3-dioxygenase gene. J. Biol. Chem. 271(32): 19140-19145.
Kordula T, Rydel RE, Brigham EF, Horn F, Heinrich PC, Travis J. 1998 Feb. Oncostatin M and the interleukin-6 and soluble interleukin-6 receptor complex regulate alpha1-antichymotrypsin expression in human cortical astrocytes. J. Biol. Chem. 273(7): 4112-4118.
Kotenko SV, Gallagher G, Baurin VV, Lewis-Antes A, Shen M, Shah NK, Langer JA, Sheikh F, Dickensheets H, Donnelly RP. 2003 Jan. IFN-lambdas mediate antiviral protection through a distinct class II cytokine receptor complex. Nat. Immunol. 4(1): 69-77.
Kunz C, Focke F, Saito Y, Schuermann D, Lettieri T, Selfridge J, Schär P. 2009 Apr. Base excision by thymine DNA glycosylase mediates DNA-directed cytotoxicity of 5-fluorouracil. PLoS Biol. 7(4): e91.
Lang R, Pauleau A, Parganas E, Takahashi Y, Mages J, Ihle JN, Rutschman R, Murray PJ.

2003 Jun. SOCS3 regulates the plasticity of gp130 signaling. Nat. Immunol. 4(6): 546-550.
Levy DE, Kessler DS, Pine R, Reich N, Darnell JEJ. 1988 Apr. Interferon-induced nuclear factors that bind a shared promoter element correlate with positive and negative transcriptional control. Genes Dev. 2(4): 383-393.
Lew DJ, Decker T, Strehlow I, Darnell JE. 1991 Jan. Overlapping elements in the guanylate-binding protein gene promoter mediate transcriptional induction by alpha and gamma interferons. Mol. Cell. Biol. 11(1): 182-191.
Lewin AR, Reid LE, McMahon M, Stark GR, Kerr IM. 1991 Jul. Molecular analysis of a human interferon-inducible gene family. Eur. J. Biochem. 199(2): 417-423.
Lewis Phillips GD, Li G, Dugger DL, Crocker LM, Parsons KL, Mai E, Blättler WA, Lambert JM, Chari RVJ, Lutz RJ, Wong WLT, Jacobson FS, Koeppen H, Schwall RH, Kenkare-Mitra SR, Spencer SD, Sliwkowski MX. 2008 Nov. Targeting HER2-positive breast cancer with trastuzumab-DM1, an antibody-cytotoxic drug conjugate. Cancer Res. 68(22): 9280-9290.
Li J, Colovai AI, Cortesini R, Suciu-Foca N. 2000 May. Cloning and functional characterization of the 5'-regulatory region of the human CD86 gene. Hum. Immunol. 61(5): 486-498.
Liao J, Fu Y, Shuai K. 2000 May. Distinct roles of the NH2- and COOH-terminal domains of the protein inhibitor of activated signal transducer and activator of transcription (STAT) 1 (PIAS1) in cytokine-induced PIAS1-Stat1 interaction. Proc. Natl. Acad. Sci. U.S.A. 97(10): 5267-5272.
Lickert H, Cox B, Wehrle C, Taketo MM, Kemler R, Rossant J. 2005 Jun. Dissecting Wnt/beta-catenin signaling during gastrulation using RNA interference in mouse embryos. Development 132(11): 2599-2609.
Lin SM, Du P, Huber W, Kibbe WA. 2008 Feb. Model-based variance-stabilizing transformation for Illumina microarray data. Nucleic Acids Res. 36(2): e11.
Lin W, Choe WH, Hiasa Y, Kamegaya Y, Blackard JT, Schmidt EV, Chung RT. 2005 Apr. Hepatitis C virus expression suppresses interferon signaling by degrading STAT1. Gastroenterology 128(4): 1034-1041.
Linsen SEV, de Wit E, Janssens G, Heater S, Chapman L, Parkin RK, Fritz B, Wyman SK, de Bruijn E, Voest EE, Kuersten S, Tewari M, Cuppen E. 2009 Jul. Limitations and possibilities of small RNA digital gene expression profiling. Nat. Methods 6(7): 474-476.
Liu B, Liao J, Rao X, Kushner SA, Chung CD, Chang DD, Shuai K. 1998 Sep. Inhibition of Stat1-mediated gene activation by PIAS1. Proc. Natl. Acad. Sci. U.S.A. 95(18): 10626-10631.
Lloyd RE, Blalock JE, Stanton GJ. 1983 Sep. Cell-to-cell transfer of interferon-induced antiproliferative activity. Science 221(4614): 953-955.
Lu L, Thai T, Calado DP, Chaudhry A, Kubo M, Tanaka K, Loeb GB, Lee H, Yoshimura A, Rajewsky K, Rudensky AY. 2009 Jan. Foxp3-dependent microRNA155 confers competitive fitness to regulatory T cells by targeting SOCS1 protein. Immunity 30(1): 80-91.
Mallet V, Vallet-Pichard A, Pol S. 2010 Apr. New trends in hepatitis C management. Presse Med 39(4): 446-451.
Masuhara M, Sakamoto H, Matsumoto A, Suzuki R, Yasukawa H, Mitsui K, Wakioka T, Tanimura S, Sasaki A, Misawa H, Yokouchi M, Ohtsubo M, Yoshimura A. 1997 Oct. Cloning and characterization of novel CIS family genes. Biochem. Biophys. Res. Commun. 239(2): 439-446.
Melzner I, Bucur AJ, Brüderlein S, Dorsch K, Hasel C, Barth TFE, Leithäuser F, Möller P. 2005 Mar. Biallelic mutation of SOCS-1 impairs JAK2 degradation and sustains phospho-

JAK2 action in the MedB-1 mediastinal lymphoma line. Blood 105(6): 2535-2542.
Merry C, Barry MG, Mulcahy F, Ryan M, Heavey J, Tjia JF, Gibbons SE, Breckenridge AM, Back DJ. 1997 Mar. Saquinavir pharmacokinetics alone and in combination with ritonavir in HIV-infected patients. AIDS 11(4): F29-33.
Meyer T, Vinkemeier U. 2004 Dec. Nucleocytoplasmic shuttling of STAT transcription factors. Eur. J. Biochem. 271(23-24): 4606-4612.
Meyer T, Vinkemeier U. 2007 Oct. STAT nuclear translocation: potential for pharmacological intervention. Expert Opin. Ther. Targets 11(10): 1355-1365.
Middeldorf I, Galm O, Osieka R, Jost E, Herman JG, Wilop S. 2010 Jul. Sequence of administration and methylation of SOCS3 may govern response to gemtuzumab ozogamicin in combination with conventional chemotherapy in patients with refractory or relapsed acute myelogenous leukemia (AML). Am. J. Hematol. 85(7): 477-481.
Minamoto S, Ikegame K, Ueno K, Narazaki M, Naka T, Yamamoto H, Matsumoto T, Saito H, Hosoe S, Kishimoto T. 1997 Aug. Cloning and functional analysis of new members of STAT induced STAT inhibitor (SSI) family: SSI-2 and SSI-3. Biochem. Biophys. Res. Commun. 237(1): 79-83.
Miyaaki H, Ichikawa T, Nakao K, Matsuzaki T, Muraoka T, Honda T, Takeshita S, Shibata H, Ozawa E, Akiyama M, Miuma S, Eguchi K. 2009 Sep. Predictive value of suppressor of cytokine signal 3 (SOCS3) in the outcome of interferon therapy in chronic hepatitis C. Hepatol. Res. 39(9): 850-855.
Miyoshi H, Fujie H, Moriya K, Shintani Y, Tsutsumi T, Makuuchi M, Kimura S, Koike K. 2004 Jun. Methylation status of suppressor of cytokine signaling-1 gene in hepatocellular carcinoma. J. Gastroenterol. 39(6): 563-569.
Montgomery SB, Griffith OL, Sleumer MC, Bergman CM, Bilenky M, Pleasance ED, Prychyna Y, Zhang X, Jones SJM. 2006 Mar. ORegAnno: an open access database and curation system for literature-derived promoters, transcription factor binding sites and regulatory variation. Bioinformatics 22(5): 637-640.
Moucari R, Asselah T, Cazals-Hatem D, Voitot H, Boyer N, Ripault M, Sobesky R, Martinot-Peignoux M, Maylin S, Nicolas-Chanoine M, Paradis V, Vidaud M, Valla D, Bedossa P, Marcellin P. 2008 Feb. Insulin resistance in chronic hepatitis C: association with genotypes 1 and 4, serum HCV RNA level, and liver fibrosis. Gastroenterology 134(2): 416-423.
Muhlethaler-Mottet A, Di Berardino W, Otten LA, Mach B. 1998 Feb. Activation of the MHC class II transactivator CIITA by interferon-gamma requires cooperative interaction between Stat1 and USF-1. Immunity 8(2): 157-166.
Ndubuisi MI, Guo GG, Fried VA, Etlinger JD, Sehgal PB. 1999 Sep. Cellular physiology of STAT3: Where's the cytoplasmic monomer? J. Biol. Chem. 274(36): 25499-25509.
Nguyen V, Zhang H, Kadakia S, Krolewski JJ [unpublished]. Attenuation of interferon-alpha signaling by SOCS-1 and SOCS-3 [Internet]. [cited 2006 Dec 29]. Available from: http://www.pathology.uci.edu/faculty/jkrolewski/51NguyenSubmitted.pdf
Nguyen VT, Benveniste EN. 2000 Aug. Involvement of STAT-1 and ets family members in interferon-gamma induction of CD40 transcription in microglia/macrophages. J. Biol. Chem. 275(31): 23674-23684.
Niculescu-Duvaz I. 2010 Jun. Trastuzumab emtansine, an antibody-drug conjugate for the treatment of HER2+ metastatic breast cancer. Curr. Opin. Mol. Ther. 12(3): 350-360.
Niwa Y, Kanda H, Shikauchi Y, Saiura A, Matsubara K, Kitagawa T, Yamamoto J, Kubo T, Yoshikawa H. 2005 Sep. Methylation silencing of SOCS-3 promotes cell growth and migration by enhancing JAK/STAT and FAK signalings in human hepatocellular carcinoma. Oncogene 24(42): 6406-6417.
Nomoto S, Kinoshita T, Kato K, Otani S, Kasuya H, Takeda S, Kanazumi N, Sugimoto H,

Nakao A. 2007 Nov. Hypermethylation of multiple genes as clonal markers in multicentric hepatocellular carcinoma. Br. J. Cancer 97(9): 1260-1265.
O'Brien CA, Manolagas SC. 1997 Jun. Isolation and characterization of the human gp130 promoter. Regulation by STATS. J. Biol. Chem. 272(23): 15003-15010.
Ogata H, Kobayashi T, Chinen T, Takaki H, Sanada T, Minoda Y, Koga K, Takaesu G, Maehara Y, Iida M, Yoshimura A. 2006 Jul. Deletion of the SOCS3 gene in liver parenchymal cells promotes hepatitis-induced hepatocarcinogenesis. Gastroenterology 131(1): 179-193.
Ogino S, Kawasaki T, Kirkner GJ, Kraft P, Loda M, Fuchs CS. 2007a Jul. Evaluation of markers for CpG island methylator phenotype (CIMP) in colorectal cancer by a large population-based sample. J Mol Diagn 9(3): 305-314.
Ogino S, Meyerhardt JA, Kawasaki T, Clark JW, Ryan DP, Kulke MH, Enzinger PC, Wolpin BM, Loda M, Fuchs CS. 2007b May. CpG island methylation, response to combination chemotherapy, and patient survival in advanced microsatellite stable colorectal carcinoma. Virchows Arch. 450(5): 529-537.
Okochi O, Hibi K, Sakai M, Inoue S, Takeda S, Kaneko T, Nakao A. 2003 Nov. Methylation-mediated silencing of SOCS-1 gene in hepatocellular carcinoma derived from cirrhosis. Clin. Cancer Res. 9(14): 5295-5298.
Owerbach D, Rutter WJ, Shows TB, Gray P, Goeddel DV, Lawn RM. 1981 May. Leukocyte and fibroblast interferon genes are located on human chromosome 9. Proc. Natl. Acad. Sci. U.S.A. 78(5): 3123-3127.
Pammer J, Reinisch C, Birner P, Pogoda K, Sturzl M, Tschachler E. 2006 Oct. Interferon-alpha prevents apoptosis of endothelial cells after short-term exposure but induces replicative senescence after continuous stimulation. Lab. Invest. 86(10): 997-1007.
Pansky A, Hildebrand P, Fasler-Kan E, Baselgia L, Ketterer S, Beglinger C, Heim MH. 2000 Mar. Defective Jak-STAT signal transduction pathway in melanoma cells resistant to growth inhibition by interferon-alpha. Int. J. Cancer 85(5): 720-725.
Pauli E, Schmolke M, Wolff T, Viemann D, Roth J, Bode JG, Ludwig S. 2008 Nov. Influenza A virus inhibits type I IFN signaling via NF-kappaB-dependent induction of SOCS-3 expression. PLoS Pathog. 4(11): e1000196.
Pearse RN, Feinman R, Shuai K, Darnell JEJ, Ravetch JV. 1993 May. Interferon gamma-induced transcription of the high-affinity Fc receptor for IgG requires assembly of a complex that includes the 91-kDa subunit of transcription factor ISGF3. Proc. Natl. Acad. Sci. U.S.A. 90(9): 4314-4318.
Pedersen IM, Cheng G, Wieland S, Volinia S, Croce CM, Chisari FV, David M. 2007 Oct. Interferon modulation of cellular microRNAs as an antiviral mechanism. Nature 449(7164): 919-922.
Pehamberger H, Soyer HP, Steiner A, Kofler R, Binder M, Mischer P, Pachinger W, Auböck J, Fritsch P, Kerl H, Wolff K. 1998 Apr. Adjuvant interferon alfa-2a treatment in resected primary stage II cutaneous melanoma. Austrian Malignant Melanoma Cooperative Group. J. Clin. Oncol. 16(4): 1425-1429.
Persico M, Capasso M, Persico E, Svelto M, Russo R, Spano D, Crocè L, La Mura V, Moschella F, Masutti F, Torella R, Tiribelli C, Iolascon A. 2007 Oct. Suppressor of cytokine signaling 3 (SOCS3) expression and hepatitis C virus-related chronic hepatitis: Insulin resistance and response to antiviral therapy. Hepatology 46(4): 1009-1015.
Persico M, Russo R, Persico E, Svelto M, Spano D, Andolfo I, La Mura V, Capasso M, Tiribelli C, Torella R, Iolascon A. 2009. SOCS3 and IRS-1 gene expression differs between genotype 1 and genotype 2 hepatitis C virus-infected HepG2 cells. Clin. Chem. Lab. Med. 47(10): 1217-1225.
Petta S, Cammà C, Di Marco V, Alessi N, Cabibi D, Caldarella R, Licata A, Massenti F,

Tarantino G, Marchesini G, Craxì A. 2008 May. Insulin resistance and diabetes increase fibrosis in the liver of patients with genotype 1 HCV infection. Am. J. Gastroenterol. 103(5): 1136-1144.
Pichiorri F, Suh S, Ladetto M, Kuehl M, Palumbo T, Drandi D, Taccioli C, Zanesi N, Alder H, Hagan JP, Munker R, Volinia S, Boccadoro M, Garzon R, Palumbo A, Aqeilan RI, Croce CM. 2008 Sep. MicroRNAs regulate critical genes associated with multiple myeloma pathogenesis. Proc. Natl. Acad. Sci. U.S.A. 105(35): 12885-12890.
Platanias LC, Uddin S, Colamonici OR. 1994 Jul. Tyrosine phosphorylation of the alpha and beta subunits of the type I interferon receptor. Interferon-beta selectively induces tyrosine phosphorylation of an alpha subunit-associated protein. J. Biol. Chem. 269(27): 17761-17764.
Pogribny IP, Starlard-Davenport A, Tryndyak VP, Han T, Ross SA, Rusyn I, Beland FA. 2010 Oct. Difference in expression of hepatic microRNAs miR-29c, miR-34a, miR-155, and miR-200b is associated with strain-specific susceptibility to dietary nonalcoholic steatohepatitis in mice. Lab. Invest. 90(10): 1437-1446.
Porter AC, Chernajovsky Y, Dale TC, Gilbert CS, Stark GR, Kerr IM. 1988 Jan. Interferon response element of the human gene 6-16. EMBO J. 7(1): 85-92.
Poynard T, Yuen M, Ratziu V, Lai CL. 2003 Dec. Viral hepatitis C. Lancet 362(9401): 2095-2100.
Qing Y, Costa-Pereira AP, Watling D, Stark GR. 2005 Jan. Role of tyrosine 441 of interferon-gamma receptor subunit 1 in SOCS-1-mediated attenuation of STAT1 activation. J. Biol. Chem. 280(3): 1849-1853.
Randall G, Panis M, Cooper JD, Tellinghuisen TL, Sukhodolets KE, Pfeffer S, Landthaler M, Landgraf P, Kan S, Lindenbach BD, Chien M, Weir DB, Russo JJ, Ju J, Brownstein MJ, Sheridan R, Sander C, Zavolan M, Tuschl T, Rice CM. 2007 Jul. Cellular cofactors affecting hepatitis C virus infection and replication. Proc. Natl. Acad. Sci. U.S.A. 104(31): 12884-12889.
Rani MRS, Croze E, Wei T, Shrock J, Josyula A, Kalvakolanu DV, Ransohoff RM. 2010 Mar. STAT-phosphorylation-independent induction of interferon regulatory factor-9 by interferon-beta. J. Interferon Cytokine Res. 30(3): 163-170.
Reid LE, Brasnett AH, Gilbert CS, Porter AC, Gewert DR, Stark GR, Kerr IM. 1989 Feb. A single DNA response element can confer inducibility by both alpha- and gamma-interferons. Proc. Natl. Acad. Sci. U.S.A. 86(3): 840-844.
Rico-Bautista E, Flores-Morales A, Fernández-Pérez L. 2006 Dec. Suppressor of cytokine signaling (SOCS) 2, a protein with multiple functions. Cytokine Growth Factor Rev. 17(6): 431-439.
Rigby RJ, Simmons JG, Greenhalgh CJ, Alexander WS, Lund PK. 2007 Jul. Suppressor of cytokine signaling 3 (SOCS3) limits damage-induced crypt hyper-proliferation and inflammation-associated tumorigenesis in the colon. Oncogene 26(33): 4833-4841.
Robertson G, Hirst M, Bainbridge M, Bilenky M, Zhao Y, Zeng T, Euskirchen G, Bernier B, Varhol R, Delaney A, Thiessen N, Griffith OL, He A, Marra M, Snyder M, Jones S. 2007 Aug. Genome-wide profiles of STAT1 DNA association using chromatin immunoprecipitation and massively parallel sequencing. Nat. Methods 4(8): 651-657.
Rogers RS, Horvath CM, Matunis MJ. 2003 Aug. SUMO modification of STAT1 and its role in PIAS-mediated inhibition of gene activation. J. Biol. Chem. 278(32): 30091-30097.
Ronni T, Matikainen S, Lehtonen A, Palvimo J, Dellis J, Van Eylen F, Goetschy JF, Horisberger M, Content J, Julkunen I. 1998 Sep. The proximal interferon-stimulated response elements are essential for interferon responsiveness: a promoter analysis of the antiviral MxA gene. J. Interferon Cytokine Res. 18(9): 773-781.
Roos G, Leanderson T, Lundgren E. 1984 Jun. Interferon-induced cell cycle changes in

human hematopoietic cell lines and fresh leukemic cells. Cancer Res. 44(6): 2358-2362.
Rutherford MN, Hannigan GE, Williams BR. 1988 Mar. Interferon-induced binding of nuclear factors to promoter elements of the 2-5A synthetase gene. EMBO J. 7(3): 751-759.
Sabates-Bellver J, Van der Flier LG, de Palo M, Cattaneo E, Maake C, Rehrauer H, Laczko E, Kurowski MA, Bujnicki JM, Menigatti M, Luz J, Ranalli TV, Gomes V, Pastorelli A, Faggiani R, Anti M, Jiricny J, Clevers H, Marra G. 2007 Dec. Transcriptome profile of human colorectal adenomas. Mol. Cancer Res. 5(12): 1263-1275.
Sasaki A, Yasukawa H, Suzuki A, Kamizono S, Syoda T, Kinjyo I, Sasaki M, Johnston JA, Yoshimura A. 1999 Jun. Cytokine-inducible SH2 protein-3 (CIS3/SOCS3) inhibits Janus tyrosine kinase by binding through the N-terminal kinase inhibitory region as well as SH2 domain. Genes Cells 4(6): 339-351.
Schindler C, Levy DE, Decker T. 2007 Jul. JAK-STAT signaling: from interferons to cytokines. J. Biol. Chem. 282(28): 20059-20063.
Schindler C, Shuai K, Prezioso VR, Darnell JEJ. 1992 Aug. Interferon-dependent tyrosine phosphorylation of a latent cytoplasmic transcription factor. Science 257(5071): 809-813.
Schmid R, Baum P, Ittrich C, Fundel-Clemens K, Huber W, Brors B, Eils R, Weith A, Mennerich D, Quast K. 2010. Comparison of normalization methods for Illumina BeadChip HumanHT-12 v3. BMC Genomics 11: 349.
Scott R, Siegrist F, Foser S, Certa U. 2011 Aug. Interferon-alpha induces reversible DNA demethylation of the interferon-induced transmembrane protein-3 core promoter in human melanoma cells. J. Interferon Cytokine Res. 31(8): 601-608.
Seegert D, Strehlow I, Klose B, Levy DE, Schindler C, Decker T. 1994 Mar. A novel interferon-alpha-regulated, DNA-binding protein participates in the regulation of the IFP53/tryptophanyl-tRNA synthetase gene. J. Biol. Chem. 269(11): 8590-8595.
Shen X, Hong F, Nguyen VA, Gao B. 2000 Sep. IL-10 attenuates IFN-alpha-activated STAT1 in the liver: involvement of SOCS2 and SOCS3. FEBS Lett. 480(2-3): 132-136.
Shi W, Banerjee A, Ritchie ME, Gerondakis S, Smyth GK. 2009. Illumina WG-6 BeadChip strips should be normalized separately. BMC Bioinformatics 10(): 372.
Shimakami T, Lanford RE, Lemon SM. 2009 Oct. Hepatitis C: recent successes and continuing challenges in the development of improved treatment modalities. Curr Opin Pharmacol 9(5): 537-544.
Short JAL. 2009. Viral evasion of interferon stimulated genes. Bioscience Horizons 2(2): 212-224.
Shows TB, Sakaguchi AY, Naylor SL, Goedell DV, Lawn RM. 1982 Oct. Clustering of leukocyte and fibroblast interferon genes of human chromosome 9. Science 218(4570): 373-374.
Shuai K. 2000 May. Modulation of STAT signaling by STAT-interacting proteins. Oncogene 19(21): 2638-2644.
Siegrist F, Certa U. 2008a. Micro RNA Induction by Interferon Alpha and a Potential Role to Interfere with SOCS. 7th Joint Conference – Montréal, Québec, Canada, October 12-16, 2008. Editor: John Hiscott. Medimont International Proceedings: 93-97.
Siegrist F, Certa U. 2008b Sep. Micro RNA induction by interferon alpha and their potential role to interfere in the negative feedback pathway. Cytokine 43(3): 284-285.
Siegrist F, Ebeling M, Certa U. 2009a Oct-Nov. Phylogenetic analysis of interferon inducible transmembrane gene family and functional aspects of IFITM3. Cytokine 48(1-2, SI): 87.
Siegrist F, Ebeling M, Certa U. 2011 Jan. The small interferon-induced transmembrane genes and proteins. J. Interferon Cytokine Res. 31(1): 183-197.
Siegrist F, Scott R, Certa U. 2010 Apr 1. Human tumor cell lines treated with interferon-

alpha-2a [Internet]. [cited 2010 May 15]. Available from: http://www.ncbi.nlm.nih.gov/geo/acc.cgi?acc=GSE21158
Siegrist F, Singer T, Certa U. 2009b Dec. MicroRNA Expression Profiling by Bead Array Technology in Human Tumor Cell Lines Treated with Interferon-Alpha-2a. Biol Proced Online 11: 113-129.
Sims SH, Cha Y, Romine MF, Gao PQ, Gottlieb K, Deisseroth AB. 1993 Jan. A novel interferon-inducible domain: structural and functional analysis of the human interferon regulatory factor 1 gene promoter. Mol. Cell. Biol. 13(1): 690-702.
Smyth GK, Yang YH, Speed T. 2003. Statistical issues in cDNA microarray data analysis. Methods Mol. Biol. 224: 111-136.
Stark GR, Friedman RL, McMahon M, Manly S, Kelly JM, Kerr IM. 1984 Dec. Induction of human mRNAs by interferon. Philos. Trans. R. Soc. Lond., B, Biol. Sci. 307(1132): 227-230.
Stark GR, Kerr IM, Williams BR, Silverman RH, Schreiber RD. 1998. How cells respond to interferons. Annu. Rev. Biochem. 67: 227-264.
Steiner E, Holzmann K, Pirker C, Elbling L, Micksche M, Sutterlüty H, Berger W. 2006 Feb. The major vault protein is responsive to and interferes with interferon-gamma-mediated STAT1 signals. J. Cell. Sci. 119(Pt 3): 459-469.
Stewart WE2. 1980 Oct. Interferon nomenclature recommendations. J. Infect. Dis. 142(4): 643.
Sun BK, Tsao H. 2008 Nov. Small RNAs in development and disease. J. Am. Acad. Dermatol. 59(5): 725-737.
Takahashi S, Doss C, Levy S, Levy R. 1990 Oct. TAPA-1, the target of an antiproliferative antibody, is associated on the cell surface with the Leu-13 antigen. J. Immunol. 145(7): 2207-2213.
Taniguchi T, Takaoka A. 2001 May. A weak signal for strong responses: interferon-alpha/beta revisited. Nat. Rev. Mol. Cell Biol. 2(5): 378-386.
Teodoridis JM, Hardie C, Brown R. 2008 Sep. CpG island methylator phenotype (CIMP) in cancer: causes and implications. Cancer Lett. 268(2): 177-186.
Tessitore A, Pastore L, Rispoli A, Cilenti L, Toniato E, Flati V, Farina AR, Frati L, Gulino A, Martinotti S. 1998 Dec. Two gamma-interferon-activation sites (GAS) on the promoter of the human intercellular adhesion molecule (ICAM-1) gene are required for induction of transcription by IFN-gamma. Eur. J. Biochem. 258(3): 968-975.
Thyrell L, Erickson S, Zhivotovsky B, Pokrovskaja K, Sangfelt O, Castro J, Einhorn S, Grandér D. 2002 Feb. Mechanisms of Interferon-alpha induced apoptosis in malignant cells. Oncogene 21(8): 1251-1262.
Tsuchimoto D, Tojo A, Asano S. 2004. A mechanism of transcriptional regulation of the CSF-1 gene by interferon-gamma. Immunol. Invest. 33(4): 397-405.
Tsukahara T, Kim S, Taylor MW. 2006 Apr. REFINEMENT: a search framework for the identification of interferon-responsive elements in DNA sequences--a case study with ISRE and GAS. Comput Biol Chem 30(2): 134-147.
Ungureanu D, Vanhatupa S, Grönholm J, Palvimo JJ, Silvennoinen O. 2005 Jul. SUMO-1 conjugation selectively modulates STAT1-mediated gene responses. Blood 106(1): 224-226.
Ungureanu D, Vanhatupa S, Kotaja N, Yang J, Aittomaki S, Jänne OA, Palvimo JJ, Silvennoinen O. 2003 Nov. PIAS proteins promote SUMO-1 conjugation to STAT1. Blood 102(9): 3311-3313.
Van der Auwera I, Yu W, Suo L, Van Neste L, van Dam P, Van Marck EA, Pauwels P, Vermeulen PB, Dirix LY, Van Laere SJ. 2010. Array-based DNA methylation profiling for breast cancer subtype discrimination. PLoS ONE 5(9): e12616.

Vanni E, Abate ML, Gentilcore E, Hickman I, Gambino R, Cassader M, Smedile A, Ferrannini E, Rizzetto M, Marchesini G, Gastaldelli A, Bugianesi E. 2009 Sep. Sites and mechanisms of insulin resistance in nonobese, nondiabetic patients with chronic hepatitis C. Hepatology 50(3): 697-706.

Vlotides G, Sörensen AS, Kopp F, Zitzmann K, Cengic N, Brand S, Zachoval R, Auernhammer CJ. 2004 Jul. SOCS-1 and SOCS-3 inhibit IFN-alpha-induced expression of the antiviral proteins 2,5-OAS and MxA. Biochem. Biophys. Res. Commun. 320(3): 1007-1014.

Waiboci LW, Ahmed CM, Mujtaba MG, Flowers LO, Martin JP, Haider MI, Johnson HM. 2007 Apr. Both the suppressor of cytokine signaling 1 (SOCS-1) kinase inhibitory region and SOCS-1 mimetic bind to JAK2 autophosphorylation site: implications for the development of a SOCS-1 antagonist. J. Immunol. 178(8): 5058-5068.

Walsh MJ, Jonsson JR, Richardson MM, Lipka GM, Purdie DM, Clouston AD, Powell EE. 2006 Apr. Non-response to antiviral therapy is associated with obesity and increased hepatic expression of suppressor of cytokine signalling 3 (SOCS-3) in patients with chronic hepatitis C, viral genotype 1. Gut 55(4): 529-535.

Wang M, Zhu Q, Ren Z, Zou L, Dou H, Hu J. 2008 Oct. [Arsenic trioxide induces socs-1 gene demethylation in myeloma cell lines]. Zhongguo Shi Yan Xue Ye Xue Za Zhi 16(5): 1064-1068.

Wang P, Hou J, Lin L, Wang C, Liu X, Li D, Ma F, Wang Z, Cao X. 2010 Nov. Inducible microRNA-155 feedback promotes type I IFN signaling in antiviral innate immunity by targeting suppressor of cytokine signaling 1. J. Immunol. 185(10): 6226-6233.

Wang Q, Miyakawa Y, Fox N, Kaushansky K. 2000 Sep. Interferon-alpha directly represses megakaryopoiesis by inhibiting thrombopoietin-induced signaling through induction of SOCS-1. Blood 96(6): 2093-2099.

Ward SV, Markle D, Das S, Samuel CE. 2002 Aug. The promoter-proximal KCS element of the PKR kinase gene enhances transcription irrespective of orientation and position relative to the ISRE element and is functionally distinct from the KCS-like element of the ADAR deaminase Promoter. J. Interferon Cytokine Res. 22(8): 891-898.

Weber A, Hengge UR, Bardenheuer W, Tischoff I, Sommerer F, Markwarth A, Dietz A, Wittekind C, Tannapfel A. 2005 Oct. SOCS-3 is frequently methylated in head and neck squamous cell carcinoma and its precursor lesions and causes growth inhibition. Oncogene 24(44): 6699-6708.

Weisenberger DJ, Siegmund KD, Campan M, Young J, Long TI, Faasse MA, Kang GH, Widschwendter M, Weener D, Buchanan D, Koh H, Simms L, Barker M, Leggett B, Levine J, Kim M, French AJ, Thibodeau SN, Jass J, Haile R, Laird PW. 2006 Jul. CpG island methylator phenotype underlies sporadic microsatellite instability and is tightly associated with BRAF mutation in colorectal cancer. Nat. Genet. 38(7): 787-793.

Weissmann C, Nagata S, Boll W, Fountoulakis M, Fujisawa A, Fujisawa JI, Haynes J, Henco K, Mantei N, Ragg H, Schein C, Schmid J, Shaw G, Streuli M, Taira H, Todokoro K, Weidle U. 1982 Sep. Structure and expression of human IFN-alpha genes. Philos. Trans. R. Soc. Lond., B, Biol. Sci. 299(1094): 7-28.

Wesoly J, Szweykowska-Kulinska Z, Bluyssen HAR. 2007. STAT activation and differential complex formation dictate selectivity of interferon responses. Acta Biochim. Pol. 54(1): 27-38.

Xu L, Massagué J. 2004 Mar. Nucleocytoplasmic shuttling of signal transducers. Nat. Rev. Mol. Cell Biol. 5(3): 209-219.

Yang G, Xu Y, Chen X, Hu G. 2007 Jan. IFITM1 plays an essential role in the antiproliferative action of interferon-gamma. Oncogene 26(4): 594-603.

Yang J, Stark GR. 2008 Apr. Roles of unphosphorylated STATs in signaling. Cell Res.

18(4): 443-451.
Yasukawa H, Misawa H, Sakamoto H, Masuhara M, Sasaki A, Wakioka T, Ohtsuka S, Imaizumi T, Matsuda T, Ihle JN, Yoshimura A. 1999 Mar. The JAK-binding protein JAB inhibits Janus tyrosine kinase activity through binding in the activation loop. EMBO J. 18(5): 1309-1320.
Yoshida T, Ogata H, Kamio M, Joo A, Shiraishi H, Tokunaga Y, Sata M, Nagai H, Yoshimura A. 2004 Jun. SOCS1 is a suppressor of liver fibrosis and hepatitis-induced carcinogenesis. J. Exp. Med. 199(12): 1701-1707.
Yoshimura A, Naka T, Kubo M. 2007 Jun. SOCS proteins, cytokine signalling and immune regulation. Nat. Rev. Immunol. 7(6): 454-465.
Yoshimura A, Nishinakamura H, Matsumura Y, Hanada T. 2005. Negative regulation of cytokine signaling and immune responses by SOCS proteins. Arthritis Res. Ther. 7(3): 100-110.
Yoshimura A, Ohkubo T, Kiguchi T, Jenkins NA, Gilbert DJ, Copeland NG, Hara T, Miyajima A. 1995 Jun. A novel cytokine-inducible gene CIS encodes an SH2-containing protein that binds to tyrosine-phosphorylated interleukin 3 and erythropoietin receptors. EMBO J. 14(12): 2816-2826.
You M, Yu DH, Feng GS. 1999 Mar. Shp-2 tyrosine phosphatase functions as a negative regulator of the interferon-stimulated Jak/STAT pathway. Mol. Cell. Biol. 19(3): 2416-2424.
Yu CL, Burakoff SJ. 1997 May. Involvement of proteasomes in regulating Jak-STAT pathways upon interleukin-2 stimulation. J. Biol. Chem. 272(22): 14017-14020.
Zeng B, Li H, Liu Y, Zhang Z, Zhang Y, Yang R. 2008 Jul. Tumor-induced suppressor of cytokine signaling 3 inhibits toll-like receptor 3 signaling in dendritic cells via binding to tyrosine kinase 2. Cancer Res. 68(13): 5397-5404.
Zhang J, Randall G, Higginbottom A, Monk P, Rice CM, McKeating JA. 2004 Feb. CD81 is required for hepatitis C virus glycoprotein-mediated viral infection. J. Virol. 78(3): 1448-1455.
Zhao W, Cha EN, Lee C, Park CY, Schindler C. 2007 Jul. Stat2-dependent regulation of MHC class II expression. J. Immunol. 179(1): 463-471.

Acknowledgments

First of all I would like to thank Prof. Ulli Certa for his substance support and mentor-ship, without Ulli all these projects could not get the attention that they needed after all. I hope we will stay in contact and share our intellectual property whenever it's possible. I would also like to thank Prof. Primo Schär for the fruitful collaborations and his personal support and the possibility to be part of many interesting projects from his lab. I am very appreciative of the support from Prof. Markus Rüegg to help me realizing completion of my thesis at the University of Basel although most of the work was done at a pharmaceutical company and for his implicit trust in my work and me.

Special thanks go to Dr. Rachel Scott for her ceaselessly patience with my delight in teasing her endlessly, but of course even more for all her help and the fruitful scientific discussions. I would especially thank Dr. Sylvia Schreiber, the post-doc who supported me most in the interferon research and cheered me up when cytokine research seemed very mysterious to me. My thanks also goes to Dr. Stefan Foser for his support whenever a smart advice was needed. 'Veel dank' also to the youngest kid in our group, Peter Noij for setting up the set for photo-shootings and all the explanation of the nano world.

Cordial thanks to all the other doctors around the lab, especially Laura Burleigh, Heather Hinton, Stefan Kustermann, Cristina Bertinetti-Lapatki, Jean-Christophe Hoflack, Markus Schmitz, Radina Kostadinova, Tobias Heckel and Christian Czech.

I am very thankful for the help *in silico* and *in vivo* from the statisticians and R experts Dr. Guido Steiner, Andreas Buness and Dr. Laurent Essioux and of course the bio-informaticians Dr. Martin Ebeling, Dr. Roland Schmucki, Dr. Laura Badi, Dr. Clemens Broger and Dr. Isabelle Wells.

I like to thank Dr. Laura Suter-Dick, Dr. Thomas Weiser and Dr. Stefan Platz not only for their signatures but also for supporting PhD students at the industry in general.

I got excellent scientific advice from Dr. Antonio Iglesias, Dr. Pia März-Weiss, Prof. Roger G. Clerc and Prof. Horst Blüthmann and would like to thank all the scientists to preserve the scientific spirit in a money ruled environment.

I am very thankful to all people who help me in setting up the environment in both of the labs and for introduction into the working techniques at Roche, especially Yvonne Burki, Monika Wilhelm-Seiler, Adriana Ille, Inga Redwanz, Ursula Nelboeck-Hochstetter, Alexandra Gerber, Sonja Fellert, Erich Kueng, Susanne Fischer, Nicholas Flint, Monika Haiker, Morgane Ravon and Judith Knehr. I would also like to thank Dr. Franziska Böss, Karen Schad, Christine Zihlmann and all the people from non-clinical safety for their nice introduction into toxicology.

I also thank Andrea Stauffer to be so interested in getting my help and patient when accepting it. Furthermore, I am glad to have met other PhD students as Caio Cesar Silva de Castro who gave me the impression of being very happy to work at such an interesting place at Roche and in Basel, Switzerland.

Of course I am very happy to have numerous co-authors who helped me in the enlargement of my publication list and are not listed elsewhere here: Dr. Thomas Singer, Linda C. Hallen, Krisztina Oroszlan-Szovik, Dr. Bernd Bohrmann, Dr. Kaspar Ulrich Truninger, Dr. Jim Selfridge, Teresa Lettieri, Annika Wirz, Angelika L. Jacobs, Eilidh

MacDougall, Prof. Josef Jiricny, Dr. Adrian Bird, Dr. Roland Steinacher.

A special thank goes to all people working for the student course every year and especially, Dr. Patric Urfer, Stefan Weis, Dr. Gregor Dernick, Dr. Adrian Roth, Ashley Hayes and Peter Jani. I am very positive that this collaboration with the University of Basel will continue in my absence (with exception of this year), because there are so many beautiful research topics to investigate on.

I would like to thank the scientists at the University of Basel for their collaboration and impressive discussions: Prof. Dr. Giulio Spagnoli, Dr. Claudia Daubenberger, Dr. Christophe Kunz, Dr. Daniel Cortazar, Dr. Faiza.Noreen, Dr. Yusuke Saito, Dr. David Schürmann, Dr. Eva Herrero Herranz and Dr. Thomas Zeis.

I would like to thank people from Roche to help me on my projects without squeezing a profit from it: Dr. Anne Vogt, Dr. Corinne Ploix, Oliver Partouche and Marc Bedoucha and all the others for explanation of their projects as Dr. Florent Revel, Dr. Raphael Poirier for example. We should not forget that all the work would not be possible without the people that look for the working environment such as Wolfgang Eufe and Markus Sprecher who were always around to help whenever there was a problem in the building.

Of course I would also like to thank all the other people from Roche and mention some other that were always around for a chat: Dr. Tobias Manigold, Dr. Claas Aiko Meyer, Dr. Daniel Breustedt, Dr. Peter Berlepsch, Anke Gehringer, Yolande Lang, Corinne Marfing, Bernard Morand and Cristina Dominguez Almendral or other for the more scientific discussions: Dr. Simon Fletcher, Dr. Daniel Chin, Endre Sebestyen, Dr. Reto Brem and Dr. Helmut Jacobsen.

Many thanks for the mental support from Sandro Gfeller, Veronique Drephal and Robert König, for their continuous acceptance for my visits despite the *limes*, also called river Rhein that separates our pharmaceutical companies.

Thanks go also to my football trainers at the FC Reinach BL, Silvan Aebischer, Alain Schaffter, Jean Schär, Stefan Krebs, Dean Krexa-Brown and Matthias Kaiser for their unremitting confidence in my goal-getter skills and the though physical education and of course all the team-mates for contributing to our success.

Moreover, thanks goes to all friends joining me in watching football games to passivate all my day-to-day problems as well as to all the fellows who made conferences enjoyable occasions, especially Dr. Steve S. Lee, Dr. Anja Langenkamp and Sonja Hänzelmann.

A special thank goes to Dr. Reto von Allmen, Andreas Flury, Dr. Severin Waldis, Dr. Alexander Lämmle, Christoph Burgdorfer, Stefanie Kropf and Marc Bärtschi who hold up my connection to Bern or to the bernese language.

I thank my godparents Anne-Marie Rufer, Heinz Siegrist, Dr. Karl Kläy and to Lotti Mäder, the person almost become godmother of me and the most innocent supporters, my godchilds Nina Siegrist and Aiko Baumgartner and my other niece and nephew Rea and Ilai and my sisters Fräne Siegrist and Daniela Siegrist-Baumgartner.

Of course the biggest gratitude goes to my parents Magdalena Siegrist-Kläy and Alfred Siegrist. There is not enough paper in the world to list all of what they gave to me.

With special intent, the last thank goes to Romy Walser for bringing in the *life* in “Work-Life Balance”.

The Small Interferon-Induced Transmembrane Genes and Proteins

Fredy Siegrist[1], Martin Ebeling[2], Ulrich Certa[1]
[1] Non-Clinical Safety and [2] Computational Biology, F. Hoffmann-La Roche Ltd., Basel, Switzerland.

Abstract

Interferon-induced transmembrane (IFITM) genes are transcribed in most tissues and are with the exception of IFITM5 interferon inducible. They are involved in early development, cell adhesion, and control of cell growth. Most IFITM genes are activated in response to bacterial and viral infections, and the exact host immune defense mechanisms are still unknown. Elevated gene expression triggered by past or chronic inflammation could prevent spreading of pathogens by limiting host cell proliferation. Accordingly, induction in cells with low basal protein levels is sufficient to drive growth arrest and a senescence-like morphology. On the other hand, loss of IFITM levels in cancer is correlated with pronounced malignancy; thus, these genes are considered as tumor suppressors. However, several cancer cells have deregulated high levels of IFITM transcripts, indicating a tumor progression stage where at least one of the interferon-controlled antiproliferative pathways has been silenced. Phylogenetic analyses of the protein coding genomic sequences suggest a single interferon-inducible gene in the common ancestor of rodents and primates. Biological functions studied so far may have evolved in parallel, and functional characterization of IFITM proteins will provide insight into innate immune defense, cancer development, and other pathways.

Introduction

Interferon-stimulated genes (ISG) are abundantly expressed in many different tissue types shortly after administration of interferon (IFN) *in vitro* and *in vivo*. These proteins have multiple functions such as antiviral, antiproliferative responses to stimulants of the immune system. Although several activities are reported for most of the genes, open questions remain concerning the biological function of IFN-activated cascades. Some members of this class have been found significantly downregulated in cancer screenings for metastatic and nonmetastatic melanomas (Brem and others 2001b). The interferon induced transmembrane (*IFITM*) genes *IFITM1*, *IFITM2*, and *IFITM3* (*IFITM1-3*) belong to the family of small ISGs. Its members are induced in response to viral infections (Martensen and Justesen 2004). The IFITM protein levels and their inducibility may play a crucial role in the IFN therapy in hepatitis C infections and in melanoma adjuvant therapy. We assessed the function of *IFITM3*, which encodes the human 1-8U protein, in melanoma cell cultures in an IFN- sensitive cell line (ME-15) (Zhang and others 2006) or in cell line D10 that shows no antiproliferative activity. In the responder line *IFITM3* is induced together with antiproliferative activity, whereas *IFITM3* shows constitutive expression in D10 (Brem and others 2003). IFN-activated antiproliferative signals can be transmitted from cell to cell *in vitro* (Lloyd and others 1983). The molecular basis of this mechanism has not been resolved yet, and a role of IFITM proteins in the transmission of the signals remains to be proven. In addition to the antiproliferative activity, several functions of the 1–8 family members have been proposed, and published interactions are summarized in

Table 1.

Discovery of IFITM and Related Gene Products

The *IFITM* gene family was first identified in a cDNA screen from IFN-treated neuroblastoma cells back in 1984 (Friedman and others 1984). Other members, such as human *IFITM5*, were discovered by genomic homology searches soon thereafter. Upon publication of the first genome drafts from rodents and humans, we realized that the genetics of the *IFITM* family was more complex than expected. Their chromosomal arrangement is not conserved between human, mouse, and rat both in length and in number of genes present in the chromosomal locus (Fig. 1). *IFITM5*, also known as bone restricted IFITM-like (BRIL) protein, is situated upstream of the human 1–8 protein chromosomal locus. The protein has recently been described as bone-specific modulator of mineralization and is significantly expressed neither in immune cells nor by IFN stimulation of sensitive cells (Moffatt and others 2008).

Beside this heterogeneous family we find some considerably conserved proteins, tumor suppressor candidate 5 (TUSC5), and proline-rich transmembrane protein 2 (PPRT2) that are not IFN inducible but share the 2 dominant hydrophobic regions. The TUSC5 shares the CD225 domain and is predominantly expressed in human cultured adipocytes (Oort and others 2007) and was described as a potential tumor suppressor (Konishi and others 2003). The closest relative to TUSC5 is the PRRT2 (Morrison and Farmer 1999). The proposed common function for these 2 proteins is an involvement in cell cycle control.

A small fraction of 14 kDa IFITM-like polypeptides turned out to be much more immunogenic in mice than the predominant lipids present in the electric organ plasma membrane of proteolipid extractions from Torpedo fish (Morel and others 1991). As expected the antibodies obtained recognized preferentially membrane structures and the antigen was postulated to be involved in cell–cell interactions based on the subcellular localization. IFITM-like proteins connected with leukocyte functions were also found in other fish after poly(I:C) stimulation, and *IFITM* is induced in sea urchins following bacterial challenge (Rast and others 2000; Johnson and others 2006; Wan and Chen 2008). The genetic arrangement in fish shows similarities to the human promoter organization with IFN- and immune and stress-related transcription factor binding sites (Johnson and others 2006).

Proteins containing CD225 domains are known from humans to bacteria, and some, but not all, vertebrate genes are IFN inducible. Below we present for the first time a comprehensive analysis on the evolution of 100 *IFITM* genes across several species using a genome-based phylogenetic approach. This allows better understanding of shared properties of IFITM proteins and discrimination of their pleiotropic functions in an evolutionary context.

Amino Acid Conservation and Functional Domains

Our analysis focuses on sequence conservation in vertebrate proteins with clear homology to human and mouse IFITM proteins. About 14–17 kDa proteins were identified in various species in response to pathogen challenge or IFN exposure. The human *IFITM* family was originally found in screens for IFN alpha (IFNα)-inducible genes. The functional importance for developmental processes was assessed in rodents, whereas uterine formation was studied in ruminants. Similar IFN-induced proteins (IIP) were detected in liver of the marble electric ray. We have compiled sequences that share a significant number of amino acid

(AA) similarities with the human and mouse IFITM proteins (Supplementary Table S1).

This set of sequences forms a group of proteins with a conserved CD225 domain and 2 exons encoding transmembrane spanning polypeptides (Fig. 1). The length of proteins included in the current analysis ranges from 102 to 157 AA with median length of 132 AA. The core AAs are highly similar in all sequences, whereas the length and identity of the distal residues is more variable. Among the sequences analyzed, mole salamander proteins have maximum length (157 AA residues), and the nonmammalian proteins show a certain degree of length polymorphism.

For easier interpretation, the AA frequency is shown graphically for BRIL-like, mammalian, and nonmammalian sequences separately in Fig. 2. This classification allows identification of a conserved aspartate-rich domain at the carboxy terminus of BRIL proteins (Fig. 2). The BRIL-specific structure is highly similar to calcium binding domains (Rigden and Galperin 2004) and may be crucial for mineralization of bones. There are some additional IFITM protein domain (IFITMD)-containing proteins. *TUSC5* (IFITMD3) and *PRRT2* (IFITMD1) are the closest relatives of the IFITM family in human code for a CD225 domain and share the position of the single *IFITM* splice site. In *TUSC5*, the first intron and the 3'-untranslated region are larger compared to *IFITM* genes and the mRNA has a second splice site just before the STOP codon. The *PRRT2* gene has an intron before the start codon and the protein has a longer amino terminal domain. In conclusion, all functional CD225 proteins in vertebrates share a single exon–exon splice junction within the highly conserved domain and are probably derived from an early duplication event in the evolution of chordates.

Phylogenetic Analysis Reveals Recent IFITM Gene Duplication

In addition to the ancient gene relationships outlined above, the IFN-inducible *IFITM* family has also significantly evolved much more recently. Human *IFITM* genes all have 2 exons separated by a short intron and are located in a cluster on the left arm of chromosome 11 (11p15.5). *IFITM5* is located upstream of the first 3 *IFITM* genes and apparently lacks any IFN response elements (Fig. 1). The *IFITM* gene structure including a conserved splice site is highly similar in vertebrates. This allows us to estimate when gene duplications such as the recent duplication leading to human *IFITM2* and *IFITM3* occurred.

The exact human gene arrangement is only replicated in the chimpanzee and orangutan genomes. Two *IFITM3*-like genes in the rhesus macaque genome cannot be unambiguously assigned as orthologs to either human *IFITM3* or *IFITM2*. In mouse, the *fragilis* gene cluster is located in the distal arm of chromosome 7 (Lange and others 2003). Four IFN-inducible protein coding genes are contained within a 60 kb region and the organization is entirely different from the human gene arrangement (Fig. 1b). The mouse proteins all have divergent termini and these distal regions may have limited relevance for protein function (Fig. 1a). We have collected sequence information for IFN-inducible *IFITM*-like proteins to calculate the evolutionary distance and relationships (Supplementary Table S1). Each candidate sequence was manually inspected for computational artifacts. For example, in the gorilla genome draft (gorGOR1 at EMBL), sequence gaps masked parts or entire coding exons and interfered with automatic splice site prediction. We excluded genes lacking the highly conserved S(V/T)K–(S/A)RD AA pattern together with a functional splice site in the center. Phylogenetic analysis of 100 *IFITM* like DNA sequences using a maximum likelihood approach (as implemented in the DNAML program of the PHYLIP package) identified separated branches for all *IFITM5* sequences and for mammalian IFN-inducible *IFITM* sequences. Nonmammalian sequences (IIP) are joined to

the branch connecting the *IFITM5* subtree to the rest of the main tree (not shown). Next, we refined the analysis by separating the 2 subfamilies *IFITM1*-3 and *BRIL*. The length of *BRIL* sequences is identical, and therefore full-length coding sequence was analyzed. In contrast, *IFITM* sequences were trimmed to the core region that could be reliably aligned. Bootstrap analysis of the mammalian *IFITM* tree provided unambiguous evidence for a single common ancestor gene before the divergence of the euarchontoglires from the remaining mammalian lineages (Fig. 3). There is only one *BRIL* gene in every species analyzed here, including the less conserved fish BRIL-like sequences (Fig. 3).

The evolutionary distance in *IFITM5* (*BRIL*) sequences is comparable to that found for other genes. In contrast, some of the *IFITM* genes, in particular the rodent *Ifitm6*, show significantly higher sequence divergence (Fig. 3). This property is frequently found in genes that lost evolutionary pressure for maintenance of the AA sequence due to loss of function, or in genes that are under positive selection to adopt a new function. *Ifitm6* and *Ifitm3* are close paralogs with similar expression patterns across tissues except for total bone marrow extracts. *Ifitm6* may have a special function in subsets of immune cells, including macrophages (Smith and others 2006). Mouse *Ifitm7* maps to chromosome 16 and is not part of the cluster on chromosome 7. It has no intron or reported functionality, but there is evidence for it being transcribed and translated, and therefore we have included this special case in the analysis. It was probably retrotranscribed from an *Ifitm1* transcript and has since then not acquired any nonsynonymous mutations or premature stop codons. As a result, this gene can be classified as a retrogen (Sakai and others 2007). The evolutionary analysis of the gene family clearly suggests that human and rodent IFITMs share some functional properties, but the situation is complicated by some obvious species-specific adaption during evolution and unclear orthology relationships.

Copy Number Variations and Pseudogenes

Initially, we screened the available genomic sequence databases for genes with homologous sequences to *IFITM3* to find genes with similar functions, expression patterns, or subcellular localization. Several hits on other human chromosomes, apart from chromosome 11, were detected. However, for none of these loci is there evidence for active transcription, and 4 copies are clearly pseudogenes due to premature stop codons or truncation of the primary sequence. Global genome analyses produced 10, 2, and 1 pseudogenes for *IFITM3*, *IFITM1*, and *IFITM2*, respectively (Zhang and others 2003). This establishes an average of 4.3 pseudogenes per *IFITM* gene and *IFITM3* made it to place 115 in the list of top pseudogene carriers in this analysis (Zhang and others 2003). Pseudogene frequency is relatively high compared to 0.5 pseudogenes per active gene on average.

Processed pseudogenes (PPG), which are retrotransposed copies of gene transcripts, have been regarded as junk or selfish DNA for a long time. The ribosomal RNA and olfactory receptor genes are the main groups of pseudogenes in our genome. Ribosomal RNA genes contribute one-third of known pseudogenes and contain no introns. Olfactory receptor genes represent another third; these are non-PPG. In addition, genes involved in immune response account for about 10% of the total (Zheng and others 2007). IFN class I pseudogenes were already recognized decades ago (Henco and others 1985). The genomic locus contains 13 pseudogenes and 17 functional IFN genes (Chen and others 2004). PPG and duplicated pseudogenic fragments are expressed in most tissues, including the germ line. They have small coding sequences (400–900 bp) and have GC contents below 53%. IFITM transcripts share the first 2 of these common properties with a

coding sequence length of 378–402 bp, but their GC content is 55%–59%. In addition to retrotransposition in the genome, exact copies of *IFITM* genes (probably originating from DNA repair events) represent an additional source involved in the generation of *IFITM* gene heterogeneity. Comparisons of individual human genomes identified hundreds of copy number variations in coding genes, including *IFITM1* (Redon and others 2006). The copy number is in normal range for *IFITM2/3* and *IFITM5*, but twice as high for *IFITM1* (3.4–4.1). However, the copy numbers of *IFNα* genes outrange it by far with values up to 11.3 copies of *IFNA7* for instance (Alkan and others 2009). Evidence for the presence of pseudogenes originating from *IFITM* genes was found already around the time of the first IFN pseudogene publication. In Northern blot experiments with 1–8 complementary DNA hybridized to multiple mRNAs between 650 and 900 nucleotides (Friedman and others 1984; Kelly and others 1985). This finding suggests transcription of some PPGs or else variable transcription of *IFITM1* and *IFITM*2/3. PPGs have few or no reported expressed sequence tags and proteins have not been detected. Therefore, *IFITM*-derived PPGs are considered to be nonfunctional (Lange and others 2003).

Both the origin and the function of transcribed PPG remain unclear, but they may influence cell cycle processes through interference in *IFITM* translation or transcription. Some pseudogene-derived small interfering RNAs are active in the regulation of gene expression during embryogenesis (Tam and others 2008). However, no *IFITM* homologous RNA sequence has been identified in screens for pseudogene derived RNAs involved in this process (Watanabe and others 2008). Therefore, *IFITM*-like PPGs are probably not involved in RNAi control of development and there is no evidence for interference on *IFITM* translation after infections.

This raises the question why there is such a high number of pseudogenes and what is their origin. IFITM proteins are abundant in germ cells and this could enable random integration of *IFITM* retropseudogenes in the genome. Another explanation is that *IFITM* transcripts have been induced by viral infection and subsequently integrated by viral reverse transcriptase in the genome (Brierley and others 2007). The best match to this recognition pattern for genomic integration is found in *IFITM5* mRNA but not in *IFITM3*, the template of most IFITM-like PPGs (http://pseudogenes.org) (Zhang and others 2003). Note that this event requires viral infection in germ cells. Therefore, random integration of *IFITM* transcripts in the genome of germ cells or their progenitors currently appears more plausible. Random integration of active genes that encode antiproliferative proteins is posing a threat to the organism and the copies are found to undergo rapid inactivation. *Ifitm7*, for example, has recently been retrotranscribed from *Ifitm1* in mice and has low transcriptional activity. The *Ifitm6* sequence is most closely related to the one of *Ifitm3* but has a much higher overall divergence compared to other members of the family and is not present in primate genomes.

The human *IFITM*2 and *IFITM3* genes are very closely related and have been treated as a copy number variation (Alkan and others 2009). Copy number varies not only in inter-species comparisons but also within human individuals (Zhang and others 2009). The *IFITM* gene locus contains sequence elements that may promote duplication events. *IFITM1* is flanked by 2 inverted repeats of 1672 bp length each (Fig. 1b). The element consists of a unique CpG sequence in the core and an unspecific LTR/ERV1 repeat with only 1 bp mismatch between the 2 copies in the human reference sequence (NCBI Build 36.1). The core of this element has a length of 736 bp and represents potential recombinogenic inverted sequences (PRIS) (Flores and others 2007). The PRIS are oriented in opposite direction and are thus potential targets for nonallelic homologous recombination, which could give rise to duplications and deletions of the *IFITM1* locus.

Comparable PRIS have been found to be inverted at high frequency in human somatic cells (Flores and others 2007). *IFITM1* inversions could lead to chromosomal rearrangements nearby and affect the inducibility of adjacent IFN-inducible genes. There are other marks of genetic rearrangements in this locus such as a tandem duplication in the 3'-untranslated region of *IFITM2* (Lewin and others 1991).

Promoter Elements Stimulated by IFNs and Alternative Regulation

The main feature that discriminates these genes is the response of human *IFITM1* and *IFITM2/3* genes to IFN gamma (IFNγ) and IFNα stimulation. Thus, promoter analysis may reveal clues that explain the differential activation. After binding of IFNα to the receptor, signaling is initiated by receptor dimerization and recruitment of Janus kinases. Subsequent steps involve phosphorylation of these kinases and receptors as well as phosphorylation and dimerization of the signal transducers and activators of transcription (STATs). Activated STAT1 dimers form IFNγ-activated transcription factor and STAT1, STAT2, and IRF9 form the initial activator complex termed ISGF3 (ISG factor 3). ISGs have specific upstream promoter elements known as interferon stimulated response element (ISRE) and gamma-activated sequence, which are targets of ISGF3 and activated STAT1 dimers, respectively.

Here we will focus on the most relevant ISRE binding-site for ISGF3 “GGAAAN(N)GAAAC” (Lewin and others 1991), and other motifs were omitted for clarity (Meraro and others 2002). RNA protection assays showed that *IFITM1* and *IFITM3* are inducible by IFNα or IFNγ signaling (McKendry and others 1991). All IFN response motifs are in proximity of the core promoter and the transcriptional start site. In addition, the recognition matrix tolerates single nucleotide insertion without significant loss in response to IFNs (Tanaka and others 2004). Modern computational search algorithms using iterative refinement of hidden Markov models detect potential ISGF3 binding sites with reliability and accuracy (Tsukahara and others 2006). Combination of relaxed motive searches with microarray data collections confirm that essential all *IFITM* genes regardless of mouse or human respond to type I or II IFNs with the exception of *IFITM5* (Samarajiwa and others 2009).

In relatively a recent duplication event of IFN-regulated *IFITM* genes the conserved ISRE evolved independently leading to differential responses to class I or II IFNs (Kelly and others 1985). All 3 human *IFITM* genes contain ISRE elements (Lewin and others 1991) and the *IFITM1* promoter has a 17 bp insertion in the corresponding position that contains 2 gamma-activated sequence elements “CTTAAGAGAAA” and “CTTCTGAGAAA,” which would explain inducibility by IFNγ.

IFN responsive sites have different relative positions in the rodent *IFITM* genes. ISREs are immediately adjacent to the *Ifitm3* and *Ifitm6* transcriptional start sites and not detectable in the core promoter of *Ifitm1*, but each mouse gene can be regulated by IFNs (Samarajiwa and others 2009). This indicates that an ISRE is not necessarily required in the core promoter for IFN responsiveness. Some potential enhancer elements have been identified in some distance to *Ifitm1* in mice (Lange and others 2003). They may confer IFN responses by long-range interactions between regulatory elements, the so-called remote enhancers that are involved in the formation of chromatin loops in response to IFN beta (IFNβ), for example (Nolis and others 2009). IFN-induced gene expression depends strongly on regulation by chromatin remodeling, and Brahma-related gene 1 (BRG1) is a component of the chromatin-remodeling complex SWI/SNF, which interacts with STAT2. This interaction is required for IFNα-induced *IFITM1* expression, suggesting an important role of this epigenetic mechanism in regulation *IFITM* genes and other ISGs (Huang and

others 2002). BRG1 and Brahma form together with BRG1-associated factors the SWI2-SNF2 complex. This complex recruits TEAD1 resulting in *IFITM3* gene transcription (Cuddapah and others 2008). Further, this complex is constitutively associated with the *IFITM3* promoter *in vivo* and is involved in chromatin-remodeling during IFNα and IFNγ-stimulated gene induction (Liu and others 2002; Ni and others 2005). BRG1-associated factors complex enables binding of transcription factor SP1 to its cognate site, which is crucial for efficient IFN-stimulated gene transcription (Ni and others 2005; Nolis and others 2009). This suggests that the BRG1-containing SWI/SNF complex acts as co-activator of ISGF3, SP1, TEAD1, and CTNNB1 in the modulation of *IFITM* gene expression. In addition, CTNNB1 and bone morphogenetic protein 2 and 4 signaling is able to control the level of expression of *IFITM* genes in mouse embryonic germ cells (Saitou and others 2003; Lickert and others 2005; Young and others 2010). Aside from that, phosphorylation of p38 mitogen-activated protein kinase and activation of Akt via mTOR/p70 is required for efficient *ISG15* ISRE promoter regulation and seems to be involved in general IFN type I regulation (Kaur and others 2008). Moreover, ionizing radiation can induce *IFITM1* transcripts probably through upregulation of inactive STAT1 molecules (Clave and others 1997; Tsai and others 2007). Taken together, several pathways and mechanisms control *IFITM* transcription and tissue-specific expression during development.

Interactions in Adhesion and Receptor Complexes

IFITM1 associates in many human cell types with the cell surface antigen CD81 (Takahashi and others 1990; Bradbury and others 1992; Deblandre and others 1995). CD81 is expressed in a variety of tissues and cancers such as melanoma, and CD81-targeting functional antibodies have adhesive and antiproliferative properties (Oren and others 1990). The IFITM1/CD81 complex is involved in the β1-integrin-mediated adhesion to extracellular matrix proteins (Behr and Schriever 1995) and interacts with the B-lymphocyte antigen (CD19)/complement component receptor 2 (CR2) signal transduction complex (Tedder and others 1994). Antibodies against IFITM1 (αLeu-13) trigger homotypic aggregation of T cells (Chen and others 1984) and have an antiproliferative effect in leukemic B cells (Evans and others 1990, 1993). Therefore, IFITM proteins contribute to cell adhesion and growth control in lymphocytes and other cell types (Martensen and Justesen 2004). The CD81 interaction of Ifitm1 and Ifitm3 has also been shown in mice (Smith and others 2006). A role of Ifitm3 in cell adhesion seems to be important in rat and mice where the protein contributes to the organization of mammary glands and the germ cell niche, respectively (Zucchi and others 1998; Saitou and others 2002). Ifitm3 (Rat8) is involved in epithelial cell differentiation (Zucchi and others 1998) and coimmunoprecipitates with Fyn, a membrane-associated tyrosine kinase involved in cell cycle control (Zucchi and others 2004). The adhesive properties are partially based on an interaction of Ifitm3 with the extracellular matrix glycoprotein *osteopontin* (Opn) also known as secreted phosphoprotein 1 (El-Tanani and others 2010). Opn interacts with b1-integrins and is involved in the anchoring of hemopoietic stem cells within the endosteal niche as well as in their transmarrow migration. In addition Opn forms a complex with fibronectin and collagen within the extracellular matrix (Haylock and Nilsson 2006). Recombinant overexpression of IFITM3 in benign Rama-37 cells inhibits colony formation, cell adhesion, and cell invasion, whereas inhibition of IFITM3 in noninvasive cells enhances cell invasion (El-Tanani and others 2010).

Involvement in Embryonic Development

Ifitm3 (fragilis protein) is a very early germline marker and has proposed functions in primordial germ cell (PGC) homing in mice. Single-cell analysis of differential gene expression between founder PGCs and their somatic neighbors at the embryoid bodies stage identified *fragilis* (*Ifitm3*) and *stella* (*Dppa3*) as genes strongly and specifically expressed in PGCs (Saitou 2009). *Ifitm3* marks the onset of germ cell competence in the epiblast of pregastrula-stage mouse embryos (Tanaka and Matsui 2002). *In vivo*, *Ifitm3* levels start to increase in about 20 cells within the posterior proximal epiblast in late streak/early bud stage (E7.0–E7.5) embryos (Saitou and others 2002), and these cells undergo proliferation and migrate to the gonads. These results indicate that IFITM proteins are partial inhibitors of cell proliferation in pluripotent cells. *Ifitm1* and *Ifitm3* are differently expressed in migratory PGCs and it has been suggested that Ifitm1 is required for PGC transition from mesoderm into endoderm. Ifitm3 is sufficient to confer autonomous PGC-like homing properties to somatic cells, an effect that was shown to be mediated by the N-terminal extra-cellular domain (Tanaka and Matsui 2002; Tanaka and others 2005). In addition to PGCs, Ifitm genes are expressed in pluripotent embryonic stem cells and mice with RNAi-mediated reduced levels of *Ifitm1* have a phenotype resembling Wnt mutants Thus, it appears that Ifitm1 is a key mediator of the Wnt response during gastrulation regulating epithelialization of the somites (Lickert and others 2005). In contrast to transient knockdowns of *Ifitm1*, deletion of the entire locus on chromosome 7 has no obvious effect on embryonic development, viability, or fertility (Lange and others 2008). These obviously conflicting data require further clarification until final conclusions can be drawn.

Antiproliferative Signaling and Antiviral Activities

The best documented function of proteins containing the conserved CD225 domain (such as the IFITM family) is antiproliferative and in some cases apoptotic activity, which can be enhanced by IFNs (Gutterman 1994). IFN-mediated proliferation control can be transmitted through administration of a 17 kD protein fraction from IFNβ-treated cells (Hillman and others 1987; Deblandre and others 1995). Functional antibodies against these peptides can activate antiproliferative signaling pathways through binding of IFITM1 complexes on the cell surface (Evans and others 1990, 1993; Takahashi and others 1990; Bradbury and others 1992). We have shown previously that overexpression of IFITM3 inhibits proliferation of IFN-sensitive melanoma cells (Brem and others 2003). Silencing of IFITM1 markedly reduced the antiproliferative action of IFNγ and IFITM1 expression leads to enhanced tumor suppressor protein 53 (p53) signaling with no effect on cell cycle progression in p53-deficient cells (Yang and others 2007). Cessation in cell growth acts through inhibition of extracellular signal-regulated kinases following activation of the mitogen-activated protein kinase p53 pathway (Xu and others 2009). IFNγ activates p53 instantly through signaling of the ATM DNA damage pathway, whereas IFNα has delayed activity in this experimental system (Kim and others 2009). This is in accordance with delayed *IFITM1* induction by IFNα compared to *IFITM3* and in contrast to rapid inducibility by IFNγ. IFN-driven activation of p53 changes the morphology of cultured cells to a senescence-like stage (Siegrist and others 2009b) with distinct large flattened morphology (Kim and others 2009). We have observed a similar morphology upon recombinant expression of IFITM3 proteins together with an arrest of cell proliferation. In contrast, overexpression of IFITM2 leads to a rounded appearance typical for an apoptotic state (Joung and others 2003). FITM2 expression leads to G1 and subG1 phase arrest, which is independent on p53 activation (Daniel-Carmi and others 2009). In contrast, the IFITM1-induced G1 phase arrest is p53 dependent (Xu and others 2009). Like IFNγ, IFNβ is able to activate the ATM DNA damage pathway together with high levels of reactive oxygen

species, which results ultimately in p53-mediated senescence (Moiseeva and others 2006). Production of reactive oxygen species is affected by the IFITM3 interaction partner pre-B-cell colony-enhancing factor (Zhang and others 2008).

These findings suggest that additional pathways apart from the canonical Janus kinase (JAK)/STAT are involved in cellular senescence driven by IFITM proteins. Further, the antiproliferative action of IFITM proteins is limited in pluripotent cells and not effective in certain tumors. Elevated *Ifitm3* levels induced by nuclear transfer in bovine embryos had no effect on cell division progress, indicating a specific role for Ifitm proteins in early development (Smith and others 2007). Cell cycle time increases from 6 to 16 h in mouse nascent germ cells with fragilis expression, compared to the nonexpressing surrounding somatic cells (Saitou and others 2002). In differentiated tissue such as mouse fibroblasts, the growth rate is significantly decreased in presence of Ifitm3 (Ropolo and others 2004). In addition to the cellular functions showcased above, IFN signaling is predominantly important for effective immune responses and host defense.

Viruses such as cytomegalovirus and herpes simplex are capable of inducing IFITM gene expression (Zhu and others 1997, 1998; Navarro and others 1998; Nicholl and others 2000; Zhao and others 2009). Despite the efforts to find evidence for antiviral activity of IFITM family members, most results today are either ambiguous or not reproducible. Mouse cells are less permissive for vesicular stomatitis virus infection when human IFITM1 is expressed, demonstrating that IFITM family members can possess intrinsic antiviral activity across species (Alber and Staeheli 1996). IFITM3 expression results in reduced hepatitis C viral RNA levels, indicating an association with the antiproliferative activity of the polypeptide (Zhu and Liu 2003). Only recently, genomewide RNAi screenings have identified IFITM3 as restriction factor for influenza and flaviviruses by inhibiting viral infection at cell entry (Brass and others 2009). Further evidence for the inhibition of flaviviruses by IFITM3 and IFITM2 proteins suggests disruption of viral molecular events before translation of viral genomic RNA (Jiang and others 2010). Variable activity against pseudoviruses coated with envelope proteins from diverse RNA-viruses suggests that rather the properties of envelope proteins than the nature of the viral genome determines the antiviral activity of IFITM proteins. However, blockage of retroviruses, positive- and negative-strand RNA viruses has been detected so far, and activity against DNA viruses needs further examination. However, a transmission of antiviral signals to noninfected cells by IFITM has not been demonstrated in these studies.

Pathogen infections lead to long-lasting upregulation of IFITM proteins, suggesting a function of IFITM3 in host defense. In addition, IFITM3 might be a suitable biomarker for past or chronic inflammation. *IFITM* transcripts have higher levels in certain neurological disorders, indicating an environmental insult during brain development (Arion and others 2007).

Tissue Distribution and Localization

The subcellular localization of IFITM proteins varies in different tissues and cell types. Targeting of the proteins to their site of function probably depends on cellular factors that modify the proteins post-translationally or on protein interactions specific for transport vehicles such as caveolin vesicles (Xu and others 2009). Relocation to small vesicles is important for inhibition of virus entry (Brass and others 2009). IFITM1 localization is cell type dependent and various techniques have detected IFITM proteins in proximity to the endoplasmatic reticulum, the Golgi apparatus, or associated with the plasma membrane (Alber and Staeheli 1996; Zucchi and others 2004; Yang and others 2007). In melanoma

cell lines IFITM3 co-localizes with major histo-compatibility complex, class I (MHC-1) and tetraspanins of the cell membrane and exosomes were considered as transport rafts (Brem and others 2003). The membrane-bound fraction of IFITMs interacts with several other membrane proteins involved in adhesion and transmission of proliferation control signals (Table 1).

IFITM genes are transcribed in most adult tissues and the expression levels differ in specific cell types of the same organ (Yamashita and others 2000; Seo and others 2010). During development gene expression changes and is associated with the migratory behavior of germ cells (Saitou and others 2003; Lickert and others 2005; Tanaka and others 2005; Smith and others 2007). In melanoma cells, IFITM containing small vesicles like exosomes or the soluble form of IFITM proteins are found in culture supernatants (Siegrist and others 2009a). IFITM proteins can be processed by an unknown mechanism to be targeted for secretion or to change the subcellular localization. This mechanism probably involves cleavage of a small peptide fraction at both IFITM3 proteins ends and efficient translocation may depend on processing at the amino terminus (Siegrist and others 2009a). Tagged IFITM proteins for instance can display these degradation or modification processes occurring in 6xHis-tagged IFITM1, Ifitm6, and 3xflag-tagged BRIL proteins (Alber and Staeheli 1996; Smith and others 2006; Moffatt and others 2008).

This cleavage process is limiting localization studies because some cleavage products of IFITM fusion proteins are undetectable. In addition, the IFITM processing may regulate secretion of IFITM3 proteins and enable the transmission of antiproliferative responses in IFNα-sensitive cells or tissues (Brem and others 2003). However, an active or passive transfer of apoptotic or antiviral activity *in vitro* can be excluded based on recent experiments (Brass and others 2009; Daniel-Carmi and others 2009). A crucial step to discover an antiproliferative or antiviral signaling across cells is the identification of this processing factor. Signal transmission may involve immune cells or gap junction formation for communication apart from unknown signal transducers. Transgenic flies (*Drosophila melanogaster*) expressing human IFITM3 proteins showed no developmental defects, although the speckled subcellular localization resembled the pattern in human cells (unpublished results). This indicates that IFITM protein function requires interaction with proteins that are specific for mammalian organisms. Serial deletions or site-directed mutagenesis may lead to the identification of modified AA or sites required for protein interactions important for *IFITM* functions provided the protein scaffold is maintained after mutagenesis.

IFITM Antiproliferative and Antiviral Signaling and Discrimination of Subtypes

The antiproliferative and antiviral activity is shared between all IFITM proteins, but the efficiency can vary among different IFITMs, tissues, and cell types. A conserved function of all IFITM polypeptides is the apparent control of cell proliferation or apoptosis (Table 1). IFITM1 for instance interacts with the p53 signaling cascade, resulting in partial cell cycle arrest (Xu and others 2009). In contrast, the pro-apoptotic function of IFITM2 is largely p53 independent although decreased efficiency has been noted in p53-deficient rodent fibroblasts cells (Daniel-Carmi and others 2009). IFITM3 is the most potent inhibitor of viral entry relative to IFITM2 and IFITM1, which points to functional differentiation of protein subtypes (Brass and others 2009; Jiang and others 2010). These different activities may reside in the amino termini that are specific for IFITM2 and IFITM3 and may direct specific protein interactions for example to interfere with virion uptake or uncoating. The next steps in unveiling the mechanism will involve the identification of IFITM-interacting proteins contributing to the innate antiviral activity.

IFITM Expression and Implications in Cancer Development

IFITM expression levels are different from control tissues in many cancer samples, and upregulation and down-modulation occurs depending on the cancer type and may occur together with mutations. There are at least 5 variations in the *IFITM3* promoter consisting of repeated sequences (Seo and others 2010). In addition, single-nucleotide polymorphisms as well as insertions are frequent in the *IFITM*2 coding region (Daniel-Carmi and others 2009). This indicates either high genetic variability among humans or an enhanced somatic mutation rate in cancer necessary to deactivate the gene product. IFITM proteins have properties of tumor suppressors because they can control the cell cycle and they are modulated even before tumor formation. *IFITM* expression abnormalities occurs often in the transition from normal to premalign stages and are associated with viral infections, lesions, or inflammation.

The histological activity of hepatic steatosis in patent with chronic hepatitis C correlates with *IFITM1* levels for example (Younossi and others 2009). Further, IFITM proteins are also associated with inflammatory diseases such as ulcerative colitis and inflammatory bowel disease (Hisamatsu and others 1999; Wu and others 2007; Seo and others 2010). In addition, *IFITM* genes have been associated with the cause of cytopenia in preleukemic conditions (Pellagatti and others 2006). In this case the proliferation inhibitory action of IFITM proteins may cause ineffective hematopoiesis by promoting apoptosis or senescence. In the early stages of oncogenesis IFITM abundance may promote selection of cells that are insensitive to tumor suppressor pathways like p53, but conclusive proof for the involvement of IFITM proteins in tumor formation is still missing. Elevated *IFITM* levels are found in adenoma compared to adjacent normal mucosa and they are even higher in colon carcinoma (Zhang and others 1997; Andreu and others 2006; Tirosh and others 2007; Fan and others 2008; Nibbe and others 2009; Ma and others 2010). Cancer cells insensitive to the antiproliferative action of IFITMs are expressing higher amount of the molecule, which implies a benefit for the tumor by escaping the immune surveillance. Gastric cancer cell lines with elevated IFITM1 protein levels escape natural killer cell recognition (Yang and others 2005). Further, *IFITM3* levels are upregulated in the invasive stage of breast carcinoma (Abba and others 2004) and overexpression of IFITM1 promotes invasiveness of tumor cells *in vitro* (Yang and others 2005; Hatano and others 2008). Expression of IFITM proteins can also be reduced in certain tumor types and *IFITM1* transcription is repressed in most brain samples from astrocytoma patients (Huang and others 2000). Further, *in vitro* tumorigenesis by ras transformation results in downregulation of *IFITM* transcripts in rodent cells (Zuber and others 2000; Brem and others 2001a). Cells with deactivated IFITM function are probably selected during their cultivation and the co-expression of oncogenic transformation factors myc and ras together with IFITM2 results in diminished colony formation (Daniel-Carmi and others 2009). Consistent with these results, IFITM knockdown promotes cancer growth *in vivo* (Yang and others 2007).

The tumor suppressive *in vivo* effect may depend on the translocation of IFITM-derived peptides to exosomes that are involved in the transport of cancer antigens to dendritic cells. The high immunogenic potential of IFITM peptides supports this theory and they may act as tumor-associated antigenic peptides in MHC-1 presenting cells (Tirosh and others 2007). Depletion of IFITM expression can change the adhesive properties of cancer cells and indicates malign-formation in some cancers. The assumption that IFITM expressing cells cannot escape cellular structures in benign tumors is based on the involvement of Ifitm3 in the formation of specific dome structures by breast adenocarcinoma cells (Zucchi and others 1998). Subsequently, the correlation of IFITM reduction with cancer

progression and metastasis was examined in gene expression studies of human melanoma cell lines. Indeed, *IFITM1* and *IFITM3* levels are downregulated in metastatic melanoma cells, indicating successful escaping from the cellular cohesion in these tumor samples (Brem and others 2001b). However, there is no convincing evidence for significant correlation of metastasis and IFITM depletion in every melanoma-derived cell.

IFITM expression levels can be both full transcriptional silenced or virtually unrestricted in cancer cells insensitive to growth inhibition through IFNα-activated pathways (Certa and others 2001). *IFITM3* expression is deregulated in the nonresponder melanoma cell line D10 and overexpression of *IFITM3* does not significantly reduce cellular growth (Brem and others 2003). However, cell lines derived from different cancer samples are highly variable in *IFITM* gene expression irrespectively of their ability to respond to IFNα (Siegrist and others 2010). Recent findings of IFITM3 interaction with Opn may explain some aspects of IFITM involvement in cancer although Opn expression is variable in different tumors. *IFITM3* expression lowers apparently Opn levels and this may interfere with the function of Opn in migration and adhesion during cancer progression (El-Tanani and others 2010). The antiproliferative and adhesive properties of IFITM proteins qualify them as antagonists for tumor development provided that overexpression can be pharmacologically achieved.

There is good evidence for the involvement of positive and negative regulation of *IFITM* expression during the malignant transformation of tumors. IFN-sensitive cells may not benefit from higher IFITM levels due to the antiproliferative activity in these cells. It is feasible that *IFITM* gene levels are predictive for the outcome of IFN-based adjuvant treatment in cancer patients. *IFITM1*, usually more IFNγ associated, was not upregulated in IFNα-treated D10 but significantly in the IFNα growth-sensitive melanoma cell line ME-15 (Certa and others 2001). This indicates a contribution of IFITM1 in the response to IFN. Subsequently, the IFNα response in these cells was evaluated with different platforms to detect global changes in gene expression, including microRNA genes (Certa and others 2003; Siegrist and others 2009b, 2010). There are some differences in *IFITM* expression depending on the detection technology, and the similarities between the genes may complicate interpretation of results. ME-15 cells, for instance, have no detectable levels of *IFITM3* in absence of JAK/STAT activation (Zhang and others 2006) and show a marked growth arrest by pegylated IFNα (Foser and others 2006). In addition, melanoma xenotransplants in mice are restricted in growth mediated by IFNα or pegylated IFNα, and *IFITM* levels are upregulated among other genes in these tumors (Krepler and others 2004). In an analysis across many clinical settings, IFNα showed significant improvement of relapse-free survival for at least some melanoma patients (Garbe and others 2010). Activation of IFITM proteins by IFN administration could explain the therapeutic efficacy in cancer adjuvant therapy but there is no convincing proof so far. The correlation of IFNα sensitivity and low *IFITM* expression levels is cancer-type specific, and in contrast with our findings in melanoma cell cultures, *IFITM1* is expressed low in high-risk leukemia patients who have reduced response to IFNα therapy (Akyerli and others 2005).

IFITM levels may indicate resistance to other therapeutics and are linked to treatment outcome. Tumor cells selected for radio-resistance have enhanced STAT1 signaling, including high *IFITM1* levels, and therefore IFITM1 could contribute to survival in relapsing tumor cells (Khodarev and others 2004). In this case high levels of pluripotency markers such as *IFITM* genes indicate probably a state of slowly replicating cancer stem cells that have constitutively activated IFN pathways and are resistant to anticancer drugs as IFNs, radiotherapy, or any drug therapy that is selective for rapidly growing cells. Further, *IFITM1* is also induced by *in vitro* selection for *cis*-platinum resistance in lung cancer cells (Whiteside and others 2004). This is in contrast with the increase of *cis*-platinum

resistance in esophageal squamous cell carcinoma with experimentally reduced *IFITM1* levels (Fumoto and others 2008). Moreover, loss of *IFITM2/3* expression is a predictive factor for bad response to chemotherapy in osteosarcoma patients (Salas and others 2009).

In summary, IFITM may have different functions in different tumors and the exact role in tumorigenesis is complex. Tumorigenesis involves the inactivation of cell cycle control and attenuated DNA damage repair. Tumor suppressor protein 53 is necessary to maintain cells in an amplification-permissive state and can be regulated by IFITM proteins. Cancer cells proficient in p53 signaling may benefit from transcriptional silencing of *IFITM* genes, but virtually unrestricted *IFITM* levels in most cancer cells probably reflect resistance to IFITM-mediated proliferation control that is linked to deactivated p53 signaling. Further, amplifications in the tip of chromosome 11 are occurring frequently in tumors and affect *IFITM*, *HRAS*, and *IRF7* genes. Deficiencies in nonhomologous end-joining DNA repair could lead to duplications, inversions, and chromosomal rearrangements involving *IFITM* genes.

Conclusions

We have shown here that at least some of the *IFITM* genes have evolved only recently, and this could be crucial for effective antiviral protection and host defense. IFITM proteins protect against viral challenges dependent on the type of virus in addition to the IFITM properties. An enhanced mutation rate of these genes is probably beneficial for adaptation to genetic changes in viruses. The phylogenetic analyses, a high number of pseudogenes representing frequent duplications, the presence of the PRIS, and frequent mutations in cancer demonstrate the high mutation rate of *IFITM* genes. Antiviral genes with an elevated mutation rate are beneficial for the evasion of viral countermeasures against human innate immunity actions. One plausible action is the proapoptotic effect that may kill the host cell before the virus is able to assemble into a fully functional virion (Joung and others 2003).

Due to the progress of functional characterization of IFITM class proteins, we are now able to highlight connections between the phenotypes observed and the presence of IFITM proteins. There are good indications that the mode of IFITM-controlled antiproliferative signaling is conserved in many chordates. We have addressed possible genetic implications of duplicated *IFITM* genes. *IFITM* genes with abundant expression acquired and conserved IFN inducibility after the duplication event of the ancient *BRIL/IFITM* gene. Only few functions such as antiproliferative activities are maintained in the IFITM proteins to BRIL, and new functions have evolved that are related to innate immunity. Due to the recent development of the *IFITM* genes at evolutionary scale, functional discrimination should be considered when conclusions across the species are drawn. *IFITM3*-derived pseudogenes are relatively frequent and complicate the genetic discrimination using amplification or hybridization assays. On the basis of our evolutionary analysis, *IFITM* pseudogenes are remnants of random integration during embryogenesis and IFITM proteins are expected to play a nonessential role in germ cell progenitors in humans and mice. Common antiproliferative action and variable response to related cytokines indicates a redundancy in the system and interchangeability of the IFITM proteins in response to pathogens. We anticipate a function of at least some of the *IFITM* genes beyond the intracellular activities because IFITM fusion proteins are processed to their natural size and detectable in the supernatant of cultured cells. The elucidation of inter-cellular antiproliferative pathways would therefore link some of the less-defined IFITM functions in

innate immunity and cancer development. Finally, IFITM activators could be useful as therapeutics against viral infections and cancer.

Acknowledgments

We thank Laura Badi (Computational Biology, Roche Basel, CH) for integration and observation of public database microarray data, and we are grateful to Dr. Stefan Foser (Roche Basel, CH) to bring in many new ideas.

Author Disclosure Statement

No competing financial interests exist.

References

Abba MC, Drake JA, Hawkins KA, Hu Y, Sun H, Notcovich C, Gaddis S, Sahin A, Baggerly K, Aldaz CM. 2004. Transcriptomic changes in human breast cancer progression as determined by serial analysis of gene expression. Breast Cancer Res 6(5):R499–R513.
Akyerli CB, Beksac M, Holko M, Frevel M, Dalva K, Ozbek U, Soydan E, Ozcan M, Ozet G, Ilhan O, Gürman G, Akan H, Williams BRG, Ozçelik T. 2005. Expression of IFITM1 in chronic myeloid leukemia patients. Leuk Res 29(3):283–286.
Alber D, Staeheli P. 1996. Partial inhibition of vesicular stomatitis virus by the interferon-induced human 9–27 protein. J Interferon Cytokine Res 16(5):375–380.
Alkan C, Kidd JM, Marques-Bonet T, Aksay G, Antonacci F, Hormozdiari F, Kitzman JO, Baker C, Malig M, Mutlu O, Sahinalp SC, Gibbs RA, Eichler EE. 2009. Personalized copy number and segmental duplication maps using next-generation sequencing. Nat Genet 41(10):1061–1067.
Andreu P, Colnot S, Godard C, Laurent-Puig P, Lamarque D, Kahn A, Perret C, Romagnolo B. 2006. Identification of the ifitm family as a new molecular marker in human colorectal tumors. Cancer Res 66(4):1949–1955.
Arion D, Unger T, Lewis DA, Levitt P, Mirnics K. 2007. Molecular evidence for increased expression of genes related to immune and chaperone function in the prefrontal cortex in schizophrenia. Biol Psychiatry 62(7):711–721.
Behr S, Schriever F. 1995. Engaging cd19 or target of an antiproliferative antibody 1 on human b lymphocytes induces binding of b cells to the interfollicular stroma of human tonsils via integrin alpha 4/beta 1 and fibronectin. J Exp Med 182(5):1191–1199.
Bradbury LE, Kansas GS, Levy S, Evans RL, Tedder TF. 1992. The cd19/cd21 signal transducing complex of human b lymphocytes includes the target of antiproliferative antibody-1 and leu-13 molecules. J Immunol 149(9):2841–2850.
Brass AL, Huang I, Benita Y, John SP, Krishnan MN, Feeley EM, Ryan BJ, Weyer JL, van der Weyden L, Fikrig E, Adams DJ, Xavier RJ, Farzan M, Elledge SJ. 2009. The IFITM proteins mediate cellular resistance to influenza a h1n1 virus, west nile virus, and dengue virus. Cell 139(7):1243–1254.
Brem R, Certa U, Neeb M, Nair AP, Moroni C. 2001a. Global analysis of differential gene expression after transformation with the v-h-ras oncogene in a murine tumor model. Oncogene 20(22):2854–2858.
Brem R, Hildebrandt T, Jarsch M, Van Muijen GN, Weidle UH. 2001b. Identification of metastasis-associated genes by transcriptional profiling of a metastasizing versus a non-metastasizing human melanoma cell line. Anticancer Res 21(3B):1731–1740.
Brem R, Oraszlan-Szovik K, Foser S, Bohrmann B, Certa U. 2003. Inhibition of proliferation by 1-8u in interferon-alpha-responsive and non-responsive cell lines. Cell Mol

Life Sci 60(6):1235–1248.
Brierley I, Pennell S, Gilbert RJC. 2007. Viral RNA pseudoknots: versatile motifs in gene expression and replication. Nat Rev Microbiol 5(8):598–610.
Certa U, Seiler M, Padovan E, Spagnoli GC. 2001. High density oligonucleotide array analysis of interferon-alpha2a sensitivity and transcriptional response in melanoma cells. Br J Cancer 85(1):107–114.
Certa U, Wilhelm-Seiler M, Foser S, Broger C, Neeb M. 2003. Expression modes of interferon-alpha inducible genes in sensitive and resistant human melanoma cells stimulated with regular and pegylated interferon-alpha. Gene 315:79–86.
Chen J, Baig E, Fish EN. 2004. Diversity and relatedness among the type i interferons. J Interferon Cytokine Res 24(12):687–698.
Chen YX, Welte K, Gebhard DH, Evans RL. 1984. Induction of T cell aggregation by antibody to a 16kd human leukocyte surface antigen. J Immunol 133(5):2496–2501.
Clave E, Carosella ED, Gluckman E, Socié G. 1997. Radiation-enhanced expression of interferon-inducible genes in the kg1a primitive hematopoietic cell line. Leukemia 11(1):114–119.
Cuddapah S, Cui K, Zhao K. 2008. Transcriptional enhancer factor 1 (TEF-1/TEAD1) mediates activation of IFITM3 gene by BRGl. FEBS Lett 582(2):391–397.
Daniel-Carmi V, Makovitzki-Avraham E, Reuven E, Goldstein I, Zilkha N, Rotter V, Tzehoval E, Eisenbach L. 2009. The human 1-8d gene (IFITM2) is a novel p53 independent pro-apoptotic gene. Int J Cancer 125(12):2810–2819.
Deblandre GA, Marinx OP, Evans SS, Majjaj S, Leo O, Caput D, Huez GA, Wathelet MG. 1995. Expression cloning of an interferon-inducible 17-kda membrane protein implicated in the control of cell growth. J Biol Chem 270(40):23860–23866.
El-Tanani MK, Jin D, Campbell FC, Johnston PG. 2010. Interferon-induced transmembrane 3 binds osteopontin *in vitro*: expressed *in vivo* IFITM3 reduced opn expression. Oncogene 29(5):752–762.
Evans SS, Collea RP, Leasure JA, Lee DB. 1993. IFN-alpha induces homotypic adhesion and leu-13 expression in human B lymphoid cells. J Immunol 150(3):736–747.
Evans SS, Lee DB, Han T, Tomasi TB, Evans RL. 1990. Monoclonal antibody to the interferon-inducible protein leu-13 triggers aggregation and inhibits proliferation of leukemic B cells. Blood 76(12):2583–2593.
Fan J, Peng Z, Zhou C, Qiu G, Tang H, Sun Y, Wang X, Li Q, Le X, Xie K. 2008. Gene-expression profiling in chinese patients with colon cancer by coupling experimental and bioinformatic genomewide gene-expression analyses: identification and validation of IFITM3 as a biomarker of early colon carcinogenesis. Cancer 113(2):266–275.
Flores M, Morales L, Gonzaga-Jauregui C, Domínguez-Vidaña R, Zepeda C, Yañez O, Gutiérrez M, Lemus T, Valle D, Avila MC, Blanco D, Medina-Ruiz S, Meza K, Ayala E, García D, Bustos P, González V, Girard L, Tusie-Luna T, Dávila G, Palacios R. 2007. Recurrent dna inversion rearrangements in the human genome. Proc Natl Acad Sci USA 104(15):6099–6106.
Foser S, Redwanz I, Ebeling M, Heizmann CW, Certa U. 2006. Interferon-alpha and transforming growth factor-beta co-induce growth inhibition of human tumor cells. Cell Mol Life Sci 63(19–20):2387–2396.
Friedman RL, Manly SP, McMahon M, Kerr IM, Stark GR. 1984. Transcriptional and posttranscriptional regulation of interferon-induced gene expression in human cells. Cell 38(3):745–755.
Fumoto S, Shimokuni T, Tanimoto K, Hiyama K, Otani K, Ohtaki M, Hihara J, Yoshida K, Hiyama E, Noguchi T, Nishiyama M. 2008. Selection of a novel drug-response predictor in esophageal cancer: a novel screening method using microarray and identification of ifitm1

as a potent marker gene of cddp response. Int J Oncol 32(2):413–423.
Garbe C, Peris K, Hauschild A, Saiag P, Middleton M, Spatz A, Grob J, Malvehy J, Newton-Bishop J, Stratigos A, Pehamberger H, Eggermont A. 2010. Diagnosis and treatment of melanoma: european consensus-based interdisciplinary guideline. Eur J Cancer 46(2):270–283.
Gutterman JU. 1994. Cytokine therapeutics: lessons from interferon alpha. Proc Natl Acad Sci USA 91(4):1198–1205.
Hatano H, Kudo Y, Ogawa I, Tsunematsu T, Kikuchi A, Abiko Y, Takata T. 2008. IFN-induced transmembrane protein 1 promotes invasion at early stage of head and neck cancer progression. Clin Cancer Res 14(19):6097–6105.
Haylock DN, Nilsson SK. 2006. Osteopontin: a bridge between bone and blood. Br J Haematol 134(5):467–474.
Henco K, Brosius J, Fujisawa A, Fujisawa JI, Haynes JR, Hochstadt J, Kovacic T, Pasek M, Schamböck A, Schmid J, Todokoro K, Wälchi M, Nagata S, Weissmann C. 1985. Structural relationship of human interferon alpha genes and pseudogenes. J Mol Biol 185(2):227–260.
Hillman MCJ, Knight EJ, Blomstrom DC. 1987. A membrane protein from IFN-beta-treated daudi cells causes a cessation in cell growth. Biochem Biophys Res Commun 148(1):140–147.
Hisamatsu T, Watanabe M, Ogata H, Ezaki T, Hozawa S, Ishii H, Kanai T, Hibi T. 1999. Interferon-inducible gene family 1-8u expression in colitis-associated colon cancer and severely inflamed mucosa in ulcerative colitis. Cancer Res 59(23):5927–5931.
Huang H, Colella S, Kurrer M, Yonekawa Y, Kleihues P, Ohgaki H. 2000. Gene expression profiling of low-grade diffuse astrocytomas by cDNA arrays. Cancer Res 60(24):6868–6874.
Huang M, Qian F, Hu Y, Ang C, Li Z, Wen Z. 2002. Chromatin-remodelling factor BRG1 selectively activates a subset of interferon-alpha-inducible genes. Nat Cell Biol 4(10):774–781.
Jiang D, Weidner JM, Qing M, Pan X, Guo H, Xu C, Zhang X, Birk A, Chang J, Shi P, Block TM, Guo J. 2010. Identification of five interferon-induced cellular proteins that inhibit west nile virus and dengue virus infection. J Virol 84(16):8332–8341.
Johnson MC, Sangrador-Vegas A, Smith TJ, Cairns MT. 2006. Cloning and characterization of two genes encoding rainbow trout homologues of the IFITM protein family. Vet Immunol Immunopathol 110(3–4):357–362.
Joung I, Angeletti PC, Engler JA. 2003. Functional implications in apoptosis by interferon inducible gene product 1-8d, the binding protein to adenovirus preterminal protein. J Microbiol 41(4):295–299.
Kaur S, Sassano A, Dolniak B, Joshi S, Majchrzak-Kita B, Baker DP, Hay N, Fish EN, Platanias LC. 2008. Role of the akt pathway in mRNA translation of interferon-stimulated genes. Proc Natl Acad Sci USA 105(12):4808–4813.
Kelly JM, Gilbert CS, Stark GR, Kerr IM. 1985. Differential regulation of interferon-induced mRNAs and c-myc mRNA by alpha- and gamma-interferons. Eur J Biochem 153(2):367–371.
Khodarev NN, Beckett M, Labay E, Darga T, Roizman B, Weichselbaum RR. 2004. STAT1 is overexpressed in tumors selected for radioresistance and confers protection from radiation in transduced sensitive cells. Proc Natl Acad Sci USA 101(6):1714–1719.
Kim KS, Kang KW, Seu YB, Baek S, Kim J. 2009. Interferon-gamma induces cellular senescence through p53-dependent dna damage signaling in human endothelial cells. Mech Ageing Dev 130(3):179–188.
Konishi H, Sugiyama M, Mizuno K, Saito H, Yatabe Y, Takahashi T, Osada H, Takahashi T.

2003. Detailed characterization of a homozygously deleted region corresponding to a candidate tumor suppressor locus at distal 17p13.3 in human lung cancer. Oncogene 22(12):1892–1905.
Krepler C, Certa U, Wacheck V, Jansen B, Wolff K, Pehamberger H. 2004. Pegylated and conventional interferon-alpha induce comparable transcriptional responses and inhibition of tumor growth in a human melanoma scid mouse xenotransplantation model. J Invest Dermatol 123(4):664–669.
Lange UC, Adams DJ, Lee C, Barton S, Schneider R, Bradley A, Surani MA. 2008. Normal germ line establishment in mice carrying a deletion of the IFITM/fragilis gene family cluster. Mol Cell Biol 28(15):4688–4696.
Lange UC, Saitou M, Western PS, Barton SC, Surani MA. 2003. The fragilis interferon-inducible gene family of transmembrane proteins is associated with germ cell specification in mice. BMC Dev Biol 3:1.
Lewin AR, Reid LE, McMahon M, Stark GR, Kerr IM. 1991. Molecular analysis of a human interferon-inducible gene family. Eur J Biochem 199(2):417–423.
Lickert H, Cox B, Wehrle C, Taketo MM, Kemler R, Rossant J. 2005. Dissecting wnt/beta-catenin signaling during gastrulation using RNA interference in mouse embryos. Development 132(11):2599–2609.
Liu H, Kang H, Liu R, Chen X, Zhao K. 2002. Maximal induction of a subset of interferon target genes requires the chromatin-remodeling activity of the BAF complex. Mol Cell Biol 22(18):6471–6479.
Lloyd RE, Blalock JE, Stanton GJ. 1983. Cell-to-cell transfer of interferon-induced antiproliferative activity. Science 221(4614):953–955.
Ma Y, Zhang G, Fu X, Xia O, Zhan C, Li L, Wang Z, Wu B. 2010. Wnt signaling may be activated in a subset of peutz-jeghers syndrome polyps closely correlating to lkb1 expression. Oncol Rep 23(6):1569–1576.
Martensen PM, Justesen J. 2004. Small ISGs coming forward. J Interferon Cytokine Res 24(1):1–19.
McKendry R, John J, Flavell D, Müller M, Kerr IM, Stark GR. 1991. High-frequency mutagenesis of human cells and characterization of a mutant unresponsive to both alpha and gamma interferons. Proc Natl Acad Sci USA 88(24):11455–11459.
Meraro D, Gleit-Kielmanowicz M, Hauser H, Levi B. 2002. IFN-stimulated gene 15 is synergistically activated through interactions between the myelocyte/lymphocyte-specific transcription factors, pu.1, IFN regulatory factor-8/IFN consensus sequence binding protein, and IFN regulatory factor-4: characterization of a new subtype of IFN-stimulated response element. J Immunol 168(12):6224–6231.
Moffatt P, Gaumond M, Salois P, Sellin K, Bessette M, Godin E, de Oliveira PT, Atkins GJ, Nanci A, Thomas G. 2008. Bril: a novel bone-specific modulator of mineralization. J Bone Miner Res 23(9):1497–1508.
Moiseeva O, Mallette FA, Mukhopadhyay UK, Moores A, Ferbeyre G. 2006. DNA damage signaling and p53-dependent senescence after prolonged beta-interferon stimulation. Mol Biol Cell 17(4):1583–1592.
Morel N, Brochier G, Synguelakis M, Le Gal La Salle G. 1991. Immunological identification of a new 14 × 10(3) mr membrane-bound protein in torpedo electric organ. J Cell Sci 98 (Pt 3):351–361.
Morrison RF, Farmer SR. 1999. Role of PPARgamma in regulating a cascade expression of cyclin-dependent kinase inhibitors, p18(ink4c) and p21(waf1/cip1), during adipogenesis. J Biol Chem 274(24):17088–17097.
Navarro L, Mowen K, Rodems S, Weaver B, Reich N, Spector D, David M. 1998. Cytomegalovirus activates interferon immediate-early response gene expression and an

interferon regulatory factor 3-containing interferon-stimulated response element-binding complex. Mol Cell Biol 18(7):3796–3802.
Ni Z, Karaskov E, Yu T, Callaghan SM, Der S, Park DS, Xu Z, Pattenden SG, Bremner R. 2005. Apical role for BRG1 in cytokine-induced promoter assembly. Proc Natl Acad Sci USA 102(41):14611–14616.
Nibbe RK, Markowitz S, Myeroff L, Ewing R, Chance MR. 2009. Discovery and scoring of protein interaction subnetworks discriminative of late stage human colon cancer. Mol Cell Proteomics 8(4):827–845.
Nicholl MJ, Robinson LH, Preston CM. 2000. Activation of cellular interferon-responsive genes after infection of human cells with herpes simplex virus type 1. J Gen Virol 81(Pt 9):2215–2218.
Nolis IK, McKay DJ, Mantouvalou E, Lomvardas S, Merika M, Thanos D. 2009. Transcription factors mediate long-range enhancer-promoter interactions. Proc Natl Acad Sci USA 106(48):20222–20227.
Oort PJ, Warden CH, Baumann TK, Knotts TA, Adams SH. 2007. Characterization of TUSC5, an adipocyte gene co-expressed in peripheral neurons. Mol Cell Endocrinol 276(1–2):24–35.
Oren R, Takahashi S, Doss C, Levy R, Levy S. 1990. Tapa-1, the target of an antiproliferative antibody, defines a new family of transmembrane proteins. Mol Cell Biol 10(8):4007–4015.
Pellagatti A, Cazzola M, Giagounidis AAN, Malcovati L, Porta MGD, Killick S, Campbell LJ, Wang L, Langford CF, Fidler C, Oscier D, Aul C, Wainscoat JS, Boultwood J. 2006. Gene expression profiles of CD34+ cells in myelodysplastic syndromes: involvement of interferon-stimulated genes and correlation to fab subtype and karyotype. Blood 108(1):337–345.
Rast JP, Pancer Z, Davidson EH. 2000. New approaches towards an understanding of deuterostome immunity. Curr Top Microbiol Immunol 248:3–16.
Redon R, Ishikawa S, Fitch KR, Feuk L, Perry GH, Andrews TD, Fiegler H, Shapero MH, Carson AR, Chen W, Cho EK, Dallaire S, Freeman JL, González JR, Gratacòs M, Huang J, Kalaitzopoulos D, Komura D, MacDonald JR, Marshall CR, Mei R, Montgomery L, Nishimura K, Okamura K, Shen F, Somerville MJ, Tchinda J, Valsesia A, Woodwark C, Yang F, Zhang J, Zerjal T, Zhang J, Armengol L, Conrad DF, Estivill X, Tyler-Smith C, Carter NP, Aburatani H, Lee C, Jones KW, Scherer SW, Hurles ME. 2006. Global variation in copy number in the human genome. Nature 444(7118):444–454.
Rigden DJ, Galperin MY. 2004. The dxdxdg motif for calcium binding: multiple structural contexts and implications for evolution. J Mol Biol 343(4):971–984.
Ropolo A, Tomasini R, Grasso D, Dusetti NJ, Cerquetti MC, Iovanna JL, Vaccaro MI. 2004. Cloning of ip15, a pancreatitis-induced gene whose expression inhibits cell growth. Biochem Biophys Res Commun 319(3):1001–1009.
Saitou M. 2009. Germ cell specification in mice. Curr Opin Genet Dev 19(4):386–395.
Saitou M, Barton SC, Surani MA. 2002. A molecular programme for the specification of germ cell fate in mice. Nature 418(6895):293–300.
Saitou M, Payer B, Lange UC, Erhardt S, Barton SC, Surani MA. 2003. Specification of germ cell fate in mice. Philos Trans R Soc Lond B Biol Sci 358(1436):1363–1370.
Sakai H, Koyanagi KO, Imanishi T, Itoh T, Gojobori T. 2007. Frequent emergence and functional resurrection of processed pseudogenes in the human and mouse genomes. Gene 389(2):196–203.
Salas S, Jézéquel P, Campion L, Deville J, Chibon F, Bartoli C, Gentet J, Charbonnel C, Gouraud W, Voutsinos-Porche B, Brouchet A, Duffaud F, Figarella-Branger D, Bouvier C. 2009. Molecular characterization of the response to chemotherapy in conventional

osteosarcomas: predictive value of hsd17b10 and IFITM2. Int J Cancer 125(4):851–860.
Samarajiwa SA, Forster S, Auchettl K, Hertzog PJ. 2009. Interferome: the database of interferon regulated genes. Nucleic Acids Res 37(Database issue):D852–D857.
Seo GS, Lee JK, Yu JI, Yun KJ, Chae SC, Choi SC. 2010. Identification of the polymorphisms in IFITM3 gene and their association in a korean population with ulcerative colitis. Exp Mol Med 42(2):99–104.
Siegrist F, Ebeling M, Certa U. 2009a. Phylogenetic analysis of interferon inducible transmembrane gene family and functional aspects of IFITM3. Cytokine 48(1–2, Spec Issue):87.
Siegrist F, Scott RW, Certa U. 2010. Human tumor cell lines treated with interferon-alpha-2a [Internet]. Gene Expression Omnibus, National Center for Biotechnology Information. [cited 2010 May 16]. Available at www.ncbi.nlm.nih.gov/geo/acc.cgi?acc=GSE21158
Siegrist F, Singer T, Certa U. 2009b. Microrna expression profiling by bead array technology in human tumor cell lines treated with interferon-alpha-2a. Biol Proced Online 11(1):113–129.
Smith C, Berg D, Beaumont S, Standley NT, Wells DN, Pfeffer PL. 2007. Simultaneous gene quantitation of multiple genes in individual bovine nuclear transfer blastocysts. Reproduction 133(1):231–242.
Smith RA, Young J, Weis JJ, Weis JH. 2006. Expression of the mouse fragilis gene products in immune cells and association with receptor signaling complexes. Genes Immun 7(2):113–121.
Takahashi S, Doss C, Levy S, Levy R. 1990. Tapa-1, the target of an antiproliferative antibody, is associated on the cell surface with the leu-13 antigen. J Immunol 145(7):2207–2213.
Tam OH, Aravin AA, Stein P, Girard A, Murchison EP, Cheloufi S, Hodges E, Anger M, Sachidanandam R, Schultz RM, Hannon GJ. 2008. Pseudogene-derived small interfering rnas regulate gene expression in mouse oocytes. Nature 453(7194):534–538.
Tanaka SS, Matsui Y. 2002. Developmentally regulated expression of mil-1 and mil-2, mouse interferon-induced transmembrane protein like genes, during formation and differentiation of primordial germ cells. Mech Dev 119 Suppl 1:S261–S267.
Tanaka SS, Nagamatsu G, Tokitake Y, Kasa M, Tam PPL, Matsui Y. 2004. Regulation of expression of mouse interferon-induced transmembrane protein like gene-3, IFITM3 (mil-1, fragilis), in germ cells. Dev Dyn 230(4):651–659.
Tanaka SS, Yamaguchi YL, Tsoi B, Lickert H, Tam PPL. 2005. IFITM/mil/fragilis family proteins IFITM1 and IFITM3 play distinct roles in mouse primordial germ cell homing and repulsion. Dev Cell 9(6):745–756.
Tedder TF, Zhou LJ, Engel P. 1994. The cd19/cd21 signal transduction complex of B lymphocytes. Immunol Today 15(9):437–442.
Tirosh B, Daniel-Carmi V, Carmon L, Paz A, Lugassy G, Vadai E, Machlenkin A, Bar-Haim E, Do M, Ahn IS, Fridkin M, Tzehoval E, Eisenbach L. 2007. “1-8 interferon inducible gene family”: putative colon carcinoma-associated antigens. Br J Cancer 97(12):1655–1663.
Tsai M, Cook JA, Chandramouli GVR, DeGraff W, Yan H, Zhao S, Coleman CN, Mitchell JB, Chuang EY. 2007. Gene expression profiling of breast, prostate, and glioma cells following single versus fractionated doses of radiation. Cancer Res 67(8):3845–3852.
Tsukahara T, Kim S, Taylor MW. 2006. Refinement: a search framework for the identification of interferon-responsive elements in dna sequences—a case study with ISRE and gas. Comput Biol Chem 30(2):134–147.
Wan X, Chen X. 2008. Molecular cloning and expression analysis of interferon-inducible transmembrane protein 1 in large yellow croaker pseudosciaena crocea. Vet Immunol Immunopathol 124(1–2):99–106.

Watanabe T, Totoki Y, Toyoda A, Kaneda M, Kuramochi-Miyagawa S, Obata Y, Chiba H, Kohara Y, Kono T, Nakano T, Surani MA, Sakaki Y, Sasaki H. 2008. Endogenous sirnas from naturally formed dsrnas regulate transcripts in mouse oocytes. Nature 453(7194):539–543.
Whiteside MA, Chen D, Desmond RA, Abdulkadir SA, Johanning GL. 2004. A novel time-course cDNA microarray analysis method identifies genes associated with the development of cisplatin resistance. Oncogene 23(3):744–752.
Wu F, Dassopoulos T, Cope L, Maitra A, Brant SR, Harris ML, Bayless TM, Parmigiani G, Chakravarti S. 2007. Genome-wide gene expression differences in crohn's disease and ulcerative colitis from endoscopic pinch biopsies: insights into distinctive pathogenesis. Inflamm Bowel Dis 13(7):807–821.
Xu Y, Yang G, Hu G. 2009. Binding of IFITM1 enhances the inhibiting effect of caveolin-1 on ERK activation. Acta Biochim Biophys Sin 41(6):488–494.
Yamashita T, Hashimoto S, Kaneko S, Nagai S, Toyoda N, Suzuki T, Kobayashi K, Matsushima K. 2000. Comprehensive gene expression profile of a normal human liver. Biochem Biophys Res Commun 269(1):110–116.
Yang G, Xu Y, Chen X, Hu G. 2007. IFITM1 plays an essential role in the antiproliferative action of interferon-gamma. Oncogene 26(4):594–603.
Yang Y, Lee J, Kim KY, Song HK, Kim JK, Yoon SR, Cho D, Song KS, Lee YH, Choi I. 2005. The interferon-inducible 9–27 gene modulates the susceptibility to natural killer cells and the invasiveness of gastric cancer cells. Cancer Lett 221(2):191–200.
Young JC, Dias VL, Loveland KL. 2010. Defining the window of germline genesis *in vitro* from murine embryonic stem cells. Biol Reprod 82(2):390–401.
Younossi ZM, Afendy A, Stepanova M, Hossain N, Younossi I, Ankrah K, Gramlich T, Baranova A. 2009. Gene expression profile associated with superimposed non-alcoholic fatty liver disease and hepatic fibrosis in patients with chronic hepatitis c. Liver Int 29(9):1403–1412.
Zhang F, Gu W, Hurles ME, Lupski JR. 2009. Copy number variation in human health, disease, and evolution. Annu Rev Genomics Hum Genet 10:451–481.
Zhang J, Lang HP, Huber F, Bietsch A, Grange W, Certa U, McKendry R, Güntherodt H, Hegner M, Gerber C. 2006. Rapid and label-free nanomechanical detection of biomarker transcripts in human RNA. Nat Nanotechnol 1(3):214–220.
Zhang L, Zhou W, Velculescu VE, Kern SE, Hruban RH, Hamilton SR, Vogelstein B, Kinzler KW. 1997. Gene expression profiles in normal and cancer cells. Science 276(5316):1268–1272.
Zhang LQ, Adyshev DM, Singleton P, Li H, Cepeda J, Huang S, Zou X, Verin AD, Tu J, Garcia JGN, Ye SQ. 2008. Interactions between PBEF and oxidative stress proteins—a potential new mechanism underlying PBEF in the pathogenesis of acute lung injury. FEBS Lett 582(13):1802–1808.
Zhang Z, Harrison PM, Liu Y, Gerstein M. 2003. Millions of years of evolution preserved: a comprehensive catalog of the processed pseudogenes in the human genome. Genome Res 13(12):2541–2558.
Zhao H, Boije H, Granberg F, Pettersson U, Svensson C. 2009. Activation of the interferon-induced STAT pathway during an adenovirus type 12 infection. Virology 392(2):186–195.
Zheng D, Frankish A, Baertsch R, Kapranov P, Reymond A, Choo SW, Lu Y, Denoeud F, Antonarakis SE, Snyder M, Ruan Y, Wei C, Gingeras TR, Guigó R, Harrow J, Gerstein MB. 2007. Pseudogenes in the encode regions: consensus annotation, analysis of transcription, and evolution. Genome Res 17(6):839–851.
Zhu H, Cong JP, Mamtora G, Gingeras T, Shenk T. 1998. Cellular gene expression altered by human cytomegalovirus: global monitoring with oligonucleotide arrays. Proc Natl Acad

Sci USA 95(24):14470–14475.
Zhu H, Cong JP, Shenk T. 1997. Use of differential display analysis to assess the effect of human cytomegalovirus infection on the accumulation of cellular rnas: induction of interferon-responsive RNAs. Proc Natl Acad Sci USA 94(25):13985–13990.
Zhu H, Liu C. 2003. Interleukin-1 inhibits hepatitis c virus subgenomic RNA replication by activation of extracellular regulated kinase pathway. J Virol 77(9):5493–5498.
Zuber J, Tchernitsa OI, Hinzmann B, Schmitz AC, Grips M, Hellriegel M, Sers C, Rosenthal A, Schäfer R. 2000. A genome-wide survey of ras transformation targets. Nat Genet 24(2):144–152.
Zucchi I, Montagna C, Susani L, Vezzoni P, Dulbecco R. 1998. The rat gene homologous to the human gene 9–27 is involved in the development of the mammary gland. Proc Natl Acad Sci USA 95(3):1079–1084.
Zucchi I, Prinetti A, Scotti M, Valsecchi V, Valaperta R, Mento E, Reinbold R, Vezzoni P, Sonnino S, Albertini A, Dulbecco R. 2004. Association of rat8 with fyn protein kinase via lipid rafts is required for rat mammary cell differentiation *in vitro*. Proc Natl Acad Sci USA 101(7):1880–1885.

Tables, Figures and Legends

Adhesion	Antiproliferative	Antiviral	Apoptosis	Development	Cell-migration	Tumor progression	Miscellaneous	Species	Gene	IFITM protein interactions	References
■								Hs	IFITM1		Chen1984
	■							Hs	IFITM		Hillman1987
■	■							Hs	IFITM1	CD81 CD81	Evans1990, 1993 Takahashi1990 Bradbury1992
■	■							Hs	IFITM1	CD81	Deblandre1995
	■							Hs	IFITM3		Brem2003
	■					■		Hs	IFITM1		Yang2007
	■						■	Hs	IFITM3	PBEF	Zhang2008
	■							Hs	IFITM1	CAV1	Xu2009
■	■					■	■	Hs Rn	IFITM3 Ifitm3	Spp1	El-Tanani2010
		■						Hs Ca Mm	IFITM1		Alber1996
		■						Hs	IFITM3 IFITM1-2		Brass2009
			■					Hs	IFITM2	Gal4	Joung2003
			■			■		Hs Mm Rn	IFITM2 Ifitm2		Daniel- Carmi2009
							■	Hs	IFITM1-3		Arion2007

Adhesion	Antiproliferative	Antiviral	Apoptosis	Development	Cell-migration	Tumor progression	Miscellaneous	Species	Gene	IFITM protein interactions	References
	■			■		■		Rn	Ifitm3	Fyn	Zucchi1998 Zucchi2004
■	■			■				Mm	Ifitm3		Saitou2002
	■			■				Hs Ca Mm	Ifitm3		Ropolo2004
				■	■			Mm	Ifitm3/1		Tanaka2005
				■	■		■	Mm	Ifitm1		Lickert2005
						■	■	Mm	Ifitm1/3	CD81	Smith2006
				■				Mm	Ifitm1-6		Lange2008
				■				Bt	Ifitm3		Smith2007
						■		Hs	IFITM3		Huang2000
						■		Hs	IFITM1/2		Brem2001
						■	■	Hs	IFITM1		Yang2005
						■		Hs	IFITM1/3		Khodarev2004
						■		Hs	IFITM2/3		Salas2009
							■	Tm Mm			Morel1991

Table 1 Pleiotropic Functions of Interferon Induced Transmembrane Proteins

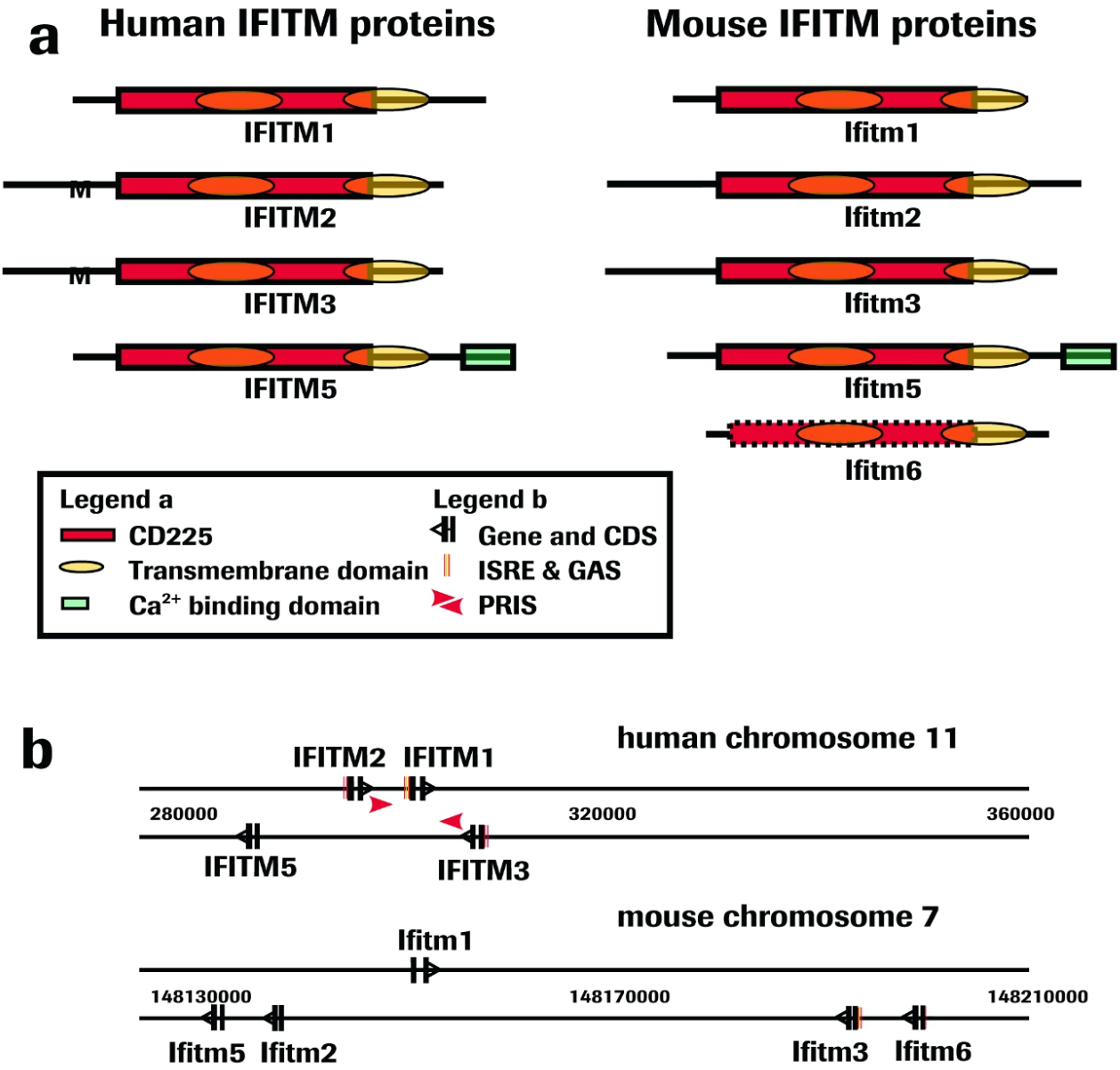

Figure 1 (a) Structural display of human and mouse IFITM proteins 9–27/fragilis2 (*IFITM1*), 1-8D/fragilis3 (*IFITM2*), 1-8U/fragilis (*IFITM3*), fragilis5 (*Ifitm6*), and BRIL/fragilis4 (*IFITM5*); mil4 (*Ifitm7*) is not shown. **(b)** Chromosomal localization of *IFITM* genes in human and mouse. There are 2 interferon stimulated response elements (ISRE) (red) in each promoter of human *IFITM* genes and additional gamma-activated sequence (yellow) in *IFITM1*. Two potential recombinogenic inverted sequence (PRIS) are indicated by *red arrowheads*, genes are shown as *arrows*, and protein coding sequence as vertical bars. IFITM, Interferon induced transmembrane; BRIL, bone restricted IFITM-like.

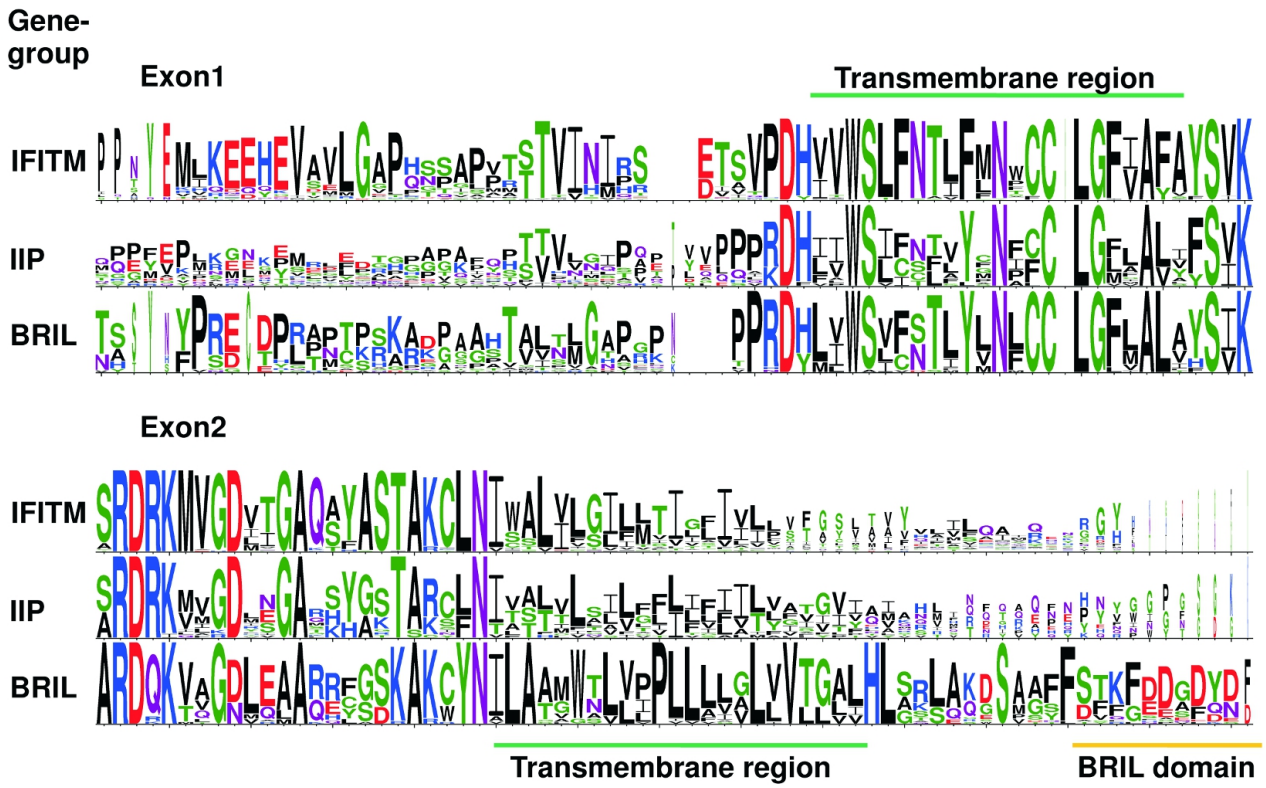

Figure 2. Amino acid (AA) occurrence in putative homologs of IFITM1-3, IFITM5 (BRIL), and nonmammalian homologs of fish interferon-inducible proteins (IIP). Probability is calculated from 55 mammalian IFITM homologs, 27 IFITM5, and BRIL-like AA sequences in fish or 17 IIPs. Consensus AA sequences of human, mouse, and rat were used to search for homologs in complete genomes; whole genome shot-gun contigs and additional sequences were taken from publications. All sequences were manually screened for presence of a single 300–2500 base spanning intron (or up to 6,500 bases in lizard). Exceptions with no intron are *Ifitm7* from mouse, *IFITM* from dasypus, 3 *BRIL* from fish, and 10 nonmammalian *IIP* sequences. Protein sequences, including an IFITM-like sequence from arrow-worms, were aligned with the CLUSTALW in MEGA 4. Global pairwise alignment is shown for the region 71 AAs before and after the conserved exon splice-junction. Potentially calcium binding domain of BRIL is highlighted by a *yellow bar* and predicted trans-membrane regions are indicated by a *green bar*. The CD225 domain has the same length in all but one (IFITM0 from horse) of the sequences analyzed. In human IFITM1, it corresponds to amino acid positions Pro34 to Thr97. Sequence logos were generated from translated coding sequences using the web-based program WEBLOGO 3.

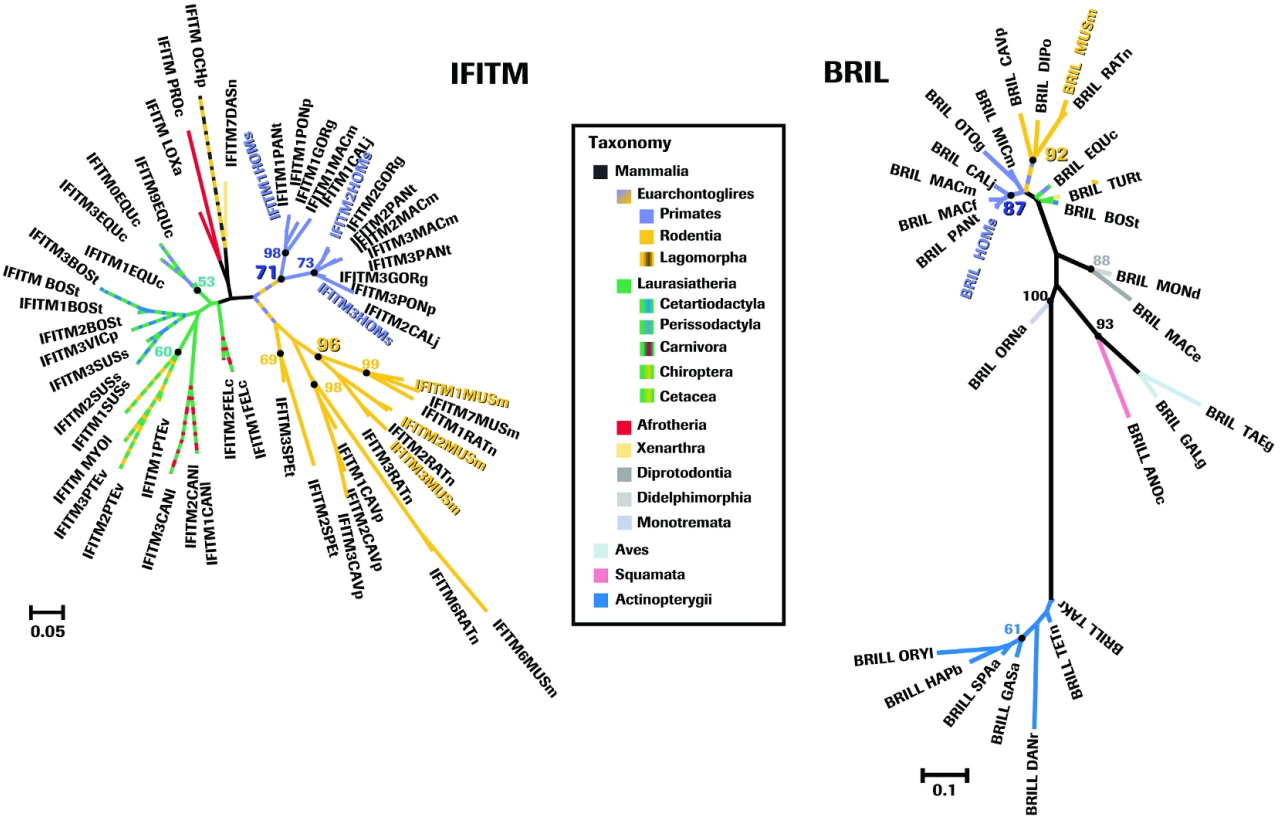

Figure 3. Phylogenetic tree for trimmed coding sequences of 55 mammalian variants of *IFITM*s (*left*) and 27 identified *BRIL* and related sequences (*right*). Fish *IIP* sequences and other ambiguous sequences were not taken into account for generation of these trees. Phylogenetic analyses were performed on the coding DNA sequences using the maximum likelihood method program DNAML in PHYLIP (Phylogeny Interference Package version 3.68) distributed by the author. There were a total of 312 and 441 nucleotide positions in the final data sets. The evolutionary history was inferred using the maximum likelihood method for DNA sequences. Default settings were changed to “not rough” calculation and allowing global rearrangements. HMM rates were defined with 2 categories of rates one and 3 with probability 0.66 and 0.34. For each set the optimal tree with the sum of branch length *IFITM* = 4.56979 and *BRIL* = 4.58961 is shown as radiation tree with branch lengths in the units of expected nucleotide substitutions per site. The branches were colored by common biological classes (and orders) and human and mouse sequence names are colored. Bootstrap values are shown for branches of interest based on 100 replicates. Highlighted numbers indicate the high probability for gene duplication during speciation of primates. Sequence names were annotated in the following way: mammalian *IFITM5* sequences and unknown genes showing a similar, specific domain at the C-terminus were named *BRIL*, and similar sequences in other species *BRILL* (BRIL like proteins) accordingly. Species with only 1 detected gene were named IFITM in mammals and interferon-induced protein in others. Numbering of genes is based on the present analysis and does not claim to correspond to other databases and publications.

Antiproliferative Activity of the Human IFN-α-Inducible Protein IFI44

Hallen, L.C.[1], Burki, Y.[1], Ebeling, M.[1], Broger, C.[2], Siegrist, F.[1] , Oroszlan-Szovik K.[2], Bohrmann B.[2], Certa, U. [1] and [#]Foser, S. [1]

[1]Roche Center for Medical Genomics, [2]Pharma Research Basel, F. Hoffmann-La Roche Ltd., 4070 Basel, Switzerland.
Running title: Expression mode of IFI44 in human cell lines
[#]Dr. Stefan Foser
Tel. +41 61 688 1111
FAX +41 61 688 1448
E-mail Stefan.foser@roche.com

Abstract
The interferon-α (IFN-α)-inducible protein IFI44 is associated with hepatitis C virus (HCV) infection, and its function is unknown. We show here in two human melanoma cell lines (ME15 and D10) that transcription starts 4 h after induction, and peak protein levels are reached 24 h after stimulation. We show by immunofluorescence, viral overexpression, and cellular fractionation that IFI44 is a cytoplasmic protein. Overexpression of IFI44 cDNA induces an antiproliferative state *in vitro*, even in cells that are not responsive to IFN-α. IFI44 contains a perfect GTP binding site but has no homology to known GTPases or G proteins. Based on these results, we propose a model in which IFI44 binds intracellular GTP, and this depletion abolishes extracellular signal-regulated kinase (ERK) signaling and results finally in cell cycle arrest.

Keywords: interferon-α; signaling; GTP binding proteins; IFI44

Introduction

Chronic infection with hepatitis C virus (HCV) is the most common form of chronic viral hepatitis in the developed world with 170 million infected individuals worldwide. The chronic infection is often silent and may be discovered during routine blood screening. Symptoms are typically absent, and only liver biopsies demonstrate disease progress and severity. The therapy of chronic hepatitis is still unsatisfactory, and the only agent with proven benefit is cotherapy of pegylated interferon-2A (IFN-2A) with the viral polymerase inhibitor ribavirin (Feld and Hoofnagle, 2005; Hoofnagle, 1998; Zeuzem et al., 2001). Only 50% of individuals infected with HCV genotype 1 respond to antiviral therapy, and the responders increase to 80% in nongenotype 1 infections. The host and pathogen factors that cause therapy failure are still unknown, and efforts have started to identify host-encoded candidate genes using global transcriptional analysis in patient samples and cell lines (Bain et al., 2006; Basu et al., 2006; Certa et al., 2003; Foser et al., 2003; Patzwahl et al., 2001; Walters et al., 2006). One gene that is consistently upregulated following IFN-α therapy or *in vitro* stimulation of cell lines was termed IFI44. It was initially discovered in association with microtubular structures in an HCV-infected chimpanzee, and more than a decade later, nothing is known about its possible function (Honda et al., 1990). Recently, it was included in a genetic screen aimed at discovering biomarkers for predisposition of responsiveness to therapy for chronic hepatitis C (Hwang et al., 2006). Most genes included in this study had about 10 single nucleotide polymorphisms (SNPs) in the noncoding promoter region, with the exception of IFI44, where a nonsynonymous amino acid change (Arg/Trp) occurs in the ninth position of the protein sequence, which points perhaps to a role in HCV pathogenesis or host defense. This feature and its consistent high-level induction by IFN-α and HCV raise the possibility that IFI44 has antiviral activity. In this paper, we assess the function of IFI44 by studying its induction kinetics in a number of human cell lines as well as its subcellular localization, and we demonstrate antiproliferative activity.

Materials and Methods

Antibodies

Antibodies against a peptide conjugate of IFI44 (amino acid residues 271–285, GLCRDDIFYILNGNIRDRYQFNPMESIKLNHHDYIDSPSL) were raised in rabbits using standard immunologic techniques (Eurogentec/ LIEGE Science Park, Belgium). Anti-IFI44 serum (rabbit 247) was used at 1:1000 dilution for Western blots and diluted 1:100 for immunofluorescence. Preimmune serum was used as a control to establish the assay conditions (data not shown). Goat antirabbit IgG (HL) horseradish peroxidase (HRP) conjugate was obtained from BioRad (Basel, Switzerland), and Alexa Fluor 488 goat antirabbit IgG (H+L) and Alexa Fluor 568 goat antirabbit IgG (HL) were purchased from Invitrogen (Basel, Switzerland).

Cell lines.

ME15 and D10 have been described previously, and all other cell lines were purchased from the ATCC cell culture collection (Rockville, MD) and cultured at 37°C in a 5% CO2 atmosphere in RPMI 1640 medium (GIBCO Life Sciences, Paisley, U.K.) supplemented with 10% fetal bovine serum (FBS), L-glutamine (2 mM), sodium pyruvate (1 mM), nonessential amino acids, antibiotics, and 10 mM HEPES buffer (Certa et al., 2003).

Cell proliferation assay.

Cells from each line (5000 cells) were grown in triplicate over a period of 5 days in 96-well plates with the appropriate treatment. Cell density was measured using a commercial colorimetric assay as described. (Foser et al., 2003). The mean of the OD reading was determined and used to calculate the standard deviation (SD) from the mean value. The averaged data were used to calculate the percent of control to obtain comparable values

within the set of experiments. The maximal deviation from the mean at day 4 was 3.2% (data not shown).

Immunefluorescence and immunoblotting.

Immunodetection of IFI44 was carried out as described with the serum dilutions indicated (Brem et al., 2003).

Recombinant expression of IFI44 in semliki forest virus.

The IFI44 coding sequence was amplified with total cellular ME15 cDNA as template by PCR using primers with internal BglII cloning sites (forward primer 5-GTACAACAATCAAGATCTAGGCAGTGAC-3; position 71–100 in NM_006417; backward primer 5-GAATTTACGTGAACCTTTCAGATCTCTAT-3; position 1388–1418 in NM_006417). The BglII-digested PCR fragment was subcloned into pCR 2.1-TOPO for sequence verification. The correct IFI44 cDNA was cloned into SFV-PD for expression (SFVIFI44), and viral stocks were prepared as describe (Lundstrom et al., 2001). The $SFV^{IFN\alpha}$ viral stock was a gift from Dr. S. Clure (Biocenter of the University of Basel).

Cell fractionation

ME15 and D10 cells were lysed and fractionated using a commercial kit and the instructions supplied (Qiagen Qproteome Cell Compartment Kit, Qiagen AG, 8634 Hombrechtikon, Switzerland).

mRNA quantification

The cell lines A549, LS174T, HCT116, MIA PaCa-2, AsPC-1, D10, and ME15 were grown without (control) or with 100 U/mL human IFN-2A (Roferon, F. Hoffmann-La Roche Ltd., Basel, Switzerland) for 4 or 24 h. Total RNA was extracted with TRI reagent (Molecular Research Center, Inc., Cincinnati, OH), and biotin-labeled using a commercial kit and the protocol supplied (Agilent Technologies, Basel, Switzerland). Labeled, unfragmented cRNA (500 ng) of each cell line was hybridized to commercial microarrays using the manufacturer's protocol (Sentrix HumanRef-8 Expression BeadChips; Illumina, Inc., San Diego, CA). Data were collected using a confocal scanner (Illumina beadstation), and data analysis was performed using Illumina Beadstudio (*www.illumina.com*) and RACE-A software (Certa et al., 2003).

Results and Discussion

Expression mode of IFI44

Inhibition of HCV replication by IFN-α occurs within hours after stimulation, which implies that host defense genes show immediate-early induction (Guo, Bichko and Seeger, 2001). In Figure 1, we analyze the kinetics of IFI44 mRNA and protein induction by IFN-α relative to control genes in a panel of IFN-α-sensitive and resistant cell lines. Four hours after cytokine stimulation, efficient induction of IFI44 mRNA occurs in ME15, D10, and AsPC-1, whereas A549, LS174T, HCT116, and MIA PaCa-2 are poor responders (Fig. 1A). A similar induction pattern appears for the early induced control gene IFIT3, with the exception of MIA PaCa-2, where this particular gene is efficiently induced after 4 h (Fig. 1B). In contrast to IFI44 and IFIT3, 6-16 shows peak levels of mRNA 8 h after stimulation, which eliminates it as an immediate-early host defense gene (Fig. 1C). At this point, we found it important to show induction of IFI44 at the protein level by probing immunoblots of IFN-α-treated ME15 and D10 cells (for details, see Materials and Methods). Induction of IFI44 protein is clearly evident 8 h after stimulation in both lines (Fig. 1D), which is consistent with the mRNA induction kinetics. Removal of IFN-α 24 h after induction results in clear decline of IFI44 protein, which classifies IFI44 as a *bona fide* IFN-α response gene.

Cellular localization of IFI44

IFI44 was originally found in microtubular aggregates in hepatocytes of non-A, non-B (NANB) virus-infected chimpanzees (Honda et al., 1990). Nothing is known about the subcellular localization of IFI44 in human tissues or cell lines. To address this question, we chose the human melanoma cell lines ME15 and D10 because IFN-α stimulation induces significant amounts of IFI44 protein (Fig.1). In both lines, fluoresecent patch-like structures are consistently detected in the nuclei in nonstimulated cells (Fig. 2A, B). Upon IFN-α treatment, the nuclear signal fades, and a uniform cytoplasmic fluorescence appears, which is consistent with the data shown in Figure 1D. When untreated ME15 cells are transfected with an SFV that overexpresses IFI44 protein (SFV^{IFI44}), a similar diffuse cytoplasmic fluorescence with higher intensity appears, which proves specificity of the anti-IFI44 rabbit serum (Fig. 2C). Control infection with virus vehicle alonedoes not cause any changes in the IFI44 detection pattern (data not shown). The immunofluorescence with anti-IFI44 serum clearly differs from a typical microtubular staining pattern obtained with serum against -tubulin (Fig. 2C, right).

We thus applied cell fractionation as an independent approach to confirm this conclusion (Fig. 3). In fractionated ME15 and D10 cell lysates, IFI44 is detectable only in the cytoplasmic fraction and is absent in the membrane, nuclear, and particularly the cytoskeleton fraction, where it would be expected as a microtubule-associated protein. In this assay, we failed to confirm the nuclear localization of IFI44 in uninduced ME15 or D10 cells, which might be related to insufficient sensitivity, shedding during the preparation of nuclei, or other technical issues (Figs. 2 and 3). We conclude based on two independent assays that IFI44 is a cytoplasmic protein in human melanoma cell lines and is associated with microtubular structures. IFI44 was first identified in density gradient-enriched microtubular aggregates with a monoclonal antibody (mAb) from HCV-infected chimpanzee livers, and, therefore, any protein present in these complexes is microtubule associated. This is the first report describing *in situ* detection of IFI44, and detection in microtubular aggregates might be cross-contamination related to the high abundance of IFI44 in HCV-infected liver cells. Alternatively, although less likely, subcellular localization of IFI44 might be cell type specific.

Comparative genomics analysis of human IFI44

With the availability of complete genome sequences of a number of relevant organisms, it became possible to identify functional domains of any protein by sequence homology. Such an analysis can provide important clues for the potential function of an uncharacterized protein. We performed a computer-aided homology search with human IFI44 in the genomes of bat (*Myotis lucifugus*), cow, dog, rabbit, mouse, amphioxus, and rat. In all species analyzed (including some fish species, for which no data are shown), we identified IFI44 homologs with 80% sequence identity (Fig. 4). However, none of the conserved sequence blocks corresponded to any known functional protein domain motif, with the exception of the sequence GP(I/V/T)GAGK, which is a GTPbinding site. This now classifies IFI44 as a potential GTP-binding protein, and its overall high interspecies conservation points to an important biologic function.

Antiproliferative activity of IFI44

A hallmark of IFNs is the ability to induce antiproliferative activity. Transfection of the small IFN-α-inducible protein 1-8U, for instance, leads to a complete arrest of cell division (Brem et al., 2003). On the other hand, GTP-binding proteins, like the IFN-α-inducible GTPase p47, are involved in host defense against such viruses as HCV and HIV (MacMicking, 2004). Cell cycle arrest of infected cells is an important aspect of virus defense because it inhibits spread of the pathogen through blocking of cell division. To test whether IFI44 has

antiproliferative activity, we overexpressed IFI44 in ME15 and D10 cells by infection withSFV^{IFI44} or SFV as control and measured cell proliferation over a period of 4 days (Fig. 5A). In both cell lines,SFV^{IFI44} infection induced significant growth inhibition of about 20% in ME15 and D10 at day 4 relative to the control virus-infected cultures. As an additional control, we infected ME15 and D10 cells with $SFV^{IFN\alpha}$, which is a recombinant virus that expresses secreted recombinant IFN-2A. We also included reference cultures in the analysis that received standard treatment with 100 U/mL IFN-α (Fig. 5B). As expected, proliferation of $SFV^{IFN\alpha}$ infected or IFNα-treated ME15 cells was strongly inhibited regardless of the IFN-α delivery, whereas growth of D10 cells was essentially unaffected by either treatment. This also eliminated the concern that viral infection might cause growth arrest. Thus, recombinant expression of IFI44 alone is sufficient to inhibit cell proliferation regardless of the IFN-α response state of the cell. This finding points to a direct mechanism of action that does not require the presence or activity of any additional IFN-α-inducible proteins. Our sequence analysis (Fig. 4) opened the possibility that the highly conserved GTP-binding site present in all IFI44 orthologs has functional significance. In mouse, the p47 group of IFN-inducible GTPases with antiproliferative activity has been strongly implicated in host defense against bacterial, viral, and protozoan pathogens (MacMicking, 2004). The molecular weight range of 47–50kDa of these enzymes is similar to that of IFI44 (50461 Da), which opened the attractive possibility that IF44 is perhaps a novel member of this group. To our surprise, only the GTP binding motif (GXXXXGKS) is shared between IFI44 and the GTPase panel,and rest of the IFI44 amino acid sequence has no homology to this group of enzymes (data not shown). In particular, the G3 (DXXG) and G4 (TKXD) motifs that are found in all p47 type GTPases at equivalent positions are absent in IFI44 (MacMicking, 2004). Another category of GTP-binding proteins are the well-studied G proteins, which transmit signals of G protein-coupled receptors (GPCRs) to the adenylate cyclase signaling cascade. One well-studied downstream enzyme associated with cell proliferation is the mitogen-activated protein kinase (MAPK), also termed extracellular signal-regulated kinase (ERK). ERK cascade activity couples cytokine or growth factor signaling to proliferation through G proteins. (Stork and Schmitt, 2002). We relied again on sequence alignment for the possible classification of IFI44 as a G protein. However, typical G proteins, such as Ras, are smaller and plasma membrane associated, and known G proteins are not inducible and less abundant than IFI44. Finally, G proteins form trimeric complexes, and no protein interaction is documented for IFI44 in the Database of Interacting Proteins (*www.dip.doembi.ucla.edu/dip*).

We conclude that it is unlikely that IFI44 is a GTPase or G protein, and its high abundance after IFN-α induction might be key to its function. Pharmacologic GTP depletion induces apoptosis and cell cycle arrest of insulin-secreting cells by inhibition cAMP signaling to downstream cascades, such as ERK.(Li et al., 1998). The relatively high abundance of IFI44 after IFN-α stimulation together with its cellular localization lead to the following hypothesis. IFI44 binds intracellular GTP and depletes the cytoplasmic pools, which would cause inhibition cAMP-mediated signaling downstream of the ERK cascade and the ultimate arrest of cell division. The fact that IFI44 levels decline without IFN-α stimulus (Fig. 1D) would allow normal cell growth after successful virus defense. We are currently testing this plausible hypothesis experimentally by analyzing G protein signaling in stable IFI44-transfected cells. Strikingly, the most potent drug known against HCV, the guanosin analog ribavirin depletes intracellular GTP pools, and IFI44 might be its natural homolog (Leyssen et al., 2005).

Acknowledgments
We thank Dr. Karl Weyer (Roche Basel, Switzerland) for the gift of monopegylated IFN-2A (K134) and Dr. S. Clure (Biocenter of the University of Basel, Switzerland). We are grateful to Dr. Martin Grigorov (NRC, Lausanne, Switzerland) for the initial detection of the GTP-binding motif in IFI44 and Dr. Gary Peltz (Roche Palo Alto, CA) for substantial improvements to the manuscript. We thank Prof. Fridolin Leopold, University of Munich, for his interest in this work and his critical input.

Figures / Legends

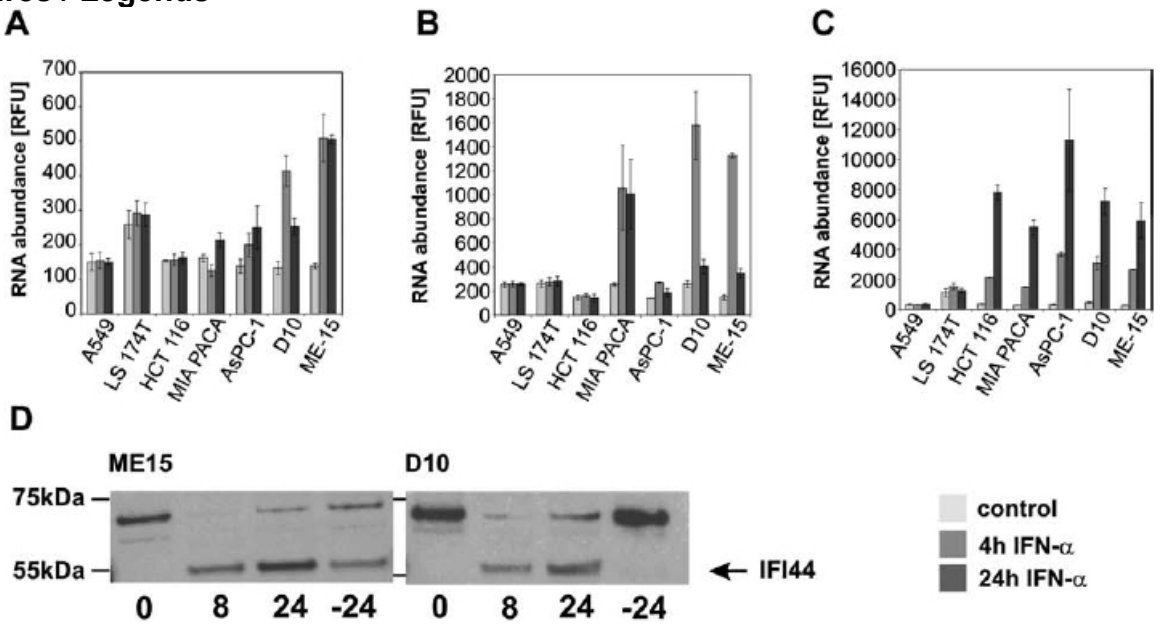

Figure 1. Kinetics of IFI44 induction in IFN-α-sensitive and resistant human cell lines. **(A)** IFI44 induction with 100 U/mL IFN-α in a panel of human cell lines. In AsPC-1, ME15, and D10, efficient expression of IFI44 mRNA occurs early, 4 h after stimulation, whereas the IFI44 gene is virtually noninducible in A549, LS174T, HCT116, and MIA PaCa-2. **(B)** Induction kinetics of the primary response gene IFIT3 and of the secondary gene 6-16 **(C)** in the same panel of cell lines. mRNA abundance was measured in parallel using commercial DNA microarrays. **(D)** Immunoblot detection of IFI44 protein in ME15 and D10 4 or 24 h after IFN-α stimulation. As expected for a *bona fide* response gene, continued cultivation without IFN-α results in protein decay. IFI44 protein was detected with rabbit serum raised against an immunogenic peptide fragment of IFI44. The serum crossreacts with a larger, unknown protein, which is not IFN-α inducible. The position of IFI44 is marked by an arrow.

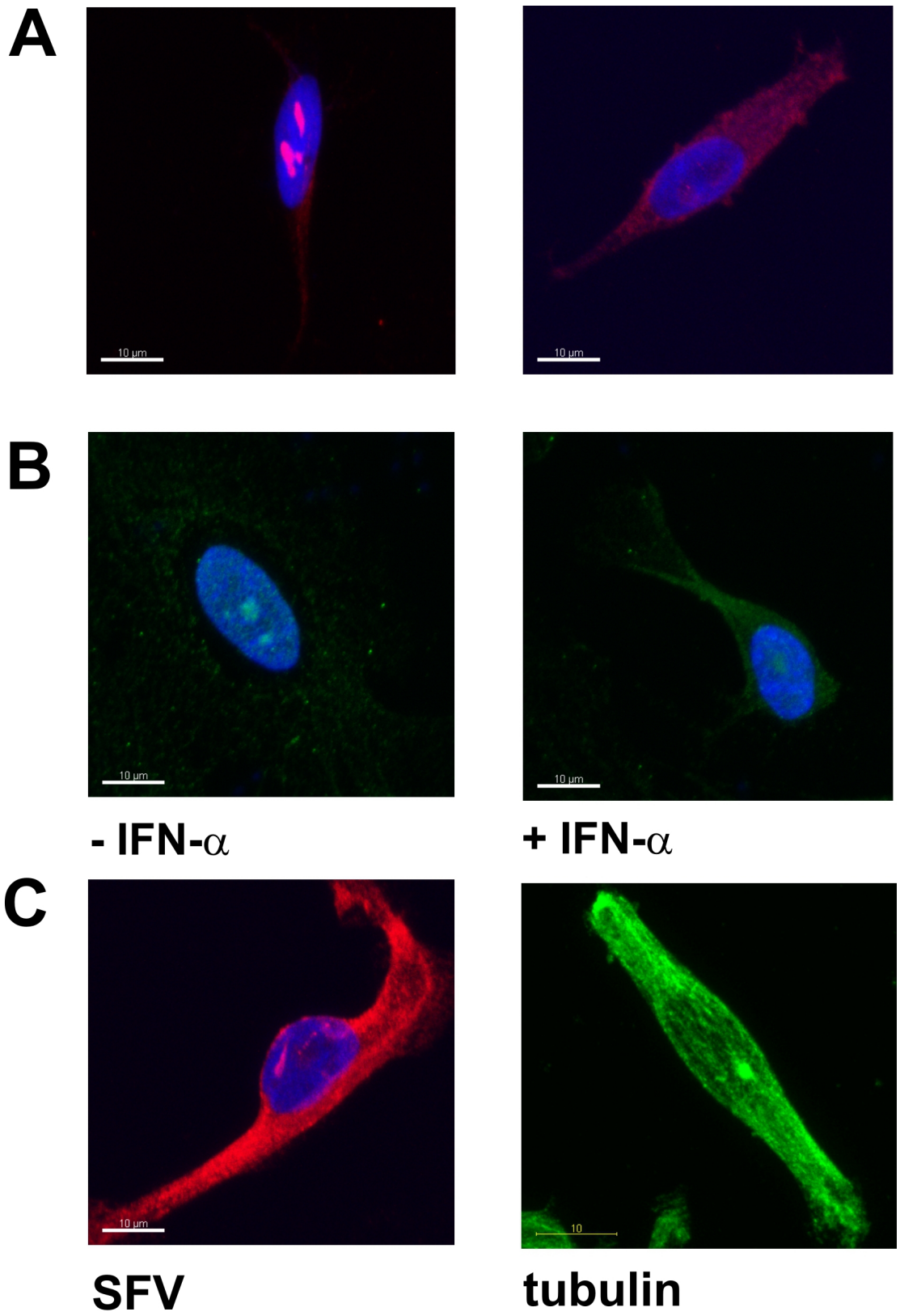

Figure 2. Cellular localization of IFI44 by immunofluorescence. **(A)** ME15 or **(B)** D10 cells were incubated with 1000 U IFN-α for 24 h, followed by fixation and staining with a polyclonal rabbit antibody raised against an immunogenic peptide of IFI44. Antibody/antigen complexes were labeled with a secondary antibody conjugated with red (ME15) or green (D10) fluorochromes. In noninduced cells, some fluorescent patches are consistently detectable in the nucleus of ME15 and D10 cells (left). After IFN-α stimulation,

red (ME15) or green (D10), the nuclear signal fades, and diffuse fluorescence of the cytoplasm appears. **(C)** ME15 cells infected with an SFV that expresses recombinant IFI44 (left) or a typical microtubular staining pattern obtained with antitubulin antibodies in ME15 cells as reference (right).

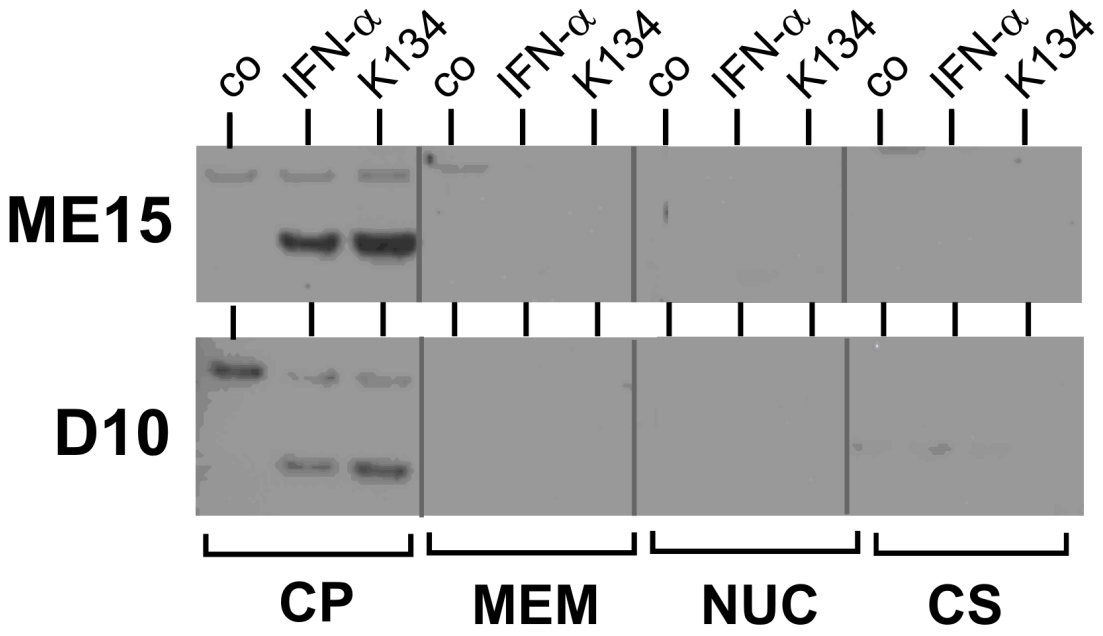

Figure 3. Immunoblot detection of IFI44 in cellular fractions of ME15 (top) or D10 (bottom) cells. Uninduced cells (co) and cells induced with IFN-α or K134 for 24 h (a lysine 134 monopegylated form of IFN-α) were lysed and fractionated by differential centrifugation into cytoplasm (CP), membranes (MEM), nuclei (NUC), and cytoskeleton (CS) using a commercial kit (for details, see Materials and Methods). Equal amounts of total protein were separated by SDS-PAGE, immobilized on membranes, and probed with IFI44 rabbit serum. Consistent with Figure 2, IFI44 is detectable only in the cytoplasm and virtually absent in the remaining fractions, including cytoskeleton and nucleus.

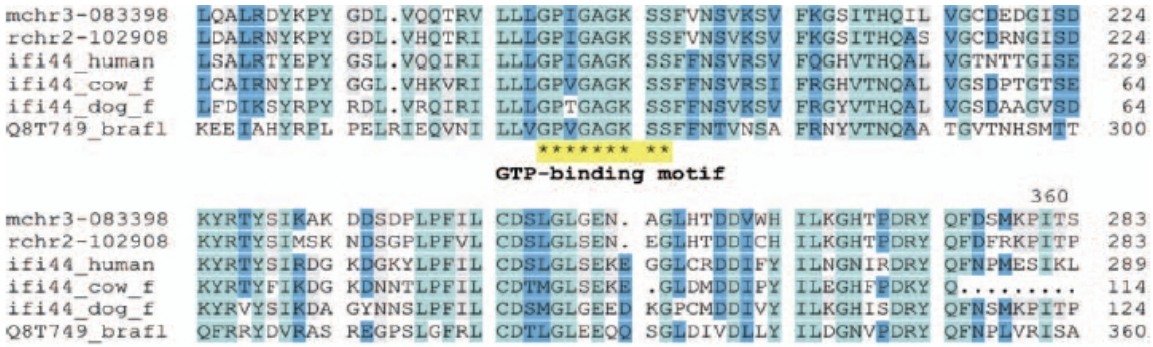

Figure 4. Comparative genomics analysis of IFI44. The coding sequences of IFI44 orthologs of human, mouse, rat, cow, dog, bat, and fish were aligned, and conserved amino acid blocks are highlighted in blue. A GTP-binding motif found in all known GTPases and G proteins is showcased in yellow (Pavlovic et al., 1993).

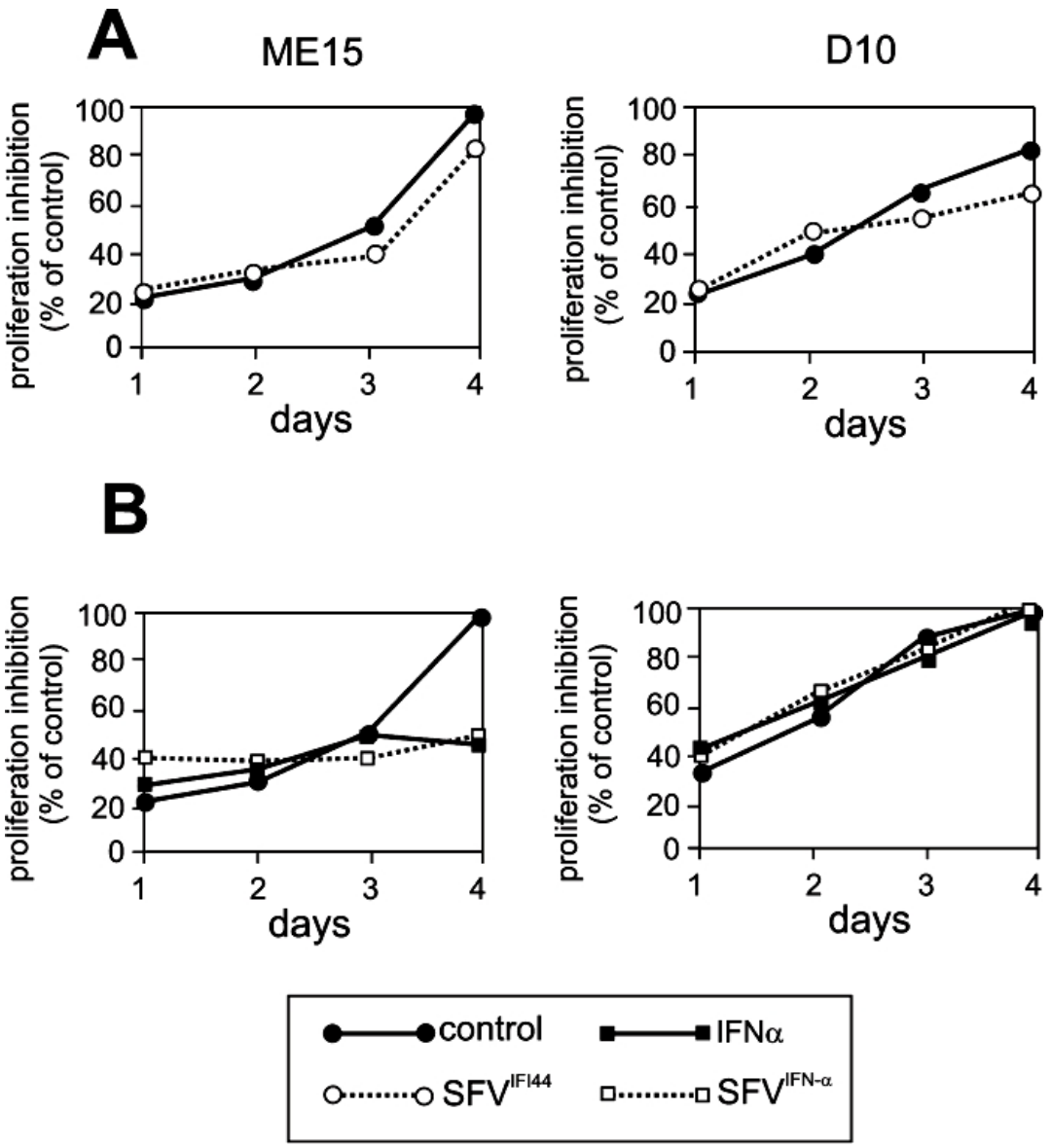

Figure 5. Antiproliferative activity of IFI44. **(A)** ME15 (IFN-α sensitive) or D10 (IFN-α resistant) cells were infected either with SFV vector control or with a virus stock that overexpresses IFI44(SFV^{IFI44}) Proliferation was measured in triplicate cultures over a period of 4 days using a calometric assay and expressed as percent of control (for details, see Materials and Methods). **(B)** As reference, ME15 and D10 cells were stimulated with IFN-α and, in addition, infected with an SFV that expresses secreted recombinant IFN-α (SFV$^{IFNα)}$. Control cells in **B** were grown without IFN-α or viral stock. Consistent with the literature, both IFN-α formulations inhibited only the growth of ME15 cells, whereas D10 proliferation was essentially unaffected. Notably, SFV^{IFI44} infection affected the growth of both cell lines to a similar extent.

References

Feld JJ, Hoofnagle JH. Mechanism of action of interferon and ribavirin in treatment of hepatitis C. *Nature* 2005;436:967–972.

Hoofnagle JH. Therapy of viral hepatitis. *Digestion* 1998;59: 563–578.

Zeuzem S, Heathcote J E, Martin N, Nieforth K, Modi M. Peginterferon alfa-2a (40 kDa) monotherapy: a novel agent for chronic hepatitis C therapy. *Expert Opin. Invest. Drugs* 2001;10:2201–2213.

Bain VG, Yoshida EM, Kaita, KD, Swain MG, Heathcote EJ, Garcia A, Moore PA, Yu R, McHutchison JG, Subramanian GM. Dynamics of interferon-specific gene expression in peripheral blood of interferon alfa-naive patients with genotype 1 chronic hepatitis C infection treated with albumin-interferon alfa. *Hepatol. Res.* 2006;35:256–262.

Basu A, Meyer K, Lai KK, Saito K, Di Bisceglie AM, Grosso LE, Ray RB, Ray R. Microarray analyses and molecular profiling of Stat3 signaling pathway induced by hepatitis C virus core protein in human hepatocytes *Virology* 2006;349:347–358.

Certa U, Wilhelm-Seiler M, Foser S, Broger C, Neeb M. Expression modes of interferon-alpha inducible genes in sensitive and resistant human melanoma cells stimulated with regular and pegylated interferon-alpha. *Gene* 2003;315:79–86.

Foser S, Weyer K, Huber W, Certa U. Improved biological and transcriptional activity of monopegylated interferon-alpha-2a isomers. *Pharmacogenomics J.* 2003;3:312–319.

Patzwahl R, Meier V, Ramadori G, Mihm S. Enhanced expression of interferon-regulated genes in the liver of patients with chronic hepatitis C virus infection: detection by suppression-subtractive hybridization. *J. Virol.* 2001;75:1332–1338.

Walters KA, Smith MW, Pal S, Thompson JC, Thomas MJ, Yeh MM, Thomas DL, Fitzgibbon M, Proll S, Fausto N, Gretch DR, Carithers RL, Shuhart MC, Katze MG. Identification of a specific gene expression pattern associated with HCV-induced pathogenesis in HCV and HCV/HIV-infected individuals. *Virology* 2006;350:453–464.

Honda Y, Kondo J, Maeda T, Yoshiyama Y, Yamada E, Shimizu Y K, Shikata T, Ono Y. Isolation and purification of a non-A, non-B hepatitis-associated microtubular aggregates protein. *J. Gen. Virol.* 1990;71:1999–2004.

Hwang Y, Chen EY, Gu ZJ, Chuang WL, Yu ML, Lai MY, Chao YC, Lee CM, Wang JH, Dai CY, Shian-Jy Bey M, Liao YT, Chen PJ, Chen DS. Genetic predisposition of responsiveness to therapy for chronic hepatitis C. *Pharmacogenomics* 2006;7:697–709.

Brem R, Oraszlan-Szovik K, Foser S, Bohrmann B, Certa U. Inhibition of proliferation by 1-8U in interferon-alpha-responsive and non-responsive cell lines. *Cell. Mol. Life Sci.* 2003;60:1235–1248.

Lundstrom K, Rotmann D, Hermann D, Schneider EM, Ehrengruber MU. Novel mutant Semliki Forest virus vectors: gene expression and localization studies in neuronal cells. *Histochem. Cell Biol.* 2001;115:83–91.

Guo JT, Bichko VV, Seeger C. Effect of alpha interferon on the hepatitis C virus replicon. *J. Virol.* 2001;75:8516–8523.

MacMicking JD. IFN-inducible GTPases and immunity to intracellular pathogens. *Trends Immunol.* 2004;25:601–609.

Pavlovic J, Schroder A, Blank A, Pitossi F, Staeheli P. Mx proteins: GTPases involved in the interferon-induced antiviral state. *Ciba Found. Symp.* 1993;176:233–243.

Stork PJ, Schmitt JM. Crosstalk between cAMP and MAP kinase signaling in the regulation of cell proliferation. *Trends Cell Biol.* 2002;12:258–266.

Li G, Segu VB, Rabaglia ME, Luo RH, Kowluru A, Metz SA. Prolonged depletion of guanosine triphosphate induces death of insulin-secreting cells by apoptosis. *Endocrinology* 1998;139: 3752–3762.

Leyssen P, Balzarini J, De Clercq E, Neyts J. The predominant mechanism by which ribavirin exerts its antiviral activity *in vitro* against flaviviruses and paramyxoviruses is mediated by inhibition of IMP dehydrogenase. *J. Virol.* 2005;79:1943–1947.

Phylogenetic analysis of interferon inducible transmembrane gene family and functional aspects of IFITM3.

Fredy Siegrist[1], Martin Ebeling[2], Ulrich Certa[1]
[1] RNAi Safety & Genomics, F. Hoffmann-La Roche Ltd., Basel Switzerland,
[2] Computational Biology, F. Hoffmann-La Roche Ltd., Basel Switzerland.

Abstract

Interferon inducible transmembrane (IFITM) proteins are involved in early development, cell adhesion and the inhibition of cell growth in response to interferons (IFN). These genes can be transcribed in most tissues capable of IFN signaling with the exception of bone-specific IFITM5/BRIL. They are clustered within a distinct region in the vicinity of IFITM5 which shows highest homology to corresponding genes in most other vertebrate species. Some processed pseudogenes lacking the single intron are spread over investigated genomes and apparently do not code for functional proteins. Phylogenetic analysis of the protein coding sequences point to the presence of a single interferon inducible IFITM in the ancestor of rodents and primates. The distinct functions studied so far in primates and rodents may have evolved in parallel but should not be casually inferred based on identical gene names. Cancer cells tend to have deregulated levels of IFITM transcripts. IFITM3 reintroduced into cell lines with low basal levels is sufficient to drive growth arrest and a senescence-like morphology. Overexpressed IFITM3 proteins are moved from inner cell organelles to the membrane in small caveolae-like compartments. Nevertheless they can be isolated from the culture medium and show intracellular processing when attached to a protein tag. IFN alpha-induced growth inhibitory signals are transmitted from mouse to human cells and may be carried by IFITM proteins. According to our results, IFITM3 protein expression alone is not sufficient to transfer growth-inhibitory signals. However, high IFITM levels in tumor cells may point to a progression state where one of the IFN-controlled antiproliferative pathways has been switched off.

IFITM genes in cancer

IFITM gene expression levels are altered in cancer cells (Brem et al, 2001). We have found both full transcriptional silenced and virtually unrestricted expression of IFITM3 genes in melanoma cells. IFITM3 is important for development (Smith C et al, 2007) and underlies epigenetic regulation by DNA methylation. Cancer patients with a hypermethylator phenotype show an aberrant methylation status of IFITM promoter sequences. Tumor suppressor protein p53 proficient cancer cells may benefit from transcriptional silencing of IFITM genes and p53 deficient cells may even profit from high abundance of IFITM transcripts by potential anti-proliferative signaling to adjacent normal cells or by regulation of the immune system.

Abbreviations

BRIL: (protein)	Bone marrow restricted IFITM like
CDS:	Coding sequence
IFITM: (gene)	Interferon inducible transmembrane
IFN (IFNα):	Interferon (alpha)
IIP:	Interferon induced protein (in fish)
IQR:	Inter quartile range
GAS: sequence/site	(Interferon) gamma activated
ISRE: element	Interferon-stimulated response
SNAP-tag®:	Small protein based on human O^6-alkylguanine- DNA-alkyltransferase
9-27 / 1-8D / 1-8 U:	human IFITM 1/2/3 protein synonyms (see figure legend 2)

CD225 domain proteins and consensus sequence of IFITM and BRIL

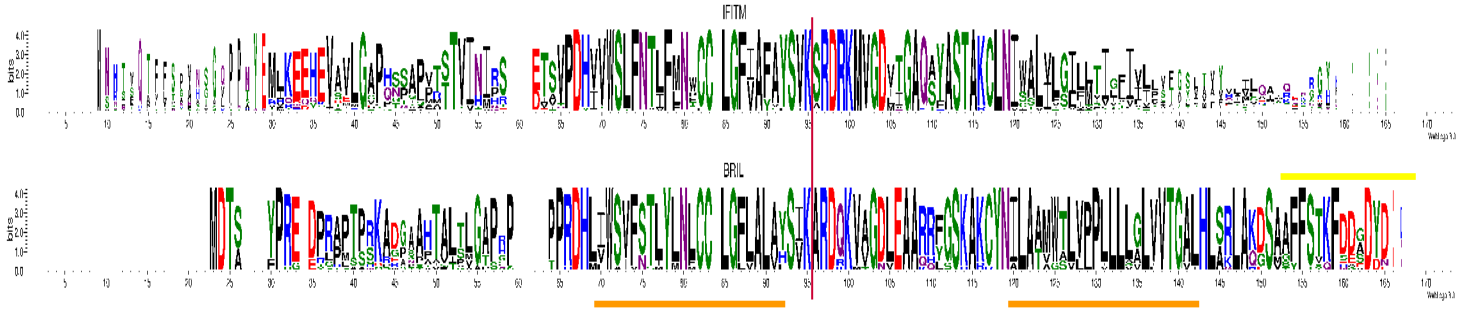

Figure 1

Amino-acid occurrence in putative homologues of IFITM1-3 (top) and IFITM5 (BRIL) proteins (bottom). Probability is calculated from genomic sequences of 55 mammalian (IFITM1-3 and homologous) or 17 different mammals and one bird (IFITM5) genes. The conserved exon splice-junction is indicated by a vertical line. Potentially calcium binding domain of BRIL is highlighted by a yellow line above and predicted trans-membrane regions are underlined in orange.

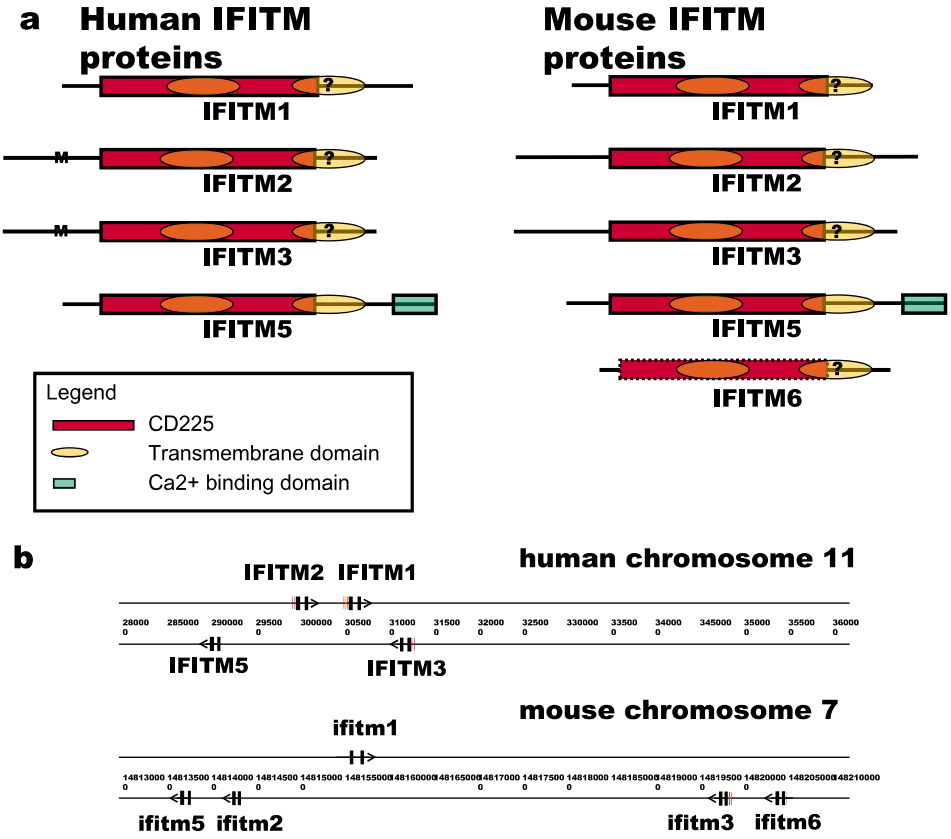

Figure 2 A) Structural diagram of human and mouse IFITM proteins 9-27 / fragilis2 (IFITM1), 1-8D / fragilis3 (IFITM2), 1-8U / fragilis (IFITM3), fragilis5 (ifitm6) and BRIL / fragilis4 (IFITM5), mil4 (ifitm7) is not shown.B) Mapping of IFITM genes to human and mouse chromosome locus. There are 2 ISRE promoter elements (red) in IFITM1-3 and an additional GAS (yellow) in IFITM1 (Lewin et al, 1991).

Phylogenetic analysis

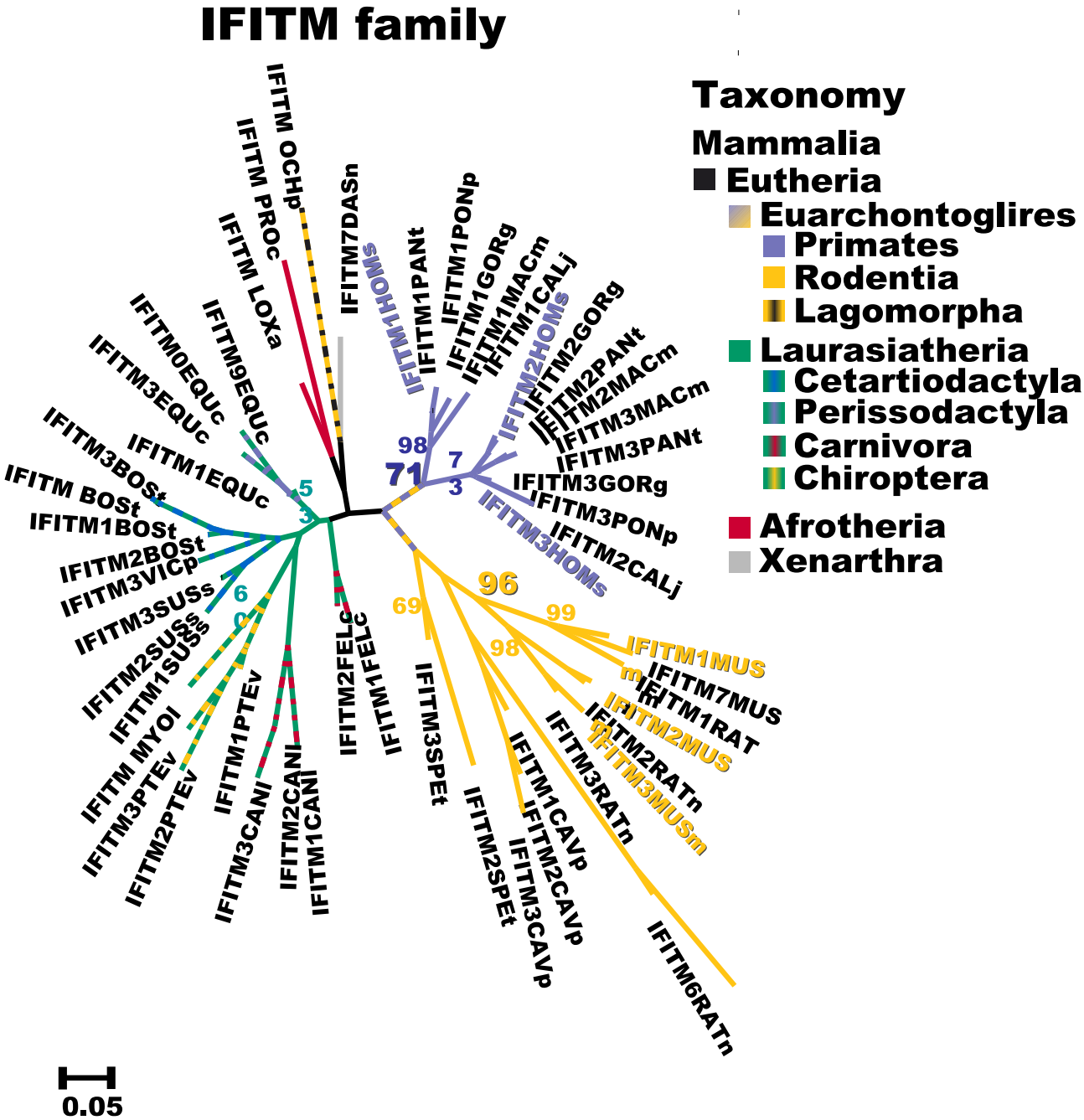

Figure 3 Phylogenetic tree (maximum likelihood approach) for trimmed CDS sequences of 55 mammalian variants of IFITMs. Identified BRIL sequences, fish IIP sequences and other, ambiguous sequences were not taken into account for this analysis. Bootstrap values based on 100 replicates are shown for branches of interest. Enlarged numbers indicate the high probability for occurrence of a singe common ancestor for all primate interferon induced transmembrane genes and one for all Old World rats and mice (Murinæ).

The interferon induced protein family members in humans IFITM1, IFITM2 and IFITM3, share more DNA homology within their taxonomic order than to homologues in other vertebrates, suggesting one common ancestor of these sequences when rodents and rabbits separated from primates (figure 3).
IFITM5, also described as bone marrow restricted IFITM like (BRIL, Moffatt et al, 2008),

has homologs in many species among the jawed vertebrates (not shown). In contrast to IFITM1-3, BRIL has a highly conserved aspartate-rich domain of probably calcium ion binding function at its C-terminus (see figure 1).
A clear ordering of the rodent-specific IFITM6 fails within the interferon regulated IFITM proteins. This gene shows higher mutation rates when assuming descent from the same ancestor, thus its evolution resembles that of an antiviral gene with positive selection pressure or reflects the mutation rate of a dying gene. The sequences of primates and rodents look clearly separated, suggesting a single gene in the ancestor of placental mammals.

Cellular localization, secretion and processing of IFITM3 fusion proteins

IFITM proteins are transferred in caveolae like vesicles to the cell membrane (Xu et al, 2009) and can be detected in the supernatant of constitutively expressing cells and IFN-treated cells at comparable levels to ISG15 (d'Cunha et al, 1996). Fusion proteins in human cells were processed to endogenous protein size (figure 4a), similarly to the mouse model (Smith RA et al, 2006). Processed IFITM proteins may act as tumor-associated antigenic peptides (Tirosh et al, 2007) in all MHC class I presenting cells. We have suggested that secreted IFITM3 proteins could interact with receptors on other cells (Brem et al, 2003), but so far we could not demonstrate transfer of 1-8 protein.
Processed amino-terminal and intact carboxy-terminal SNAP-tagged fusion proteins could be found in concentrated supernatants (figure 4b). IFITM3 sensitive cell lines with knocked-in fusion protein are initially blocked in proliferation and adopt a senescence like morphology. The majority of these cells regain proliferative ability only when IFITM3 expression is strongly diminished. This effect is stronger when the protein is tagged at the C terminus and predominantly processed to endogenous protein size.

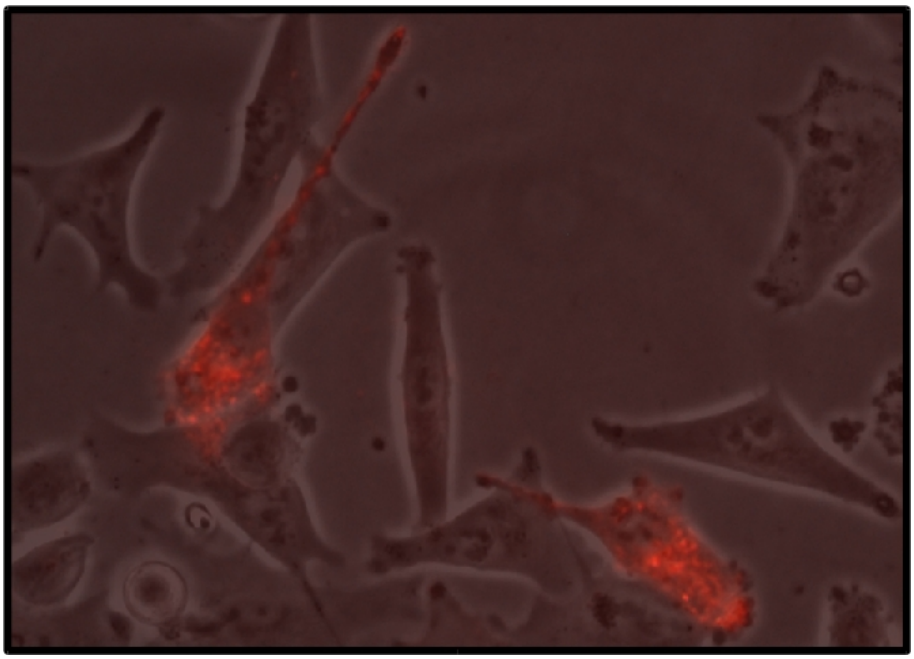

Figure 5 Live cell imaging of TMR star labeled human IFITM3 SNAP tag fusion (N-tag) proteins. ME-15 (melanoma) cells were labeled 16 hours after transfection of plasmid and incubated for 4 hours to allow protein trans-location. Overlay of fluorescence and phase contrast (25%) channels is shown.

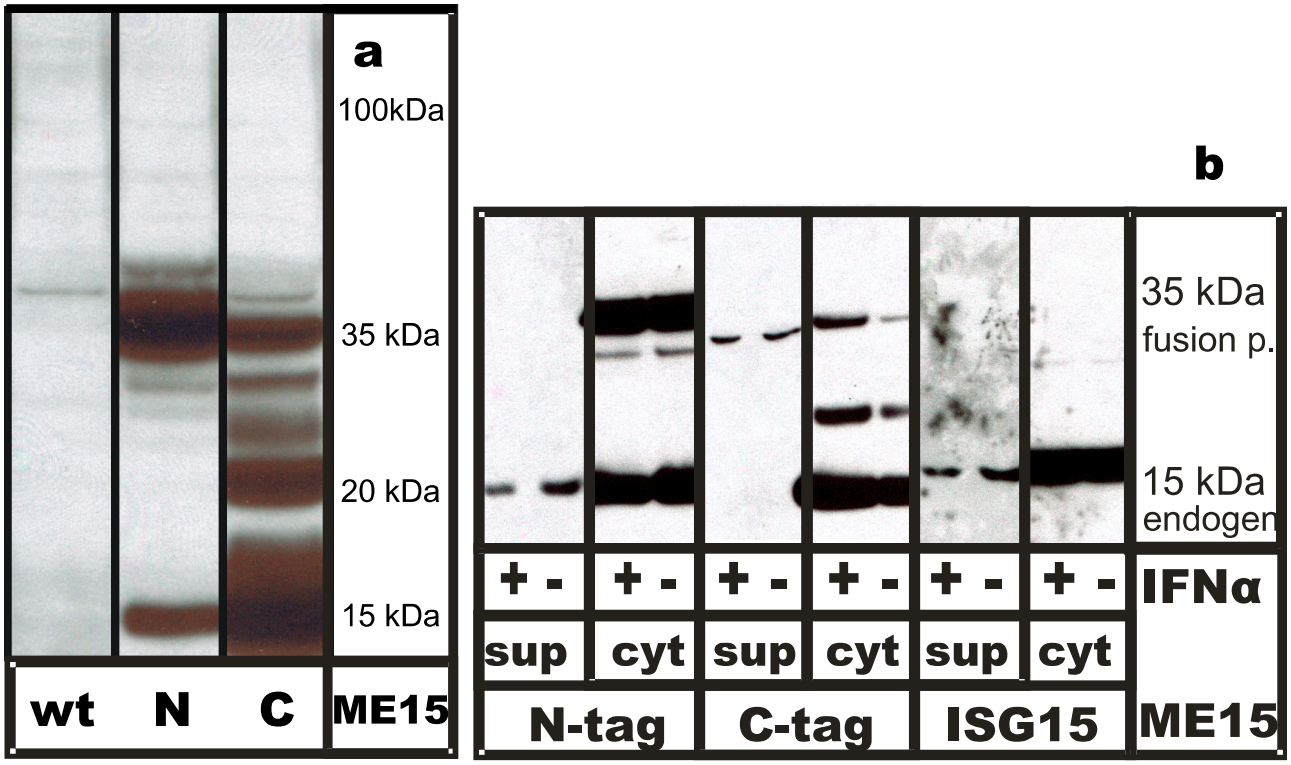

Figure 4 A) Degradation pattern of amino-terminal SNAP-tagged (N-tag) and carboxy-terminal SNAP-tagged IFITM3-fusion proteins (35 kDa) and unspecific antibody binding (wt). B) Detection of processed IFITM3 (15 kDa), fusion-proteins (35 kDa) and endogenous ISG15 protein (15 kDa) in the supernatant (sup) and cytosolic protein (cyt) levels under IFN alpha (+) or PBS treatment (- control).

Co-cultures – no observable effect of growth arrest signal transduction

Anti-proliferative signals can be transmitted from one cell to the other when the interferon system has been activated (Lloyd et al, 1983). IFITM1-3 proteins are able to inhibit cell growth (Hillman et al, 1987, Deblandre et al, 1995, Brem et al, 2003, Ropolo et al, 2004). IFITM proteins are also known to interact with receptor complexes (Smith RA et al, 2006). 1-8 proteins are able to bind viral proteins and induce apoptosis in infected cells (Joung et al, 2003). IFITM proteins drive cells to senescence by interaction with the ATM-p53 pathway (Kim et al, 2009) . Overexpression of IFITM3 genes in tumor cells is sufficient to drive them into senescence.
We investigated the potential of 1-8U protein to be transmitted from one cell to the adjacent and to act as a co-receptor, by blocking with antibodies. A transfer of protein or a significant change in the proliferation rate was not observed in our experiments. In addition, there was no significant benefit for growth sensitive tumors cells when anti-serum against 1-8 proteins was added to the culture medium. In conclusion, we have demonstrated that expression of IFITM3 genes is not sufficient for the transfer of interferon induced anti-proliferative signals in our model system.

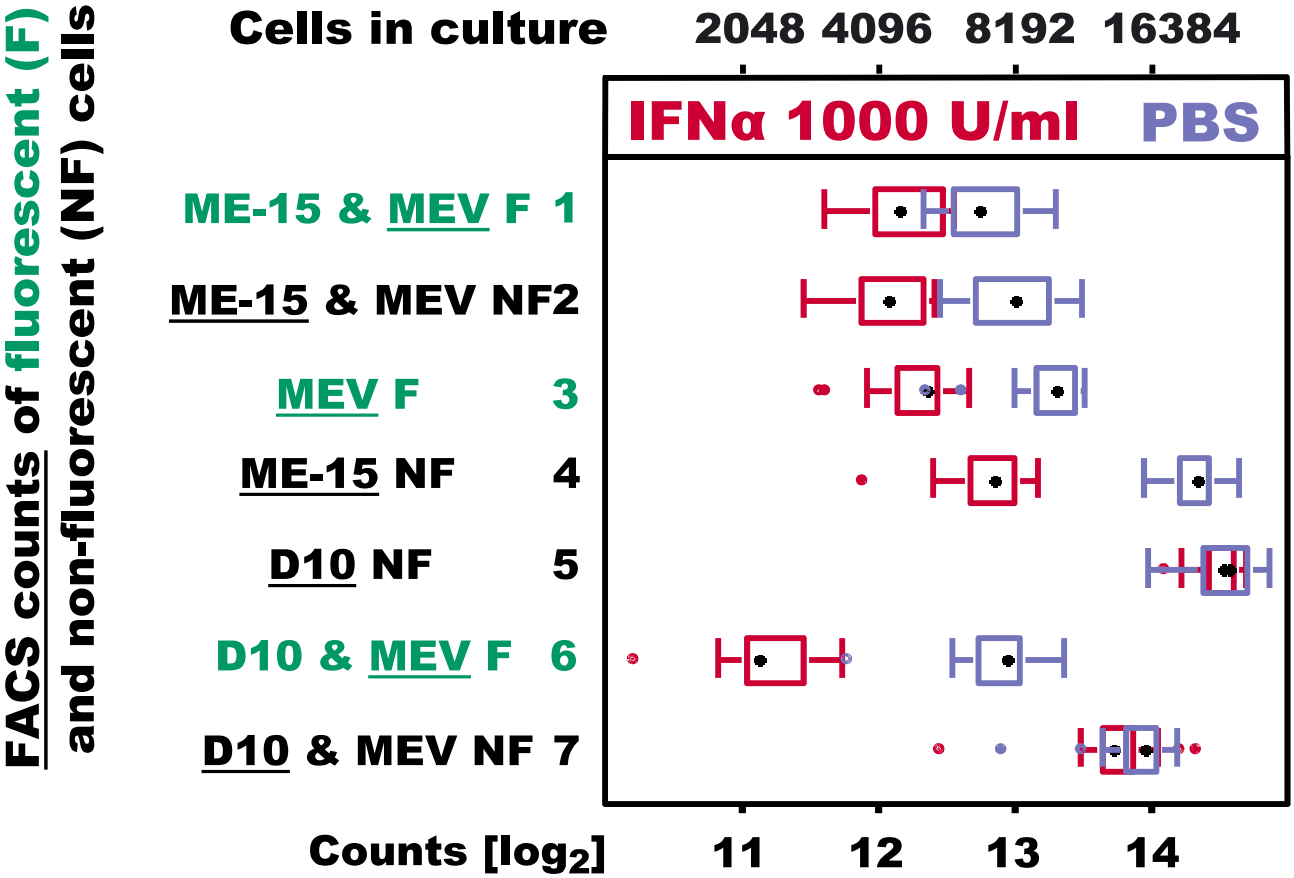

Figure 6 Effects of IFITM3 in co-cultures and interferon alpha treatment. Cell counts of interferon alpha (red) or control treated cultures (blue) sorted by fluorescence signal. Human melanoma cells were grown alone (lines 3-5), fluorescent labeled cells (MEV) were cultured with their unlabeled counterpart (lines 1+2) or with IFITM3 positive cells (D10) that show no growth response to IFN alpha treatment (lines 6+7). Box-and-whisker plot show median (black dot), lower and upper quartile (box), range (whiskers, 1.5x IQR) and outliers (colored dots) of (log2) counted cell numbers by FACS (Fluorescence-Activated Cell Sorting).The culture medium was optionally supplemented by dilution series of IFITM3 anti-serum or preimmunization serum. Serum treatment resulted in growth advantage (p-value = 0.01) independent of IFITM3 antibodies (p-value = 0.31), variance shown here arise partially from increased rabbit serum levels.

Venus protein was a gift from the Miyawaki lab (Nagai et al, 2002).

Conclusions

IFITM gene locus is a hot spot of gene duplications and mutations
IFITM1-3 multiplied and evolved only recently
► shared functions in all mammalian variants
IFITM proteins are processed and found in extracellular compartments
IFITM3 expression is sufficient for cellular senescence
but not for anti-proliferative cell to cell signaling

References

Brem R, Hildebrandt T, Jarsch M, Van Muijen GN, Weidle UH. Identification of metastasis-

associated genes by transcriptional profiling of a metastasizing versus a non-metastasizing human melanoma cell line. *Anticancer Res*. **2001** May-Jun;21(3B):1731-40.

Brem R, Oraszlan-Szovik K, Foser S, Bohrmann B, Certa U. Inhibition of proliferation by 1-8U in interferon-alpha-responsive and non-responsive cell lines. *Cell Mol Life Sci*. **2003** Jun;60(6):1235-48.

D'Cunha J, Knight E Jr, Haas AL, Truitt RL, Borden EC. Immunoregulatory properties of ISG15, an interferon-induced cytokine. *Proc Natl Acad Sci U S A*. **1996** Jan 9;93(1):211-5.

Deblandre GA, Marinx OP, Evans SS, Majjaj S, Leo O, Caput D, Huez GA, Wathelet MG. Expression cloning of an interferon-inducible 17-kDa membrane protein implicated in the control of cell growth. *J Biol Chem*. **1995** Oct 6;270(40):23860-6.

Hillman MC Jr, Knight E Jr, Blomstrom DC. A membrane protein from IFN-beta-treated Daudi cells causes a cessation in cell growth. *Biochem Biophys Res Commun*. **1987** Oct 14;148(1):140-7.

Kim KS, Kang KW, Seu YB, Baek SH, Kim JR. Interferon-gamma induces cellular senescence through p53-dependent DNA damage signaling in human endothelial cells. *Mech Ageing Dev*. **2009** Mar;130(3):179-88.

Joung I, Angeletti PC, Engler JA. Functional Implications in Apoptosis by Interferon Inducible Gene Product 1-8D, the Binding Protein to Adenovirus Preterminal Protein. *J Microbiol*. **2003**;41(4):295-9.

Lewin AR, Reid LE, McMahon M, Stark GR, Kerr IM. Molecular analysis of a human interferon-inducible gene family. *Eur J Biochem*. **1991** Jul 15;199(2):417-23.

Lloyd RE, Blalock JE, Stanton GJ. Cell-to-cell transfer of interferon-induced antiproliferative activity. *Science*. **1983** Sep 2;221(4614):953-5.

Moffatt P, Gaumond MH, Salois P, Sellin K, Bessette MC, Godin E, de Oliveira PT, Atkins GJ, Nanci A, Thomas G. Bril: a novel bone-specific modulator of mineralization. J *Bone Miner Res*. **2008** Sep;23(9):1497-508.

Nagai T, Ibata K, Park ES, Kubota M, Mikoshiba K, Miyawaki A. A variant of yellow fluorescent protein with fast and efficient maturation for cell-biological applications. *Nat Biotechnol*. **2002** Jan;20(1):87-90.

Ropolo A, Tomasini R, Grasso D, Dusetti NJ, Cerquetti MC, Iovanna JL, Vaccaro MI. Cloning of IP15, a pancreatitis-induced gene whose expression inhibits cell growth. *Biochem Biophys Res Commun*. **2004** Jul 2;319(3):1001-9.

Smith C, Berg D, Beaumont S, Standley NT, Wells DN, Pfeffer PL. Simultaneous gene quantitation of multiple genes in individual bovine nuclear transfer blastocysts. *Reproduction*. **2007** Jan;133(1):231-42.

Smith RA, Young J, Weis JJ, Weis JH. Expression of the mouse fragilis gene products in immune cells and association with receptor signaling complexes. *Genes Immun*. **2006** Mar;7(2):113-21.

Tirosh B, Daniel-Carmi V, Carmon L, Paz A, Lugassy G, Vadai E, Machlenkin A, Bar-Haim E, Do MS, Ahn IS, Fridkin M, Tzehoval E, Eisenbach L. '1-8 interferon inducible gene family': putative colon carcinoma-associated antigens. *Br J Cancer*. **2007** Dec 17;97(12):1655-63.

Xu Y, Yang G, Hu G. Binding of IFITM1 enhances the inhibiting effect of caveolin-1 on ERK activation. Acta Biochim Biophys Sin (Shanghai). 2009 Jun;41(6):488-94.

MicroRNA Expression Profiling by Bead Array Technology in Human Tumor Cell Lines Treated with Interferon-Alpha-2a

Fredy Siegrist, Thomas Singer, and Ulrich Certa
Pharmaceutical Research, Global Preclinical Safety (PRN), F. Hoffmann-La Roche Ltd., 4070 Basel, Switzerland

Biol Proced Online. 2009 December; 11(1): 113–129.
Published online 2009 July 23. doi: 10.1007/s12575-009-9012-1.

Key words: MicroRNAs, Oligonucleotide Array Sequence Analysis, Interferons, Melanoma, Hepatoma, Reverse Transcriptase Polymerase Chain Reaction, Suppressor of Cytokine Signaling Proteins

Abstract

MicroRNAs are positive and negative regulators of eukaryotic gene expression that modulate transcript abundance by specific binding to sequence motifs located prevalently in the 3′ untranslated regions of target messenger RNAs (mRNA). Interferon-alpha-2a (IFNα) induces a large set of protein coding genes mediating antiproliferative and antiviral responses. Here we use a global microarray-based microRNA detection platform to identify genes that are induced by IFNα in hepatoma- or melanoma-derived human tumor cell lines. Despite the enormous differences in expression levels between these models, we were able to identify microRNAs that are upregulated by IFNα in both lines suggesting the possibility that interferon-regulated microRNAs are involved in the transcriptional repression of mRNA relevant to cytokine responses.

Introduction

The gene expression patterns of tumor-derived cell lines differ greatly, as do their responses to antiproliferative effects of interferons (IFNs). The cause of this variation has been under investigation for more than 40 years, but only basic regulatory mechanisms of interferon signaling are understood today. Small regulatory genome encoded RNAs, such as microRNAs, have recently attracted attention in genomic research. New methods to analyze the levels of these regulatory elements are now commercially available, but the power of these techniques is still discussed extensively. Our study was designed to compare two methods for microRNA detection with respect to usefulness in defined cell culture assays. The experimental design assesses variation between the two cell lines and the treatment effects of IFNα.

A hallmark of the therapeutic activity of type I interferons is the induction of antiproliferative activity mediated by the upregulation of several hundred response genes with pleiotropic functions (1). These genes can be divided into two major classes based on the kinetic properties of induction (2). Primary response genes (PRGs) are upregulated within 24 h after the cytokine signal and the secondary response genes (SRGs) are induced following day1 when the activity of the PRGs decays. In contrast to SRGs, all PRGs studied to date contain bona fide interferon response elements in the promoter region, which are required for binding of the interferon-stimulated gene factor 3 (ISGF3) complex and for janus kinase/signal transducer of transcription (JAK/STAT)-pathway-mediated signaling. Expression of PRGs is turned off by proteins termed suppressors of cytokine signaling (SOCS) (3). As the nomenclature indicates, this class of polypeptides has the capacity to

interfere and silence other cytokine-induced signaling cascades (for review see (4)). SOCS1 for instance is part of the early inducible PRG cluster and down modulation occurs together with the other genes before onset of SRG expression. It is believed that feedback inhibition of JAK/STAT signaling by SOCS1 represses transcriptome modulation of IFNα signaling (5). Regulation of SOCS protein translation by interferon-regulated microRNAs (IRmiRs) would enhance the potential of cytokine fine regulation. It has been reported that miR-19 antagonists lead to higher SOCS1 levels and miR-19 mimics can repress SOCS1 reporter constructs, thus obviously supporting the bioinformatic predictions that SOCS1 is a direct target of miR-19 (6). Inhibition of SOCS activity could for instance prolong the duration of cytokine activity, which has obvious clinical implications.

Following the discovery of microRNAs in virtually all higher eukaryotic organisms significant research efforts were initiated to address the function of these catalytic oligonucleotides which are the natural counterparts of synthetic small inhibitory RNAs (siRNAs) used for experimental gene silencing (for review see (7)). MicroRNAs are positive and negative modulators of the expression of entire gene clusters that contain complementary microRNA recognition sequence motifs in the 3′-UTR. Today, prediction of microRNA target genes by homology-based algorithms is still ambiguous (8). The activity of one or several microRNAs could explain suppression of the entire PRG cluster provided that microRNA abundance is regulated by IFNα. Alternatively, microRNA-mediated degradation of transcripts encoding negative regulatory proteins would also abolish PRG expression and restore IFNα responsiveness.

Some recent reports showed that interferon beta (IFNβ) stimulation can boost microRNA levels in cell culture together with inhibition of viral replication (9). At this point it is an open question whether this induction is IFNβ specific or a shared feature of all type I interferons. To investigate whether microRNA are also involved in regulation of IFNα response, we used two human-tumor-derived cell lines: the melanoma line ME-15 (10) and the hepatoma line HuH7 (11). We have chosen these cell lines as models, because we have a good understanding of the IFNα responses at the mRNA and the protein levels in these cell lines. Further we chose to use a melanoma cell line because IFN is also used for treatment of this cancer type. HuH7 is commonly used as a model for testing antiviral effects of IFN in the HCV replicon system. In both models efficient responses to IFNα have been shown at the functional and transcriptional level. IFNα response genes carry response elements in their promoter region and these motifs are responsible for gene expression with similar efficiency in many cell types. Therefore we expected to find a similar regulated set of genes in both lines given that IRmiR genes are regulated by the same mechanism, whereas some constitutively expressed microRNA genes were expected to be cell type specific for functional reasons. We have chosen a DNA-microarray-based technology (Illumina) for the multi-parallel expression analysis of all known human microRNAs (http://microrna.sanger.ac.uk/; Release 10.0: August 2007). This method allowed us to process total RNA as template, allowing the possibility of mRNA gene expression profiling in further experiments. Briefly, annealing of microRNA specific primers combined with enzymatic polyadenylation allows multi-parallel polymerase chain reaction (PCR)-mediated amplification of individual microRNAs. The output of this step is a DNA amplicon library that reflects to a large extent the original stoichiometry of mature microRNAs in a cell or tissue (12). PCR amplification is performed with fluorescently labeled primers, which allows quantitative signal detection by conventional confocal laser scanning.

Materials and Methods

Cell Culture, Interferon Treatment, and RNA Precipitation

Melanoma cells (ME-15) were cultured in RPMI 1640 with L-Glutamine supplemented with non-essential amino acids and sodium pyruvate (1 mM) and hepatoma (HuH7) cells were cultured in DMEM + GlutaMAX. Both media contained 10% FBS. All cell culture reagents were purchased from Invitrogen (GIBCO®). Roferon (Interferon alpha2a, ROCHE) was diluted in fresh medium to a final concentration of 1,000 U/mL and control cultures were grown without cytokine. Cells were cultured at 37°C in a humidified atmosphere containing 5% CO2. Total RNA preparation was carried out using TRIZOL (Invitrogen) total RNA extraction using 1/2 volume of 1-bromo-3-chloro-propane (molecular biology grade, SIGMA) as chloroform substitute. For efficient recovery of small RNAs, DNA LoBind tubes (Eppendorf) were used and all centrifugation steps were performed at maximum speed and 4°C in an Eppendorf 5417R centrifuge. Total RNA was precipitated with 2 vol of 2-propanol (Fluka) at −20°C for at least 16 h. The RNA pellet was washed with 75% ethanol (Merck), dried, and dissolved in DEPC-treated water (Ambion). The RNA was quantified with Quant-iT™ RiboGreen® RNA Assay (Invitrogen) as suggested by Illumina.

Illumina Bead Array MicroRNA Detection

Starting with 500 ng/sample of total RNA, mature microRNAs were amplified with the Illumina human v1 MicroRNA expression profiling kit containing primers for 743 human microRNAs. The resulting amplicons were hybridized to a 96 sample universal probe capture array and fluorescent signals were detected by confocal laser scanning. All steps were performed according to Illumina's instructions manual.

Data Processing and Statistical Analysis

The data was processed with Beadstudio software (version 3.1.3, gene expression module 3.3.8) including the calculation of detection p values based on negative control bead signals. Log-transformation, loess normalization (13) and statistical analysis were performed with R (2.8.1) (14) using the package lumi (1.8.3) (15) and software contained therein, in particular limma (2.16.4) (16). Statistical models were chosen as follows: a linear model (limma t statistics) with two separate coefficients for HuH7 and ME-15 cells was used for the selection of differently expressed genes shown in Fig. 1 and Table 1. Statistics represented in the tables were calculated by testing the two indicated conditions as independent factors. In Table 1, p values were adjusted by the false discovery rate method (17). Treatment effects shown in Table 2b and Fig. 3a were modeled with two coefficients (cell line, treatment) for time point 4 h, p values arise from t statistics. Normalized relative fluorescence levels were calculated by 2^mean (of log2 transformed, loess normalized values). Change factors (CHF) were calculated as fold change on the linear scale minus 1 as previously described (2). Raw data, non-normalized, and normalized microRNA expression data have been submitted to the Gene Expression Omnibus with accession number GSE16421.

Quantitative PCR and Data Processing
microRNA levels were measured using TaqMan® microRNA assays (Applied Biosystems) using the TaqMan® MicroRNA reverse transcription (RT) kit with TaqMan® 2× universal PCR master mix (No AmpErase® UNG) as recommended by the supplier. Ten nanograms of total RNA was used as input for amplification using the samples used for microarray analysis. Reversed transcriptase products were diluted 1:15 and measured on an ABI 7900HT fast real-time PCR system. Technical replicates were run on three different plates (one with 40 cycles and two with 50 cycles) and threshold for cycling time (CT) calculation

was set for all probes to 0.2. For estimation of endogenous small RNA content, the nucleolar RNA RNU48 was used as control and reference.
Standard error (Δx) was calculated by the average standard error of treated and untreated MNE for biological replicates.

Results and Discussion

The following technical aspects have to be considered for result interpretation. The dataset of the microRNA bead array assay is not directly comparable to gene expression arrays where in vitro translated transcripts are directly hybridized to the probes. Moreover Illumina's bead array technology tends to have higher background fluorescence levels and lower change factor values than Genechips from Affymetrix. Background (average of negative control signals) and noise (standard deviation of negative probes from each sample) were 528 ± 60 and 229 ± 67, respectively. The density of all samples shows a bimodal distribution peaking around the background fluorescent levels and the robust levels (approximately 12,000). The curve is skewed to the right and peak density height is found in the ratio 4:1 considering all probes (data not shown). The distribution of probes detected in all samples (detection p value threshold at 0.01) has a plateau ranging from about 2,000 close to the detectors maximum capacity of 2^16 relative fluorescent units (12). As expected, the correlation of data coming from biological replicates $r^2 = 0.952 \pm 0.028$ (not normalized) and $r^2 = 0.956 \pm 0.022$ (after loess normalization and log-transformation) was lower than for technical replicates $r^2 > 0.97$ (12). We preferred loess normalization to quantile normalization because the later was too aggressive for the given small probe numbers.
As a first step we wished to address the robustness of the microRNA array in probe detection by selecting microRNA genes that are detected under all experimental conditions with high statistical significance in all biological triplicates (detection p value < 0.01). In each set of triplicate samples (control, 4 h or 24 h, IFNα stimulation) we detect approximately 270 genes that fulfill the above criteria. This corresponds to roughly a third of microRNAs available for detection in the assay system. Furthermore, this result suggests indirectly that IFNα treatment does not induce global changes in microRNA gene expression, but it modulates rather the expression of individual genes.
Today it is well established that microRNA expression patterns are cell and tissue type specific, which is consistent with a role in cell differentiation and biological function (8). Thus we expected to detect genes with preferential expression in either hepatoma or melanoma cells as these cell lines are derived from different tumors. Indeed, when all experimental conditions and data points are included in the data analysis about 150 microRNAs genes show preferential expression in either HuH7 or ME-15 cells (Fig. 1).

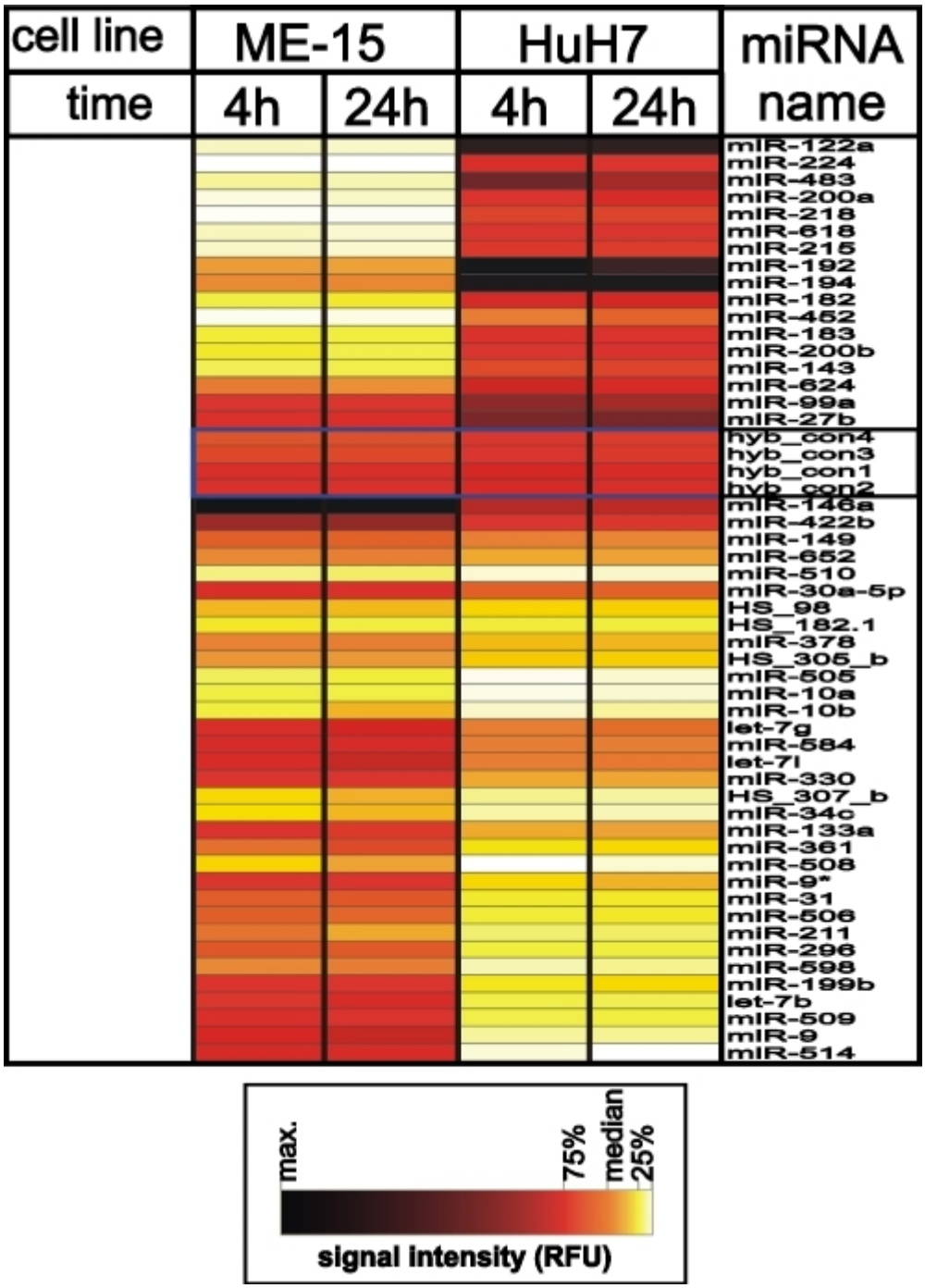

Fig. 1 Differential microRNA expression in human melanoma (ME-15) and hepatoma (HuH7) cells. microRNA expression levels were compared in two cell lines at two different time points and corrected for the treatment effect. The 50 most significant (p value below 10^{-12}) microRNA expression values from untreated samples are shown in a heat diagram including hybridization controls as reference for technical variance. White indicates noise levels, yellow indicates the first quartile, orange the median, red the third quartile, and black maximum expression levels. The intensity data, significance values and the IFNα-dependent expression levels are summarized in Table 1.

	Control						Interferon-alpha treated					
		4 h			24 h			4 h			24 h	
	ME-15	**HuH7**	**CHF**	**ME-15**	**HuH7**	**CHF**	**ME-15**	**HuH7**	**CHF**	**ME-15**	**HuH7**	**CHF**
microRNAs rated higher in HuH7												
hsa-miR-122a	685	30,912	44.14***	704	32,058	44.51***	717	30,459	41.46***	876	29,044	32.17***
hsa-miR-224	359	10,085	27.07***	345	7,358	20.31***	358	8,183	21.87***	333	7,483	21.44***
hsa-miR-483	915	23,671	24.87***	811	18,073	21.29***	849	17,784	19.95***	802	17,554	20.88***
hsa-miR-200a	517	8,392	15.22***	667	13,543	19.29***	722	11,317	14.68***	500	12,649	24.30***
hsa-miR-218	405	5,654	12.96***	417	6,527	14.64***	419	5,764	12.76***	431	6,155	13.29***
hsa-miR-618	700	7,549	9.78***	649	8,128	11.52***	651	8,042	11.35***	616	7,416	11.03***
hsa-miR-215	638	6,826	9.71***	829	6,013	6.25***	663	6,641	9.02***	723	6,501	7.99***
hsa-miR-192	3,956	34,724	7.78***	3,401	34,181	9.05***	4,021	29,382	6.31***	3,343	33,293	8.96***
hsa-miR-194	4,410	32,950	6.47***	4,142	32,991	6.96***	4,700	33,182	6.06***	4,410	32,422	6.35***
hsa-miR-182	1,575	11,480	6.29 ***	2,541	13,088	4.15***	2,227	12,512	4.62***	3,067	13,907	3.53***
hsa-miR-452	434	2,284	4.27***	707	3,326	3.70***	530	3,378	5.37***	636	3,028	3.76***
hsa-miR-183	1,763	8,748	3.96***	2,123	8,945	3.21***	2,000	8,984	3.49***	2,129	8,258	2.88***
hsa-miR-200b	1,934	7,551	2.90***	1,692	9,633	4.69***	1,705	9,393	4.51***	1,911	10,855	4.68***
hsa-miR-143	1,355	5,087	2.75***	1,775	7,167	3.04***	1,698	5,688	2.35***	1,765	7,519	3.26***
hsa-miR-624	4,852	13,418	1.77**	4,188	11,593	1.77***	4,479	11,718	1.62**	3,872	10,539	1.72**
hsa-miR-99a	8,653	20,232	1.34**	8,887	20,645	1.32***	9,064	18,019	0.99**	8,870	19,506	1.20**
hsa-miR-27b	10,067	22,544	1.24**	11,924	23,914	1.01***	11,564	23,044	0.99***	12,182	24,515	1.01**
microRNAs rated higher in ME-15												
hsa-miR-146a	36,976	15,721	−1.35**	33,410	16,103	−1.07***	35,166	15,137	−1.32***	35,688	19,962	−0.79***
hsa-miR-422b	19,264	7,759	−1.48**	19,962	7,832	−1.55***	20,641	7,462	−1.77***	17,453	7,152	−1.44***
hsa-miR-149	5,868	2,246	−1.61**	6,195	2,030	−2.05***	6,061	1,743	−2.48***	5,477	2,418	−1.26**
hsa-miR-510	1,051	368	−1.86***	1,489	396	−2.76***	1,435	366	−2.92***	1,053	384	−1.74***
hsa-miR-30a-5p	10,664	3,717	−1.87**	10,223	3,700	−1.76***	10,686	3,477	−2.07***	10,466	4,538	−1.31***
HS_98	3,274	1,065	−2.08**	3,225	859	−2.76***	3,445	965	−2.57***	2,850	750	−2.80***
hsa-miR-340	4,583	1,443	−2.18**	4,218	1,220	−2.46***	4,664	1,061	−3.40***	3,078	933	−2.30***
HS_182.1	1,965	615	−2.2**	1,687	606	−1.79**	1,903	562	−2.39***	1,844	534	−2.45***
hsa-miR-378	4,619	1,371	−2.37**	4,975	1,364	−2.65***	4,994	1,213	−3.12***	4,188	1,237	−2.38***
HS_305_b	4,105	1,207	−2.40*	3,853	833	−3.63***	4,278	977	−3.38***	3,688	1,076	−2.43***
hsa-miR-505	1,312	343	−2.83***	2,070	342	−5.05***	2,050	360	−4.70***	2,030	362	−4.60***
hsa-miR-10a	1,570	350	−3.48**	1,592	350	−3.55***	1,828	360	−4.07***	1,880	352	−4.34***
hsa-miR-10b	1,695	378	−3.49**	2,929	371	−6.89***	3,564	411	−7.67***	4,297	382	−10.26***
hsa-let-7g	10,720	2,302	−3.66**	16,046	3,077	−4.21***	13,792	2,854	−3.83***	15,435	2,568	−5.01***
hsa-miR-584	11,643	2,261	−4.15***	12,717	1,873	−5.79***	12,394	1,912	−5.48***	12,616	1,674	−6.54***
hsa-let-7i	11,701	2,255	−4.19**	16,410	2,707	−5.06***	15,319	2,251	−5.80***	15,718	2,563	−5.13***
hsa-miR-330	9,029	1,653	−4.46***	9,684	1,670	−4.80***	9,432	1,397	−5.75***	7,773	1,380	−4.63***
HS_307_b	2,453	444	−4.52***	4,188	443	−8.45***	3,669	407	−8.01***	3,318	448	−6.41***
hsa-miR-34c	2,292	412	−4.56**	3,303	426	−6.75***	3,524	381	−8.25***	2,403	404	−4.95**
hsa-miR-133a	9,270	1,594	−4.82***	7,942	1,662	−3.78***	8,488	1,435	−4.92***	6,495	1,783	−2.64***
hsa-miR-361	5,234	828	−5.32***	7,641	755	−9.13***	7,356	875	−7.41***	7,904	706	−10.19***
hsa-miR-508	2,552	325	−6.86**	4,280	376	−10.39***	3,965	357	−10.09***	4,013	336	−10.96***
hsa-miR-9*	8,372	1,039	−7.06***	10,114	940	−9.76***	10,027	1,263	−6.94***	9,948	843	−10.81***
hsa-miR-31	5,967	661	−8.03***	5,742	720	−6.97***	6,619	657	−9.07***	5,978	728	−7.21***
hsa-miR-506	5,855	625	−8.37***	6,125	713	−7.59***	5,916	665	−7.90***	5,602	675	−7.30***
hsa-miR-211	5,147	476	−9.81***	3,218	490	−5.57***	3,833	471	−7.14**	5,575	464	−11.01***
hsa-miR-296	6,194	570	−9.86***	5,913	504	−10.72***	6,441	557	−10.57***	4,369	532	−7.21***
hsa-miR-598	4,445	401	−10.09***	4,475	386	−10.59***	4,934	424	−10.63***	4,127	367	−10.24***
hsa-miR-199b	9,081	775	−10.71***	9,478	916	−9.35***	9,629	865	−10.13***	8,059	911	−7.85***
hsa-let-7b	8,236	539	−14.28***	12,563	475	−25.44***	12,150	500	−23.30***	12,309	452	−26.24***
hsa-miR-509	10,413	536	−18.44***	10,346	512	−19.22***	9,966	548	−17.20***	9,311	529	−16.62***
hsa-miR-9	12,587	422	−28.85***	15,870	447	−34.50***	15,502	418	−36.09***	16,402	429	−37.26***
hsa-miR-514	12,065	364	−32.16***	13,112	358	−35.64***	12,201	315	−37.74***	12,355	355	−33.83***

	Control						Interferon-alpha treated					
	4 h			24 h			4 h			24 h		
	ME-15	HuH7	CHF	ME-15	HuH7	CHF	ME-15	HuH7	CHF	ME-15	HuH7	CHF
Hybdridization controls												
array_hyb_con4	6,404	7,110	0.11	7,724	6,684	−0.16	7,031	6,739	−0.04	6,964	6,746	−0.03
array_hyb_con3	6,923	7,681	0.11	7,833	7,368	−0.06	7,422	7,054	−0.05	6,906	7,365	0.07
array_hyb_con1	10,779	11,868	0.10	11,812	11,728	−0.0.01	11,436	11,382	0.00	11,059	11,522	0.04
array_hyb_con2	10,258	11,145	0.09	11,382	10,829	−0.05	11,075	10,650	−0.04	9,997	10,283	0.03

Table 1 Cell line differences in microRNA expression

Table 1 shows the expression data for the most significant genes including change factors and significance score as reference. Among these differentially expressed genes there are three members of the let-7 family, which has properties of tumor suppressor genes (for review see (18)). Therefore it is not surprising that the members of this well-known microRNA gene family are deregulated in the analyzed cancer cells too. Furthermore, the different developmental stage of our cancer cell lines is expected to have left a genomic fingerprint where some microRNA genes are expressed in one but not the other cell line (19). Consistent with this, expression of some microRNAs is strictly cell type specific and barely detectable in the other cell type (Fig. 2a), for example the liver-specific miR-122a and miR-192 (20).

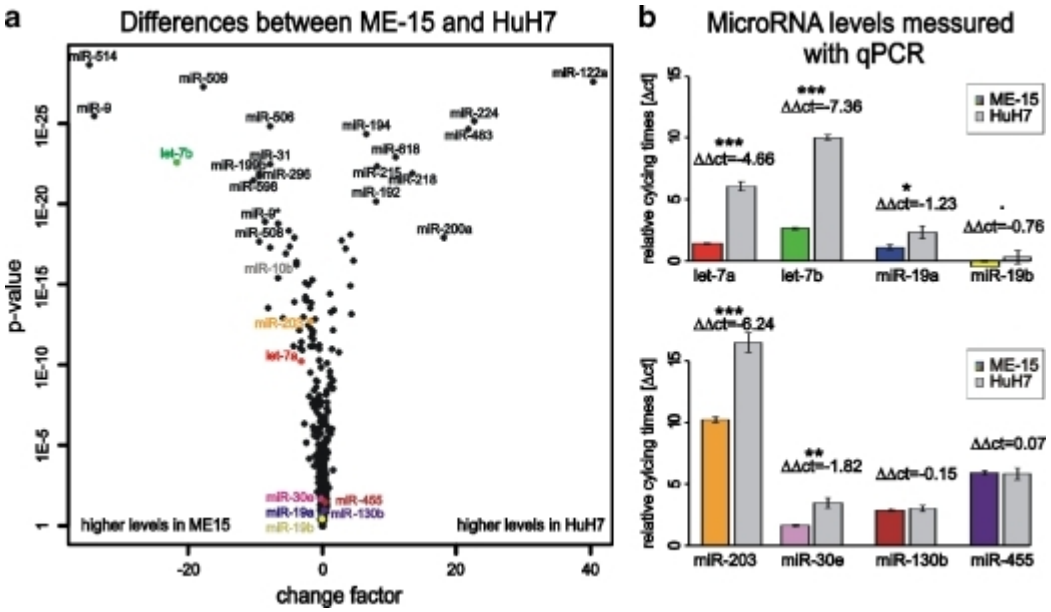

*Fig. 2 Cell line specific microRNA expression Volcano plot (a) display demonstrates the multi-variant biological diversity of microRNA expression in ME-15 or HuH7 cells. The estimated fold-change value (change factor) is plotted on the X-axis against the p value (limma t statistics) in logarithmic scale on the Y-axis. A linear model, using the expression values of untreated ME-15 cells at 4 h as base together with three parameters to estimate differences in time, treatment, or cell line. The top ranked and qPCR measured microRNAs are annotated. b Quantitative PCR validation of microarray data using eight selected microRNAs. Input total RNA came from independent cell cultures. Data are shown as relative cycling times (ΔCT) calculated with endogenous control RNU18 for ME-15 (color-filled bars) and HuH7 (gray). Error bars represent ΔCT±Δx (standard deviation of biological replicates). ΔΔCT are noted above the bars together with the significance codes for t statistics (0 '***', 0.001 '**', 0.01 '*', 0.05 '.', and 0.1 " 1).*

	Control						Interferon-alpha treated					
	4 h			24 h			4 h			24 h		
a	ME-15	HuH7	CHF	ME-15	HuH7	CHF	ME-15	HuH7	CHF	ME-15	HuH7	CHF
Validated microRNAs												
hsa-miR-19a	13,617	6,726	−1.02	18,318	17,178	−0.07	19,226	17,409	−0.10	14,425	14,079	−0.02
hsa-miR-19b	13,365	9,406	−0.42	25,463	22,438	−0.13	21,532	20,625	−0.04	18,039	17,440	−0.03
hsa-miR-30e-5p	9,497	6,838	−0.39	13,045	11,321	−0.15	12,643	10,887	−0.16	13,230	11,809	−0.12
hsa-let-7a	15,244	4,335	−2.52.	28,304	6,181	−3.58 ***	22,226	6,386	−2.48***	30,449	5,612	−4.43***
hsa-let-7b	8,236	539	−14.28***	12,563	475	−25.44***	12,150	500	−23.30 ***	12,309	452	−26.24***
hsa-miR-203	907	325	−1.79**	1,155	348	2.32***	1,302	359	−2.63***	1,186	5,757	−1.07**
hsa-miR-130b	5,700	8,316	−0.46	13,023	13,880	0.07	9,994	14,055	0.41	12,053	12,432	0.03
hsa-miR-455	2,677	2,604	−0.03	3,944	5,285	0.34*	3,437	5,927	0.72**	3,262	5,342	0.64*
	ME-15						HuH7					
b	4 h			24 h			4 h			24 h		
	−IFNa	+IFNa	CHF	−IFNa	+IFNa	CHF	−IFNa	+IFNa	CHF	−IFNa	+IFNa	CHF
Interferon-regulated microRNAs												
hsa-miR-33b	1,226	3,484	1.84**	2,888	2,318	−0.25	476	1,113	1.34**	1,306	1,851	0.42***
hsa-miR-33	2,631	7,352	1.79	9,774	5,764	−0.70*	1,887	6,645	2.52.	8,893	2,726	−2.26
hsa-miR-126*	2,221	5,409	1.44*	5,578	6,111	0.10	4,749	6,410	0.35.	5,687	5,803	0.02***
hsa-miR-10b	1,695	3,564	1.10*	2,929	4,297	0.47**	378	411	0.09	371	382	0.03
hsa-miR-551b	2,085	4,169	1.00*	4,423	3,419	−0.29	1,804	4,979	1.76*	5,221	4,865	−0.07
hsa-miR-137	1,037	1,966	0.90	2,523	2,872	0.14	1,613	3,155	0.96**	3,429	3,598	0.05
hsa-miR-138	2,158	4,074	0.89*	4,709	3,701	−0.27	725	828	0.14	903	859	−0.05
hsa-miR-130b	5,700	9,994	0.75	13,023	12,053	−0.08	8,316	14,055	0.69**	13,880	12,432	−0.12
hsa-miR-101	6,701	11,387	0.70	13,088	11,688	−0.12	3,569	10,871	2.05**	10,445	10,796	0.03
hsa-miR-140	7,339	12,236	0.67	15,512	15,931	0.03	3,058	5,976	0.95*	6,135	7,221	0.18
HS_92	829	1,356	0.64.	1,246	1,179	−0.06	407	587	0.44	492	478	−0.03
hsa-miR-362	1,382	2,234	0.62*	2,144	2,276	0.06	1,907	2,737	0.43*	2,456	2,519	0.03
hsa-miR-19b	13,365	21,532	0.61**	25,463	18,039	−0.41	9,406	20,625	1.19*	22,438	17,440	−0.29
hsa-miR-130a	13,031	20,878	0.60.	27,571	23,048	−0.20	17,884	31,012	0.73*	33,801	28,875	−0.17
hsa-miR-579	552	816	0.48.	992	1,053	0.06	729	1,362	0.87*	1,250	1,308	0.05
hsa-miR-29b	23,138	34,148	0.48.	32,691	29,710	−0.10	8,737	17,989	1.06*	20,599	17,405	−0.18.
hsa-miR-19a	13,617	19,226	0.41*	18,318	14,425	−0.27	6,726	17,409	1.59.	17,178	14,079	−0.22.
hsa-miR-338	1,298	1,813	0.40.	1,870	1,603	−0.17	2,363	4,603	0.95.	5,109	4,088	-0.25
hsa-miR-590	1,403	1,949	0.39.	1,545	1,367	−0.13	669	1,068	0.60.	884	847	−0.04
hsa-miR-545	1,455	1,973	0.36.	2,149	1,720	−0.25*	829	1,371	0.65**	1,573	1,393	−0.13
hsa-miR-30e-5p	9,497	12,643	0.33	13,045	132,030	0.01	6,838	10,887	0.59*	11,321	11,809	0.04
hsa-miR-570	1,989	2,576	0.30.	2,397	2,610	0.09	2,213	3,739	0.69*	4,312	3,708	−0.16
hsa-miR-301	13,621	17,531	0.29*	16,321	15,142	−0.08	5,646	10,460	0.85*	10,925	10,295	−0.06.
hsa-miR-561	517	621	0.20	568	464	−0.22**	683	1,157	0.69**	1,149	941	−0.22
HS_250	4,284	1,813	−1.36.	740	983	0.33	3,688	2,337	−0.58	1,195	1,303	0.09
	ME-15						HuH7					
c	4 h			24 h			4 h			24 h		
	−IFNa	+IFNa	CHF	−IFNa	+IFNa	CHF	−IFNa	+IFNa	CHF	−IFNa	+IFNa	CHF
Validated microRNAs												
hsa-miR-19a	13,617	19,226	0.41*	18,318	14,425	−0.27	6,726	17,409	1.59.	17,178	14,079	−0.22
hsa-miR-19b	13,365	21,532	0.61**	25,463	18,039	−0.41	9,406	20,625	1.19*	22,438	17,440	−0.29.
hsa-miR-30e-5p	9,497	12,643	0.33	13,045	13,230	0.01	6,838	10,887	0.59*	11,321	11,809	0.04
hsa-let-7a	15,244	22,226	0.46	28,304	30,449	0.08	4,335	6,386	0.47.	6,181	5,612	−0.10
hsa-let-7b	8,236	12,150	0.48*	12,563	2,309	−0.02	539	500	−0.08	475	452	−0.05
hsa-miR-203	907	1,302	0.44*	1,155	1,186	0.03	325	359	0.10	348	575	0.665**

Table 2 Modulation of microRNA expression by IFNα — 4 and 24 h after stimulation

Bead-array-based microRNA detection technology, including the bio-statistic analysis, is currently not well established or widely used and we have applied a commercial PCR-based assay to confirm the array data for some microRNAs that cover different expression levels and change factors. In contrast to mRNA profiling, where RT-PCR-based assays are considered as gold standard for data validation, new generation deep sequencing is considered as the method of choice for microRNA quantification but is not available in our research institute. For the microRNAs let-7 a/b, miR-19 a/b, and miR-203, the PCR-based quantification method (Fig. 2b) confirmed the direction of change found with microarray technology (Table 2a). Expression of miR-130b and miR-455 was at similar levels in both assays. The correlation calculated for the eight tested microRNAs was acceptable: multiple r^2 from f test of mean relative cycling times (ΔCT) to mean log2 microarray expression values was 0.9279. Differences of absolute levels between the microRNA targets probably results from different hybridization properties of the microarray probes and variation in the performance of Taqman primers for the specific microRNA on the other side.

Assuming that any IFNα relevant microRNA will have the same kinetics as the mRNA for PRGs, we looked at the regulation of microRNA genes in our experiment. These IRmiRs should respond to IFNα stimulation preferentially in both cell lines, because this would be a good indication of a general mechanism in the IFNα response. Within the 25 most significantly regulated genes (Table 2b), only one gene (HS_250) is downregulated. A general upregulation of transcripts is consistent with classic IFNα signaling seen for mRNAs. However, the maximal observed change factor with high significance was 1.84 (miR-33b in Table 2b) which is clearly lower than the values seen for protein coding mRNAs (2). We also included an expression analysis 24 h after IFNα stimulation in order to detect microRNA genes that show either delayed induction or remain activated at comparable levels to the 4 h stimulus. Based on our data set, the majority of the microRNA response genes show no further induction, but rather moderate downregulation 24 h after induction. This finding is not surprising as we expected immediate early impact of IFNα-mediated primary signaling.

We also measured the IFNα response in the same experiment and for the same microRNAs (Table 2c). When we analyze the IFNα effect at the early time point in both cell lines we find all the validated microRNAs to be upregulated (Fig. 3a). The magnitude of upregulation and the basal expression levels of the microRNA-19a and 19b are similar in both cell lines (Fig. 3b, top). This and the finding that miR-19 regulates SOCS1 (4) may be relevant for the regulation of cytokine signaling. let-7a and let-7b had higher levels in the melanoma-cell-line-derived samples compared HuH7, but the induction by IFNα in ME-15 could not be reproduced by RT-PCR (Fig. 3b, bottom). In both assays accurate fold changes are difficult to calculate, if the baseline expression level is close to background noise or the detection limit. An example of a gene at the detection limit is miR-203, which is not detectable without IFNα treatment in HuH7 cells (Table 2c). Upon IFNα stimulation (24 h in HuH7) the microRNA is detectable above background suggesting minimal induction. Consequently a solid change factor cannot be calculated, which is consistent with the high variance obtained by qPCR (ME-15). This result is in fact not surprising, because both technologies rely on logarithmic PCR amplification of microRNA templates. At low expression levels, both technologies show relatively high variation in biological replicates, which should be considered for data interpretation. Interestingly, miR-203 has a putative binding site for ISGF3 in the promoter region, which would enable IFNα-dependent upregulation. miR-30 has been reported to be IFNβ inducible, although the subclass measured was not specified by the authors (9). We decided to analyze the most promising candidate (miR-30e-5p) present in our microarray dataset (Fig. 3a in gray).

Detection of miR-30e failed in ME-15 cells due to technical problems, but induction in HuH7 was similar to miR-19a/b.

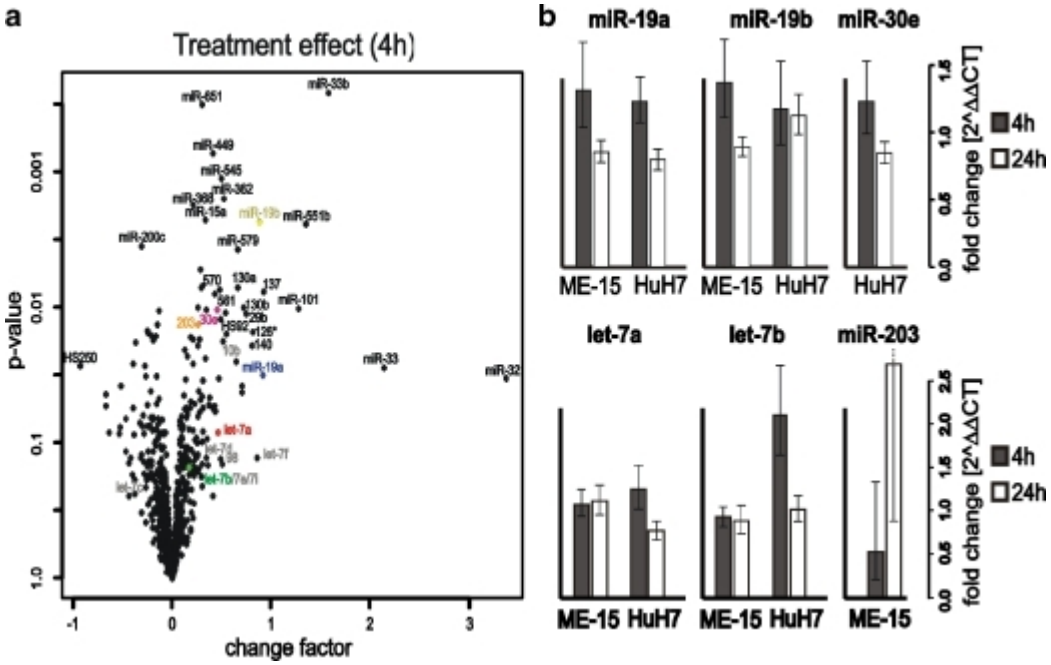

Fig. 3 IFNα-dependent modulation of microRNA expression. a Volcano plot display of IFNα induced microRNA upregulation 4 h after induction. The change factor values (2^log factor change −1) are plotted on the X-axis against the p value in logarithmic scale on the Y-axis. Top-rated microRNAs are annotated together with the let-7 family members. b Confirmation of IFNα effect for selected microarray data by qPCR. The CT-values are the average of three technical and three biological replicates and changes were calculated with 2^ΔMNE (mean normalized expression values). Error bars show 2^ΔMNE±Δx (average standard error of treated and untreated MNE) from biological triplicates. miR-30e failed to amplify in ME-15 and miR-203 was below the detection limit in HuH7. Expression values were normalized against endogenous snoRNA RNU48 levels.

Some technology-related questions remain open. The microRNA assay measures essentially the number of amplicons generated by RT-PCR for each transcript. Thus the signal is an indirect measurement of transcript abundance as compared to classical mRNA microarray platforms, where the target mRNA is directly labeled during linear amplification by in vitro transcription. As a consequence, change factor calculations for amplicon-based assays are ambiguous.

In summary, Illumina's bead array technology is well suited for multi-parallel profiling of microRNAs expressed in different cell types or tissues. We were also able to detect IFNα-inducible microRNA genes although the changes observed were moderate and biological significance remains to be proven. Like most microarray-based detection technologies the technical variability among identical samples is low compared to biological variations of individual cell cultures. At this point it is important to note that variation among biological samples occurs and is independent of the parameters that are measured. Consistent with IFNα-dependent induction of mRNAs we find that virtually all modulated microRNA genes are upregulated. However, the IFNα-induced changes detected in our study are relatively small compared to the changes induced by IFNβ in HuH7 cells (9). Finally, it is noteworthy that IRmiRs have similar kinetic properties to their mRNA counterparts. miR-10b for instance is induced early in ME-15 and remains upregulated, while miR-19 abundance

ceases after 24 h. In general, the majority of IRmiR genes were reset to basal levels after 24 h and further studies are needed for kinetic classification. Thus, our study adds another level of complexity to the dynamic regulation IFNα signaling and other mechanisms like epigenetic promoter methylation are currently under intense investigation in our laboratories.

Acknowledgements

We thank Dr. Guido Steiner and Andreas Buness (F. Hoffmann-La Roche Ltd.) for their support in bioinformatics and statistics, Dr. Martin Ebeling (F. Hoffmann-La Roche Ltd.) for the comparative genomic evaluation of microRNA-targeted transcripts and Prof. Dr. Giulio Spagnoli (University Hospital Basel) for the gift of the ME-15 melanoma cell line. Finally, we are grateful to Heather Hinton (F. Hoffmann-La Roche Ltd.) for critical reading of the manuscript and to Dr. Laura Suter-Dick (F. Hoffmann-La Roche Ltd.) for sharing lab space and introduction into GCP sampling.

References

1. Borden EC, Sen GC, Uze G, Silverman RH, Ransohoff RM, Foster GR, et al. Interferons at age 50: past, current and future impact on biomedicine. Nat Rev Drug Discov. 2007;6(12):975–990.
2. Certa U, Wilhelm-Seiler M, Foser S, Broger C, Neeb M. Expression modes of interferon-alpha inducible genes in sensitive and resistant human melanoma cells stimulated with regular and pegylated interferon-alpha. Gene. 2003;315:79–86.
3. Zimmerer JM, Lesinski GB, Kondadasula SV, Karpa VI, Lehman A, Raychaudhury A, et al. IFN-alpha-induced signal transduction, gene expression, and antitumor activity of immune effector cells are negatively regulated by suppressor of cytokine signaling proteins. J Immunol. 2007;178(8):4832–4845.
4. Yoshimura A, Naka T, Kubo M. SOCS proteins, cytokine signalling and immune regulation. Nat Rev Immunol. 2007;7(6):454–465.
5. Song MM, Shuai K. The suppressor of cytokine signaling (SOCS) 1 and SOCS3 but not SOCS2 proteins inhibit interferon-mediated antiviral and antiproliferative activities. J Biol Chem. 1998;273(52):35056–35062.
6. Pichiorri F, Suh SS, Ladetto M, Kuehl M, Palumbo T, Drandi D, et al. MicroRNAs regulate critical genes associated with multiple myeloma pathogenesis. Proc Natl Acad Sci U S A. 2008;105(35):12885–12890.
7. Bartel DP. MicroRNAs: genomics, biogenesis, mechanism, and function. Cell. 2004;116(2):281–297.
8. Friedman RC, Farh KK, Burge CB, Bartel D. Most mammalian mRNAs are conserved targets of microRNAs. Genome Res. 2009;19(1):92–105.
9. Pedersen IM, Cheng G, Wieland S, Volinia S, Croce CM, Chisari FV, et al. Interferon modulation of cellular microRNAs as an antiviral mechanism. Nature. 2007;449(7164):919–922.
10. Lüscher U, Filgueira L, Juretic A, Zuber M, Lüscher NJ, Heberer M, et al. The pattern of cytokine gene expression in freshly excised human metastatic melanoma suggests a state of reversible anergy of tumor-infiltrating lymphocytes. Int J Cancer. 1994;57(4):612–619.
11. Nakabayashi H, Taketa K, Miyano K, Yamane T, Sato J. Growth of human hepatoma cells lines with differentiated functions in chemically defined medium. Cancer Res. 1982;42(9):3858–3863.
12. Chen J, Lozach J, Garcia EW, Barnes B, Luo S, Mikoulitch I, et al. Highly sensitive and specific microRNA expression profiling using BeadArray technology. Nucleic Acids Res. 2008;36(14):e87.
13. Bolstad B, Irizarray R, Astrand M, Speed T. A comparison of normalization methods for high density oligonucleotide array data based on bias and variance. Bioinformatics. 2003;19:185–193.
14. R Development Core Team. R: A language and environment for statistical computing. Vienna, Austria: R Foundation for Statistical Computing 2008. URL: http://www.R-project.org.

Micro RNA induction by Interferon alpha and their potential role to interfere in the negative feedback pathway.

Fredy Siegrist and Ulrich Certa
RNAi Safety, F. Hoffmann-La Roche LTD, Basel Switzerland.

Poster Session Topic:
PP 5 – Gene Regulation: Transcriptional and Post-transcriptional Mechanisms

Keywords: Suppressors of Cytokine Signaling, Interferon alpha, JAK/STAT, miRNA microarrays, negative feedback, cytokine memory

Abstract

Suppressors of Cytokine Signaling (SOCS) Family Proteins are rapidly transcribed after Interferon alpha 2a (IFNa) treatment. They are involved in silencing the general pathways induced by Interferon, especially the Janus kinase / signal transducers and activators of transcription (JAK/STAT) pathways. SOCS1 and SOCS3 mRNA is barely detectable in most cultured cells but upon IFNa stimulation their levels increase rapidly. Their maximal expression levels differ markedly in cultured cancer cell lines, perhaps due to their epigenetic status. Peak SOCS3 mRNA are reached three hours after IFNa induction followed by rapid degradation within a few hours. These results suggest post-transcriptional regulation of SOCS3 mRNA expression. In addition to various protein coding genes, also levels of certain micro RNA's (miRNA) are modulated by IFNa. The 3' UTR of SOCS1, SOCS3 and SOCS6 share conserved binding sites for IFNa inducible miRNAs. Here we propose a model of how the SOCS dependent negative feedback pathway of Interferon may be influenced by RNA interference. This regulation suggests an important role in controlling the suppressor's protein levels. Moreover, the involvement of miRNAs may contribute to an Interferon mediated cytokine memory.

Predicted miRNA binding sites for SOCS1 and SOCS3

Conserved binding sites for miRNA families were scanned using Target-Scan. Especially the miRNAs lying at the very 3' end: let-7, miR-30, miR-19, miR-203 were upregulated after Interferon challenge.
A genome wide scan for the occurrence of miR-30 and miR-19 sites in close proximity in 3'-UTRs showed that only 41 transcripts had gap of less than 150 base pairs between these two sites, including SOCS1, SOCS3 and SOCS6 mRNA.

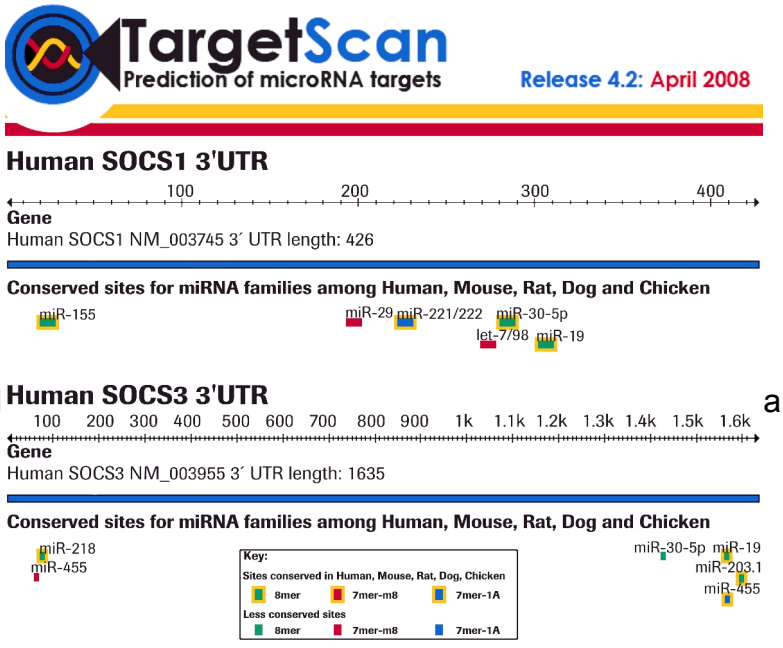

a

Genomic context of miRNA-203 has a conserved ISRE transcription factor binding site

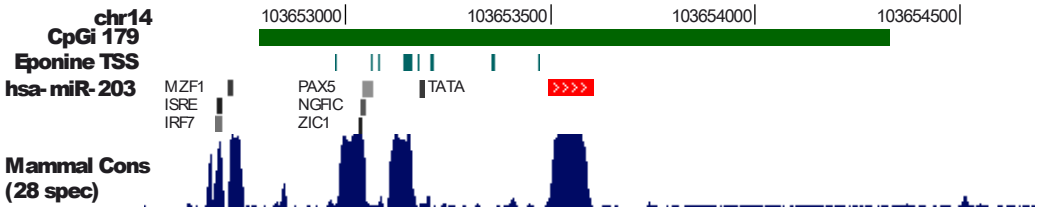

The miR-203 gene shows a similar context as an interferon stimulated gene. The miR coding site is covered by a CpG island. There are several transcription start sites and transcription factor binding sites, including one for ISGF3, upstream and 11 polyA sites downstream.

Model of miRNA mediated cytokine memory

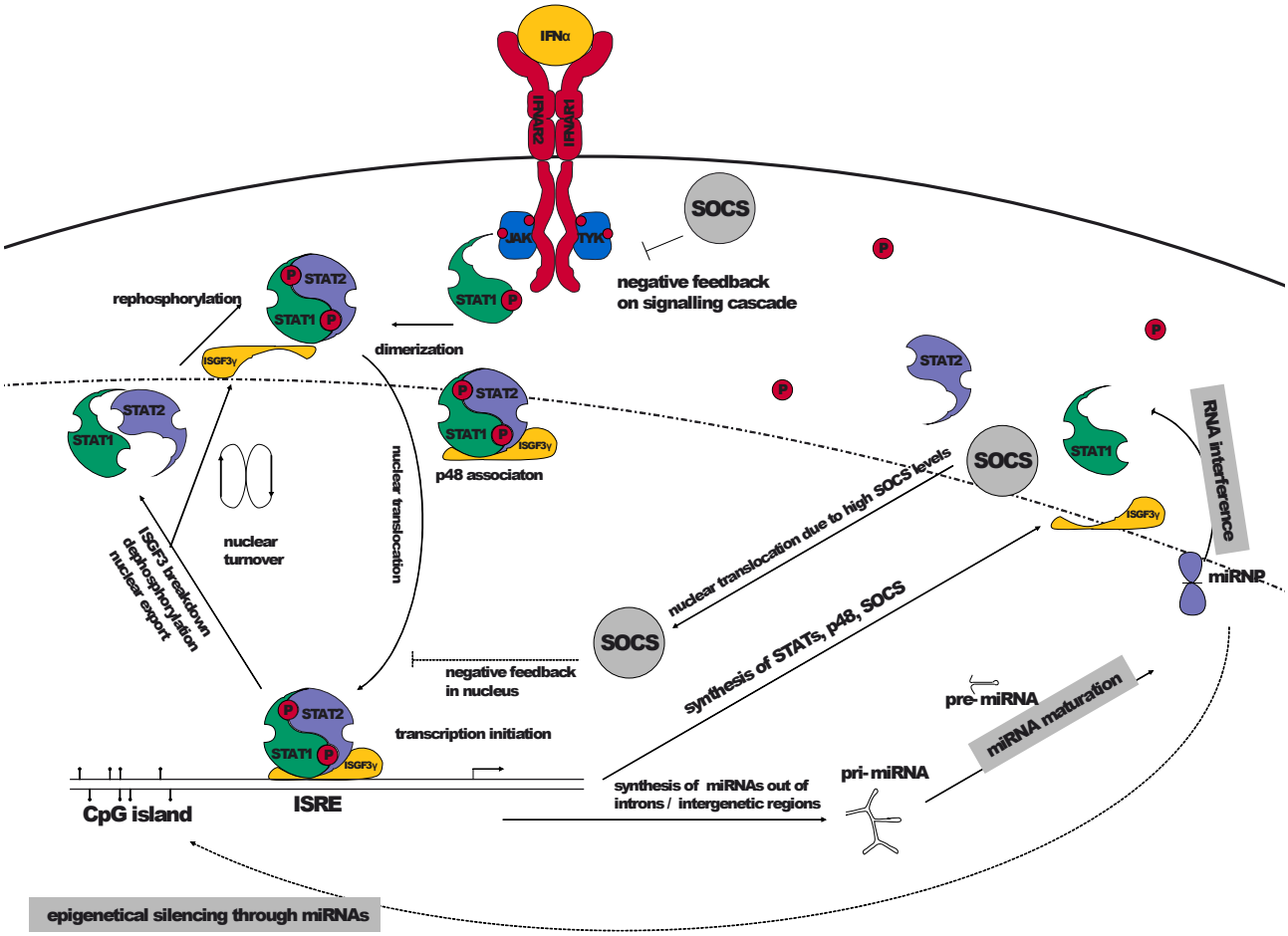

Model showing the induction of the negative feedback loop of Interferon alpha (SOCS protein expression), the action of their presumed negative regulators (miRNAs) and their potential to contribute to long term cytokine memory through epigenetic regulation.

miRNA levels after Interferon stimulation

Mature miRNA levels were affected early (after 4 hours incubation) by Interferon alpha addition to cell culture media. This effect was washed out after 24 hours, when only few, specific miRNAs were regulated (see table on the lower right). The effect is spread over many miRNAs and every single expression level needs confirmation by qPCR.
The tables show upregulated miRNA which have target sequences in the very 3'-UTR regions of SOCS1 or SOCS3. Both, miR-30 and let7 levels have been reported to increase after cytokine stimulation. Pedersen IM et al. (2007) showed a three fold upregulation of miR-30 when HuH7 cells were stimulated with Interferon beta. This miR had no effect on their studied effect (viral replication). Meng F et al. (2007) postulated that the let-7 miRNA enhancement after Il-6 treatment may target SOCS1 to degradation and by that interfere in the Stat-3 pathway.

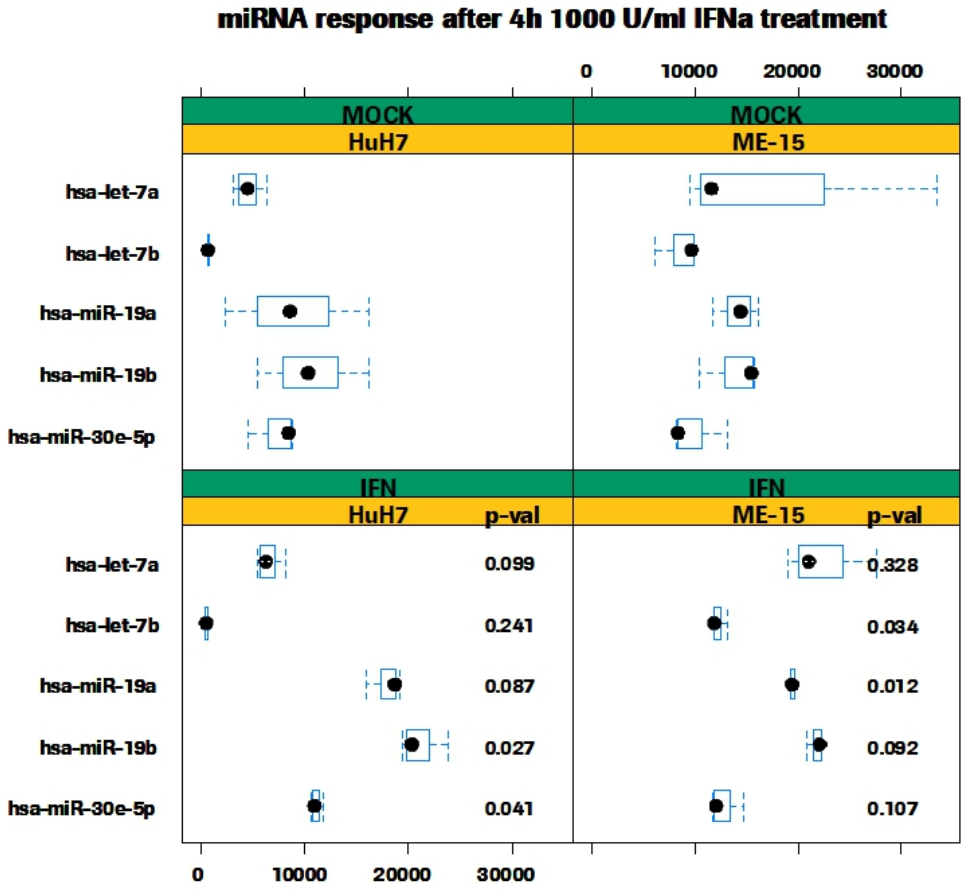

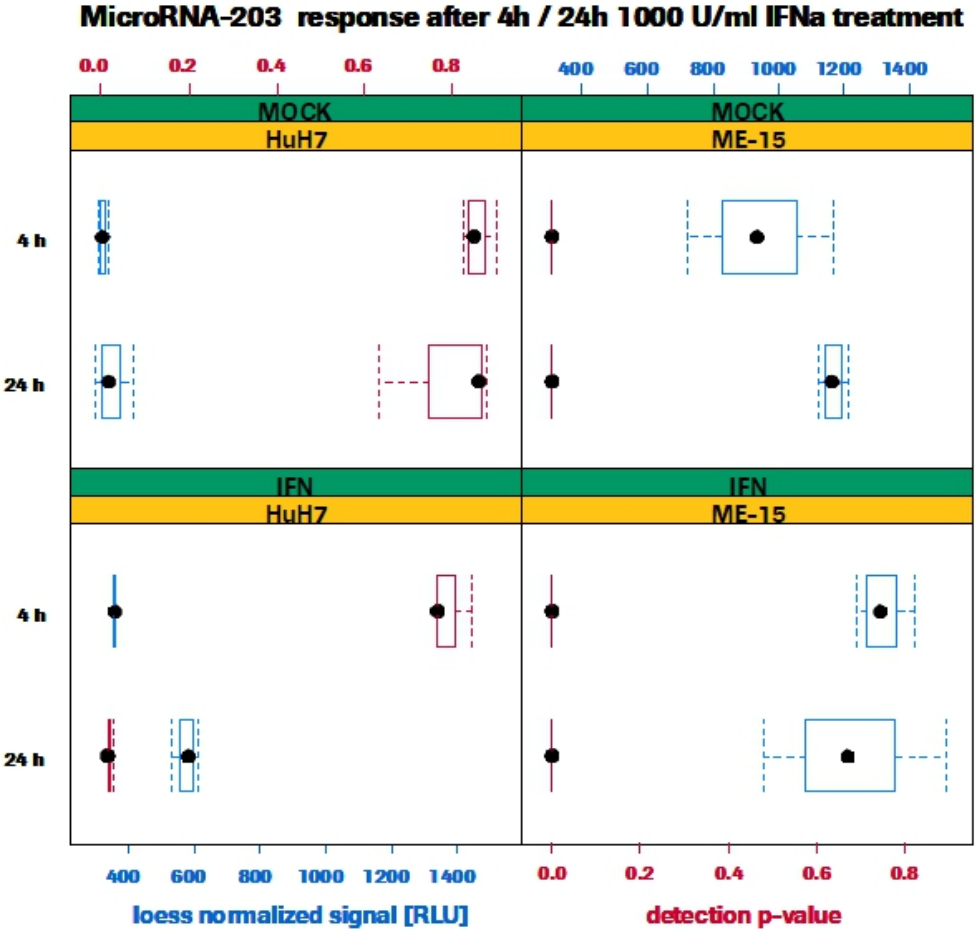

miRNA mediated degradation of SOCS1

After cytokine stimulation SOCS1 mRNA is produced and translated. Let-7 binding is inhibited or is not sufficient for degradation. The presence of several miRNA bound to the transcript will lead to translational blockage and degradation of the mRNA.

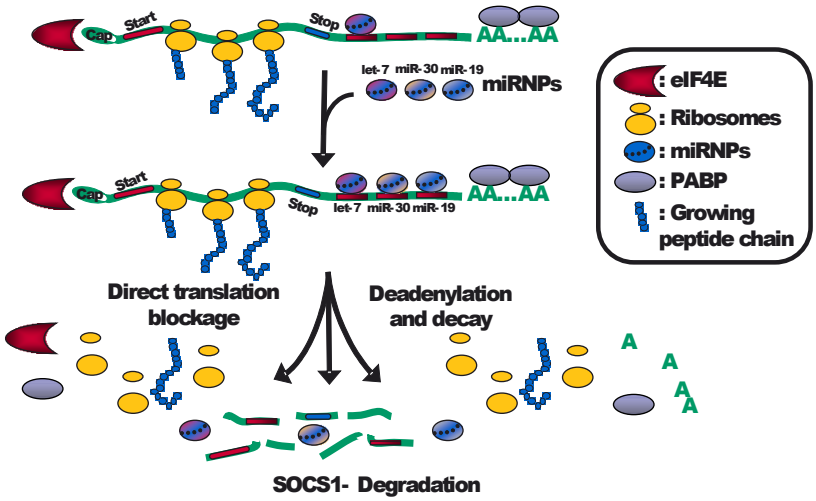

Discussion – Interfering in the SOCS pathway

A rapid degradation of SOCS-proteins after their induction is needed to restore cell responsiveness to cytokine stimulation. Restricted SOCS proteins levels are crucial to control their suppressing function (Lee KH, 2007). An insertion in the SH2 domain of SOCS3 is accountable for destabilizing the protein (Babon JJ, 2006), but this would be unprofitable unless its mRNA levels peak shortly after cytokine signalling.
In contrast to the large screening study (Landgraf P, 2007) that has not found any substantial changes in miRNA profiles after Interferon alpha, beta and gamma treatment, we have found evidence for a global change of miRNA expression after stimulation with IFNa supplemented medium. Therefore we propose a model where several miRNA are needed for a potent decay of SOCS mRNA and consequently their protein levels. Systems where changes of a single miRNA against SOCS were analyzed showed positive results (Pichiorri F, 2008, for the regulation of SOCS1 3'-UTR by miR-19). Others had brought no measurable effect, thus these miRs have been claimed not to act as negative regulators (Lena AM, 2008, no regulation of SOCS3 levels by expressing pre-miR-203). Our microarray analysis depicted immediate regulation of many miRNAs followed by restoration to mock treated levels after 24 hours, similar to expression of early response genes (Hallen LC, 2007). Accordingly, we conclude that several miRNA, bearing the potential to target SOCS transcripts to degradation, are involved and hence needed for a fast restoration steady-state SOCS protein levels. This may be achieved by rapid transcription of primary miRNAs derived either from intergenetic regions, that carry Interferon response elements (eg. miR-203) or from introns of early response genes. Alternatively, maturation of pre-miRNA could be influenced by Interferon regulated genes. Our previous findings (Brem R, 2003) suggested an epigenetic genome alteration following prolonged Interferon alpha exposure. Our model proposes contribution of Interferon regulated miRNAs to long term epigenetic gene silencing.

References

Pedersen IM, Cheng G, Wieland S, Volinia S, Croce CM, Chisari FV, David M. *Nature*. 2007 Oct 18;449(7164):919-22. Interferon modulation of cellular microRNAs as an antiviral mechanism. [PMID: 17943132]

Meng F, Henson R, Wehbe-Janek H, Smith H, Ueno Y, Patel T. *J Biol Chem.* 2007 Mar 16;282(11):8256-64. Epub 2007 Jan 12, The MicroRNA let-7a modulates interleukin-6-dependent STAT-3 survival signaling in malignant human cholangiocytes. [PMID: 17220301]

Lee KH, Moon KJ, Kim HS, Yoo BC, Park S, Lee H, Kwon S, Lee ES, Yoon S. *FEBS Lett.* 2008 Jun 25;582(15):2319-24. Epub 2008 Jun 4. Increased cytoplasmic levels of CIS, SOCS1, SOCS2, or SOCS3 are required for nuclear translocation. [PMID: 18538139]

Babon JJ, McManus EJ, Yao S, DeSouza DP, Mielke LA, Sprigg NS, Willson TA, Hilton DJ, Nicola NA, Baca M, Nicholson SE, Norton RS. *Mol Cell.* 2006 Apr 21;22(2):205-16. The structure of SOCS3 reveals the basis of the extended SH2 domain function and identifies an unstructured insertion that regulates stability. [PMID: 16630890]

Landgraf P, Rusu M, Sheridan R, Sewer A, Iovino N, Aravin A, Pfeffer S, Rice A, Kamphorst AO, Landthaler M, Lin C, Socci ND, Hermida L, Fulci V, Chiaretti S, Foà R, Schliwka J, Fuchs U, Novosel A, Müller RU, Schermer B, Bissels U, Inman J, Phan Q, Chien M, Weir DB, Choksi R, De Vita G, Frezzetti D, Trompeter HI, Hornung V, Teng G, Hartmann G, Palkovits M, Di Lauro R, Wernet P, Macino G, Rogler CE, Nagle JW, Ju J, Papavasiliou FN, Benzing T, Lichter P, Tam W, Brownstein MJ, Bosio A, Borkhardt A, Russo JJ, Sander C, Zavolan M, Tuschl T. *Cell.* 2007 Jun 29;129(7):1401-14. A mammalian microRNA expression atlas based on small RNA library sequencing. [PMID: 17604727]

Pichiorri F, Suh SS, Ladetto M, Kuehl M, Palumbo T, Drandi D, Taccioli C, Zanesi N, Alder H, Hagan JP, Munker R, Volinia S, Boccadoro M, Garzon R, Palumbo A, Aqeilan RI, Croce CM. *Proc Natl Acad Sci U S A.* 2008 Sep 2;105(35):12885-90. Epub 2008 Aug 26. MicroRNAs regulate critical genes associated with multiple myeloma pathogenesis. [PMID: 18728182]

Micro RNA induction by interferon alpha and a potential role to interfere with SOCS.

F Siegrist, U Certa
RNAi Safety, F. Hoffmann-La Roche LTD, Basel Switzerland.

Summary
Suppressors of Cytokine Signaling (SOCS) Family Proteins are rapidly induced by interferon alpha 2a (IFN≁) treatment. SOCS1 and SOCS3 mRNA is barely detectable in most cultured cells but upon IFN≁ stimulation transcript levels increase rapidly. Peak SOCS3 mRNA levels are reached three hours after IFN≁ induction followed by rapid degradation within a few hours. These results suggest post-transcriptional regulation of SOCS3 mRNA expression. In addition to various protein coding genes, also the levels of certain micro RNAs (miRNA) are upregulated by IFN≁. Interestingly, the 3' UTR of SOCS1, SOCS3 and SOCS6 share conserved binding sites for IFN≁ inducible miRNAs. Here we propose a model in which the SOCS dependent negative feedback pathway of type I interferons may be controlled by RNA interference.

Introduction
SOCS are involved in silencing the general pathways induced by cytokines like interferon, especially the Janus kinase / signal transducers and activators of transcription (JAK/STAT) pathways. Their maximal expression levels differ markedly in cultured cancer cell lines. Protein and mRNA levels of SOCS are decreasing rapid after induction. The fast degradation of SOCS-proteins after their induction is needed to restore cell responsiveness to cytokine stimulation. Restricted SOCS proteins levels are crucial to control their suppressing function. An insertion in the SH2 domain of SOCS3 is accountable for destabilizing the protein (Babon, 2006), but this would be inefficient unless its mRNA levels peak shortly after cytokine stimulation. A large screening study (Landgraf, 2007) showed no substantial changes in miRNA profiles after interferon alpha, beta and gamma treatment. Recently, several groups have now reported miRNA regulation after cytokine stimulation: Pedersen et al. (2007) showed upregulation of miR-30 when stimulated with interferon beta, yet this miR had no effect on viral genome replication. Meng et al. (2007) postulated that the let-7 miRNA enhancement after Il-6 treatment may result in SOCS1 degradation. In a model system miR-19 was able to downregulate SOCS1 3-UTR bearing reporters (Pichiorri, 2008). Endogenous systems are more difficult: Lena AM et al. (2008) have not observed any regulation of SOCS3 levels by expressing pre-miR-203.

Materials and Methods
Cell culture and interferon treatment: Melanoma cell lines (ME-15) were cultured in modified RPMI 1640, Hepatoma cells (HuH7) were cultured in DMEM + GlutaMAX each supplemented with 10% fetal bovine serum. Roferon (interferon ≁2a) was diluted in fresh medium to a final concentration of 1000 U/ml, for mock treatment medium w/o interferon was used. Total RNA was extracted with TRIZOL.
Microarrays: miRNA expression was profiled using Illumina technology (MicroRNA Panel v1) which detects 743 human miRs.
Bioinformatics: Conserved binding sites for miRNA families were scanned using Target-Scan (Release 4.2). The expression data were processed with beadstudio 3.1.3, gene expression module 3.3.8 (Illumina), log2 transformed, loess-normalized and statistically (t-test linear model) analyzed with R using lumi (Du, 2008) and packages used therein.

Results

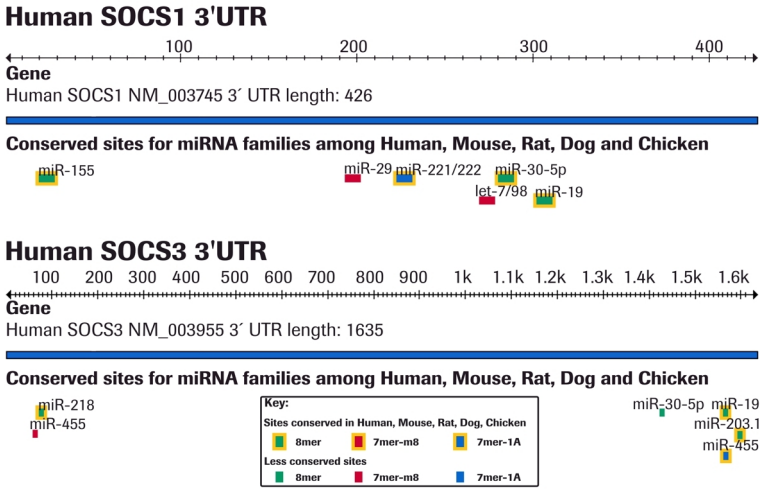

Figure 1 - Predicted miRNA binding sites for SOCS1 and SOCS3

Figure 1 shows that both, SOCS1 and SOCS3 have at the very 3' end shared miRNA binding sites: miR-30, miR-19. SOCS1 have in addition a let-7 and SOCS3 binding sites for miR-203 and miR-455. A genome wide scan for the occurrence of miR-30 and miR-19 sites in close proximity in 3'-UTRs showed that only 41 transcripts had a gap of less than 150 base pairs between these two sites, including SOCS1, SOCS3 and SOCS6.

miRNA ID	*log-2 fold change*		*average expression*		*p value (t test)*	
Cell line	ME-15	HuH7	ME-15	HuH7	ME-15	HuH7
hsa-let-7a	0.5208	0.5502	14.183	12.382	0.311	0.093
hsa-let-7b	0.5426	n/d	13.316	n/d	0.034	n/d
hsa-let-7f	0.9974	0.7784	11.550	10.388	0.320	0.114
hsa-miR-19a	0.4741	1.3691	14.011	13.440	0.016	0.075
hsa-miR-19b	0.6640	1.1257	14.074	13.804	0.010	0.023
hsa-miR-30e	0.4012	0.6647	13.445	13.106	0.108	0.038
hsa-miR-203	0.5097	0.728*	10.110	8.807*	0.035	0.002*
hsa-miR-455	0.3673	1.1958	11.598	11.961	0.030	0.077

Table 1 - SOCS1 / 3 targeting miRNA levels after interferon stimulation

Mature miRNA expression (log-2 transformed levels showed) was upregulated 4 hours (n/d no detectable levels, *miRNA only detected after 24h) after interferon alpha stimulation. In Table 1 only miRNAs are listed which have predicted and conserved target sequences in the very 3'-UTR regions of either SOCS1 or SOCS3 or both of them.

Conclusions

We found evidence for a global change of miRNA expression after stimulation with IFN≈. Basal levels of SOCS targeting miRNAs are constitutively expressed and interferon stimulation further boost their expression levels. Consequently we propose a model where several miRNA are needed for a potent decay of SOCS mRNA and consequently their protein levels. After cytokine stimulation SOCS1 mRNA is produced and translated. The binding of the ubiquitously expressed let-7 is inhibited or is not sufficient for SOCS1 degradation. Our microarray analysis depicted immediate regulation of many miRNAs followed by reset to uninduced levels after 24 hours, similar to expression of early response genes (Hallen, 2007). Accordingly, we conclude that several miRNA, with SOCS target sites are involved and hence needed for a fast restoration of steady-state SOCS protein levels (Figure 2).

Primary miRNAs are rapidly transcribed either from intergenetic regions, that carry interferon response elements (as for miR-203) or from introns of early response genes. Alternatively, maturation of pre-miRNA could be influenced by the product of other interferon regulated genes.
In conclusion, our data strongly suggest that interferon inducible miRNAs contribute to the fine-tuning of cytokine signaling.

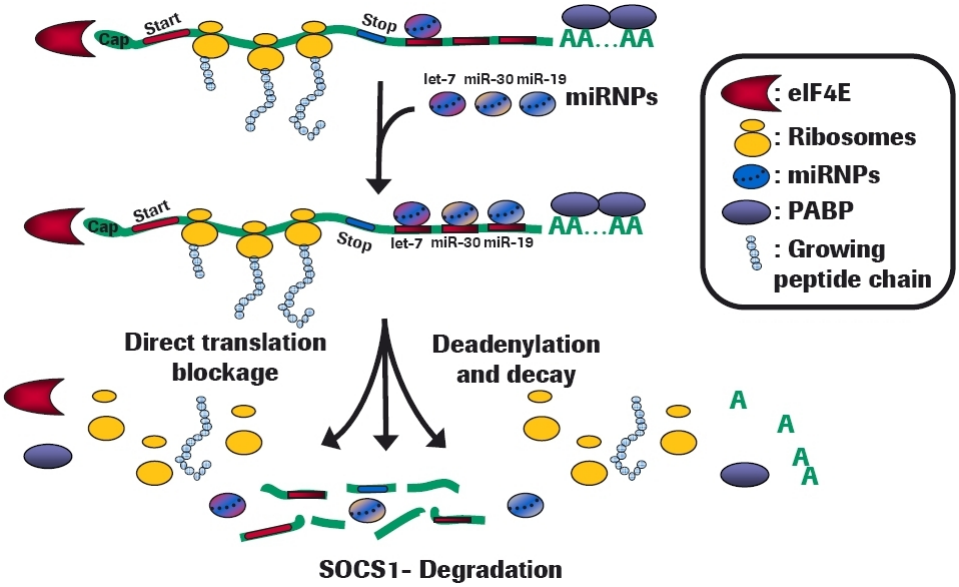

Figure 2 - Model for miRNA mediated degradation of SOCS1

References

BABON JJ et al, The structure of SOCS3 reveals the basis of the extended SH2 domain function and identifies an unstructured insertion that regulates stability Mol Cell, 2, 205-216, 2006.
LANDGRAF P et al, A mammalian microRNA expression atlas based on small RNA library sequencing, Cell, 7, 1401-1414, 2007.
PICHIORRI F et al, MicroRNAs regulate critical genes associated with multiple myeloma pathogenesis, Proc Natl Acad Sci U S A, 35, 12885-12890, 2008.
LENA AM et al, miR-203 represses 'stemness' by repressing DeltaNp63, Cell Death Differ, 7, 1187-1195, 2008.
PEDERSEN IM et al, Interferon modulation of cellular microRNAs as an antiviral mechanism, Nature, 7164, 919-922, 2007.
MENG F et al, The MicroRNA let-7a modulates interleukin-6-dependent STAT-3 survival signaling in malignant human cholangiocytes, J Biol Chem, 11, 8256-8264, 2007.
DU P et al, lumi: a pipeline for processing Illumina microarray, Bioinformatics, 13, 1547-1548, 2008.
HALLEN LC et al, Antiproliferative activity of the human IFN-alpha-inducible protein IFI44, J Interferon Cytokine Res, 8, 675-680, 2007.

Suppression of interferon alpha mediated gene expression by SOCS1 and SOCS3.

Fredy Siegrist and Ulrich Certa
Pharma Research, F. Hoffmann-La Roche AG, Grenzacherstrasse 124, Basel 4070, Switzerland.

Introduction

Name	Structure	Factors that induce expression	Critical role in cytokine signalling
CIS1/CISH		EPO, IL2, IL3, IL6, IL9, INFα, TNFα, GH, prolactin, EPO, TSLP	GH, prolactin, IL2, IL3, EPO
JAB/SSI1/SOCS1		IL2, IL3, IL4, IL6, IL7, IL9, IL13, LIF, IFNγ, IFNα/β, TNFα, GH, prolactin, EPO, TPO, TSLP, G-/GM/M-CSF, TPO, LPS, CpG	IL2, IL4, IL6, IL7, IL12, IL15, IFNα/β, IFNγ, LIF, TNFα, EPO, TPO, TSLP, GH, prolactin, insulin, leptin, LPS, CpG
CIS2/SOCS2		GH, IL6, LIF, IGF1, IFNγ, IFNα, prolactin, insulin, CTNF, cadiotropin, TSH	GH, IGF1, IL6
CIS3/SSI3/SOCS3		IL1, IL2, IL3, IL4, IL6, IL9, IL10, IL11, IL13, GH, prolactin, EPO, GM-CSF, LIF, IFNα, IFNγ, leptin, IL10, LPS, insulin, CTNF, LPS, CpG	GCSF, IL2, IL4, IL6, IL9, IL11, IL23, IFNγ, IFNα/β, LIF, leptin, prolactin, insulin, EPO
CIS7/SOCS4	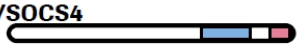		
CIS6/SOCS5	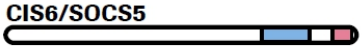	IL6, IL4	IL4, IL6
CIS4/SOCS6	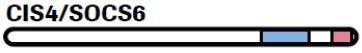		insulin
CIS5/NAP4/SOCS7	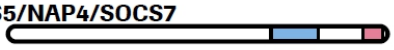		insulin

1 – Eight suppressors of cytokine signaling (SOCS) proteins are regulated by a plethora of cytokines, hormones and growth factors as well as PAMPs (1). CIS and SOCS1-3 are well characterized in their response to these factors. SOCS proteins interfere often in the same pathways in negative feed-back loops. However, regulation of some factors is ambiguous. Here, we have investigated the role of interferon α induced SOCS in regulation of the JAK/STAT pathway.

Type I interferons (IFN) find therapeutic application against HCV infection in combination with anti-viral chemical drugs. Recently, meta-analysis of IFN adjuvant therapy trials has demonstrated benefits for relapse-free survival in melanoma patients. Although cure occurs in some patients, others either do not benefit from the treatment or tend to develop a resistance to the therapy. One class of putative effector proteins is the family of suppressors of cytokine signalling (SOCS) acting in a classical negative feedback loop. In order to understand the mode of JAK-STAT signalling pathway suppression by SOCS proteins, we profiled gene expression in hepatoma and melanoma cells with constitutive SOCS protein expression and IFN-alpha-2a treatment. We found unequally enhanced SOCS1 and SOCS3 mRNA levels shortly after IFN alpha treatment of human melanoma and hepatoma model cell lines. According to the literature, SOCS1 plays an important role in suppressing IFN alpha signalling, whereas the relevance of SOCS3 is disputed. Our results indicate a potential for full range inhibition of IFN alpha-induced gene expression in different tissues by SOCS1, whereas SOCS3 mediated suppression occurs in a cell- and gene-dependent manner. These findings suggest a relationship between SOCS expression levels and response to IFN alpha / PEGASYS® treatment for HCV and cancer.

SOCS mRNA induction by IFNα

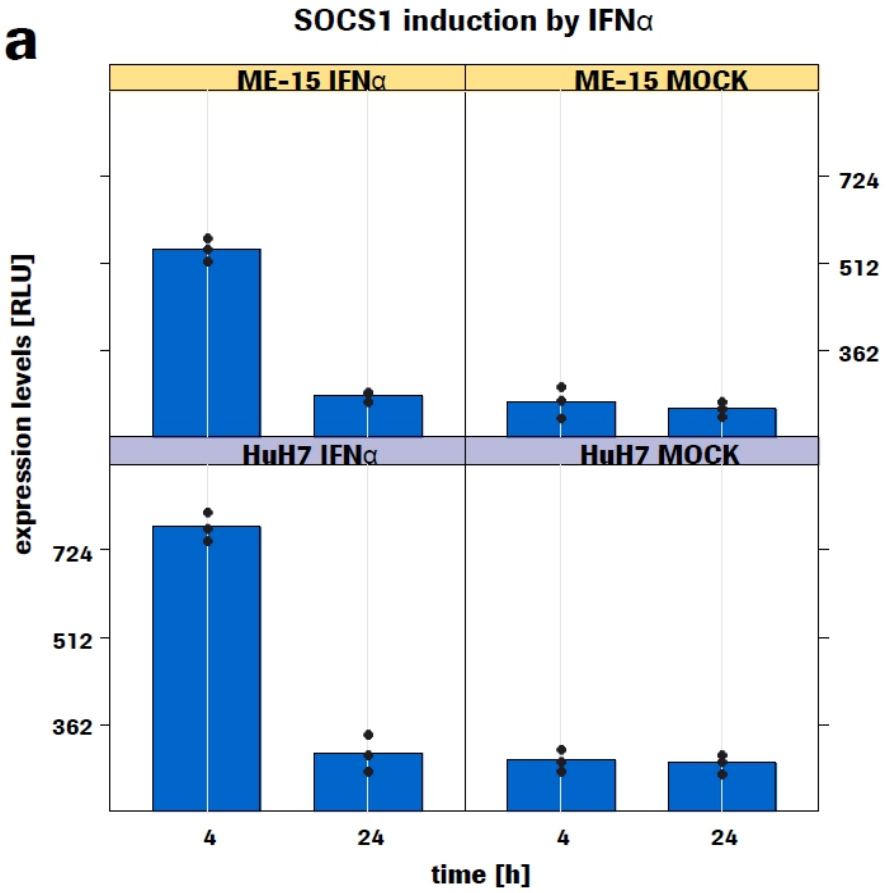

2a – SOCS1 induction by IFNα in melanoma and hepatoma cells, Gene-array [light units].

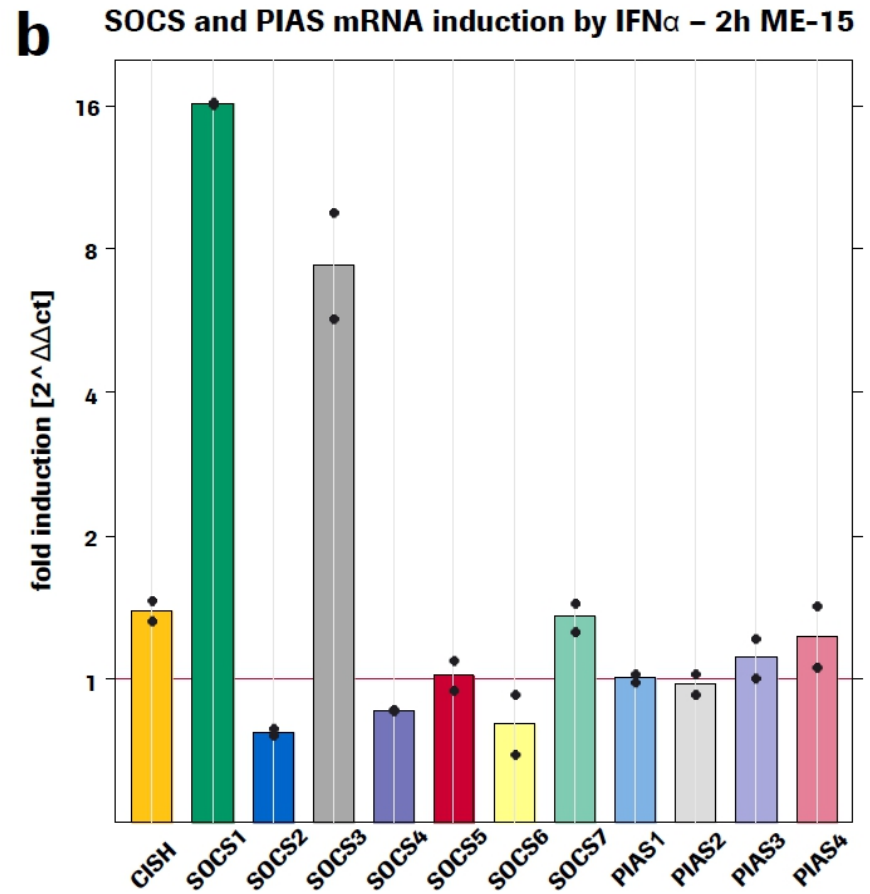

2b – SOCS and PIAS induction by IFNα in melanoma cells, RT-PCR [fold].

raw ct - values	SOCS1	SOCS3
ME-15 untreated	26	29
ME-15 max. induced	21	26
HuH7 untreated	24	29
HuH7 max. induced	21	23

2d – SOCS1 and SOCS3 induction by IFNα in melanoma and hepatoma cells, RT-PCR time-course [cycling times]

SOCS mRNA levels were elevated in several whole genome micro-array studies in combination with recombinant interferon α or pegylated interferon α (2a). SOCS1 and SOCS3 mRNA levels were induced highest among the SOCS and PIAS genes in our melanoma cell model (2b). SOCS1 and SOCS3 mRNA levels were highest at 2-6 and 1-4 hours, respectively (2c). SOCS1 fold induction was more pronounced in melanoma cells whereas SOCS3 was moderately changed therein, while SOCS3 was induced heavily in hepatoma cells compared to SOCS1 induction (2c). SOCS1 level in control cultures was higher in HuH7 cells partially explaining the lower fold induction.

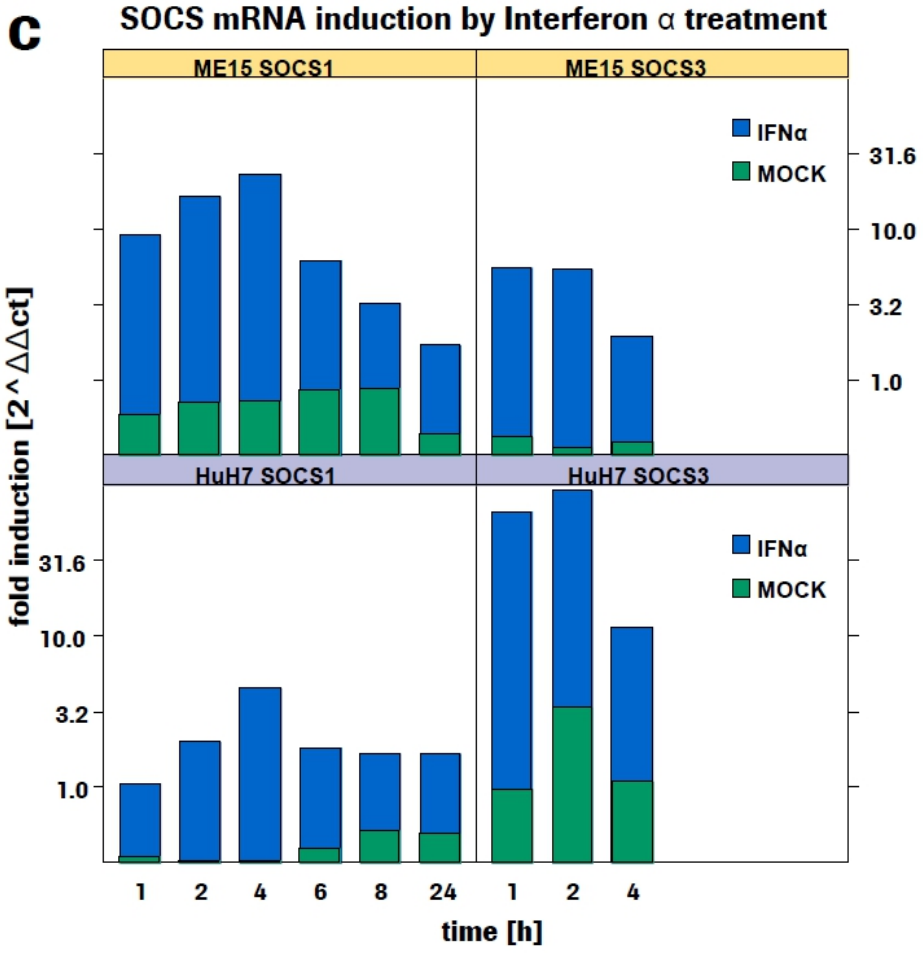

2c – SOCS1 and SOCS3 induction by IFNα in melanoma and hepatoma cells, RT-PCR time-course [fold].

Generation of SOCS expressing cell lines and IFITM3 protein response

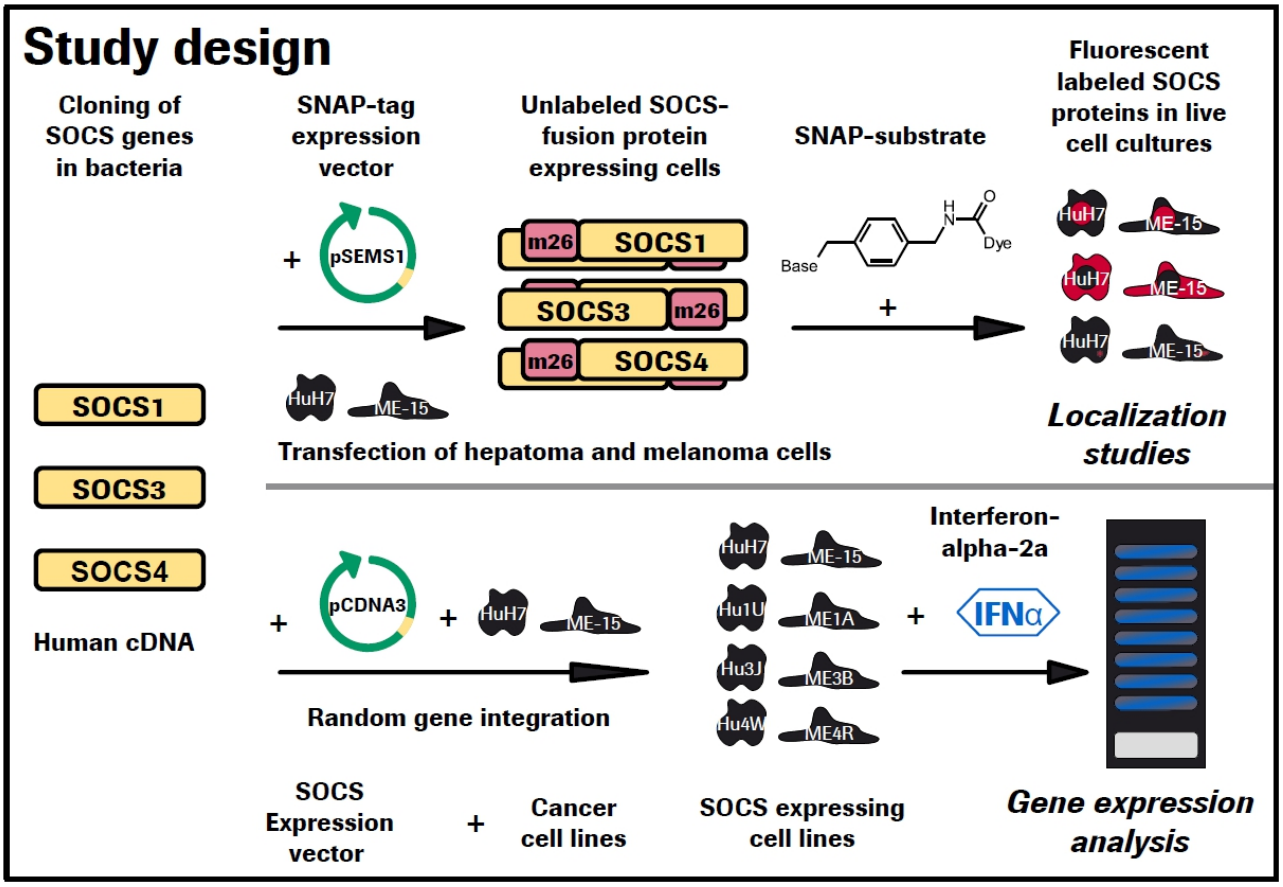

3a – Study design: SOCS proteins and IFNα response in cancer cell lines.

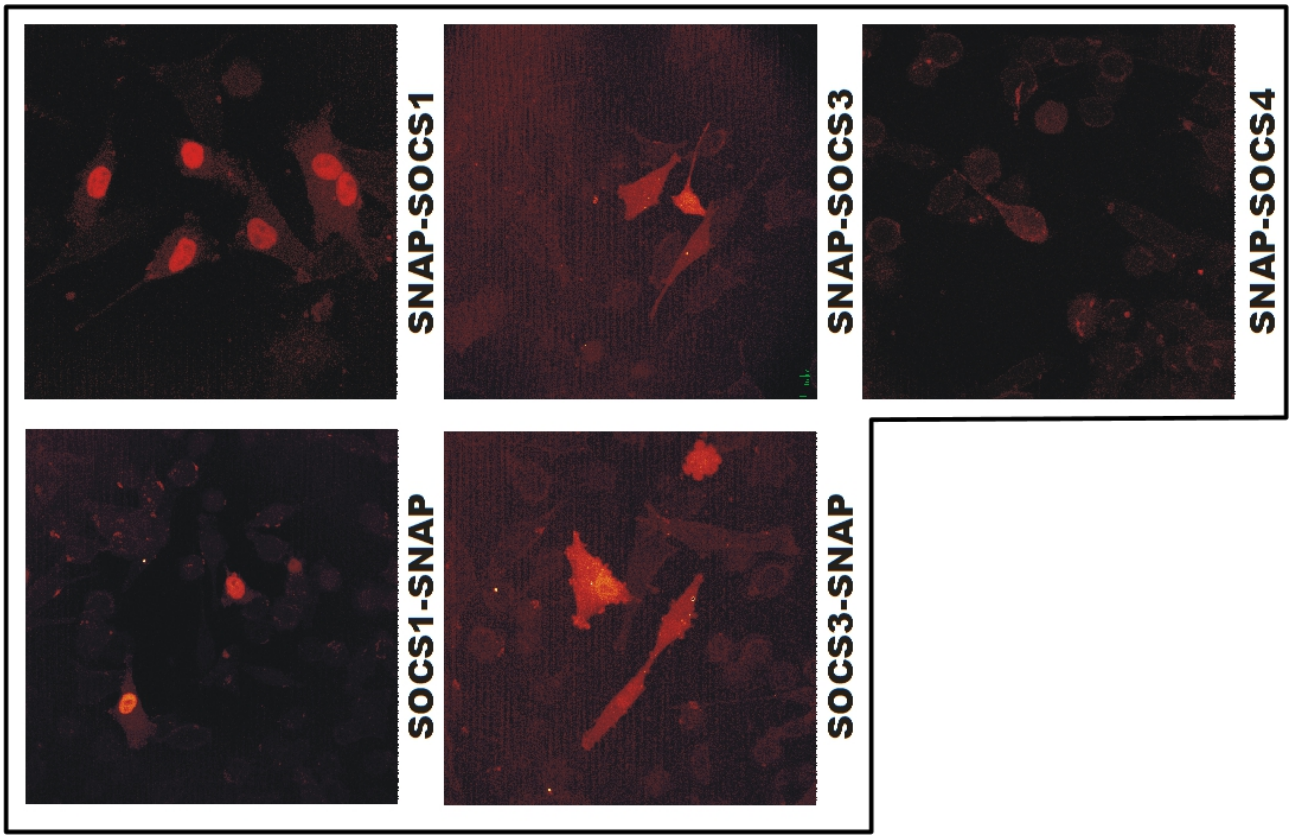

3b – SNAP labeled SOCS proteins in melanoma cell lines, confocal microscopy.

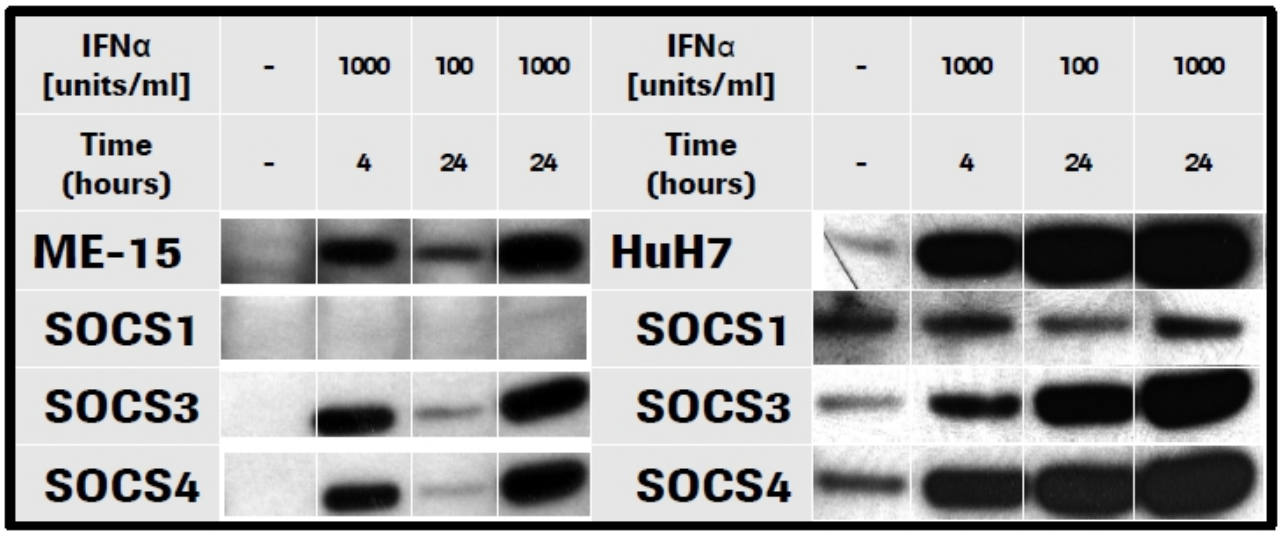

3c – ISG (IFITM3) protein induction by IFNα in melanoma and hepatoma cells,

Whole genome expression analysis of interferon response

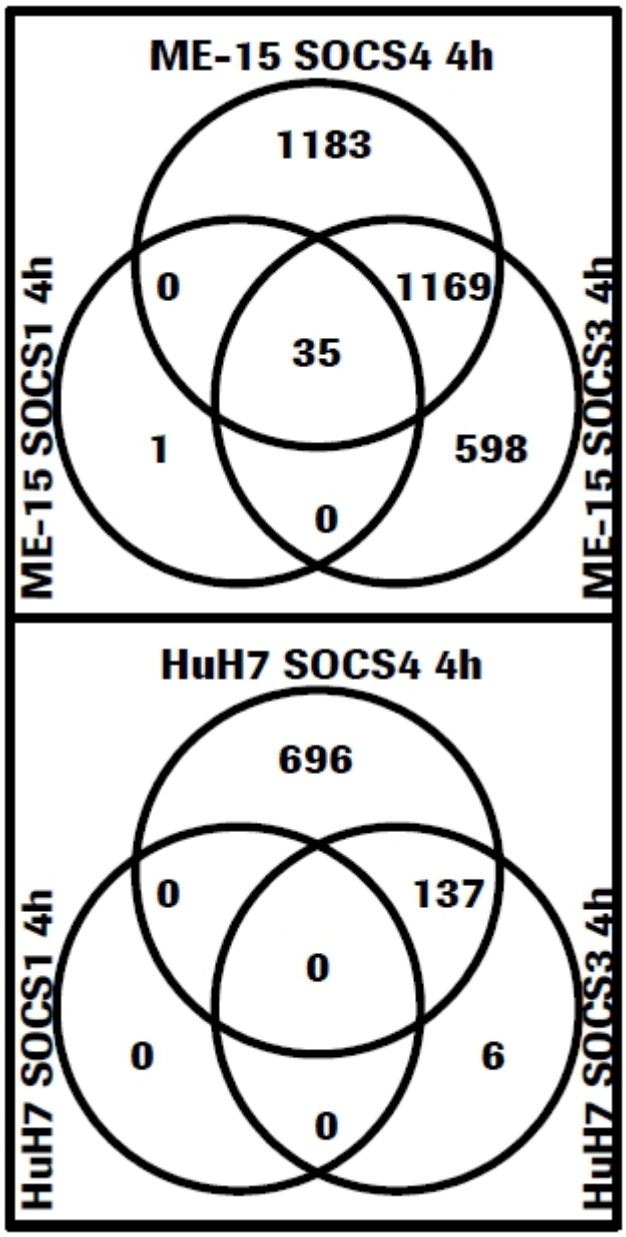

4b – Number of probes significantly changed by 4 hour IFN treatment, Gene-expression arrays [count].

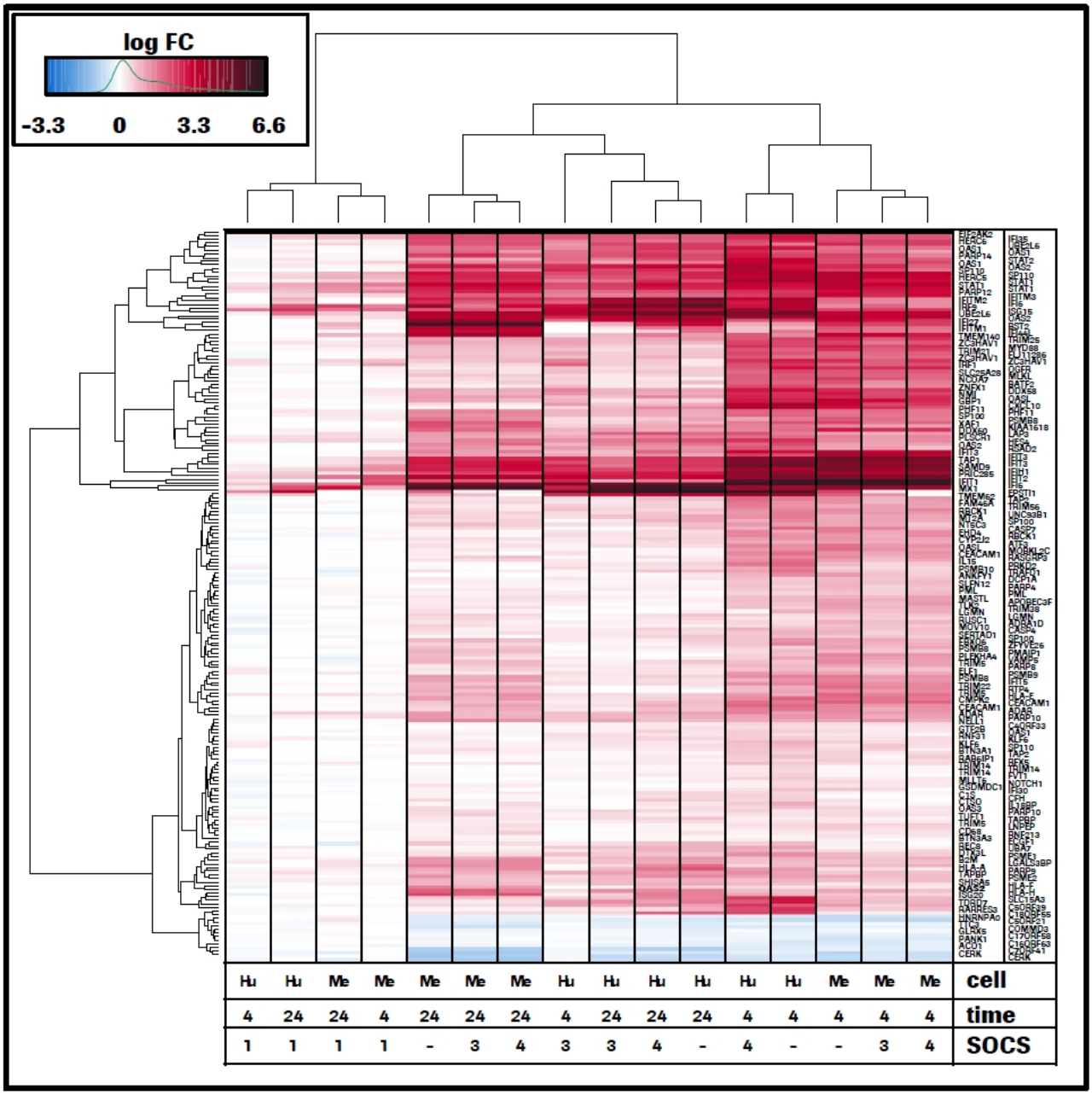

4a – Induction levels by IFN treatment, Illumina Gene-expression arrays [log2 factor change].

Induction of interferon stimulated genes (4a) and their proteins (3c) is blocked in SOCS1 expressing hepatoma and melanoma cells, whereas only SOCS3 in HuH7 cells partially interfere with IFNα gene induction (4b). SOCS3 dependent ISGs have weak IFNα response elements and they are classed rather to IFNγ and late IFNα response genes (4c).

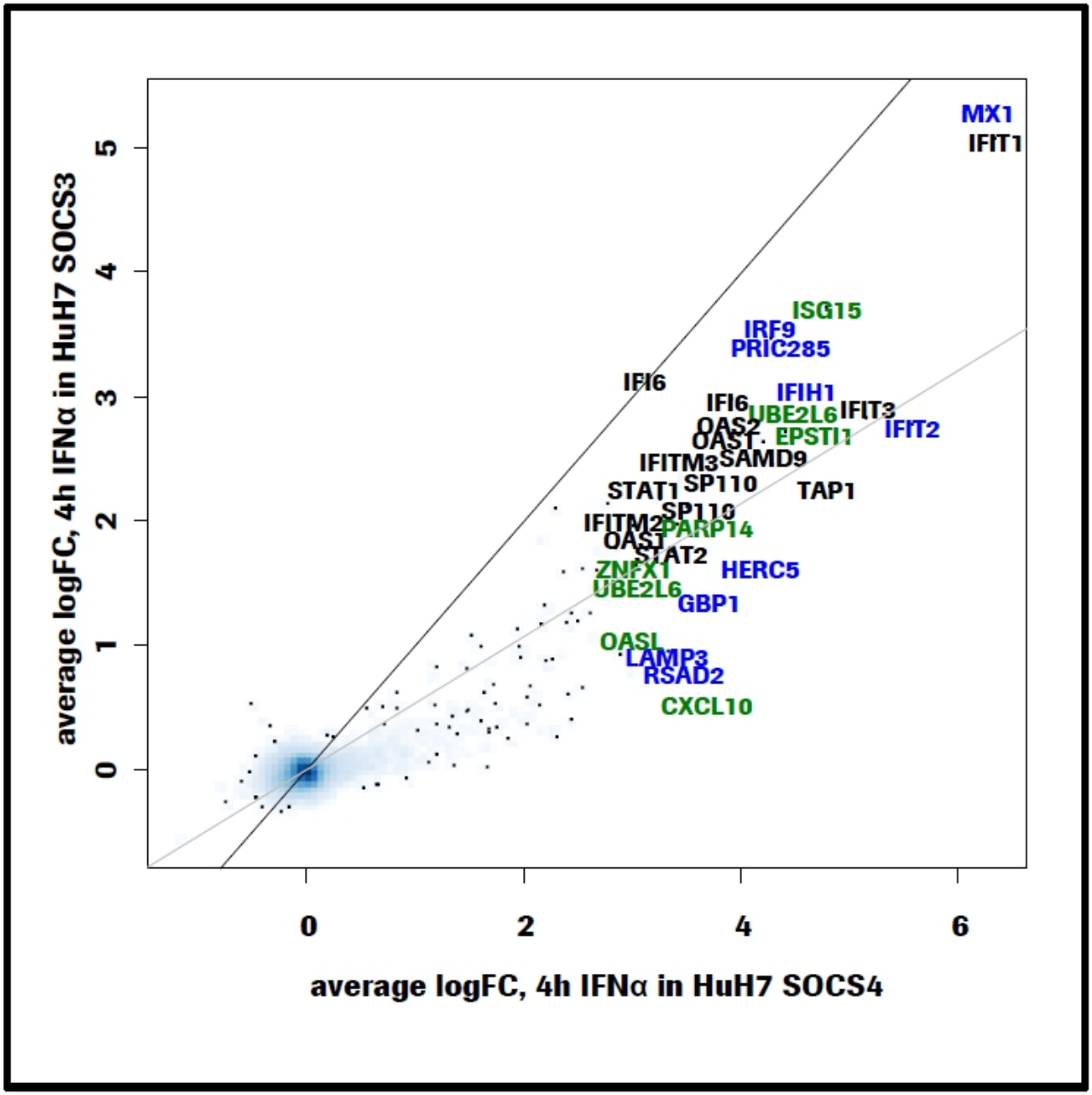

4c – Classification of SOCS3 responder genes colored by numbers of conserved ISRE-like sequences [log factor change].

MicroRNA profiling of SOCS expressing cell lines

IFNα inducible microRNAs have small changes in detection levels shortly after treatment. SOCS expressing cell lines do not differ significantly in their response (5a). However, some of the IFNα inducible microRNAs are targets or have conserved binding sites on SOCS1 and SOCS3 mRNA. SOCS translation may be hindered by these microRNAs followed by deadenylation and decay of the messenger RNA (5b). Prolonged interferon treatment (several days) results in deactivation of the microRNA maturation factor DICER. Our data strongly suggest that interferon inducible microRNAs contribute to the fine-tuning of cytokine signaling.

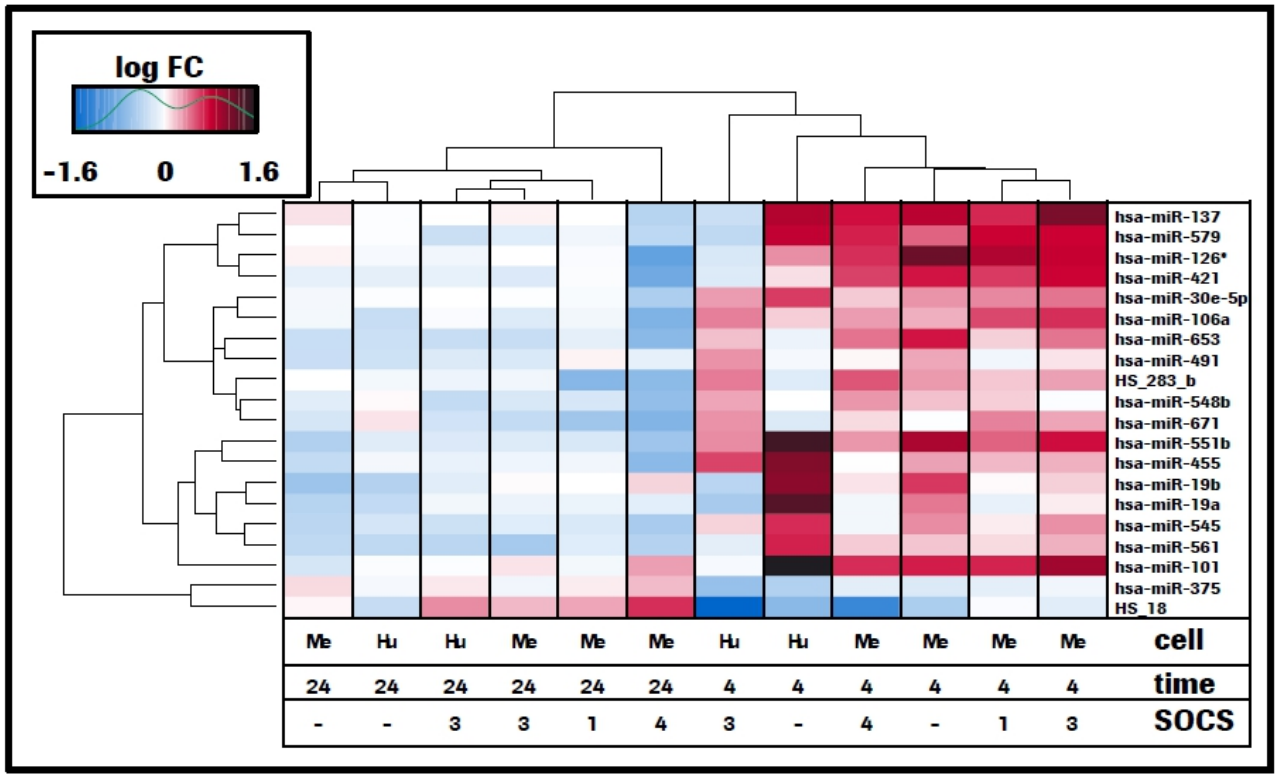

5a – Induction mature microRNA levels by IFNα treatment (4 hours) in melanoma and hepatoma cells expressing SOCS, Illumina microarrays [log2 factor change].

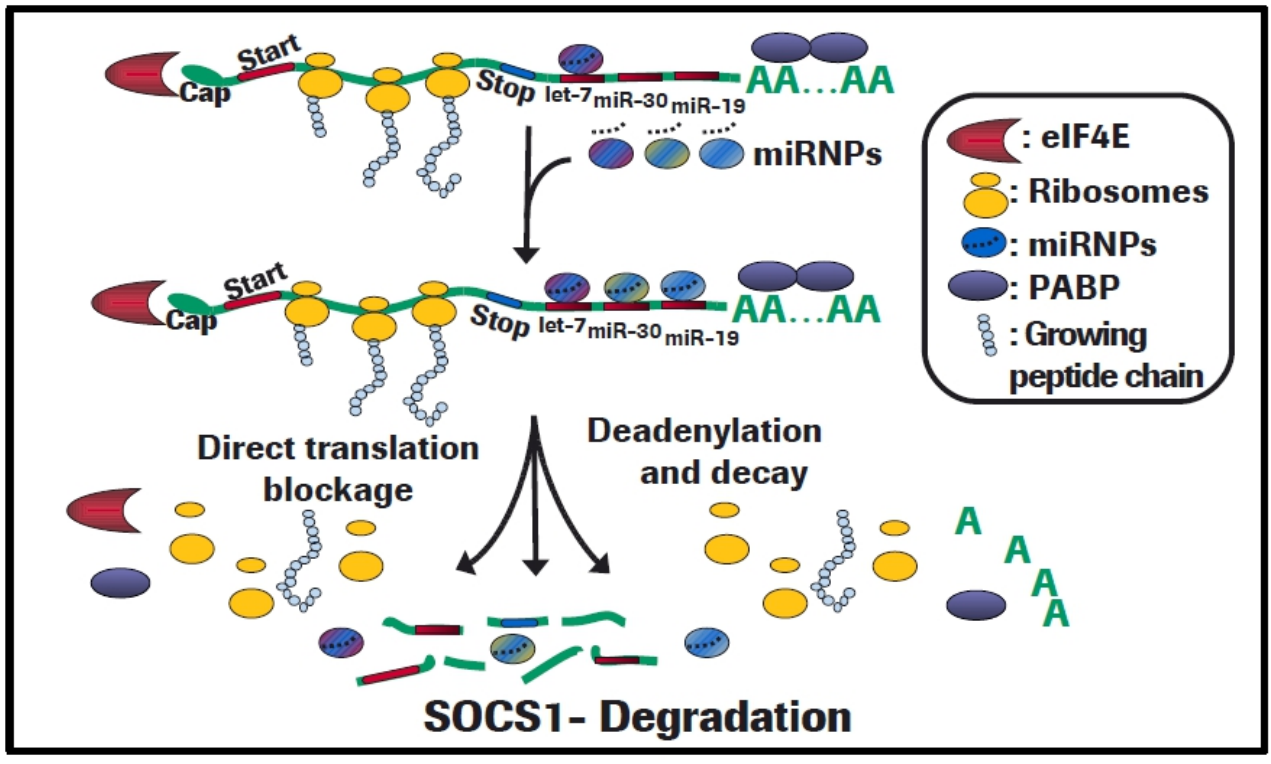

5b – Proposed mechanism of SOCS1 degradation by IFNα induced microRNAs resulting in blockage of SOCS mRNA level. SOCS induction by interferons is followed by interferon regulated microRNA maturation supporting the degradation of SOCS mRNA and thus rapid turn-over of SOCS proteins.

Conclusions

- SOCS1 is a strong inhibitor of IFNα gene induction in both melanoma and hepatocellular carcinoma cells.
- Inhibition by SOCS3 depends on specific cellular factors
- and is marginal after prolonged treatment in vitro.
- Elevated SOCS3 levels interfere with IFNα signaling in hepatocellular carcinoma cells.
- SOCS3 levels are higher in patients with insulin resistance,
- thus either factor can be a negative indicator for interferon therapy success in the treatment of hepatitis viruses.
- SOCS3 levels do not interfere with IFNα signaling in growth sensitive melanoma cells (ME-15), thus SOCS3 may not be a prognostic marker for interferon alpha response in cancer therapy.

References

Siegrist F, Singer T, Certa U. MicroRNA Expression Profiling by Bead Array Technology in Human Tumor Cell Lines Treated with Interferon-Alpha-2a. Biol Proced Online. 2009 Dec; 11 (1): 113-29.

Siegrist F, Certa U. Micro RNA Induction by Interferon Alpha and a Potential Role to Interfere with SOCS. In 7th Joint Conference – Montréal, Québec, Canada, October 12-16, 2008

Editor: John Hiscott. Medimont International Proceedings. 2008: 83-97.

Yoshimura A, Nishinakamura H, Matsumura Y, Hanada T. Negative regulation of cytokine signaling and immune responses by SOCS proteins. Arthritis Res. Ther. 2005; 7 (3): 100-10.

ORIGINAL RESEARCH

Running Header: SOCS-Proteins in IFNα silencing

Siegrist and Certa

Suppression of interferon-alpha-induced gene expression by SOCS1 and SOCS3.

Fredy Siegrist and Ulrich Certa

Non-clinical Safety, F. Hoffmann-La Roche AG, 4070 Basel, Switzerland

Corresponding Author: Ulrich Certa
Grenzacherstrasse 124
4070 Basel
Switzerland
Tel: +41 61 688 53 40
Fax: +41 61 688 14 20
e-mail: ulrich.certa@roche.com

Keywords: Interferon, Suppressor of Cytokine Signaling, Gene expression arrays

Abstract: Type I interferons (IFN) have therapeutic applications in treating hepatitis C virus (HCV) infections and as adjuvant drugs in cancer treatment. A weak antiviral and antitumor response to IFN treatment correlates with the transcriptional expression of suppressor of cytokine signaling (*SOCS*) gene family members, which act in a classical negative feedback loop. We show stronger induction of *SOCS1* and less induction of *SOCS3* mRNA levels after IFN-alpha treatment in a human melanoma cell line (ME-15) compared to a hepatoma cell line (HuH7). In order to identify which INF-induced genes (ISGs) are suppressed by SOCS protein expression, we defined the genome-wide gene expression profiles of hepatoma and melanoma cells engineered to constitutively express one SOCS protein following IFN-alpha-2a treatment. We show full repression of IFN-alpha-induced gene expression in cancer cells by SOCS1, whereas SOCS3 mediated suppression is cell type specific and affects only a subset of inducible genes. Our data further support the negative correlation of *SOCS* expression levels and transcriptional response to IFN-alpha. Inhibitors of SOCS signaling could therefore prolong the IFN-alpha responses in clinical applications such as HCV or cancer therapy.

Introduction

The suppressors of cytokine signaling (SOCS) protein family, comprising eight members, is regulated by a wide variety of cytokines, hormones, growth factors and pathogen associated molecular patterns (PAMP) (Greenhalgh *et al.* 2001). Among them, SOCS1, also known as JAK-binding protein (JAB) or STAT-induced STAT-inhibitor 1 (SSI-1), and SOCS3 can interfere in interferon (IFN) signaling through their kinase inhibitory region (KIR), whereas SOCS2 and cytokine inducible SH2-domain containing human protein (CISH) and the larger SOCS4-7 lack this domain. SOCS proteins generally downregulate the pathway that triggered their expression. They act by classical negative feedback loop mechanisms functioning as inhibitors of upstream signaling proteins including cytokine receptors (Fujimoto *et al.* 2003; Yoshimura *et al.* 2005). SOCS-mediated regulation of receptors, kinases and signal transducers, including those involved in interferon-alpha (IFNα) signaling varies dependent on cell type. The classical IFNα signaling pathway is well known and consists of a few components, which act in a serial cascade (Stark *et al.* 1998). IFNα activates the IFNα receptors (IFNARs), triggering receptor dimerization allowing the phosphorylation of the receptor-associated Janus family tyrosine kinases (JAKs). Activated JAKs regulate the activation and dimerization of the signal transducer and activator of transcription (STAT) proteins (Darnell *et al.* 1994). The STATs translocate to the nucleus to induce interferon stimulated gene (ISG) expression. STAT activation, one of the crucial steps in IFNα signaling, can be downregulated by SOCS proteins, protein tyrosine kinases and transcriptional activity can be inhibited by protein inhibitors of activated STATs (PIAS) (Shuai 2006). Among other IFNα early response genes, *SOCS1* and *SOCS3* are transcribed and translated to suppress JAK-STAT signaling concurrently through the SH2 phospho-tyrosine-binding domain, the SOCS-box and the kinase inhibitory region (Croker *et al.* 2008). SOCS1 blocks interferon signaling by binding to the INFα receptor (INFAR1), thereby masking the JAK-recognition site (Sakamoto *et al.* 1998; Fenner *et al.* 2006; Walsh *et al.* 2006). SOCS1 suppresses also interferon gamma (IFNγ) signaling through IFNγ-receptor binding, KIR dependent inhibition of JAK2 activation and binding of phosphorylated JAK2 through the SH2 domain (Starr *et al.* 2009; Endo *et al.* 1997; Yasukawa *et al.* 1999; Qing *et al.* 2005). Important for IFNα signaling through JAK1 / tyrosine kinase 2 (TYK2) is the fact that both the N-terminus and SH2 domain of SOCS1 are required for inhibition of JAK1, in contrast to JAK2 inhibition where either of these two domains alone is sufficient for kinase inhibition *in vitro* (Nicholson *et al.* 1999). Furthermore, SOCS1 is involved in kinase degradation in IFNγ-signaling through its SOCS-box motif with E3 ligase functionality leading to ubiquitination of JAK2 (Piessevaux *et al.* 2008). An unpublished report suggested TYK2 ubiquitination and consequent TYK2 degradation when overexpressing ubiquitin, TYK2 and SOCS1 *in vitro* (Nguyen *et al.* 2006) However, a recent report demonstrate the destabilization of TYK2 through SOCS1-box independent inhibition of TYK2 activation by blocking the activating ubiquitination on Lys-63 (Piganis *et al.* 2011). The degradation of the JAK1 is mediated through SOCS3 activity, in contrast to passive JAK1 inhibition by SOCS1 (Boyle *et al.* 2009). Recently, the ability of SOCS3 (KIR and SH2

domain) to inhibit JAK1, JAK2 and TYK2 has been shown *in vitro* implying that over-expressed SOCS3 is able to inhibit the kinases of classical IFNα signaling (Feng *et al.* 2012). However, this inhibition occurs with poor affinity, especially for TYK2, and is limited at physiological levels to cytokine pathways utilizing receptors with SOCS3 binding sites (Babon *et al.* 2012). SOCS1 and SOCS3 inhibit IFN mediated antiproliferative action in cancer cell lines and the expression of IFNα inducible antiviral proteins in liver cell lines (Song *et al.* 1998; Vlotides *et al.* 2004). This suggests that both SOCS1 and SOCS3 proteins are able to interfere with the IFNα signaling pathway and therefore limit the ability of IFNα therapy to control viral infections and expansion of cancer.

IFNα is used as standard therapy to treat chronic hepatitis C virus infections in combination with the antiviral nucleoside pro-drug ribavirin. The response to this treatment varies from patient to patient, and depends on the selected population, the viral genotype and other factors including steatosis, insulin resistance and high *SOCS3* expression levels in the liver (Persico *et al.* 2010; Moucari *et al.* 2008; Petta *et al.* 2008; Persico *et al.* 2007). Factors that are predictive for treatment outcome, such as HCV genotype and insulin resistance directly correlate with SOCS3 expression (Persico *et al.* 2009; Vanni *et al.* 2009). As a result, SOCS3 expression correlates with drug resistance in patients with chronic hepatitis C (CHC) (Walsh *et al.* 2006; Huang *et al.* 2007; Kim *et al.* 2009; Miyaaki *et al.* 2009). Beside of *SOCS3*, other interferon-stimulated genes (ISGs) are abundantly expressed in the liver of non-responding patients (Feld *et al.* 2007; Sarasin-Filipowicz *et al.* 2008). More non-responding HCV patients may be cured by reversal of this pre-activation of the endogenous IFN system in the liver (Sarasin-Filipowicz 2010). Therefore, strategies to modify SOCS activity may have therapeutic benefits (Starr *et al.* 2009). IFNα is also administered as adjuvant therapy in patients with metastatic melanoma after surgical removal of the tumor and in a meta-analysis patients revealed a significant benefit in relapse-free survival (Garbe *et al.* 2010). SOCS1 and SOCS3 expression is inversely correlated with cellular sensitivity to IFNα and may contribute to the resistance to the growth-inhibitory action of pro-inflammatory cytokines in clinical applications (Yoshikawa *et al.* 2001; Evans *et al.* 2007; Sakai *et al.* 2002; Roman-Gomez *et al.* 2004; Brender *et al.* 2005; Takeuchi *et al.* 2005). In line with this, high SOCS1 and SOCS3 levels indicates poor prognosis in metastatic melanoma (Li *et al.* 2004). The mechanism by which SOCS1 and SOCS3 impacts on IFNα resistance may be through STAT1 serine phosphorylation that correlates with SOCS3 levels (Fojtova *et al.* 2007). However, IFNα mediated STAT1 tyrosine phosphorylation is reduced by overexpression of SOCS1 or SOCS3 and SOCS suppression in melanoma cells results in restored sensitivity to IFNα signaling (Lesinski *et al.* 2010).

Here, we analyzed effects of SOCS1 and SOCS3 on gene transcription in IFNα signaling using genome wide profiling. We constructed SOCS1 and SOCS3 overexpressing melanoma and hepatoma cell lines to identify genes that are controlled by these suppressors and the potential therapeutic impact of our findings is discussed.

Material and methods

Plasmids

SOCS1, 3 and 4 coding sequences were cloned from RNA of ME-15 or HuH7 cells treated for two hours with INFα. Total RNA was isolated with the RNeasy Kit using QIAshredder columns for cell homogenization (Qiagen AG, Hombrechtikon, Switzerland). RNA was converted into cDNA with first strand RT-PCR kit using poly-p(dT)15 primers (Roche Applied Science, Rotkreuz, Switzerland). Protein coding sequences were amplified using *SOCS* specific primers (supplementary table 1). cDNA was sub-cloned in pCR2.1-TOPO vector and SOCS coding sequences were inserted in mammalian expression vector pcDNA3.1 NEO+ (Invitrogen, Basel, Switzerland) and pSEMS1-26m an expression vector with insertion of mammalian SNAP-tag (*26m*) coding sequence (Covalys Biosciences AG, Witterswil, Switzerland). Sequences coding for C terminally fused SNAP tag (Covalys Biosciences AG, Witterswil, Switzerland) were sub-cloned using 'non-stop' primer with deleted STOP codon (supplementary table 1) and Phusion High-Fidelity DNA Polymerase (New England Biolabs, BioConcept, Allschwil, Switzerland). From cDNA template *SOCS1*, *SOCS3* and *SOCS4* sequences were amplified with Advantage®-HF 2 PCR kit (BD Biosciences Clontech, Allschwil, Switzerland). Gel-purified DNA was sub-cloned in pCR2.1-TOPO plasmids and cut by standard restriction enzymes (Roche Applied Science, Rotkreuz, Switzerland). The expression vector pSEMS1-*26m* and pcDNA3.1 were cut and dephosphorylated with shrimp alkaline phosphatase (Roche Applied Science, Rotkreuz, Switzerland). Vector DNA and insert DNA were ligated with Rapid DNA Ligation Kit (Roche Applied Science, Rotkreuz, Switzerland) in a ratio of 1:3 and transformed in Dh5α chemically competent cells. Plasmid constructs were sequenced over the entire trans-gene region.

Cells and interferon treatment

Melanoma cells (ME-15) were cultured in RPMI 1640 with L-glutamine (2 mM) containing 10 % FBS and supplemented with non-essential amino acids (0.1 mM) and sodium pyruvate (1 mM) (RPMI *culture medium*). Hepatocyte-derived cellular carcinoma cells (HuH7) were cultured in D-MEM with GlutaMAX™-I containing 10 % FBS (D-MEM *culture medium*). All cell culture reagents were purchased from Invitrogen (Gibco®, Invitrogen, Basel, Switzerland). Roferon (Interferon-alpha-2-a, Roche Pharmaceuticals, Basel, Switzerland) was diluted in fresh *culture medium* to a final concentration of 100 or 1,000 U/ml and control cultures were grown without added cytokines. Cells were cultured at 37 °C in a humidified atmosphere containing 5 % CO_2. For the generation of stable *SOCS* expressing cells, ME-15 and HuH7 cells were transfected with Optifect (Invitrogen, Basel, Switzerland), split_one day post transfection and cultured in *culture medium* containing geneticin (*selective medium;* 800 µg/ml for ME-15 or 1.5 mg/ml for HuH7). Antibiotic-resistant clones were obtained by cultivation in *selective medium* for three weeks and single cells were plated in hybridoma cell culture dishes (Greiner bio-one, St. Gallen, Switzerland) and expanded to *SOCS*-transduced cell lines of approximately one million cells.

Cell cultures were screened for *SOCS* mRNA expression and three cell lines for each plasmid were cultured up to approximately 20 million cells. Then, induction of interferon induced transmembrane protein 3 (IFITM3) was measured to verify ISG stimulation.

Transfection and confocal microscopy

SNAP tag fusion proteins were transfected into cells with Optifect transfection reagent (Invitrogen, Basel, Switzerland), followed by a minimal incubation of 6 hours. SNAP-cell TMR-Star photostable substrate was added at a concentration of 2 µM (Covalys Biosciences AG, Witterswil, Switzerland). Cells were washed according to the manufacturer's protocol and fluorescent pictures were taken with a Leica confocal microscope DMI4000B.

Western blot analysis

Cell lysates containing protease and phosphatase inhibitory tablets (Roche Applied Science, Rotkreuz, Switzerland) were quantified with BCA protein assay (Pierce, Rockford, IL, USA), separated and blotted using the Xcell II™ system (Invitrogen, Basel, Switzerland). IFITM3 proteins were detected with primary antibody against 1-8 protein peptide (1:1000 dilution) described in (Brem *et al.* 2003), followed by horseradish peroxidase conjugated secondary antibodies (Biorad, Reinach, Switzerland). Immune complexes were detected with Supersignal West Pico chemiluminescent substrate (Pierce, Rockford, IL, USA) on Lumi-Film Chemiluminescent Detection Film (Roche Diagnostics AG, Rotkreuz, Switzerland). Pictures were digitalized on a transmitted light scanner and plot intensity profiles of probe-lanes were calculated by image processing method in ImageJ (Wayne Rasband, National Institute of Mental Health, Bethesda, MD USA). Protein levels were estimated by calculation of the area under the curve (AUC) of the IFITM3 protein signal peak using the statistical program R and the package msProcess for data preparation, baseline correction, intensity normalization and peak detection.

RT-PCR analysis

250 ng of total RNA from IFNα (1000 U/ml) treated ME-15 or HuH7 cells was analyzed with QuantiTect SYBR Green RT-PCR reagent (Applied Biosystem, Rotkreuz, Switzerland) using *SOCS* and *PIAS* specific primers (Microsynth AG, Balgach, Switzerland - supplementary table 2). Optical data were generated using a 7500 Real-Time PCR system and analyzed using the manufacturers software package SDS (Applied Biosystem, Rotkreuz, Switzerland) to generate cycling time (ct) values. Fold induction (2^ΔΔct values) were calculated in R as ration of mean normalized expression values of sample to untreated controls as described previously (Siegrist *et al.* 2009). Significance was assessed by analysis-of-variance (ANOVA) tests comparing ct values.

Gene expression microarray analysis

Total RNA was extracted from independent triplicates using the Trizol reagent (Sigma, Buchs, Switzerland). RNA was quantified using the Quant-iT™ RiboGreen® RNA Assay (Invitrogen, Basel, Switzerland) and 500 ng total RNA subjected to cDNA synthesis and subsequently in vitro transcribed to biotin labeled cRNA using the Illumina® TotalPrep RNA Amplification Kit (Ambion - Applied Biosystem, Rotkreuz, Switzerland). The protocol of miRNA microarray detection has been described previously (Siegrist *et al.* 2009). For genome-wide expression analysis 750 ng of cRNA was hybridized to HumanRef-8 v3 Expression BeadChips (Illumina, CA, USA) according to the manufacturer's protocol. Replicates were randomly distributed among slides and positions. Bead arrays were washed and stained using FluoroLink Cy3 Streptavidin (GE Healthcare AG, Glattbrugg, Switzerland). Fluorescent signals were imaged by laser scanning using the iScan system (Illumina, CA, USA). Scanner images files were processed by software supplied from the manufacturer to probe intensity files and further processed with the genome studio software (Illumina, CA, USA) without normalization and background correction. Illumina probe intensity data was processed by variance stabilization transformation (VST) (Lin *et al.* 2008) using R/Bioconductor software (lumi library) (Du *et al.* 2008), followed by quantile normalization. Significance of effects for probes was tested in R/Bioconductor (limma library) (Smyth 2004) using moderated t-test and the false discovery rate (FDR) correction method by the Benjamini and Hochberg for multiple testing. No unspecific filter was applied and multiple probes per gene were retained. Raw and normalized data is accessible at NCBI GEO database, series accession number GSE22801.

Results

SOCS expression in IFNα treated cell lines

We have previously shown variation in induction of ISG through IFNα stimulus among different cancer derived cells and reanalyzed the data for *SOCS* and *PIAS* induction (Hallen *et al.* 2007). *SOCS1* was found to be induced in most of ten cancer cell lines tested when treated with recombinant IFNα, whereas other *SOCS* and *PIAS* transcripts were not significantly regulated or not detected (NCBI GEO database, series accession number GSE21158). Eight out of ten cell lines showed induction of *SOCS1* mRNA four hours following IFNα treatment (supplementary figure 1). We confirmed the induction of *SOCS1* by IFNα in the melanoma cell line ME-15 using a more sensitive assay. Moreover, we examined all *SOCS* and *PIAS* transcripts by semi-quantitative reverse-transcription polymerase chain reaction (RT PCR). Among the genes analyzed by RT-PCR (CISH, *SOCS1-7* and *PIAS1-4)*, *SOCS1* (16.2 fold) and *SOCS3* (7.4 fold) mRNA levels were most significantly (p-value < 2e-16) induced by IFNα and their increase was considerably higher compared to the other *SOCS* and *PIAS* genes (figure 1a). A moderate upregulation of *CISH*, *SOCS7* and *PIAS4* genes (1.2-1.4 fold, 0.0025 > p-value > 0.05) was detected, but we considered that to be biologically irrelevant relative to

SOCS1 and *SOCS3*. In addition to the level of induction, we have evaluated by RT-PCR the time dependent induction levels and duration of *SOCS1* and *SOCS3* expression that may be as important for the attenuation of cytokine signaling as their maximal induction levels. *SOCS1* and *SOCS3* mRNA levels reach peak levels between two and four hours after IFNα treatment (figure 1b). In contrast to HuH7, *SOCS1* induction was more effective in melanoma cells whereas *SOCS3* induction was ten times stronger in hepatoma cells. In both cell lines *SOCS1* levels reached similar maximal induction levels in response to IFNα (Δct = 5.7±0.1 and 5.5±0.4 for ME-15 and HuH7, respectively). Typically, STAT activation declines in the first hours implying that JAK-STAT activation drives IFNα induced *SOCS1* and *SOCS3* transcription as induced levels were observed here already one hour after treatment (Maher *et al.* 2008).

Subcellular localization of SOCS proteins

Unlike the classical IFN signal regulation by SOCS1 at the cell membrane, SOCS proteins can also be found in the nucleus, where their function in cytokine signal inhibition remains unclear for many SOCS (Ben-Yair *et al.* 2002). A nuclear localization signal (NLS) sequence was identified in *SOCS1* and mutations do not affect but nevertheless impair the inhibitory function of IFNγ-induced gene expression but not STAT1 activation (Baetz *et al.* 2008; Koelsche *et al.* 2009).

To assess SOCS localization in ME-15 cells, we cloned the *SOCS1*, *SOCS3* and *SOCS4* cDNAs from IFNα treated cell lines for recombinant expression. We generated constructs in which SOCS fusions proteins with a SNAP tag are expressed that allow fluorescent labeling at different time points for dynamic subcellular localization. When labeled 16 hours after plasmid transfection, SOCS1 proteins are located in the nucleus, whereas SOCS3 proteins are equally distributed in the cytoplasm (figure 2). Attachment of the tag at the amino- or the carboxy-terminus had no influence on the subcellular localization of SOCS1 and SOCS3. Tagged SOCS4 proteins were expressed at the detection limit whereas SOCS1 and SOCS3 proteins are found express in the cytoplasm already six hours after plasmid transfection (not shown). The proteins are then translocated to their primary localization site and can be detected after 36 hours associated with compartments near the nucleus where the proteasome is localized (not shown). Our results demonstrate SOCS1 nuclear localization whereas SOCS3 is present predominantly in the cytoplasm when overexpressed in ME-15 cells.

Interferon-stimulated gene response in SOCS cell lines

To analyze the effect of SOCS1 and SOCS3 on interferon induced protein and gene expression without challenging the cells with DNA-transfection, we have generated clones of ME-15 and HuH7 cells overexpressing untagged SOCS proteins. Expression of *SOCS* mRNA and protein was confirmed by qPCR and western blot and had no visible effect on cell morphology or growth rate. We examined cell clones with high *SOCS* expression for the potential of IFNα in inducing IFITM3 protein levels to determine the functionality of the expressed SOCS proteins in this pathway. IFITM3 response levels are dependent on duration of IFNα stimulus and on the

amount of IFNα used. Therefore, monitoring of IFITM3 protein levels can be used as model ISG in these cells to control impact of SOCS proteins for both retardation and efficacy of IFNα signaling. In ME-15 cells, IFITM3 protein levels are detectable only after IFNα stimulation, whereas HuH7 cells express this protein at low basal levels (figure 3). SOCS1 expression suppresses IFITM3 protein production in both cell lines whereas the effect of SOCS3 is far less distinct. Quantification of the chemiluminescent signal shows suppression of IFITM3 protein synthesis in five out of six *SOCS1* expressing clones. One clone has a similar response as the progenitor cell line, maybe due to spontaneous mutation in the *SOCS1* gene during single cell selection. In contrast, *SOCS3* expressing ME-15 cells and all cells generated with *SOCS4* plasmid respond similar to the parental cell lines. Relative IFITM3 protein levels are lower in all three SOCS3 expressing HuH7 cells lines, each derived from a single cell clone, indicating a limited effect on IFNα signaling in these cells (figure 3). However, reduced IFITM induction does not correlate with the amount of SOCS3 in these hepatoma cells (not shown). In conclusion, we were able to generate SOCS1 expressing cell lines that fail induction of ISG protein expression in response to IFNα and SOCS3 expressing cell lines with at most partially effect on IFITM3 induction.

Genome-wide expression analysis of interferon responses in SOCS over-expressing cells lines

There are hundreds of genes induced by IFNα with different promoters and induction time. To address the question to what extend the negative impact of SOCS expression on IFNα transcriptome responses varies in different cell lines we monitored mRNA levels by Illumina gene expression microarrays. Genome-wide expression levels were analyzed in SOCS overexpressing cell lines with the corresponding two parental lines as reference and with non-stimulated controls for each condition for 2 different time points. We chose to analyze gene expression four hours after IFNα treatment, because induction of ISGs was maximal at this time *in vivo* and was followed by down-regulation of many genes (Lanford *et al.* 2006). In addition, we analyzed gene expression at 24 hours after treatment to estimate if secondary response genes are activated that are not dependent on SOCS regulated pathways such as JAK-STAT. In total, 8'658 unique genes were expressed in the majority of the samples significantly above background levels. The effect of IFNα was estimated by an analysis of variance that take into account the cell-type, time and the presence of overexpressed SOCS, IFNα treatment as well as its interaction with time and *SOCS* type as co-factors. This analysis generated 1'708 significantly changed probes representing more than 1'500 individual genes. Cluster-analysis of genes affected by SOCS proteins shows an overall suppression of ISG induction in SOCS1 expressing hepatoma and melanoma cells (figure 4). As a consequence, SOCS1 expressing cells clustered together on the sample axis due to the suppression of ISG induction. In SOCS1 expressing hepatoma cells, no probe was significantly upregulated four hours after IFNα treatment (adjusted p-value < 0.05) and only 11 probes at 24 hours (supplementary figure 2). Similarly, 36 and 12 probes were significantly changed in ME-15 SOCS1 cells at 4 hours and

24 hours, respectively. By comparing induction of ISGs in control and SOCS1-expressing cells, components of the IFNα signaling pathway themselves, *IRF9* and *STAT1*, are less affected by SOCS1 overexpression than classical interferon-stimulated response element (ISRE) bearing genes for example *IFIT1*, *IFIT2*, *IFITM3* or *OAS2* (supplementary figures 3 and 4). In contrast to SOCS1, high SOCS3 levels in melanoma cells (ME-15) do not alter the clustering of these samples (figure 4). The effect of SOCS3 in ME-15 is comparable with the one in the SOCS4 control cells and thus too marginal to draw further conclusions (supplementary figure 3). In contrast, SOCS3 expressing HuH7 cells four hour after treatment cluster with control cells of one day IFNα treatment and some probes for early ISGs are not changed in these samples (figure 4). Probes for *IFITM1*, *GBP1*, *IRF1* or *CXCL10* genes, more responsive to IFNγ than IFNα, are not significantly inducible at four hours in presence of SOCS3 (supplementary figure 4). This suggests stronger impact of SOCS3 on IFNγ activated promoter response element driven ISG expression. However, genes without ISRE element are not significantly enriched in SOCS3-suppressed probes in HuH7 cells (not shown). SOCS3 expression in the hepatoma cell line has no impact on induction of primary response genes such as *MX1*, *EIF2AK2* (PKR), *OAS1* and *OAS2* (supplementary figure 4).
Cell lines transformed with the *SOCS4* expression plasmid have low *SOCS4* mRNA levels and the IFNα response is normal (data not shown). However, transformation and selection of cell lines with any *SOCS* expressing vectors did change a panel of genes including *EFEMP1*, *NRP1*, *MAGEA8*, *IPO8*, *CD81*, *CTPS2* and *RPS6KA3*.
In conclusion, SOCS1 is potent to suppress globally ISG induction *in vitro*, whereas suppression of IFNα-induced genes by SOCS3 could only partially be observed in hepatoma cell lines.

MiRNA expression profiles in SOCS overexpressing cells

In addition to classical ISG induction, evidence is accumulating that cytokine stimulation induces miRNA transcription or maturation involved in the regulation of translation of target mRNAs. We have profiled miRNA induction by IFNα in ME-15 and HuH7 cells and detected small changes in expression levels (Siegrist *et al.* 2009). In addition to these cell lines, we have evaluated here the miRNA profiles of *SOCS1*, *SOCS3* and *SOCS4* genetically modified cell lines. As expected, principal component analysis revealed that the sample variation could be best explained by the different cell type (data not shown). During genetically modification and selection of SOCS expressing cell clones, miRNA expression patterns were largely maintained and ME-15 cells and descendants were clearly separated from the HuH7 cells. The effect of IFNα treatment was only observable at 4 hours. This result indicates that the influence of IFNα is limited to a short period after treatment and that this effect is present in all cells regardless of SOCS expression. Therefore we screened the data for miRNA genes significantly changed after 4 hours incubation. Most of the IFNα induced miRNAs that are modulated in ME-15 cells are also upregulated in SOCS expressing clones, for example *miR-10b*, *miR-551b*, *miR-137* and *miR-101* (figure 5). This indicates that miRNA regulation by IFNα is independent of regular JAK-STAT activation for many miRNAs. However, miRNAs that are clearly upregulated by IFNα in

ME-15 and HuH7 cells such as *miR-19a*, *miR-19b* and *miR-33* are not significantly upregulated in SOCS over-expressing cells. Interestingly, not only *miR-98* seems to be regulated by IFNα but the entire *let-7* family cluster to which *miR-98* belongs. Their fold changes imply only a moderate modulation of the normally ubiquitous available *let-7* miRNAs (supplementary figure 5). To conclude, IFNα treatment results in moderate modulation of miRNA abundance which was in contrast to mRNA regulation SOCS1 independent. This suggests that a passive or alternative pathway controls the transcription or maturation of miRNAs and that the response decays 4 hours after treatment.

Discussion

Efficient induction by IFNα genes requires JAK-STAT pathway signaling and stimulation of transcription factors. Here we have shown that SOCS1 overexpression results in significant suppression of ISG mRNA expression *in vitro*. In contrast, the impact of SOCS3 overexpression on IFNα signaling is moderate and secondary response genes are less affected.

SOCS EXPRESSION:

We evaluated *SOCS* expression in ME-15 cells and detected early, strong and significant upregulation of *SOCS1* and *SOCS3* mRNA. These genes are inducible by IFNα in our cell lines suggesting that the negative feedback loop in IFNα signaling is initiated. The inducibility of *SOCS3* in ME-15 cells does not reflect the situation in other melanoma cell lines, in which the *SOCS3* gene is not responsive to IFNα (Kovarik *et al.* 2005). This may reflect an inability of STAT3 to be activated in these cells, because STAT3 is important for IFNβ driven induction of *SOCS3*, whereas *SOCS1* induction depends on STAT1α and not on STAT3 or STAT2 (Qin *et al.* 2008). The promoter of *SOCS1* contains active ISRE and GAS elements that are responsible for STAT1-mediated gene transcription (Schlüter *et al.* 2000). Inducibility of *SOCS1* is not surprising since ME-15 and HuH7 cells are able to modulate many genes with ISRE and GAS elements upon IFNα stimulation. Peak upregulation of *SOCS1* and *SOCS3* occurred 4 hours and 2 hours after IFNα stimulus, respectively. This correlates perfectly with IFNβ treated cancer cells (astrocytes) with equivalent peak induction times (Qin *et al.* 2008). Here, *SOCS3* levels declined 4 hours after stimulation, which explains why we failed to detect significant *SOCS3* induction in our cancer cell line panel after 4 hours (GSE21158). The reduction of the *SOCS* response to basal levels in the liver after IL6 injection occurred after 4 hours and 8 hours for *SOCS1* and *SOCS3*, respectively (Starr *et al.* 1997). This indicates a different induction period for distinct cytokines and cell-type-specific differences in the expression of *SOCS* genes in response to the same cytokine. Other SOCS proteins are also modulated by IFNs depending in a cell type dependent manner. For example, *SOCS2* is upregulated in healthy donor PBMCs after one hour IFNα treatment (Zimmerer *et al.* 2008). Moreover, *SOCS4* downregulation can be observed by IFNλ1 (IL29) in human melanoma cell lines, whereas *SOCS6* and *SOCS1* are upregulated (Guenterberg *et al.* 2010). The induction of SOCS proteins is not restricted to cytokines but may also be regulated by pathogens themselves. *SOCS7* levels are upregulated

in HuH7 cells expressing HCV genotype 3a core protein for example (Pazienza *et al.* 2007; Pazienza *et al.* 2009). This *SOCS7* upregulation is not mediated by IFNα alone in HuH7 cells and HCV core protein-expressing hepatocytes, in line with the results presented here (Pazienza *et al.* 2010). In their study, *SOCS1* and *SOCS3* expression levels were also determined in a time course experiment in HuH7 cells but IFNα was used at lower concentration (500 U/ml) compared to this experiment. The mRNA levels stayed elevated for several days and reached a plateau after 4 hours in the case of *SOCS3* or peaked at 8 hours for *SOCS1* transcripts. We refined this study by calculating fold changes compared to non-treated levels instead of the ratio to pre-treatment levels. This may be important since undefined components in the serum-complemented medium alone such as cytokines have an impact on *SOCS* expression levels (figure 1b).

In conclusion, *SOCS1* and *SOCS3* levels are influenced in our melanoma and hepatoma cell lines and may play a role in the negative regulation of therapeutic IFNα treatment. For a better understanding of the impact of *SOCS* levels in adjuvant cancer treatment and resistance to treatment, we would suggest assessing *SOCS1* and *SOCS3* pretreatment levels and induction during clinical trials to investigate the correlation between *SOCS* levels and treatment success.

LOCALIZATION:

SOCS dependent negative feedback mechanisms is not only triggered by expression changes but also altered subcellular localization of SOCS proteins influence their function and may play a critical role in cancer (Rossa *et al.* 2012). We examined the cellular distribution of SOCS proteins in our cell lines and followed the protein localization from its synthesis to degradation by kinetic fluorescent tagging using SNAP-tag (Keppler *et al.* 2004). We favor this labeling technique because in contrast to proteins linked to a conventional fluorophore, the pool of labeled proteins is not replenished by newly synthesized proteins and the relocation of proteins during signaling processes can therefore be assessed in a time-dependent manner. Our results suggest that SOCS3 proteins are distributed throughout the cytoplasm and that in SOCS1 proteins shuttle to the nucleus early after translation in the cell lines used here. Activation of JAKs can then trigger the re-localization of SOCS1 proteins to the plasma membrane where they modulate the kinase activity (Haan *et al.* 2009). It has been shown that SOCS1 can be readily found in the nucleus (Ben-Yair *et al.* 2002), where it could interact with NFκB as part of a multimeric ubiquitin ligase complex (Maine *et al.* 2007). Other nuclear functions involve activation of DNA damage responses through binding of ATM and successive activation of p53 transcription factor mediating cellular senescence (Calabrese *et al.* 2009). Many SOCS proteins (SOCS1, SOCS2, SOCS4, SOCS5 and CISH) are upregulated in a p53 senescence state induced by constitutive STAT5 signaling. Therefore, it has been suggested that in tumor cells with aberrant and sustained STAT signaling SOCS1 may be highly abundant and localize to the nucleus. There, it may localize to DNA damage spots and activate p53 in an ATM-dependent manner. SOCS1 is believed to be the link between DNA damage signals stimulated by oncogenic activity and p53 (Mallette *et al.* 2010). Here, we have shown, that over-expressed SOCS1 can localize to the nucleus in ME-15 cells.

Protein expression and IFITM3 expression in clones:

In order to investigate the impact of SOCS expression on IFNα signaling we have generated clones from HuH7 and ME-15 cells by transfection of *SOCS* expressing vectors and selection in antibiotic medium. Similar to the marginal expression of SOCS4 tagged proteins, no upregulation of *SOCS4* mRNA or proteins could be detected in the antibiotic resistant clones. IFITM3 was readily inducible in SOCS4 clones and gene expression patterns after IFNα treatment showed no obvious difference to the progenitors. There is no evidence that *SOCS4* has an inhibitory effect on IFNα, therefore the *SOCS4* transfected cell lines act here as transfection control. A factor that may disturb the efficient expression of *SOCS4* may be miRNAs of the let-7 family (Hu *et al.* 2010). They are highly expressed in both ME-15 and HuH7 and are upregulated after IFNα treatment (Siegrist *et al.* 2009). This may explain why there was no induction of *SOCS4* mRNA detected some hours after treatment. However, this does not exclude an important function for *SOCS4* in the signaling of other cytokines for example IL6 and in STAT3 and STAT6 phosphorylation, which is not under control of SOCS1 (Hu *et al.* 2010). *IFITM3* is an ISG that is not expressed in ME-15 control cell cultures and is induced in virtually all cultured cells competent in IFNα signaling. In SOCS1-expressing clones this induction was reduced almost to control levels. In contrast, IFITM3 expression was not substantially altered in SOCS3-expressing derivatives. This is probably due to the dependence of IFITM3 on interferon-stimulated gene factor 3 activation. Thus, we conclude that the activation of STAT1-STAT2 complexes is less affected by SOCS3 in our cell lines. We addressed this question in a genome-wide approach to define gene-sets that are regulated by SOCS3 interaction in IFNα activated pathways.

Transcriptome analysis:

Liver cell cultures (HepG2) with stable *SOCS1* and *SOCS3* expression inhibit STAT1 and STAT3 phosphorylation and the expression of antiviral IFNα response genes such as *Mx A*, *OAS1*, *OAS2* and *OAS3* (Vlotides *et al.* 2004). Our results confirm efficient suppression of IFNα mediated transcriptional changes in SOCS1-overexpressing cell lines, but we did not observe an inhibition of the upregulation of these antiviral genes in SOCS3-overexpressing HuH7 cells. This indicates that over several weeks of SOCS3 expression, HuH7 cells adapted to the new situation and partially reduced the impact of the suppressor gene. Here we show that the effect of SOCS proteins is more pronounced in the first hours than after one day. In *SOCS3* knockout mice, ISG expression is higher after cytokine stimulus, probably due to an increased duration of STAT1 activation (Croker *et al.* 2003). Thus, it may be feasible to expect a decrease in duration of STAT1 activation in SOCS3 overexpressing cell lines given that STAT3 activation is not altered. This results in the regulation of both the quantity and type of STAT signal generated from the IFNAR observed here. However, since only HuH7 cells could be classified as responders to SOCS3 overexpression this type of signaling seems either to be absent in ME-15 cells or was silenced during clonal selection.
In contrast to the diffuse regulation of gene expression in SOCS3 HuH7 cells, SOCS1

expression in both cell lines affected all IFNα induced genes. However, a small number of genes resisted the negative regulation of SOCS1 in all cell lines, to some extent. Genes participating in the JAK-STAT pathway downstream of IFNα themselves, including *STAT1* and *IRF9*, were over-represented in this group. IFNβ driven induction of *IRF9* in SOCS1 overexpressing cells does not depend on STAT-phosphorylation and this explains that *IRF9* induction is less affected by SOCS1 negative regulation (Rani *et al.* 2010). We conclude from this and from our data that SOCS1 blocks JAK-STAT signaling pathway more specifically than accessory signals independent of IFNAR phosphorylation.

In order to generate a gene list with less than 5 % of false negatives we applied false discovery rate correction to the p-values of the moderated limma statistics. We observed that most of the probes that are upregulated in SOCS1-expressing cell lines and that do not met the p-value < 0.05 criteria are well known ISGs or are clearly upregulated in the control cells. This implies that the moderate t-statistics and false discovery rate adjustment may underestimate the total number of ISGs in our experiment. Consequently, even more than 1'500 genes are likely to be regulated by IFNα in our cell culture model. Additionally, only a very few genes are downregulated after IFNα treatment and one-tailed p-value calculation may be closer to reality and would result in more significantly upregulated genes.

miRNA induction by IFNA and SOCS targeting

In the last years several miRNAs have been shown to be regulated by various pathogens and cytokines including IFNs. As an example, the miRNA expression profile of HuH7 cells treated with IFNβ revealed *miR-30* as an interferon induced gene (Pedersen *et al.* 2007). Our results confirmed upregulation of this miRNA by IFNα (Siegrist *et al.* 2009) and *SOCS1* and *SOCS3* have each a conserved *miR-30* binding site in their 3'-UTR mRNA region (Siegrist *et al.* 2008). The miRNA profile of IFNβ treated HuH7 cells expressing the HCV replicon has been published after generation of our data (Gong *et al.* 2010). In comparision, no significant downregulation of *miR-550* by IFNα is detected here and IFNβ-upregulated miRNAs were not induced. These disparities may be due to differences between IFNα and IFNβ, the detection method or the absence of an HCV replicon in our system.

In addition to modulation of miRNA gene expression, prolonged IFNα treatment deactivates the miRNA maturation factor *DICER* (Wiesen *et al.* 2009). This may have a direct impact on HCV replication since viral replication is inhibited by targeting *DICER* using siRNAs in HuH7 cells (Randall *et al.* 2007). Our data strongly suggest that interferon inducible miRNAs contribute to the fine-tuning of cytokine signaling as part of a rapid response. Several miRNAs have been reported to influence SOCS mRNA, which may represent an effective mechanism of limiting SOCS mRNA expression for a limited period after the IFN stimulus. Therefore, SOCS1 degradation may be triggered by IFNα-induced miRNAs resulting in a reduction of SOCS mRNA level. We have thus hypothesized that SOCS induction by IFNs is followed by IFN-regulated miRNA maturation supporting the degradation of SOCS mRNA and therefore leading to fast turn-over of SOCS proteins (Siegrist and Certa 2008). We show there that the regulation of miRNA is not pronounced and we conclude that several miRNAs must be involved for efficient

SOCS mRNA targeting. A miRNA family that is induced by IFNα in our experiment is the *let-7* family cluster including *miR-98*. These miRNAs (*let-7d, let-7f-2 and let-7i*) have been associated with *SOCS1* and *SOCS3* targeting (Meng *et al.* 2007; Zhang *et al.* 2011a; Bakre *et al.* 2012). Additionally, other SOCS genes (*CISH* and *SOCS4*) are targeted by the *let-7* and *miR-98* family after pathogen challenge (Hu *et al.* 2009; Hu *et al.* 2010). In addition, *SOCS1* is targeted by *miR-19* and this regulation is associated with pathogenesis of multiple myeloma (Pichiorri *et al.* 2008). Interestingly, *miR-19a* and *miR-19b* are significantly regulated in ME-15 and HuH7 cells but less so in SOCS-expressing derivatives based on our data. Moreover, overexpressed *miR-30b* and *miR-155* target SOCS1 in T-cells and miR-155 is also induced by IFNβ in macrophages during osteoclastogenesis (Chang *et al.* 2012; Zhang *et al.* 2012). This is important, because *miR-155* is upregulated by lipopolysaccharide (LPS), regulates a wide range of regulatory pathways and promotes cytokine production (Tili *et al.* 2007; Xiao *et al.* 2009; Cardoso *et al.* 2012). IRF3 may play a negative feedback role by suppression of *miR-155* and counteracts the induction of SOCS1 by IL1/IFNγ treatment (Tarassishin *et al.* 2011). In agreement with published data we were not able to detect any regulation of *miR-155* (Lu *et al.* 2009; Wang *et al.* 2009; Jiang *et al.* 2010). However, *miR-155* gets induced by LPS and may therefore act as the limiting factor in the SOCS1 negative feedback loop in reaction to LPS (Androulidaki *et al.* 2009). In addition to bacterial infections, viral induction of *miRNA-155* promotes type I IFN signaling through targeting of SOCS1 by *miRNA-155*, finally suppressing viral replication (Wang *et al.* 2010). However, since *miR-155* levels were not significantly changed in our experiment, the destabilizing effect on *SOCS1* levels was unaffected by IFNα. There are also conserved patterns in the *SOCS3* 3'-UTR mRNA, which contain target-sequences recognizable by *miR-203* (Sonkoly *et al.* 2007). Based on the negative correlation of miRNA expression and *SOCS3* expression in psoriasis, a biological regulation has been suggested (Sun *et al.* 2008), but results of SOCS3 targeting experiments by *miR-203* remain controversial. On the one hand, overexpression of *miR-203* does not decrease *SOCS3* mRNA levels in vitro (Lena *et al.* 2008). However, recent findings show efficient targeting of *SOCS3* luciferase reporter constructs by *miR-203 or miR-483* in mice (Wei *et al.* 2010; Ma *et al.* 2012). In human cells, *miR-203* is bound to *SOCS3* 5'-UTR and antagomir for *miR-203* have a positive effect on SOCS3 levels and enhances chemosensitivity of breast cancer cells (Moffatt *et al.* 2011; Ru *et al.* 2011).

In summary, there are many miRNAs that have an impact on *SOCS* mRNA stability and even more may be involved in interfering with *SOCS* translation according to bioinformatic analyses (Friedman *et al.* 2009). Targeting of mRNA is followed by deadenylation and decay of the messenger RNA. This regulation supports other control mechanism for SOCS protein expression levels. First, SH2 domain of SOCS3 for instance contains an unstructured PEST (proline-, glutamic-acid, serine- and threonine-rich) motif, which negatively affects protein stability (Babon *et al.* 2006). Second, the N-terminal region of SOCS3 is also involved in protein instability through the presence of Lys-6, a major ubiquitination site (Sasaki *et al.* 2003). Last, the functions and stability of SOCS1 and SOCS3 proteins are modulated by the SUMO-

modifying protein PIM1 (Chen *et al.* 2002; Peltola *et al.* 2004). This clearly indicates how important *SOCS* regulatory factors are for unimpaired cytokine signaling

Potential of miRNA regulation as therapy

Antagomirs (anti-sense oligonucleotides) or miRNA mimics may be activated to limit SOCS proteins due to their importance in regulating SOCS expression. Despite the fact that miRNAs control *SOCS* translation it is not clear whether IFN-regulated changes in miRNA levels have an impact on the IFN antiviral effect. The most important miRNA for efficient HCV replication is *miR-122* in HuH7 cells (Jopling *et al.* 2005; Jangra *et al.* 2010). Here, we could not detect a significant effect of IFNα on *miR-122* expression in HuH7 cells neither at 4 nor at 24 hours. This is also true for mouse livers where *miR-122* does not belong to the early ISG (Sarasin-Filipowicz *et al.* 2009a). Besides acting as proviral agent, *miR-122* has been linked to target *SOCS3* responsiveness by modulation of SOCS3 promoter methylation status and silencing of miR-122 increases expression of IFNα response genes (Yoshikawa *et al.* 2012). Interestingly, non-responder patients have significant lower *miR-122* levels (Sarasin-Filipowicz *et al.* 2009a) and supplementation with *miR-122* does not increase production of the core protein or virus particles (Jangra *et al.* 2010). This supports the hypothesis that even low levels could allow HCV replication *in vivo*. Therefore, marginal reduction of *miR-122* levels may not be limiting for HCV replication in HuH7 cells. It is therefore very unlikely that miRNAs mediate antiviral IFN responses against HCV (Sarasin-Filipowicz 2010). However, a total blockage of *miR-122* in chimpanzees lowered HCV titer without effect on viral resistance and resulted in normalization of ISG levels. Moreover, it has been shown that *miRNA-122* positively regulates a step in the life cycle of HCV other than its translation (Jangra *et al.* 2010). Thus, antagonizing *miR-122* could be used to convert IFN non-responders to responders (Lanford *et al.* 2010).
In conclusion, we propose that miRNAs can limit the duration of *SOCS* expression. However, antagonizing this effect may only make sense where certain *SOCS*-targeting miRNAs are expressed at higher levels than normal and therapeutic manipulation of IFNα regulation of miRNA expression for better antiviral responses appears to have no chances of success. For the special case in HCV, the effect of IFNα on DICER may support blocking of *miR-122* maturation, which is important for the HCV life cycle. Finally, therapeutic antagonizing of *miR-122* by miravirsen (Santaris Pharma SPC3649, LNA-antimiR-122) to improve or replace current therapy against HCV is promising and clinical phase 2a was completed recently (ClinicalTrials.gov # NCT01200420).

Therapeutic implications

Deregulation of *SOCS1* and *SOCS3* can be found in patients with HCV and is associated with HCC and melanoma. On the one hand, antiviral, anti-tumor and antiproliferative effects of IFNα in the treatment of these diseases are markedly reduced when SOCS proteins are overexpressed. On the other hand, signaling through growth factors and inflammatory cytokines is enhanced when *SOCS* expression is silenced and this may induce the risk for cancer formation and its growth potential. Abundant *SOCS* expression interferes with antiviral and

antitumor properties of therapeutic IFNα and inactivation of *SOCS* transcriptional regulation translate to carcinogenic conditions. Thus, the use of SOCS inhibitors and activators as therapeutics bears a huge potential.

Viral infection leads to excessive cytokine stimulation and expression of SOCS proteins, what may indicate insufficiency in inflammatory signaling and resistance to IFNα. HCV core protein seems to be directly involved in the induction of *SOCS1* and *SOCS3* mRNA (Zhang *et al.* 2011b; Bode *et al.* 2003; El-Zayadi *et al.* 2012). The expression of SOCS proteins then leads to a desensitization of the cells towards IFNα. The refractoriness in response to IFNα correlates with expression of SOCS proteins and other factors such as insulin or leptin resistance (Dai *et al.* 2009). Moreover, HCV induced SOCS expression is dependent on the HCV core protein sequence, reduces levels of insulin receptor substrate and may account for both insulin resistance and lack of IFNα therapy response (Pascarella *et al.* 2011; El-Zayadi and Anis 2012). This argues that the negative influence of *SOCS* levels on anti-viral treatment can be monitored using symptoms such as body mass index (Kamal *et al.* 2002; Gylvin *et al.* 2009). In practice, it seems that the reduction of insulin resistance by diet restriction and physical exercise may increase the number of patients that benefit from IFNα therapy (Machado *et al.* 2009). Additionally, alcohol induces the expression of *SOCS,* thereby inhibits IFNα-based innate immunity in hepatocytes and contributes to the chronicity of hepatitis infection and poor therapy efficacy (Norkina *et al.* 2008; Ye *et al.* 2010). Elimination of SOCS proteins can prolong IFN signaling and STAT activation and thereby increases efficient viral clearance and supports survival of otherwise lethal infection (Fenner *et al.* 2006; Yasukawa *et al.* 2003). Therefore, SOCS inhibitors may prolong therapeutic effects of IFNs, decrease injection frequency and finally increase comfort for patients and reduce health care costs. However, the clinical applicability of SOCS inhibitors for re-sensitization of IFNα non-responders in HCV therapy remains to be demonstrated. Moreover, results from IFNα stimulated blood cells of different type of responders neither showed a correlation with *SOCS1* inducibility nor SOCS1 non-stimulated levels (personal communication M. Mitsuhashi, Hitachi Chemical Research Center). In contrast, lack of SOCS1 suppression at baseline levels or 7 days after treatment in blood could predict failure to achieve SVR in CHC patients (Younossi *et al.* 2012). Therefore, selection of patients that may benefit of therapeutic SOCS inhibitors is not trivial. Moreover, development of an effective therapeutic SOCS inhibitor is challenging for three reasons. First, *SOCS1* levels are not elevated longer than 3 hours after initial IFNα administration in mice and this short period could probably not be long enough to generate a significant benefit (Sarasin-Filipowicz *et al.* 2009b). Second, even if *SOCS3* levels stay significantly upregulated longer than this in mice with continuously high serum concentrations of IFNα, *SOCS3* or *STAT3* deficient mice also show prolonged IFNα refractoriness (Sarasin-Filipowicz *et al.* 2009b). For these two reasons, adjuvant therapy with SOCS inhibitors could probably be only of limited benefit for the patient. Finally, unspecific delivery of SOCS inhibitors may alter development of immune cells or impede stem cell maintenance, enhance risk of cancer formation or interfere with other antiviral pathways for example mediated by mTOR activation (Shao *et al.* 2010). This contradicts an

important impact of SOCS proteins in IFNα desensitization during treatment of CHC patients. Other factors than SOCS1, such as the ubiquitin specific peptidase USP18, have been associated with loss of treatment effect during prolonged administration (Randall *et al.* 2006; Sarasin-Filipowicz *et al.* 2009b). Furthermore, new formulations of IFNα are available or in development, for example pegylated interferon, albuferon, oral interferons or type III IFN (IFNλ) that shows fewer side effects. These improvements in IFN therapy can reduce injection rates and healthcare costs and improve acceptance of drug intake in HCV patients. Another promising approach is direct targeting of viral proteins using small chemicals to avoid host factor differences such as high *SOCS* levels. However, effective immune response in patients is probably still needed for long-term clearance of the virus.

In contrast to enhanced levels in non-responders to antiviral IFNα therapy, the inactivation of *SOCS* gene expression can be an important factor in carcinogenesis to limit growth control. Deregulation of *SOCS1* can be observed in the pre-malignant tumor stage in HCV infected patients (Yoshida *et al.* 2004). In the later stage of hepatocellular carcinomas following HCV infection the *SOCS1* promoter is frequently hypermethylated and silencing of the suppressor supports cancer growth (Yoshikawa *et al.* 2001; Yoshimura 2006; Yang *et al.* 2003). The impact of SOCS proteins in the development of tumors is confirmed by hepatocyte specific deletion of *SOCS3* promoting hepatitis C related hepatocellular carcinoma (Ogata *et al.* 2006). Moreover, *SOCS1* suppression can lead to spontaneous cancer formation in mice (Hanada *et al.* 2006). In addition, selective *SOCS3* deletion in intestinal epithelial cells leads to STAT3 hyperactivation and enhanced colon tumorigenesis following injury and inflammation (Rigby *et al.* 2007). STAT3 is also activated in *SOCS3* deficient liver cells when liver regenerative conditions are simulated (Riehle *et al.* 2008).

The knockdown of endogenous *SOCS* levels or the silencing of the cytokine response through *SOCS* promoter methylation could therefore result in a growth advantage to cancer cells. DNA methylation in the promoter of *SOCS* genes is frequently observed in various cancers (Yoshikawa *et al.* 2001; Galm *et al.* 2003; Nagai *et al.* 2003; Komazaki *et al.* 2004; Evans *et al.* 2007; Capello *et al.* 2008; Chu *et al.* 2010). In addition, SOCS1 promoter hypermethylation can be detected even in the pre-malignant stage of HCV infected patients (Yoshida *et al.* 2004). Therefore, *SOCS1* can be classified as an anti-oncogene in hepatitis-induced carcinogenesis. The mechanism how proliferation rates in HCC cells are increased by *SOCS* promoter methylation is probably linked to enhanced activation of STAT proteins involved in growth signaling. Because SOCS proteins limit cancer growth, SOCS proteins can be assigned as tumor suppressors (Elliott *et al.* 2008). Therefore, SOCS proteins or mimics may be useful to control cancer growth when SOCS promoters are inactivated or in inflammatory diseases where cytokine signaling is out of control. It has been shown that adenoviral mediated *SOCS3* transfer inhibits growth and increases radio-sensitivity of non-small cell lung cancer cells of the cells (Lin *et al.* 2010). In addition, overexpression of *SOCS3* promotes preclinical antitumor activity against malignant pleural mesothelioma (Iwahori *et al.* 2011). A reduction of side effects may be achieved by using only parts of the SOCS proteins. A small molecule mimicking SOCS proteins

is TKIP (tyrosine-kinase inhibitor peptide). TKIP is able to inhibit JAK2-mediated phosphorylation of STAT1 (Flowers *et al.* 2004; Waiboci *et al.* 2007). TKIP suppresses also the proliferation of prostate cancer cell lines, in which STAT3 is constitutively activated (Mujtaba *et al.* 2005; Flowers *et al.* 2005). Thus, an efficient drug-delivery system with TKIP has a great potential to treat cancer and inflammatory diseases (Yoshimura *et al.* 2007). However, we can only speculate on the consequences of using SOCS mimics or antagonists in the clinics and on the role of SOCS proteins in human disease at the moment but it may be beneficial to treat viral infections and cancer by modulation of SOCS expression and its activity.

In contrast to SOCS agonists, the use of SOCS inhibitors may enhance the therapeutic outcome in IFN-based cancer treatment because knockdown of SOCS transcripts results in an increase in IFN mediated STAT phosphorylation (Lesinski *et al.* 2010). In renal cell carcinoma for example, suppression of SOCS3 increases susceptibility to IFNα (Tomita *et al.* 2011). However, discussion is ongoing whether IFNα-based therapy is mainly acting on the cancer cells or on immune cells. The administration of IFNα increase the survival of wild-type mice but not STAT1-deficient mice challenged with STAT1-proficient tumor cells, suggesting that IFNs mediate their antitumor effects mainly through acting on the immune cells (Lesinski *et al.* 2003). Moreover, the immunomodulatory effect of IFNα is important for antitumor action in mice and is regulated by SOCS proteins (Zimmerer *et al.* 2007). Systemic therapy could therefore enhance both the anti-proliferative action of IFNα in cancer cells as well as antitumor effects of hematopoietic cells at the same time. Gene expression changes by IFNα stimulation are similar in PBMC of melanoma patients *in vitro* and *in vivo* (Zimmerer *et al.* 2008). Therefore, the antitumor immunomodulatory potential of SOCS inhibitors together with IFNα may be screened in the lab from blood samples of cancer patients. A similar approach is the down-modulation of *SOCS* gene expression by siRNA therapy or by a dominant negative form of the protein. Suppression of *SOCS1* using siRNA technology enhances the antiproliferative effects induced by IFNγ (Takahashi *et al.* 2008). Therefore, therapeutic siRNAs targeting *SOCS1* may also improve the growth inhibitory effects of IFNα in cancer treatment or inhibitors that target *SOCS1* and *SOCS3* activity may be used to reactivate IFNα mediated antitumor effects in metastatic melanoma cells. The ability of dendritic cells to induce strong antitumor immunity by enhanced antigen presentation can be significantly enhanced by targeting *SOCS1* with siRNA (Shen *et al.* 2004). In addition, administration of these siRNAs by a nanotube carrier reduces tumor growth in mice (Yang *et al.* 2006). As an auxiliary effect, siRNAs against *SOCS1* and *SOCS3* can improve insulin sensitivity and ameliorate hepatic steatosis (Ueki *et al.* 2005). In summary, on the one hand SOCS inhibitors may be used to enhance antitumor and antiviral properties of immune cells and to reduce cancer growth and viral proliferation in cells. On the other hand SOCS agonist could be used to regain control of proliferation in cancer cells.

Conclusion

Our results indicate that *SOCS* levels are important in the treatment of diseases like HCV or cancer with cytokines. SOCS targeting therapies are in development motivated by the possibility

that changes in *SOCS* levels during IFNα therapy may reflect refractoriness to cytokine stimulation by silencing antiviral and antiproliferative effect of the protein based drug. Here we have shown that over-expression of *SOCS1* is very potent in suppression of gene induction by high doses of IFNα *in vitro*. Interferon stimulated protein expression was less reduced by overexpression of *SOCS3* and no effect on gene expression patterns could be observed in melanoma-derived *SOCS3* overexpressing cells. This shows that IFNα sensitive tumor-derived cells that is proficient in upregulating *SOCS3* in response to cytokine stimulation can be both responsive or not to high SOCS3 expression levels. This may also be true in the clinics where patients benefit differently from IFNα treatment. We suggest therefore to measure *SOCS1* and *SOCS3* levels whenever feasible before and during the treatment for a better understanding of the factors that are involved in resistance to IFNα therapy. Finally, the capacity of rapid feedback regulation could be assessed by monitoring of *SOCS* induction some minutes after the first injection and adjustment of IFNα concentration or the use of SOCS inhibitors may be taken into account to improve therapy outcome.

Acknowledgments

The authors thank Dr. L. Burleigh, Roche, West Sussex, UK and Dr. R. Walser, University of Basel, Switzerland for critical review of the manuscript. Thanks are also due to Dr. T. Singer, Roche, Basel, Switzerland for continuous advice and support.

Disclosures

The author reports no conflicts of interest in this work.

References

References

Androulidaki A, Iliopoulos D, Arranz A, Doxaki C, Schworer S, Zacharioudaki V, Margioris AN, Tsichlis PN, Tsatsanis C. 2009 Aug. The kinase Akt1 controls macrophage response to lipopolysaccharide by regulating microRNAs. Immunity 31(2): 220-231.

Babon JJ, Kershaw NJ, Murphy JM, Varghese LN, Laktyushin A, Young SN, Lucet IS, Norton RS, Nicola NA. 2012 Feb. Suppression of cytokine signaling by SOCS3: characterization of the mode of inhibition and the basis of its specificity. Immunity 36(2): 239-250.

Babon JJ, McManus EJ, Yao S, DeSouza DP, Mielke LA, Sprigg NS, Willson TA, Hilton DJ, Nicola NA, Baca M, Nicholson SE, Norton RS. 2006 Apr. The structure of SOCS3 reveals the basis of the extended SH2 domain function and identifies an unstructured insertion that regulates stability. Mol. Cell 22(2): 205-216.

Baetz A, Koelsche C, Strebovsky J, Heeg K, Dalpke AH. 2008 Dec. Identification of a nuclear localization signal in suppressor of cytokine signaling 1. FASEB J. 22(12): 4296-4305.

Bakre A, Mitchell P, Coleman JK, Jones LP, Saavedra G, Teng M, Tompkins SM, Tripp RA. 2012 Nov. Respiratory syncytial virus modifies microRNAs regulating host genes that affect virus replication. J. Gen. Virol. 93(Pt 11): 2346-2356.
Ben-Yair L, Slaaby R, Herman A, Cohen Y, Biener E, Moran N, Yoshimura A, Whittaker J, De Meyts P, Herman B, Gertler A. 2002 Aug. Preparation and expression of biologically active prolactin and growth hormone receptors and suppressor of cytokine signaling proteins 1, 2, 3, and 6 tagged with cyan and yellow fluorescent proteins. Protein Expr. Purif. 25(3): 456-464.
Bode JG, Ludwig S, Ehrhardt C, Albrecht U, Erhardt A, Schaper F, Heinrich PC, Häussinger D. 2003 Mar. IFN-alpha antagonistic activity of HCV core protein involves induction of suppressor of cytokine signaling-3. FASEB J. 17(3): 488-490.
Boyle K, Zhang J, Nicholson SE, Trounson E, Babon JJ, McManus EJ, Nicola NA, Robb L. 2009 Mar. Deletion of the SOCS box of suppressor of cytokine signaling 3 (SOCS3) in embryonic stem cells reveals SOCS box-dependent regulation of JAK but not STAT phosphorylation. Cell. Signal. 21(3): 394-404.
Brem R, Oraszlan-Szovik K, Foser S, Bohrmann B, Certa U. 2003 Jun. Inhibition of proliferation by 1-8U in interferon-alpha-responsive and non-responsive cell lines. Cell. Mol. Life Sci. 60(6): 1235-1248.
Brender C, Lovato P, Sommer VH, Woetmann A, Mathiesen A, Geisler C, Wasik M, Ødum N. 2005 Feb. Constitutive SOCS-3 expression protects T-cell lymphoma against growth inhibition by IFNalpha. Leukemia 19(2): 209-213.
Calabrese V, Mallette FA, Deschênes-Simard X, Ramanathan S, Gagnon J, Moores A, Ilangumaran S, Ferbeyre G. 2009 Dec. SOCS1 links cytokine signaling to p53 and senescence. Mol. Cell 36(5): 754-767.
Capello D, Deambrogi C, Rossi D, Lischetti T, Piranda D, Cerri M, Spina V, Rasi S, Gaidano G, Lunghi M. 2008 May. Epigenetic inactivation of suppressors of cytokine signalling in Philadelphia-negative chronic myeloproliferative disorders. Br. J. Haematol. 141(4): 504-511.
Cardoso AL, Guedes JR, Pereira de Almeida L, Pedroso de Lima MC. 2012 Jan. miR-155 modulates microglia-mediated immune response by down-regulating SOCS-1 and promoting cytokine and nitric oxide production. Immunology 135(1): 73-88.
Chang C, Zhang Q, Liu Z, Clynes RA, Suciu-Foca N, Vlad G. 2012 Apr. Downregulation of inflammatory microRNAs by Ig-like transcript 3 is essential for the differentiation of human CD8(+) T suppressor cells. J. Immunol. 188(7): 3042-3052.
Chen XP, Losman JA, Cowan S, Donahue E, Fay S, Vuong BQ, Nawijn MC, Capece D, Cohan VL, Rothman P. 2002 Feb. Pim serine/threonine kinases regulate the stability of Socs-1 protein. Proc. Natl. Acad. Sci. U.S.A. 99(4): 2175-2180.
Chu P, Yeh C, Hsu NC, Chang Y, Chang J, Yeh K. 2010. Epigenetic alteration of the SOCS1 gene in hepatocellular carcinoma. Swiss Med Wkly 140: w13065.
Croker BA, Kiu H, Nicholson SE. 2008 Aug. SOCS regulation of the JAK/STAT signalling pathway. Semin. Cell Dev. Biol. 19(4): 414-422.
Croker BA, Krebs DL, Zhang J, Wormald S, Willson TA, Stanley EG, Robb L, Greenhalgh CJ, Förster I, Clausen BE, Nicola NA, Metcalf D, Hilton DJ, Roberts AW, Alexander WS. 2003 Jun. SOCS3 negatively regulates IL-6 signaling in vivo. Nat. Immunol. 4(6): 540-545.
Dai C, Huang J, Hsieh M, Hou N, Lin Z, Chen S, Hsieh M, Wang L, Chang W, Chuang W, Yu M. 2009 Apr. Insulin resistance predicts response to peginterferon-alpha/ribavirin combination therapy in chronic hepatitis C patients. J. Hepatol. 50(4): 712-718.
Darnell JEJ, Kerr IM, Stark GR. 1994 Jun. Jak-STAT pathways and transcriptional activation in response to IFNs and other extracellular signaling proteins. Science 264(5164): 1415-1421.
Du P, Kibbe WA, Lin SM. 2008 Jul. lumi: a pipeline for processing Illumina microarray. Bioinformatics 24(13): 1547-1548.
El-Zayadi A, Anis M. 2012 Jan. Hepatitis C virus induced insulin resistance impairs response to anti viral therapy. World J. Gastroenterol. 18(3): 212-224.
Elliott J, Hookham MB, Johnston JA. 2008 Jun. The suppressors of cytokine signalling E3 ligases behave as tumour suppressors. Biochem. Soc. Trans. 36(Pt 3): 464-468.
Endo TA, Masuhara M, Yokouchi M, Suzuki R, Sakamoto H, Mitsui K, Matsumoto A, Tanimura S, Ohtsubo M, Misawa H, Miyazaki T, Leonor N, Taniguchi T, Fujita T, Kanakura Y, Komiya S, Yoshimura A. 1997 Jun. A new protein containing an SH2 domain that inhibits JAK kinases. Nature 387(6636): 921-924.
Evans MK, Yu C, Lohani A, Mahdi RM, Liu X, Trzeciak AR, Egwuagu CE. 2007 Mar. Expression of SOCS1 and SOCS3 genes is differentially regulated in breast cancer cells in response to proinflammatory cytokine and growth factor signals. Oncogene 26(13): 1941-1948.

Feld JJ, Nanda S, Huang Y, Chen W, Cam M, Pusek SN, Schweigler LM, Theodore D, Zacks SL, Liang TJ, Fried MW. 2007 Nov. Hepatic gene expression during treatment with peginterferon and ribavirin: Identifying molecular pathways for treatment response. Hepatology 46(5): 1548-1563.
Feng Z, Chandrashekaran IR, Low A, Speed TP, Nicholson SE, Norton RS. 2012 Mar. The N-terminal domains of SOCS proteins: a conserved region in the disordered N-termini of SOCS4 and 5. Proteins 80(3): 946-957.
Fenner JE, Starr R, Cornish AL, Zhang J, Metcalf D, Schreiber RD, Sheehan K, Hilton DJ, Alexander WS, Hertzog PJ. 2006 Jan. Suppressor of cytokine signaling 1 regulates the immune response to infection by a unique inhibition of type I interferon activity. Nat. Immunol. 7(1): 33-39.
Flowers LO, Johnson HM, Mujtaba MG, Ellis MR, Haider SMI, Subramaniam PS. 2004 Jun. Characterization of a peptide inhibitor of Janus kinase 2 that mimics suppressor of cytokine signaling 1 function. J. Immunol. 172(12): 7510-7518.
Flowers LO, Subramaniam PS, Johnson HM. 2005 Mar. A SOCS-1 peptide mimetic inhibits both constitutive and IL-6 induced activation of STAT3 in prostate cancer cells. Oncogene 24(12): 2114-2120.
Fojtova M, Boudny V, Kovarik A, Lauerova L, Adamkova L, Souckova K, Jarkovsky J, Kovarik J. 2007 Jul. Development of IFN-gamma resistance is associated with attenuation of SOCS genes induction and constitutive expression of SOCS 3 in melanoma cells. Br. J. Cancer 97(2): 231-237.
Friedman RC, Farh KK, Burge CB, Bartel DP. 2009 Jan. Most mammalian mRNAs are conserved targets of microRNAs. Genome Res. 19(1): 92-105.
Fujimoto M, Naka T. 2003 Dec. Regulation of cytokine signaling by SOCS family molecules. Trends Immunol. 24(12): 659-666.
Galm O, Yoshikawa H, Esteller M, Osieka R, Herman JG. 2003 Apr. SOCS-1, a negative regulator of cytokine signaling, is frequently silenced by methylation in multiple myeloma. Blood 101(7): 2784-2788.
Garbe C, Peris K, Hauschild A, Saiag P, Middleton M, Spatz A, Grob J, Malvehy J, Newton-Bishop J, Stratigos A, Pehamberger H, Eggermont A. 2010 Jan. Diagnosis and treatment of melanoma: European consensus-based interdisciplinary guideline. Eur J Cancer 46(2): 270-283.
Gong B, Xie Q, Xiang X, Wang L, Zhao G, An F, Wang H, Lin L, Yu H, Bao S. 2010 Jun. Effect of ribavirin and interferon beta on miRNA profile in the hepatitis C virus subgenomic replicon-bearing Huh7 cells. Int. J. Mol. Med. 25(6): 853-859.
Greenhalgh CJ, Hilton DJ. 2001 Sep. Negative regulation of cytokine signaling. J. Leukoc. Biol. 70(3): 348-356.
Guenterberg KD, Grignol VP, Raig ET, Zimmerer JM, Chan AN, Blaskovits FM, Young GS, Nuovo GJ, Mundy BL, Lesinski GB, Carson WE3. 2010 Feb. Interleukin-29 binds to melanoma cells inducing Jak-STAT signal transduction and apoptosis. Mol. Cancer Ther. 9(2): 510-520.
Gylvin T, Ek J, Nolsøe R, Albrechtsen A, Andersen G, Bergholdt R, Brorsson C, Bang-Berthelsen CH, Hansen T, Karlsen AE, Billestrup N, Borch-Johnsen K, Jørgensen T, Pedersen O, Mandrup-Poulsen T, Nerup J, Pociot F. 2009 Mar. Functional SOCS1 polymorphisms are associated with variation in obesity in whites. Diabetes Obes Metab 11(3): 196-203.
Haan S, Wüller S, Kaczor J, Rolvering C, Nöcker T, Behrmann I, Haan C. 2009 Aug. SOCS-mediated downregulation of mutant Jak2 (V617F, T875N and K539L) counteracts cytokine-independent signaling. Oncogene 28(34): 3069-3080.
Hallen LC, Burki Y, Ebeling M, Broger C, Siegrist F, Oroszlan-Szovik K, Bohrmann B, Certa U, Foser S. 2007 Aug. Antiproliferative activity of the human IFN-alpha-inducible protein IFI44. J. Interferon Cytokine Res. 27(8): 675-680.
Hanada T, Kobayashi T, Chinen T, Saeki K, Takaki H, Koga K, Minoda Y, Sanada T, Yoshioka T, Mimata H, Kato S, Yoshimura A. 2006 Jun. IFNgamma-dependent, spontaneous development of colorectal carcinomas in SOCS1-deficient mice. J. Exp. Med. 203(6): 1391-1397.
Hu G, Zhou R, Liu J, Gong A, Chen X. 2010 Jul. MicroRNA-98 and let-7 regulate expression of suppressor of cytokine signaling 4 in biliary epithelial cells in response to Cryptosporidium parvum infection. J. Infect. Dis. 202(1): 125-135.
Hu G, Zhou R, Liu J, Gong A, Eischeid AN, Dittman JW, Chen X. 2009 Aug. MicroRNA-98 and let-7 confer cholangiocyte expression of cytokine-inducible Src homology 2-containing protein in response to microbial challenge. J. Immunol. 183(3): 1617-1624.
Huang Y, Feld JJ, Sapp RK, Nanda S, Lin J, Blatt LM, Fried MW, Murthy K, Liang TJ. 2007 Feb.

Defective hepatic response to interferon and activation of suppressor of cytokine signaling 3 in chronic hepatitis C. Gastroenterology 132(2): 733-744.
Iwahori K, Serada S, Fujimoto M, Nomura S, Osaki T, Lee CM, Mizuguchi H, Takahashi T, Ripley B, Okumura M, Kawase I, Kishimoto T, Naka T. 2011 Aug. Overexpression of SOCS3 exhibits preclinical antitumor activity against malignant pleural mesothelioma. Int. J. Cancer 129(4): 1005-1017.
Jangra RK, Yi M, Lemon SM. 2010 Jul. Regulation of hepatitis C virus translation and infectious virus production by the microRNA miR-122. J. Virol. 84(13): 6615-6625.
Jiang S, Zhang H, Lu M, He X, Li Y, Gu H, Liu M, Wang E. 2010 Apr. MicroRNA-155 functions as an OncomiR in breast cancer by targeting the suppressor of cytokine signaling 1 gene. Cancer Res. 70(8): 3119-3127.
Jopling CL, Yi M, Lancaster AM, Lemon SM, Sarnow P. 2005 Sep. Modulation of hepatitis C virus RNA abundance by a liver-specific MicroRNA. Science 309(5740): 1577-1581.
Kamal SM, Fehr J, Roesler B, Peters T, Rasenack JW. 2002 Oct. Peginterferon alone or with ribavirin enhances HCV-specific CD4 T-helper 1 responses in patients with chronic hepatitis C. Gastroenterology 123(4): 1070-1083.
Keppler A, Pick H, Arrivoli C, Vogel H, Johnsson K. 2004 Jul. Labeling of fusion proteins with synthetic fluorophores in live cells. Proc. Natl. Acad. Sci. U.S.A. 101(27): 9955-9959.
Kim K, Lin W, Tai AW, Shao R, Weinberg E, De Sa Borges CB, Bhan AK, Zheng H, Kamegaya Y, Chung RT. 2009 Apr. Hepatic SOCS3 expression is strongly associated with non-response to therapy and race in HCV and HCV/HIV infection. J. Hepatol. 50(4): 705-711.
Koelsche C, Strebovsky J, Baetz A, Dalpke AH. 2009 Aug. Structural and functional analysis of a nuclear localization signal in SOCS1. Mol. Immunol. 46(13): 2474-2480.
Komazaki T, Nagai H, Emi M, Terada Y, Yabe A, Jin E, Kawanami O, Konishi N, Moriyama Y, Naka T, Kishimoto T. 2004 Apr. Hypermethylation-associated inactivation of the SOCS-1 gene, a JAK/STAT inhibitor, in human pancreatic cancers. Jpn. J. Clin. Oncol. 34(4): 191-194.
Kovarik A, Fojtova M, Boudny V, Adamkova L, Lauerova L, Kovarik J. 2005 Dec. Interferon-gamma, but not interferon-alpha, induces SOCS 3 expression in human melanoma cell lines. Melanoma Res. 15(6): 481-488.
Lanford RE, Guerra B, Lee H, Chavez D, Brasky KM, Bigger CB. 2006 May. Genomic response to interferon-alpha in chimpanzees: implications of rapid downregulation for hepatitis C kinetics. Hepatology 43(5): 961-972.
Lanford RE, Hildebrandt-Eriksen ES, Petri A, Persson R, Lindow M, Munk ME, Kauppinen S, Ørum H. 2010 Jan. Therapeutic silencing of microRNA-122 in primates with chronic hepatitis C virus infection. Science 327(5962): 198-201.
Lena AM, Shalom-Feuerstein R, Rivetti di Val Cervo P, Aberdam D, Knight RA, Melino G, Candi E. 2008 Jul. miR-203 represses 'stemness' by repressing DeltaNp63. Cell Death Differ. 15(7): 1187-1195.
Lesinski GB, Anghelina M, Zimmerer J, Bakalakos T, Badgwell B, Parihar R, Hu Y, Becknell B, Abood G, Chaudhury AR, Magro C, Durbin J, Carson WE3. 2003 Jul. The antitumor effects of IFN-alpha are abrogated in a STAT1-deficient mouse. J. Clin. Invest. 112(2): 170-180.
Lesinski GB, Zimmerer JM, Kreiner M, Trefry J, Bill MA, Young GS, Becknell B, Carson WE3. 2010. Modulation of SOCS protein expression influences the interferon responsiveness of human melanoma cells. BMC Cancer 10: 142.
Li Z, Metze D, Nashan D, Müller-Tidow C, Serve HL, Poremba C, Luger TA, Böhm M. 2004 Oct. Expression of SOCS-1, suppressor of cytokine signalling-1, in human melanoma. J. Invest. Dermatol. 123(4): 737-745.
Lin SM, Du P, Huber W, Kibbe WA. 2008 Feb. Model-based variance-stabilizing transformation for Illumina microarray data. Nucleic Acids Res. 36(2): e11.
Lin Y, Lin C, Tsai Y, Weng H, Li Y, You L, Chen J, Jablons DM, Yang C. 2010 Dec. Adenovirus-mediated SOCS3 gene transfer inhibits the growth and enhances the radiosensitivity of human non-small cell lung cancer cells. Oncol. Rep. 24(6): 1605-1612.
Lu L, Thai T, Calado DP, Chaudhry A, Kubo M, Tanaka K, Loeb GB, Lee H, Yoshimura A, Rajewsky K, Rudensky AY. 2009 Jan. Foxp3-dependent microRNA155 confers competitive fitness to regulatory T cells by targeting SOCS1 protein. Immunity 30(1): 80-91.
Ma N, Li F, Li D, Hui Y, Wang X, Qiao Y, Zhang Y, Xiang Y, Zhou J, Zhou L, Zheng X, Gao X. 2012 Feb. Igf2-derived intronic miR-483 promotes mouse hepatocellular carcinoma cell proliferation. Mol. Cell. Biochem. 361(1-2): 337-343.
Machado MV, Cortez-Pinto H. 2009. Insulin resistance and steatosis in chronic hepatitis C. Ann Hepatol 8 Suppl 1: S67-75.

Maher SG, Sheikh F, Scarzello AJ, Romero-Weaver AL, Baker DP, Donnelly RP, Gamero AM. 2008 Jul. IFNalpha and IFNlambda differ in their antiproliferative effects and duration of JAK/STAT signaling activity. Cancer Biol. Ther. 7(7): 1109-1115.
Maine GN, Mao X, Komarck CM, Burstein E. 2007 Jan. COMMD1 promotes the ubiquitination of NF-kappaB subunits through a cullin-containing ubiquitin ligase. EMBO J. 26(2): 436-447.
Mallette FA, Moiseeva O, Calabrese V, Mao B, Gaumont-Leclerc M, Ferbeyre G. 2010 Jun. Transcriptome analysis and tumor suppressor requirements of STAT5-induced senescence. Ann. N. Y. Acad. Sci. 1197: 142-151.
Meng F, Henson R, Wehbe-Janek H, Smith H, Ueno Y, Patel T. 2007 Mar. The MicroRNA let-7a modulates interleukin-6-dependent STAT-3 survival signaling in malignant human cholangiocytes. J. Biol. Chem. 282(11): 8256-8264.
Miyaaki H, Ichikawa T, Nakao K, Matsuzaki T, Muraoka T, Honda T, Takeshita S, Shibata H, Ozawa E, Akiyama M, Miuma S, Eguchi K. 2009 Sep. Predictive value of suppressor of cytokine signal 3 (SOCS3) in the outcome of interferon therapy in chronic hepatitis C. Hepatol. Res. 39(9): 850-855.
Moffatt CE, Lamont RJ. 2011 Jul. Porphyromonas gingivalis induction of microRNA-203 expression controls suppressor of cytokine signaling 3 in gingival epithelial cells. Infect. Immun. 79(7): 2632-2637.
Moucari R, Asselah T, Cazals-Hatem D, Voitot H, Boyer N, Ripault M, Sobesky R, Martinot-Peignoux M, Maylin S, Nicolas-Chanoine M, Paradis V, Vidaud M, Valla D, Bedossa P, Marcellin P. 2008 Feb. Insulin resistance in chronic hepatitis C: association with genotypes 1 and 4, serum HCV RNA level, and liver fibrosis. Gastroenterology 134(2): 416-423.
Mujtaba MG, Flowers LO, Patel CB, Patel RA, Haider MI, Johnson HM. 2005 Oct. Treatment of mice with the suppressor of cytokine signaling-1 mimetic peptide, tyrosine kinase inhibitor peptide, prevents development of the acute form of experimental allergic encephalomyelitis and induces stable remission in the chronic relapsing/remitting form. J. Immunol. 175(8): 5077-5086.
Nagai H, Naka T, Terada Y, Komazaki T, Yabe A, Jin E, Kawanami O, Kishimoto T, Konishi N, Nakamura M, Kobayashi Y, Emi M. 2003. Hypermethylation associated with inactivation of the SOCS-1 gene, a JAK/STAT inhibitor, in human hepatoblastomas. J. Hum. Genet. 48(2): 65-69.
Nguyen V, Zhang H, Kadakia S, Krolewski JJ [unpublished]. Attenuation of interferon-alpha signaling by SOCS-1 and SOCS-3 [Internet]. [cited 2006 Dec 29]. Available from: http://www.pathology.uci.edu/faculty/jkrolewski/51NguyenSubmitted.pdf
Nicholson SE, Willson TA, Farley A, Starr R, Zhang JG, Baca M, Alexander WS, Metcalf D, Hilton DJ, Nicola NA. 1999 Jan. Mutational analyses of the SOCS proteins suggest a dual domain requirement but distinct mechanisms for inhibition of LIF and IL-6 signal transduction. EMBO J. 18(2): 375-385.
Norkina O, Dolganiuc A, Catalano D, Kodys K, Mandrekar P, Syed A, Efros M, Szabo G. 2008 Sep. Acute alcohol intake induces SOCS1 and SOCS3 and inhibits cytokine-induced STAT1 and STAT3 signaling in human monocytes. Alcohol. Clin. Exp. Res. 32(9): 1565-1573.
Ogata H, Kobayashi T, Chinen T, Takaki H, Sanada T, Minoda Y, Koga K, Takaesu G, Maehara Y, Iida M, Yoshimura A. 2006 Jul. Deletion of the SOCS3 gene in liver parenchymal cells promotes hepatitis-induced hepatocarcinogenesis. Gastroenterology 131(1): 179-193.
Pascarella S, Clément S, Guilloux K, Conzelmann S, Penin F, Negro F. 2011 Jun. Effects of hepatitis C virus on suppressor of cytokine signaling mRNA levels: comparison between different genotypes and core protein sequence analysis. J. Med. Virol. 83(6): 1005-1015.
Pazienza V, Clément S, Pugnale P, Conzelman S, Foti M, Mangia A, Negro F. 2007 May. The hepatitis C virus core protein of genotypes 3a and 1b downregulates insulin receptor substrate 1 through genotype-specific mechanisms. Hepatology 45(5): 1164-1171.
Pazienza V, Clément S, Pugnale P, Conzelmann S, Pascarella S, Mangia A, Negro F. 2009 May. Gene expression profile of Huh-7 cells expressing hepatitis C virus genotype 1b or 3a core proteins. Liver Int. 29(5): 661-669.
Pazienza V, Vinciguerra M, Andriulli A, Mangia A. 2010 Jul. Hepatitis C virus core protein genotype 3a increases SOCS-7 expression through PPAR-{gamma} in Huh-7 cells. J. Gen. Virol. 91(Pt 7): 1678-1686.
Pedersen IM, Cheng G, Wieland S, Volinia S, Croce CM, Chisari FV, David M. 2007 Oct. Interferon modulation of cellular microRNAs as an antiviral mechanism. Nature 449(7164): 919-922.
Peltola KJ, Paukku K, Aho TLT, Ruuska M, Silvennoinen O, Koskinen PJ. 2004 May. Pim-1 kinase inhibits STAT5-dependent transcription via its interactions with SOCS1 and SOCS3.

Blood 103(10): 3744-3750.
Persico M, Capasso M, Persico E, Svelto M, Russo R, Spano D, Crocè L, La Mura V, Moschella F, Masutti F, Torella R, Tiribelli C, Iolascon A. 2007 Oct. Suppressor of cytokine signaling 3 (SOCS3) expression and hepatitis C virus-related chronic hepatitis: Insulin resistance and response to antiviral therapy. Hepatology 46(4): 1009-1015.
Persico M, Iolascon A. 2010 Mar. Steatosis as a co-factor in chronic liver diseases. World J. Gastroenterol. 16(10): 1171-1176.
Persico M, Russo R, Persico E, Svelto M, Spano D, Andolfo I, La Mura V, Capasso M, Tiribelli C, Torella R, Iolascon A. 2009. SOCS3 and IRS-1 gene expression differs between genotype 1 and genotype 2 hepatitis C virus-infected HepG2 cells. Clin. Chem. Lab. Med. 47(10): 1217-1225.
Petta S, Cammà C, Di Marco V, Alessi N, Cabibi D, Caldarella R, Licata A, Massenti F, Tarantino G, Marchesini G, Craxì A. 2008 May. Insulin resistance and diabetes increase fibrosis in the liver of patients with genotype 1 HCV infection. Am. J. Gastroenterol. 103(5): 1136-1144.
Pichiorri F, Suh S, Ladetto M, Kuehl M, Palumbo T, Drandi D, Taccioli C, Zanesi N, Alder H, Hagan JP, Munker R, Volinia S, Boccadoro M, Garzon R, Palumbo A, Aqeilan RI, Croce CM. 2008 Sep. MicroRNAs regulate critical genes associated with multiple myeloma pathogenesis. Proc. Natl. Acad. Sci. U.S.A. 105(35): 12885-12890.
Piessevaux J, Lavens D, Peelman F, Tavernier J. 2008 Oct-Dec. The many faces of the SOCS box. Cytokine Growth Factor Rev. 19(5-6): 371-381.
Piganis RAR, De Weerd NA, Gould JA, Schindler CW, Mansell A, Nicholson SE, Hertzog PJ. 2011 Sep. Suppressor of cytokine signaling (SOCS) 1 inhibits type I interferon (IFN) signaling via the interferon alpha receptor (IFNAR1)-associated tyrosine kinase Tyk2. J. Biol. Chem. 286(39): 33811-33818.
Qin H, Niyongere SA, Lee SJ, Baker BJ, Benveniste EN. 2008 Sep. Expression and functional significance of SOCS-1 and SOCS-3 in astrocytes. J. Immunol. 181(5): 3167-3176.
Qing Y, Costa-Pereira AP, Watling D, Stark GR. 2005 Jan. Role of tyrosine 441 of interferon-gamma receptor subunit 1 in SOCS-1-mediated attenuation of STAT1 activation. J. Biol. Chem. 280(3): 1849-1853.
Randall G, Chen L, Panis M, Fischer AK, Lindenbach BD, Sun J, Heathcote J, Rice CM, Edwards AM, McGilvray ID. 2006 Nov. Silencing of USP18 potentiates the antiviral activity of interferon against hepatitis C virus infection. Gastroenterology 131(5): 1584-1591.
Randall G, Panis M, Cooper JD, Tellinghuisen TL, Sukhodolets KE, Pfeffer S, Landthaler M, Landgraf P, Kan S, Lindenbach BD, Chien M, Weir DB, Russo JJ, Ju J, Brownstein MJ, Sheridan R, Sander C, Zavolan M, Tuschl T, Rice CM. 2007 Jul. Cellular cofactors affecting hepatitis C virus infection and replication. Proc. Natl. Acad. Sci. U.S.A. 104(31): 12884-12889.
Rani MRS, Croze E, Wei T, Shrock J, Josyula A, Kalvakolanu DV, Ransohoff RM. 2010 Mar. STAT-phosphorylation-independent induction of interferon regulatory factor-9 by interferon-beta. J. Interferon Cytokine Res. 30(3): 163-170.
Riehle KJ, Campbell JS, McMahan RS, Johnson MM, Beyer RP, Bammler TK, Fausto N. 2008 Jan. Regulation of liver regeneration and hepatocarcinogenesis by suppressor of cytokine signaling 3. J. Exp. Med. 205(1): 91-103.
Rigby RJ, Simmons JG, Greenhalgh CJ, Alexander WS, Lund PK. 2007 Jul. Suppressor of cytokine signaling 3 (SOCS3) limits damage-induced crypt hyper-proliferation and inflammation-associated tumorigenesis in the colon. Oncogene 26(33): 4833-4841.
Roman-Gomez J, Jimenez-Velasco A, Castillejo JA, Cervantes F, Barrios M, Colomer D, Heiniger A, Torres A. 2004 Jan. The suppressor of cytokine signaling-1 is constitutively expressed in chronic myeloid leukemia and correlates with poor cytogenetic response to interferon-alpha. Haematologica 89(1): 42-48.
Rossa CJ, Sommer G, Spolidorio LC, Rosenzweig SA, Watson DK, Kirkwood KL. 2012. Loss of expression and function of SOCS3 is an early event in HNSCC: altered subcellular localization as a possible mechanism involved in proliferation, migration and invasion. PLoS ONE 7(9): e45197.
Ru P, Steele R, Hsueh EC, Ray RB. 2011 Jul. Anti-miR-203 Upregulates SOCS3 Expression in Breast Cancer Cells and Enhances Cisplatin Chemosensitivity. Genes Cancer 2(7): 720-727.
Sakai I, Takeuchi K, Yamauchi H, Narumi H, Fujita S. 2002 Oct. Constitutive expression of SOCS3 confers resistance to IFN-alpha in chronic myelogenous leukemia cells. Blood 100(8): 2926-2931.
Sakamoto H, Yasukawa H, Masuhara M, Tanimura S, Sasaki A, Yuge K, Ohtsubo M, Ohtsuka A, Fujita T, Ohta T, Furukawa Y, Iwase S, Yamada H, Yoshimura A. 1998 Sep. A Janus kinase

inhibitor, JAB, is an interferon-gamma-inducible gene and confers resistance to interferons. Blood 92(5): 1668-1676.
Sarasin-Filipowicz M. 2010 Jan. Interferon therapy of hepatitis C: molecular insights into success and failure. Swiss Med Wkly 140(1-2): 3-11.
Sarasin-Filipowicz M, Krol J, Markiewicz I, Heim MH, Filipowicz W. 2009a Jan. Decreased levels of microRNA miR-122 in individuals with hepatitis C responding poorly to interferon therapy. Nat. Med. 15(1): 31-33.
Sarasin-Filipowicz M, Oakeley EJ, Duong FHT, Christen V, Terracciano L, Filipowicz W, Heim MH. 2008 May. Interferon signaling and treatment outcome in chronic hepatitis C. Proc. Natl. Acad. Sci. U.S.A. 105(19): 7034-7039.
Sarasin-Filipowicz M, Wang X, Yan M, Duong FHT, Poli V, Hilton DJ, Zhang D, Heim MH. 2009b Sep. Alpha interferon induces long-lasting refractoriness of JAK-STAT signaling in the mouse liver through induction of USP18/UBP43. Mol. Cell. Biol. 29(17): 4841-4851.
Sasaki A, Inagaki-Ohara K, Yoshida T, Yamanaka A, Sasaki M, Yasukawa H, Koromilas AE, Yoshimura A. 2003 Jan. The N-terminal truncated isoform of SOCS3 translated from an alternative initiation AUG codon under stress conditions is stable due to the lack of a major ubiquitination site, Lys-6. J. Biol. Chem. 278(4): 2432-2436.
Schlüter G, Boinska D, Nieman-Seyde SC. 2000 Feb. Evidence for translational repression of the SOCS-1 major open reading frame by an upstream open reading frame. Biochem. Biophys. Res. Commun. 268(2): 255-261.
Shao R, Zhang L, Peng LF, Sun E, Chung WJ, Jang JY, Tsai W, Hyppolite G, Chung RT. 2010 Jun. Suppressor of cytokine signaling 3 suppresses hepatitis C virus replication in an mTOR-dependent manner. J. Virol. 84(12): 6060-6069.
Shen L, Evel-Kabler K, Strube R, Chen S. 2004 Dec. Silencing of SOCS1 enhances antigen presentation by dendritic cells and antigen-specific anti-tumor immunity. Nat. Biotechnol. 22(12): 1546-1553.
Shuai K. 2006 Feb. Regulation of cytokine signaling pathways by PIAS proteins. Cell Res. 16(2): 196-202.
Siegrist F, Certa U. 2008. Micro RNA Induction by Interferon Alpha and a Potential Role to Interfere with SOCS. 7th Joint Conference – Montréal, Québec, Canada, October 12-16, 2008. Editor: John Hiscott. Medimont International Proceedings: 93-97.
Siegrist F, Singer T, Certa U. 2009 Dec. MicroRNA Expression Profiling by Bead Array Technology in Human Tumor Cell Lines Treated with Interferon-Alpha-2a. Biol Proced Online 11: 113-129.
Smyth GK. 2004. Linear models and empirical bayes methods for assessing differential expression in microarray experiments. Stat Appl Genet Mol Biol 3: Article3.
Song MM, Shuai K. 1998 Dec. The suppressor of cytokine signaling (SOCS) 1 and SOCS3 but not SOCS2 proteins inhibit interferon-mediated antiviral and antiproliferative activities. J. Biol. Chem. 273(52): 35056-35062.
Sonkoly E, Wei T, Janson PCJ, Sääf A, Lundeberg L, Tengvall-Linder M, Norstedt G, Alenius H, Homey B, Scheynius A, Ståhle M, Pivarcsi A. 2007. MicroRNAs: novel regulators involved in the pathogenesis of psoriasis ? PLoS ONE 2(7): e610.
Stark GR, Kerr IM, Williams BR, Silverman RH, Schreiber RD. 1998. How cells respond to interferons. Annu. Rev. Biochem. 67: 227-264.
Starr R, Fuchsberger M, Lau LS, Uldrich AP, Goradia A, Willson TA, Verhagen AM, Alexander WS, Smyth MJ. 2009 Oct. SOCS-1 binding to tyrosine 441 of IFN-gamma receptor subunit 1 contributes to the attenuation of IFN-gamma signaling in vivo. J. Immunol. 183(7): 4537-4544.
Starr R, Willson TA, Viney EM, Murray LJ, Rayner JR, Jenkins BJ, Gonda TJ, Alexander WS, Metcalf D, Nicola NA, Hilton DJ. 1997 Jun. A family of cytokine-inducible inhibitors of signalling. Nature 387(6636): 917-921.
Sun BK, Tsao H. 2008 Nov. Small RNAs in development and disease. J. Am. Acad. Dermatol. 59(5): 725-737.
Takahashi Y, Kaneda H, Takasuka N, Hattori K, Nishikawa M, Watanabe Y, Takakura Y. 2008 Aug. Enhancement of antiproliferative activity of interferons by RNA interference-mediated silencing of SOCS gene expression in tumor cells. Cancer Sci. 99(8): 1650-1655.
Takeuchi K, Sakai I, Narumi H, Yasukawa M, Kojima K, Minamoto Y, Fujisaki T, Tanimoto K, Hara M, Numata A, Gondo H, Takahashi M, Fujii N, Masuda K, Fujita S. 2005 Feb. Expression of SOCS3 mRNA in bone marrow cells from CML patients associated with cytogenetic response to IFN-alpha. Leuk. Res. 29(2): 173-178.
Tarassishin L, Loudig O, Bauman A, Shafit-Zagardo B, Suh H, Lee SC. 2011 Dec. Interferon

regulatory factor 3 inhibits astrocyte inflammatory gene expression through suppression of the proinflammatory miR-155 and miR-155*. Glia 59(12): 1911-1922.
Tili E, Michaille J, Cimino A, Costinean S, Dumitru CD, Adair B, Fabbri M, Alder H, Liu CG, Calin GA, Croce CM. 2007 Oct. Modulation of miR-155 and miR-125b levels following lipopolysaccharide/TNF-alpha stimulation and their possible roles in regulating the response to endotoxin shock. J. Immunol. 179(8): 5082-5089.
Tomita S, Ishibashi K, Hashimoto K, Sugino T, Yanagida T, Kushida N, Shishido K, Aikawa K, Sato Y, Suzutani T, Yamaguchi O. 2011 Jan. Suppression of SOCS3 increases susceptibility of renal cell carcinoma to interferon-α. Cancer Sci. 102(1): 57-63.
Ueki K, Kadowaki T, Kahn CR. 2005 Oct. Role of suppressors of cytokine signaling SOCS-1 and SOCS-3 in hepatic steatosis and the metabolic syndrome. Hepatol. Res. 33(2): 185-192.
Vanni E, Abate ML, Gentilcore E, Hickman I, Gambino R, Cassader M, Smedile A, Ferrannini E, Rizzetto M, Marchesini G, Gastaldelli A, Bugianesi E. 2009 Sep. Sites and mechanisms of insulin resistance in nonobese, nondiabetic patients with chronic hepatitis C. Hepatology 50(3): 697-706.
Vlotides G, Sörensen AS, Kopp F, Zitzmann K, Cengic N, Brand S, Zachoval R, Auernhammer CJ. 2004 Jul. SOCS-1 and SOCS-3 inhibit IFN-alpha-induced expression of the antiviral proteins 2,5-OAS and MxA. Biochem. Biophys. Res. Commun. 320(3): 1007-1014.
Waiboci LW, Ahmed CM, Mujtaba MG, Flowers LO, Martin JP, Haider MI, Johnson HM. 2007 Apr. Both the suppressor of cytokine signaling 1 (SOCS-1) kinase inhibitory region and SOCS-1 mimetic bind to JAK2 autophosphorylation site: implications for the development of a SOCS-1 antagonist. J. Immunol. 178(8): 5058-5068.
Walsh MJ, Jonsson JR, Richardson MM, Lipka GM, Purdie DM, Clouston AD, Powell EE. 2006 Apr. Non-response to antiviral therapy is associated with obesity and increased hepatic expression of suppressor of cytokine signalling 3 (SOCS-3) in patients with chronic hepatitis C, viral genotype 1. Gut 55(4): 529-535.
Wang P, Hou J, Lin L, Wang C, Liu X, Li D, Ma F, Wang Z, Cao X. 2010 Nov. Inducible microRNA-155 feedback promotes type I IFN signaling in antiviral innate immunity by targeting suppressor of cytokine signaling 1. J. Immunol. 185(10): 6226-6233.
Wang X, Zhao Q, Matta R, Meng X, Liu X, Liu C, Nelin LD, Liu Y. 2009 Oct. Inducible nitric-oxide synthase expression is regulated by mitogen-activated protein kinase phosphatase-1. J. Biol. Chem. 284(40): 27123-27134.
Wei T, Orfanidis K, Xu N, Janson P, Ståhle M, Pivarcsi A, Sonkoly E. 2010 Sep. The expression of microRNA-203 during human skin morphogenesis. Exp. Dermatol. 19(9): 854-856.
Wiesen JL, Tomasi TB. 2009 Mar. Dicer is regulated by cellular stresses and interferons. Mol. Immunol. 46(6): 1222-1228.
Xiao C, Rajewsky K. 2009 Jan. MicroRNA control in the immune system: basic principles. Cell 136(1): 26-36.
Yang B, Guo M, Herman JG, Clark DP. 2003 Sep. Aberrant promoter methylation profiles of tumor suppressor genes in hepatocellular carcinoma. Am. J. Pathol. 163(3): 1101-1107.
Yang R, Yang X, Zhang Z, Zhang Y, Wang S, Cai Z, Jia Y, Ma Y, Zheng C, Lu Y, Roden R, Chen Y. 2006 Dec. Single-walled carbon nanotubes-mediated in vivo and in vitro delivery of siRNA into antigen-presenting cells. Gene Ther. 13(24): 1714-1723.
Yasukawa H, Misawa H, Sakamoto H, Masuhara M, Sasaki A, Wakioka T, Ohtsuka S, Imaizumi T, Matsuda T, Ihle JN, Yoshimura A. 1999 Mar. The JAK-binding protein JAB inhibits Janus tyrosine kinase activity through binding in the activation loop. EMBO J. 18(5): 1309-1320.
Yasukawa H, Ohishi M, Mori H, Murakami M, Chinen T, Aki D, Hanada T, Takeda K, Akira S, Hoshijima M, Hirano T, Chien KR, Yoshimura A. 2003 Jun. IL-6 induces an anti-inflammatory response in the absence of SOCS3 in macrophages. Nat. Immunol. 4(6): 551-556.
Ye L, Wang S, Wang X, Zhou Y, Li J, Persidsky Y, Ho W. 2010 Nov. Alcohol impairs interferon signaling and enhances full cycle hepatitis C virus JFH-1 infection of human hepatocytes. Drug Alcohol Depend 112(1-2): 107-116.
Yoshida T, Ogata H, Kamio M, Joo A, Shiraishi H, Tokunaga Y, Sata M, Nagai H, Yoshimura A. 2004 Jun. SOCS1 is a suppressor of liver fibrosis and hepatitis-induced carcinogenesis. J. Exp. Med. 199(12): 1701-1707.
Yoshikawa H, Matsubara K, Qian GS, Jackson P, Groopman JD, Manning JE, Harris CC, Herman JG. 2001 May. SOCS-1, a negative regulator of the JAK/STAT pathway, is silenced by methylation in human hepatocellular carcinoma and shows growth-suppression activity. Nat. Genet. 28(1): 29-35.
Yoshikawa T, Takata A, Otsuka M, Kishikawa T, Kojima K, Yoshida H, Koike K. 2012. Silencing

of microRNA-122 enhances interferon-α signaling in the liver through regulating SOCS3 promoter methylation. Sci Rep 2: 637.
Yoshimura A. 2006 Jun. Signal transduction of inflammatory cytokines and tumor development. Cancer Sci. 97(6): 439-447.
Yoshimura A, Naka T, Kubo M. 2007 Jun. SOCS proteins, cytokine signalling and immune regulation. Nat. Rev. Immunol. 7(6): 454-465.
Yoshimura A, Nishinakamura H, Matsumura Y, Hanada T. 2005. Negative regulation of cytokine signaling and immune responses by SOCS proteins. Arthritis Res. Ther. 7(3): 100-110.
Younossi ZM, Birerdinc A, Estep M, Stepanova M, Afendy A, Baranova A. 2012. The impact of IL28B genotype on the gene expression profile of patients with chronic hepatitis C treated with pegylated interferon alpha and ribavirin. J Transl Med 10: 25.
Zhang J, Zhao H, Chen J, Xia B, Jin Y, Wei W, Shen J, Huang Y. 2012 Sep. Interferon-β-induced miR-155 inhibits osteoclast differentiation by targeting SOCS1 and MITF. FEBS Lett. 586(19): 3255-3262.
Zhang M, Liu F, Jia H, Zhang Q, Yin L, Liu W, Li H, Yu B, Wu J. 2011a Aug. Inhibition of microRNA let-7i depresses maturation and functional state of dendritic cells in response to lipopolysaccharide stimulation via targeting suppressor of cytokine signaling 1. J. Immunol. 187(4): 1674-1683.
Zhang Y, Ma CJ, Ni L, Zhang CL, Wu XY, Kumaraguru U, Li CF, Moorman JP, Yao ZQ. 2011b Mar. Cross-Talk between Programmed Death-1 and Suppressor of Cytokine Signaling-1 in Inhibition of IL-12 Production by Monocytes/Macrophages in Hepatitis C Virus Infection. J. Immunol. 186(5): 3093-3103.
Zimmerer JM, Lesinski GB, Kondadasula SV, Karpa VI, Lehman A, Raychaudhury A, Becknell B, Carson WE3. 2007 Apr. IFN-alpha-induced signal transduction, gene expression, and antitumor activity of immune effector cells are negatively regulated by suppressor of cytokine signaling proteins. J. Immunol. 178(8): 4832-4845.
Zimmerer JM, Lesinski GB, Ruppert AS, Radmacher MD, Noble C, Kendra K, Walker MJ, Carson WE3. 2008 Sep. Gene expression profiling reveals similarities between the in vitro and in vivo responses of immune effector cells to IFN-alpha. Clin. Cancer Res. 14(18): 5900-5906.

Figures

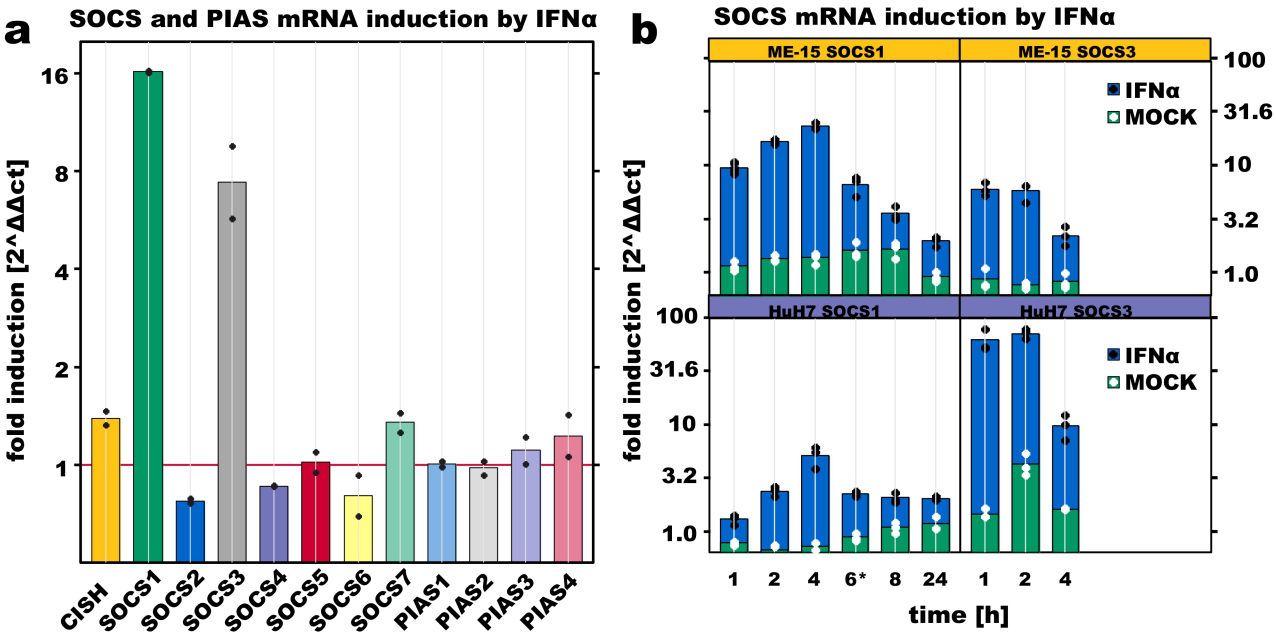

Figure 1 *SOCS* and *PIAS* mRNA induction by IFNα.
a – ME-15 cells were supplemented 2 hours before lysis with 1 % culture medium without or with IFNα (1000 U/ml). Fold changes from RT-PCR are relative to the average of *GAPDH* and *RPL32* endogenous controls and to untreated controls. Fold change for separate calculation of biological duplicates are shown as black dots.
b – Time course analysis of *SOCS1* and *SOCS3* induction by IFNα in a melanoma and hepatoma cell line. ME-15 and HuH7 cells were cultivated for 1, 2, 4, 8 or 24 hours after addition of 1 % IFNα (1000 U/ml) or control medium. Time-point 6* indicates treatment for 4 hours and replacement of medium from reference cell cultures for 2 hours. RT-PCR fold changes are relative to *RPL32* endogenous control and to pre-treatment levels. Fold changes for triplicates calculated separately are shown as black and white dots for INFα treated and non-treated samples, respectively. Endogenous *SOCS1* levels were higher in HuH7 control cultures according to ct values, which partially explain the lower fold induction.

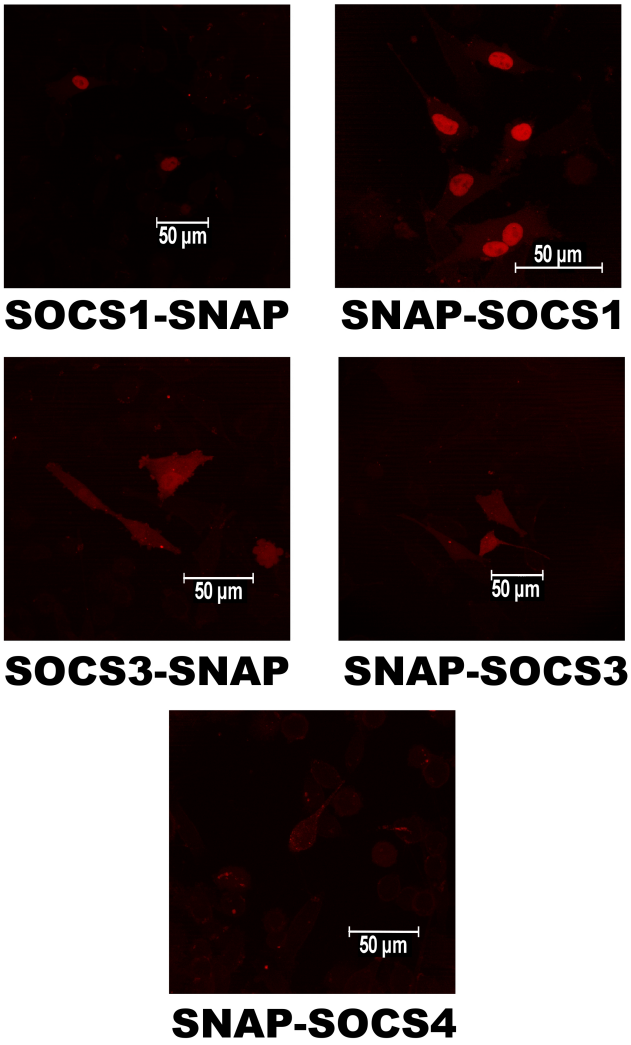

Figure 2 Subcellular localization of SOCS1, SOCS3 and SOCS4 in ME-15 melanoma cells.
ME-15 cells were transfected with expression plasmid pSEMS*1-26m* for N- and C-terminal SNAP-tagged SOCSs and cultured for 16 hours in chamber-slides before the proteins were covalently linked to the TMR-Star fluorescent substrate. Images were recorded with a 40x objective on a confocal microscope and original size is indicated with scale-bars of 50 µm.

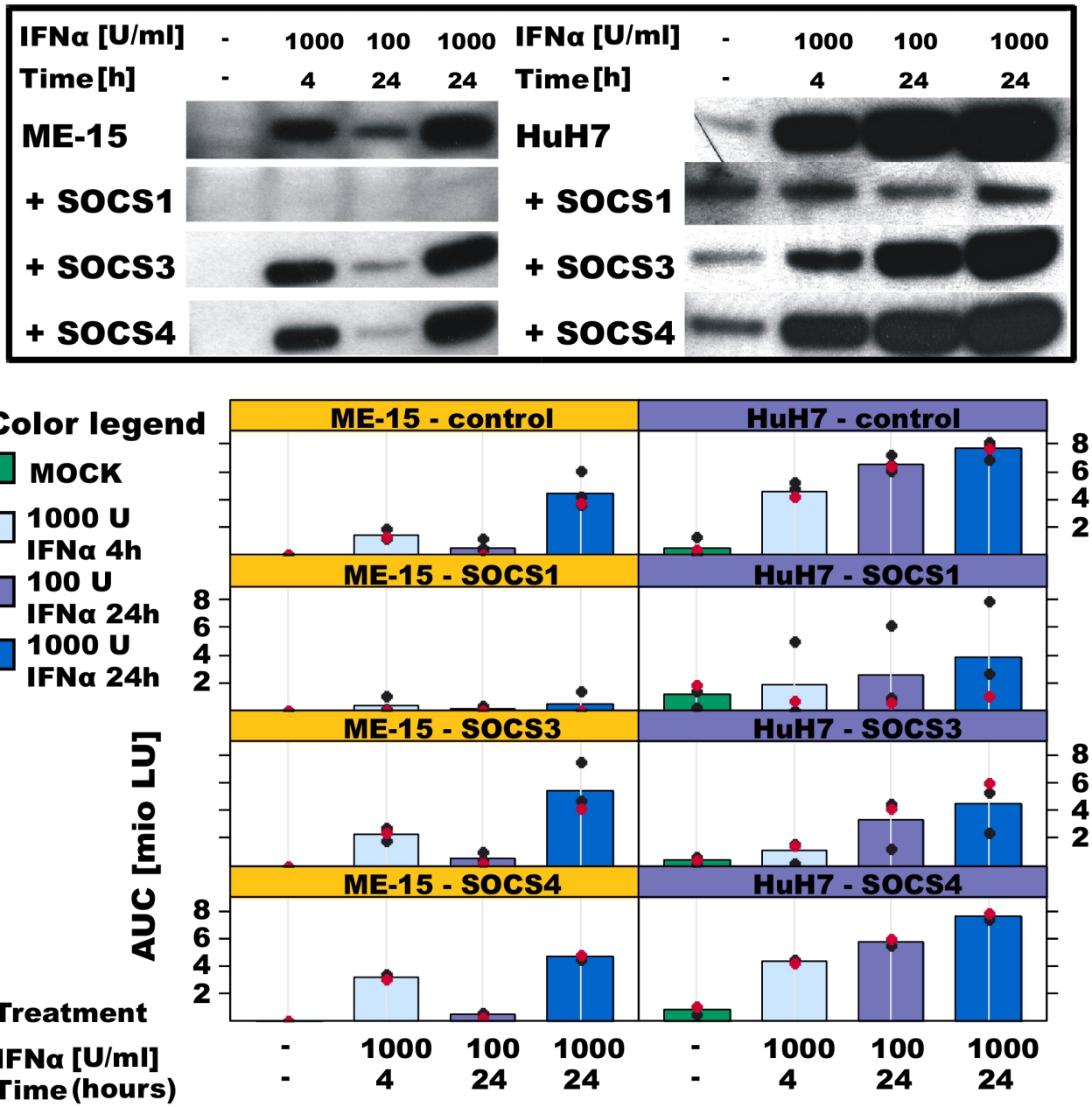

Figure 3 Effect on SOCS overexpression on IFITM3 protein induction by IFNα.

Western blots analysis of IFNα induced IFITM3 protein expression in melanoma and hepatoma cells. ME-15 and HuH7 cells were cultured in medium containing 100-1000 U/ml IFNα for 4 or 24 hours. Cell lysates were analysed by immunoblotting with an anti-IFITM antibody. Results for cell lines used in the microarray experiment are shown in the upper part and their signal intensities are represented as red dots in the graphs below. IFITM3 protein induction was quantified three times in untransfected cells, in three cells lines each derived from *SOCS1*- and *SOCS3*-pcDNA3.1 transfection and two with *SOCS4* control. Protein content was calculated based on the area under the curve (AUC) above background from chemiluminescent signals of the peak in the IFITM3 band region from immunoblots.

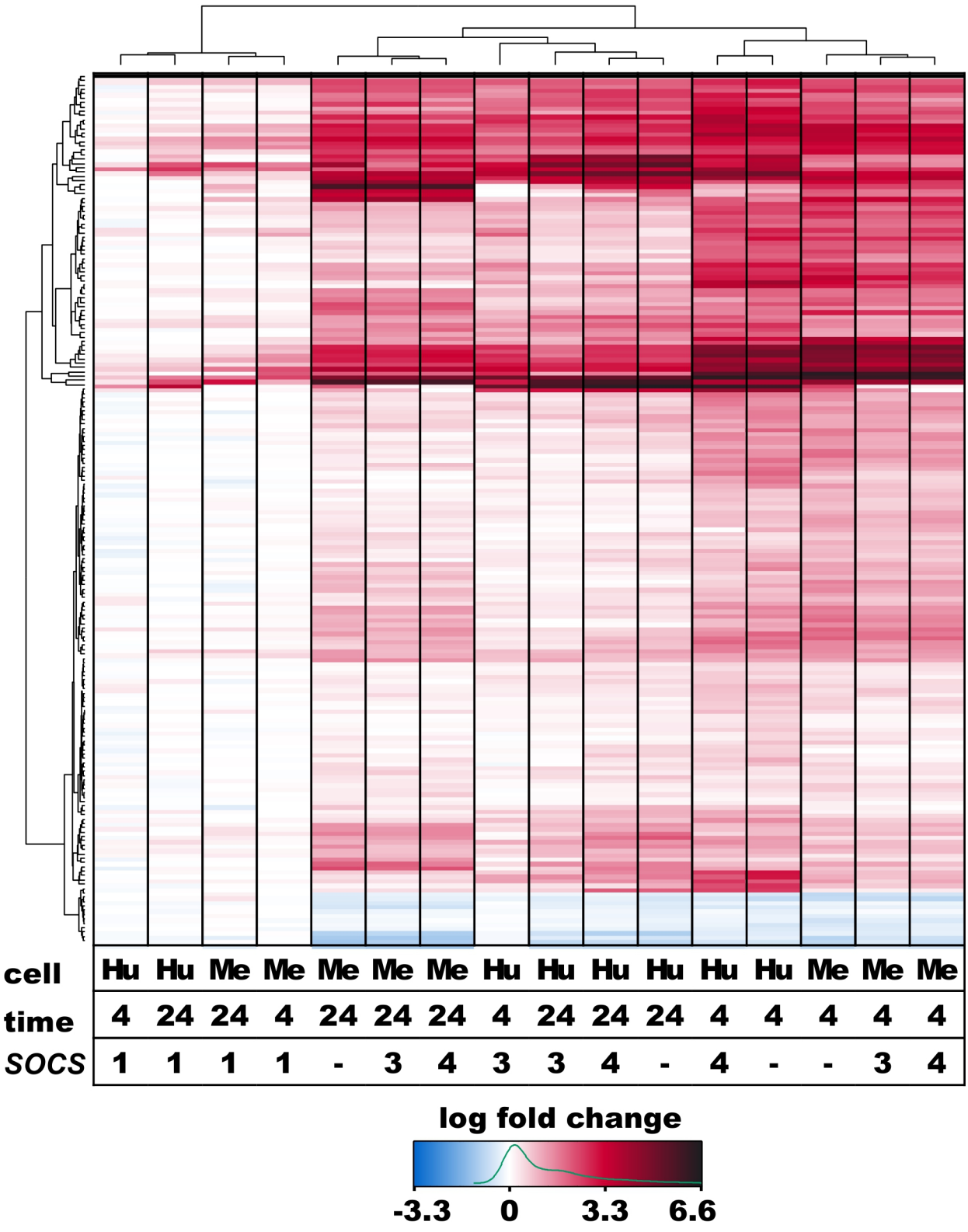

Figure 4 IFNα-stimulated whole genome expression profiles.
Parent and SOCS expressing ME-15 and HuH7 cell lines were cultured for 4 or 24 hours in normal or IFNα -containing (1000 U/ml) medium. Log2 factor changes were calculated from Illumina gene-expression arrays. Heat map shows a hierarchical clustering of the 250 most significant probes (p-value < 1.4×10^{-7}). Blue color indicates downregulation, white represents unchanged mRNA levels and red color upregulation. Density distribution for maximal or minimal changes is shown in green in the color legend.

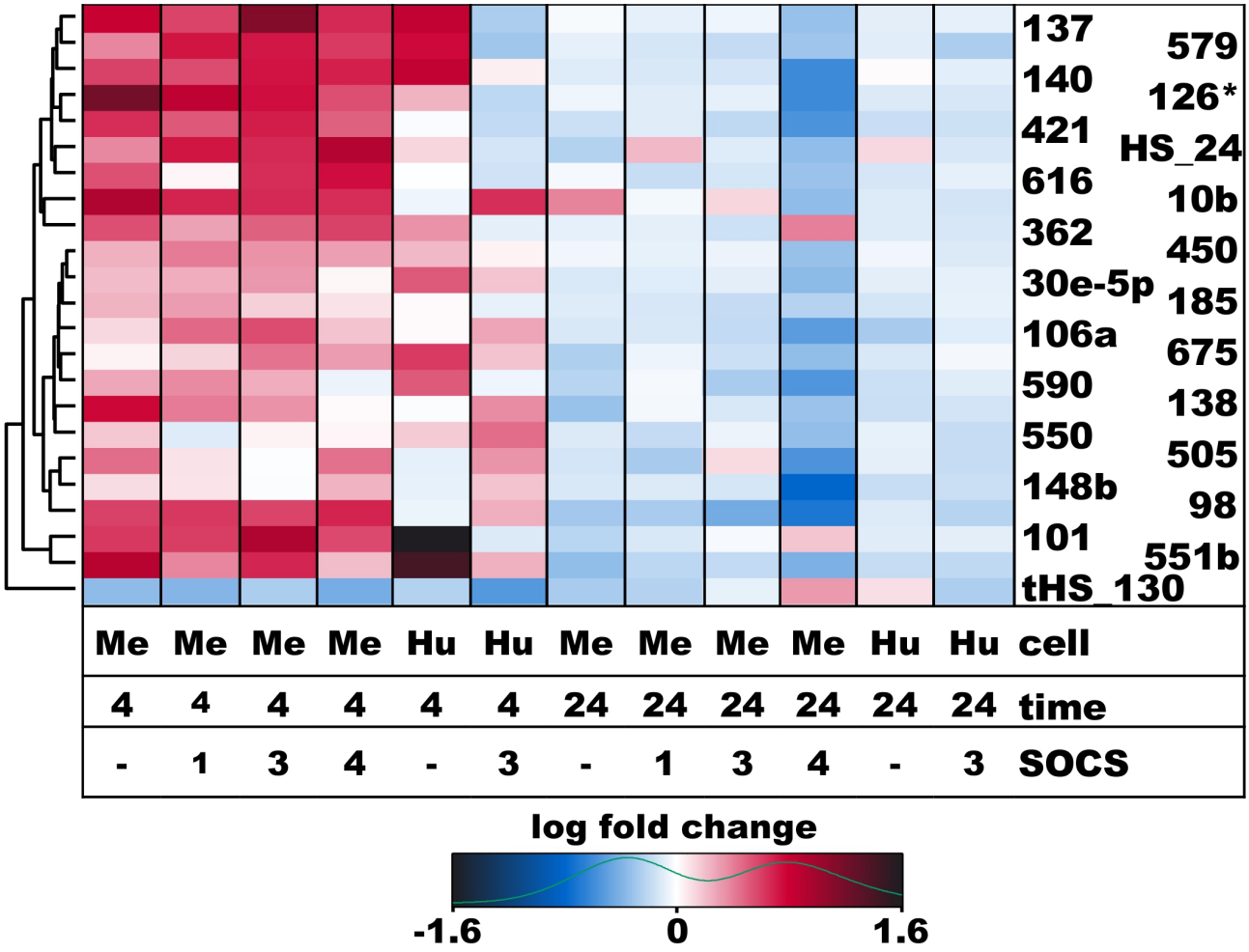

Figure 5 MiRNA profiling of SOCS-expressing cell lines.
Melanoma and hepatoma cells stably overexpressing SOCS proteins were treated with 1000U/ml IFNα for 4 and 24 hours. MiRNA probe intensities were assessed by Illumina microarrays and significant probes identified by an ANOVA model of the 4 hours time-point values correcting for cell type (p-value < 0.05). Log2 factor change values were clustered for probes and maximal (2^1.6=3 fold change) or minimal (2^-1.6=-0.33) changes indicated as a density distribution in the color legend.

Gene	RefSeq ID	Start	End	Orientation	Sequence
SOCS1	NM_003745.1	155	175	forward	taggatccgccgccATGGTAGCACACAACCAGGTG
SOCS1	NM_003745.1	790	767	reverse	tgccggaattcTCAAATCTGGAAGGGGAAGGAGCT
SOCS1	NM_003745.1	787	782	non-stop	tgccggaattcAATCTG
SOCS3	NM_003955.3	413	436	forward	cgtggatccgcCGCCATGGTCACCCACAGCAAGTT
SOCS3	NM_003955.3	1095	1070	reverse	ccccgaattGTTAAAGCGGGGCATCGTACTGGTCC
SOCS3	NM_003955.3	1091	1087	non-stop	cttcccgaattcAAGCG
SOCS4	NM_080867.2	436	460	forward	caaggatccgccgcCATGGCAGAAAATAATGAAAATATT
SOCS4	NM_080867.2	1759	1736	reverse	tgttagaattcCTAGCATGGCTGTTCTGGTGCATC
SOCS4	NM_080867.2	1756	1745	non-stop	agaattcGCATTGCTGTTC

Supplementary Table 1 Primer sequences for molecular cloning of *SOCS* genes

The sequence match with the RefSeq mRNA sequence are given in capital letters and in small letters the auxiliary nucleotide for introduction of restriction enzyme target sites and Kozak sequence are indicated. For primers matching to the reverse copy strand of the mRNA indicated have higher start than end positions.

Gene	RefSeq ID	orientation	Prod.size	Start	End	Tm	GC%	Sequence 5' - 3'
CISH	NM_145071.2	forward	**121**	476	496	54.11	47.62	ATGCCAGAAGGCACGTTCTTA
	NM_013324.5	reverse		596	577	54.79	60.00	GGAAGCTGGAGTCGGCATAC
SOCS1	NM_003745.1	forward	**140**	377	396	55.21	60.00	GACGCCTGCGGATTCTACTG
		reverse		516	496	55.02	57.14	GAGGCCATCTTCACGCTAAGG
SOCS2	NM_003877.3	forward EB	**107**	726	749	55.35	50.00	ACAGGATGGTACTGGGGAAGTATG
		reverse		832	806	56.51	44.44	AGGTAGTCTGAATGCGAGCTATCTCTA
SOCS3	NM_003955.3	forward	**148**	489	510	56.17	54.54	TTCAGCTCCAAGAGCGAGTACC
		reverse		636	617	54.74	55.00	AGCTGTCGCGGATCAGAAAG
SOCS4	NM_080867.2	forward	**129**	1203	1225	54.37	43.48	TGCAGTTGGAAACACCTCCTAAA
	NM_199421.1	reverse		1331	1310	54.67	50.00	GTGCTTCGGCTGCGTATTTATC
SOCS5	NM_014011.4	forward	**104**	1173	1193	55.68	52.38	AGGCAGAAGCAGCGTCAGATA
	NM_144949.2	reverse		1276	1254	55.79	52.17	GGCACGAGGCAGTGTATGTAATC
SOCS6	NM_004232.3	forward	**122**	1368	1389	54.27	50.00	CTCCTGGGGTTGCAAGAGTTTA
		reverse		1489	1469	55.13	52.38	ACGTGTGATTGGTCCCCAGTA
SOCS7	NM_014598.2	forward EB	**137**	1605	1624	55.35	55.00	TTCCAGGACTGCCACCAACT
		reverse		1741	1721	53.97	57.14	CAGTGGGAGATCTGGGATGTG
PIAS1	NM_016166.1	forward	**104**	1679	1699	53.73	52.38	GGCATCCTTTCCACATGACAC
		reverse		1782	1762	54.94	52.38	GGCAAGCAAGGAGGTGTTGTA
PIAS2	NM_173206.2	forward	**140**	416	437	55.07	50.00	TGGTGGCTCATCACCTGTAGAA
	NM_004671.2	reverse EB		555	531	54.15	44.00	GCATCTCAAATGTGGGCTTAGTATC
PIAS3	NM_006099.3	forward	**129**	1658	1678	54.19	52.38	GGAGCCGACATCCAAGGTTTA
		reverse		1786	1766	54.95	57.14	GGTCCCTCGGTACTGGAAGAA
PIAS4	NM_015897.2	forward EB	**133**	453	473	53.56	52.38	CCACCGAATTAGTCCCACAGA
		reverse EB		585	566	55.52	55.00	ACGACCTGCACGGCTTTAAC
RPL32	NM_000994.3	forward	**111**	353	373	54.79	47.62	GTGCTGCTGATGTGCAACAAA
		reverse		463	443	55.12	57.14	GGTGACTCTGATGGCCAGTTG
GAPDH	NM_0024046.3	forward	**300**	639	668	66.07	56.67	TGCCATCACTGCCACCCAGAAGACTGTGGA
		reverse		938	909	66.20	60.00	TGCTCAGTGTAGCCCAGGATGCCCTTGAGG

Supplementary Table 2 qPCR primer sequences for RT-PCR *SOCS* and *PIAS* mRNA quantification

qPCR primers were selected to generate a product size of 100 to 150 bp (100 as optimal). Primers covering an exon boundary were given preference. Primers for CISH, SOCS4, SOCS5 and PIAS2 are designed to amplify both transcript variants alpha and beta, the position are given for the first mRNA sequence and have a perfect match in the second on other positions (*in italic*). Primer that span over an exon boundary are marked with EB.

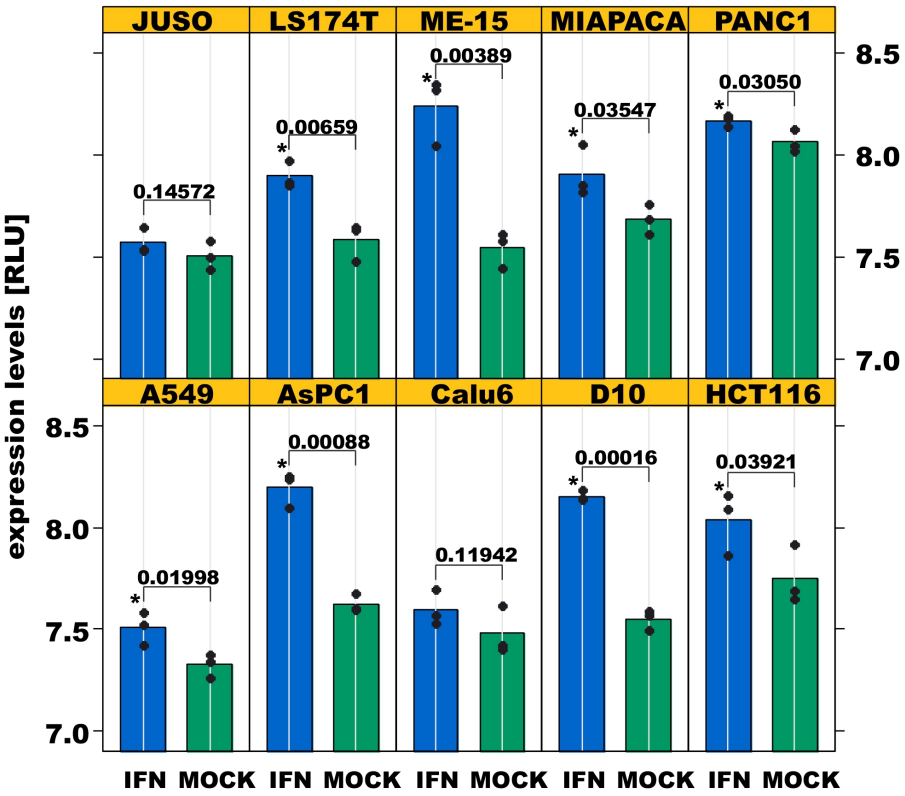

Supplementary Figure 1 SOCS1 mRNA induction by IFNα in ten carcinoma cell lines
Cells were grown in RPMI 1640 medium with IFNα (100 U/ml) for 4 hours or without IFNα (mock). The experimental details have been previously reported (Hallen *et al.* 2007) and data submitted to NCBI GEO database with accession number GSE21158. Expression levels are indicated as log relative luciferase levels (RLU). 8 out of 10 cell lines have significantly higher SOCS1 levels after addition of IFNα based on a one-tailed t-test (* indicates p-values below 0.05).

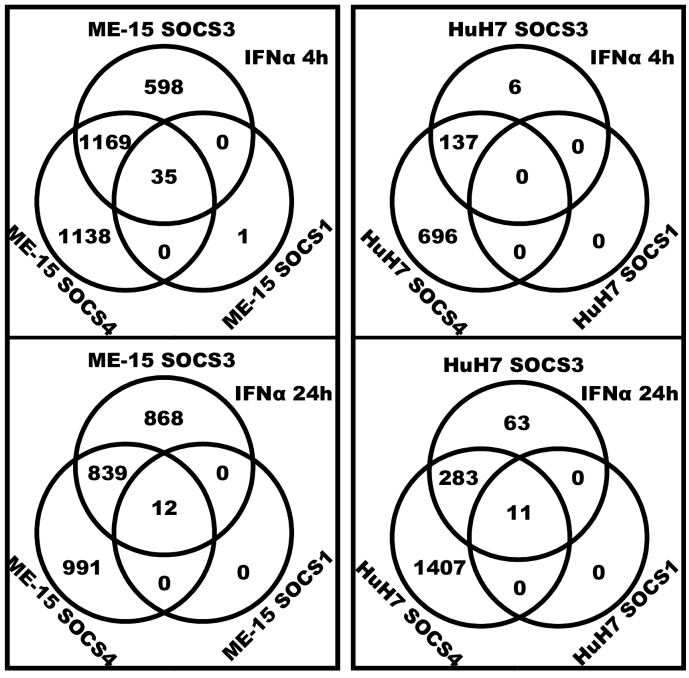

Supplementary Figure 2 Venn diagrams of IFNα induced probes
Number of probes significantly changed (fdr adjusted p-value < 0.05) by IFNα treatment in HuH7 and ME-15 cell lines derived by SOCS1, SOCS3 and SOCS4 construct transfection.

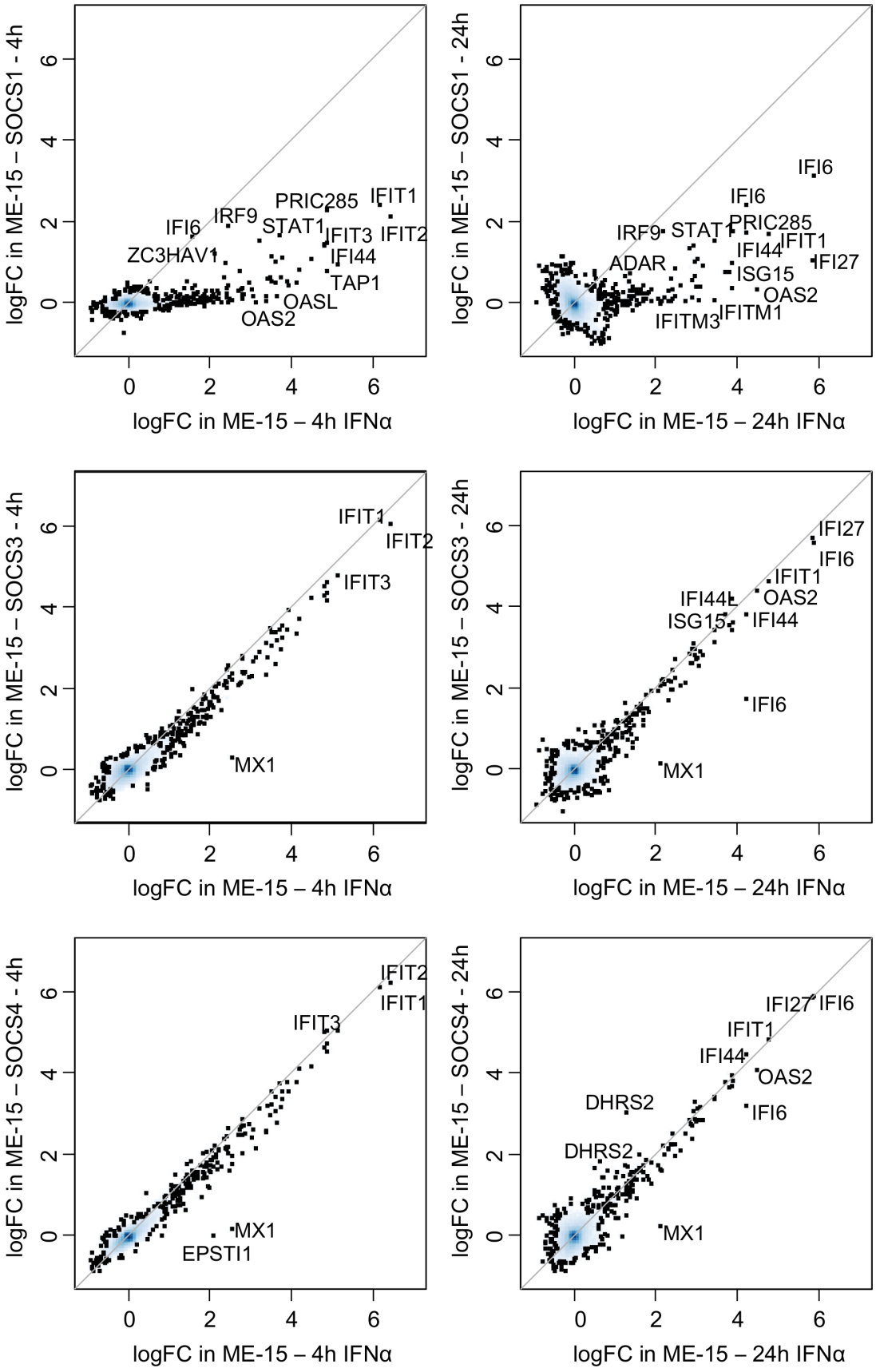

Supplementary Figure 3 Scatter-plot of SOCS ME-15 cell lines

Log factor change of control cells (ME-15) on the x-axis is plotted against log factor change of SOCS1-, SOCS3- or SOCS4-expressing cells on the y-axis. SOCS4 overexpression is only marginal and thus no effect is expected. Some probes are annotated manually for better orientation across all samples and to stress discordant values.

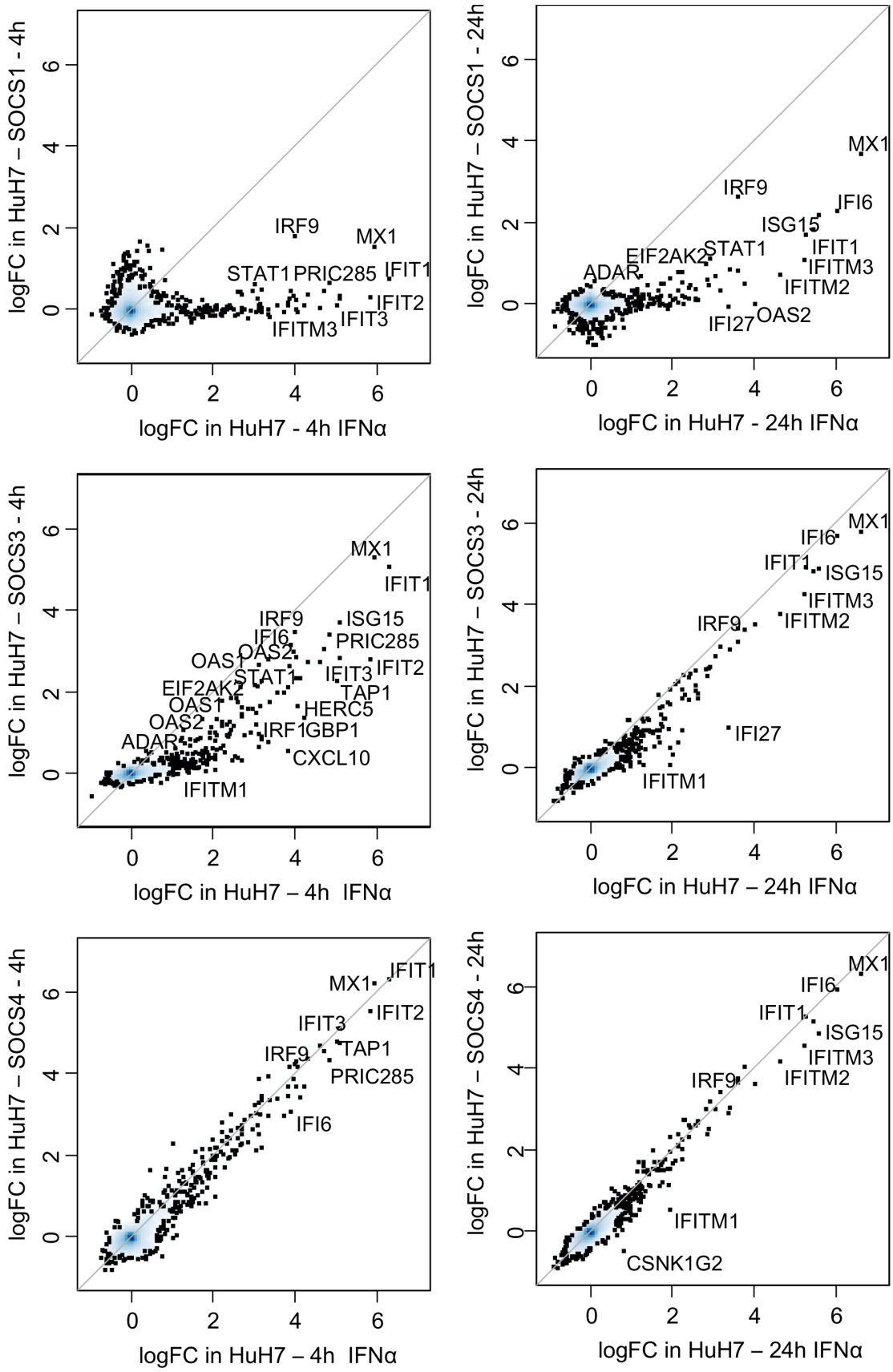

Supplementary Figure 4 Scatter-plot of SOCS HuH7 cell lines

Log factor change of control cells (HuH7) on the x-axis is plotted against log factor change of SOCS1-, SOCS3- or SOCS4-expressing cells on the y-axis. SOCS4 overexpression is only marginal and thus no effect is expected. Some probes are annotated manually for better orientation across all samples and to stress discordant values.

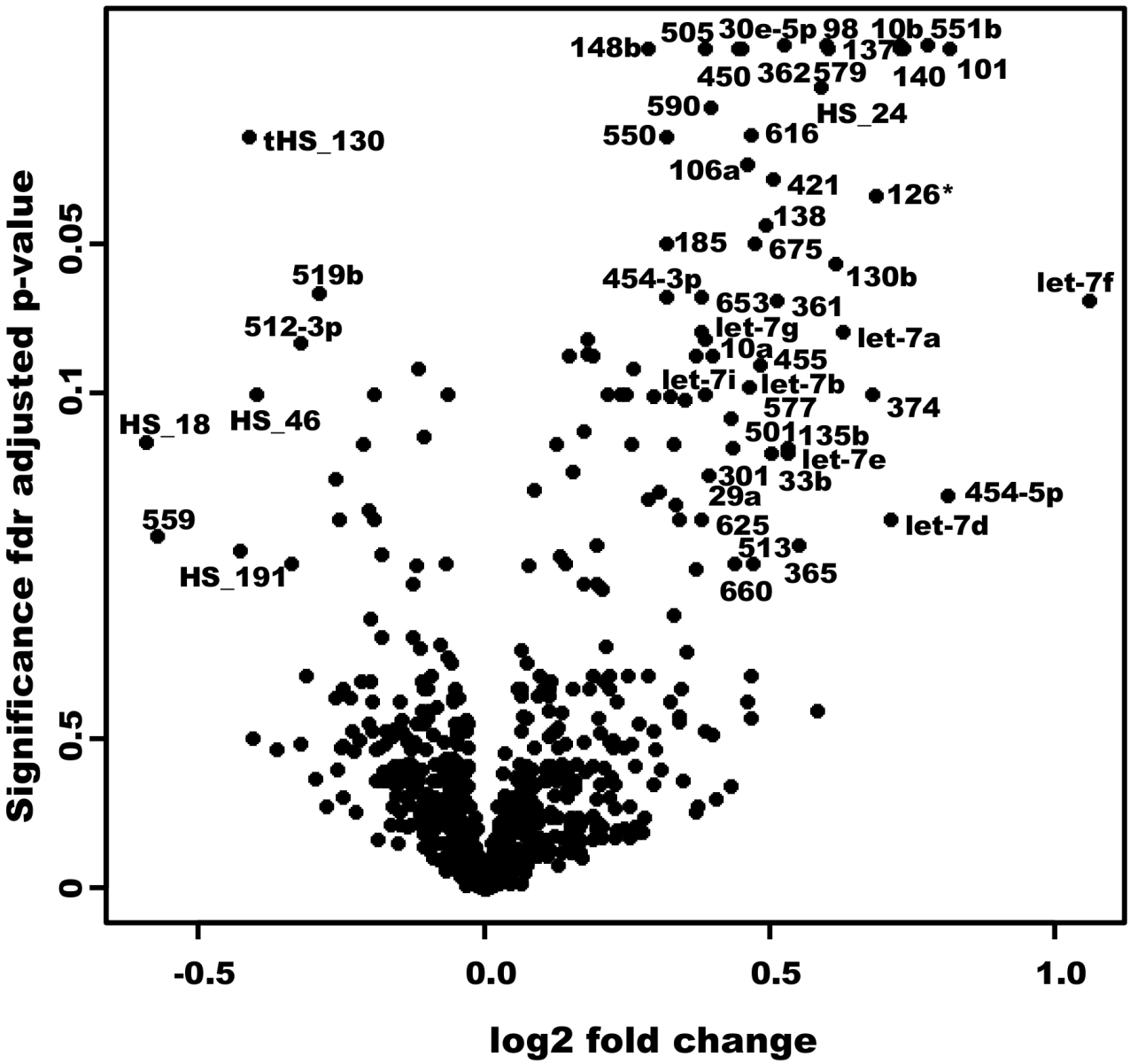

Supplementary Figure 5 Volcano-plot of IFNα-induced miRNAs

Cell lines were treated for four hours with IFNα. Microarray intensities from individual miRNA probes of HuH7 and ME-15 cell lines and SOCS-expressing derivatives were recorded using bead arrays. Probability for change by IFNα treatment (fdr adjusted p-value) is plotted against the intensity of the change (log2 fold changes). Annotations are given as numbers for miRNAs from Sanger miRBase (http://microrna.sanger.ac.uk/; Release 10.0: August 2007) or with prefix HS or tHS for 272 miRNAs according to annotation given by Illumina 'taken from the literature'.

Integrating transcriptome and epigenome analyses to identify DNA methylation changes associated with colorectal carcinogenesis.

Patric Urfer [1] and Fredy Siegrist [2], Faiza Noreen [1], Stefan Weis [1], Ulrich Certa [2], Kaspar Truninger [3], Primo Schär [1]

[1] Department of Biomedicine, Basel, [2] Roche, Basel, [3] Regional Hospital (SRO), Langenthal

Abstract

INTRODUCTION: Epigenetic silencing of tumor suppressor genes contributes significantly to malignant transformation in colorectal cancer (CRC). Silencing occurs by aberrant DNA methylation in gene promoters. METHODS: To identify genomic sequences undergoing aberrant methylation at early stages of colorectal carcinogenesis, we integrated results from three different genomic analyses: i) Gene expression profiling of 32 matched pairs of colorectal adenoma and normal mucosa tissues to identify gens downregulated early in carcinogenesis; ii) gene expression analysis of a CRC cell line showing wide-spread DNA hypermethylation (SW48) before and after 5-Aza-Cytidine/Trichostatin A induced demethylation to identify targets of methylation dependent gene silencing; and iii) DNA methylation profiling of matched primary tumor (CRC), cancer-associated mucosa (CAM) and blood from two colorectal cancer patients to identify cancer-specific methylation targets. Aberrant methylation at newly discovered targets were validated and cancer-specific methylation cut-offs determined by quantitative methylation-specific PCR in matched CRC, CAM and blood samples from 106 CRC patients. To assess “normal methylation” at these targets, we analyzed colorectal mucosa tissues (NM) from 31 healthy subjects. RESULTS: By integrating the results of these genome-wide analyses, we identified a number of potent targets that are specifically hypermethylated in an appreciable number of CRCs; e.g. FOXF1 was hypermethylated in 67% of cancers, CA4 in 21%, NPY1R in 19%, IFITM1 in 15% and GREM1 in 13%. FOXF1 hypermethylation turned out to be a strong marker for right sided neoplasia with a sensitivity of 91% (29/32). A panel consisting of all five markers and the two tumor suppressor genes MGMT and hMLH1 specifically identified 82% of all (87/106) and 94% of right sided colorectal cancers (30/32). CONCLUSION: The combination of genome-wide analyses of gene expression and DNA methylation in strategically matched samples is a powerful approach to identify hypermethylation targets fulfilling specific criteria. In our case, this strategy led to the discovery of a panel of novel and potent markers of colorectal carcinogenesis.

Introduction

Epigenetic silencing of tumor suppressor genes contributes significantly to malignant transformation in colorectal cancer (CRC). Silencing occurs by aberrant DNA methylation in gene promoters. Proposed mechanisms by which gene silencing occurs include DNA methylation and histone protein modification. Together, these epigenetic modifications determine the chromatin state and the accessibility of gene promoters. Gene silencing by aberrant promoter methylation appears to occur early in colorectal carcinogenesis since adenomas already display a different DNA methylation profile compared to normal colorectal tissue. This observation makes DNA methylation a promising diagnostic tool for cancer.

Aim of this project

To identify novel diagnostic DNA methylation targets in colorectal cancer which

- are detectable early in colorectal carcinogenesis
- show methylation-dependent gene expression (functional relevance)
- are cancer-specifically hypermethylated

To this end, we integrated the results of three different genome-wide analyses and validated the resulting candidate methylation markers with a newly established sensitive and quantitative methylation-specific PCR (qMSP) assay in 106 colorectal cancer patients and 31 healthy individuals.

Methods

Genome-wide analyses: Affymetrix Human Genome U133 Plus 2.0: Raw gene expression data generated by GeneChip Operating Software (Affymetrix) were imported into ROCHE Affymetrix Chip Experiment Analysis (RACE-A) Software and normalized per chip (i.e., to the median of all values on a given array) and per gene (i.e., to the median expression level of the given gene across all samples). Probes were selected, which had expression values of > 110 % in normal tissue in at least 30 of 32 of the adenoma samples. Boxplot-Jitter plots of 2092 probes in 32 patients representing 1249 unique genes, were computed using R software and Bioconductor.

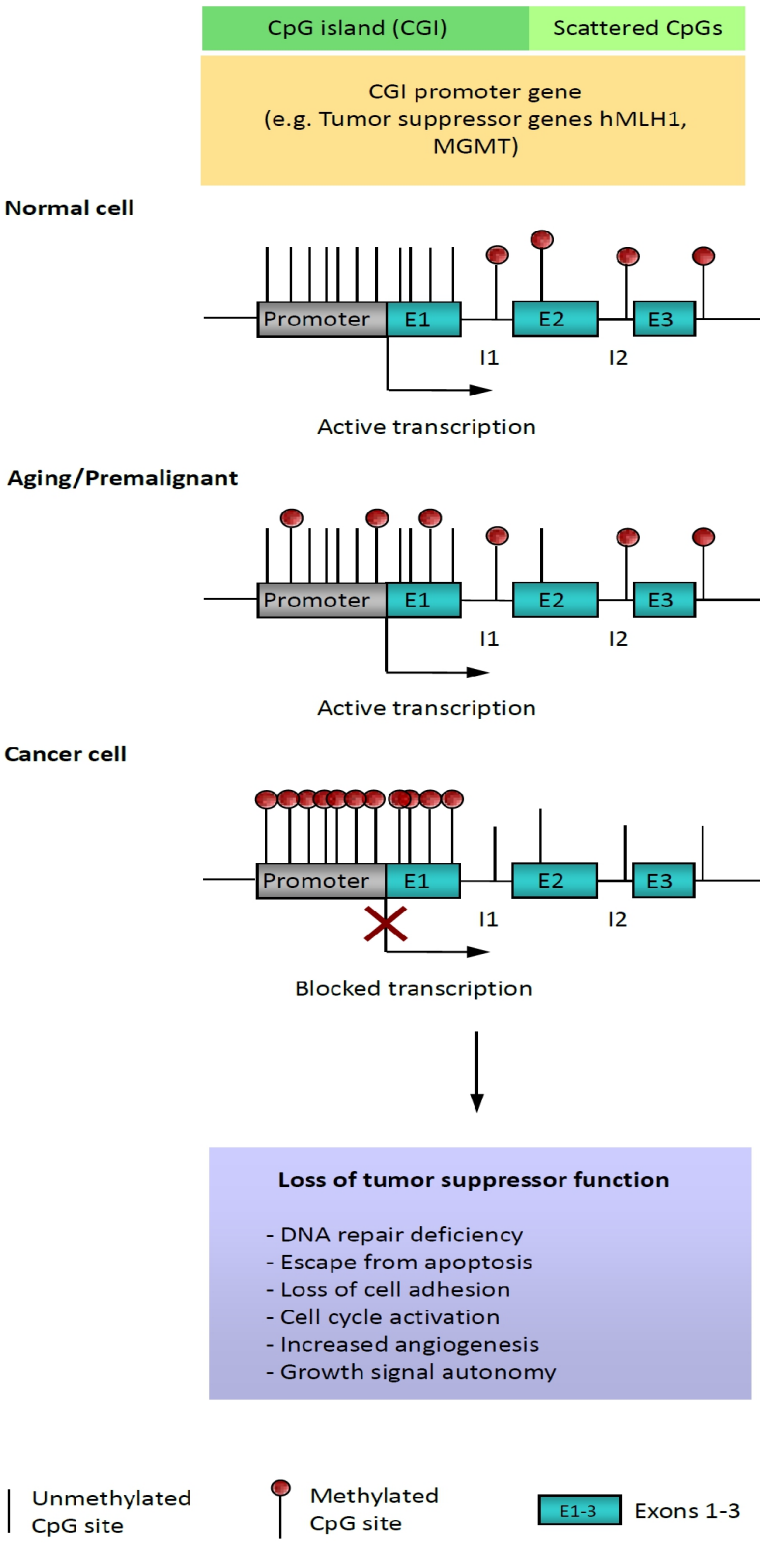

60% of genes contain dense clusters of CpG-dinucleotids in their promoters (CpG island=CGI), which regulate transcription. In a normal cell, the CGIs of tumor suppressor genes are unmethylated allowing the transcription of the gene. In ageing cells the CGI becomes progressively methylated by unknown mechanisms. Exceeding a critical level of methylation the transcription of the tumor suppressor gene is irreversibly blocked.

Illumina HumanWG-6 v3 Expression BeadChip: Illumina probe intensity data was processed by variance stabilization transformation (VST) using R/Bioconductor software (affy library), followed by quantile normalization. Significance of effects for probes was tested by in R/Bioconductor (limma library) using moderated t-test and the false discovery rate (fdr) method by the Benjamini and Hochberg for multiple testing correction. Probes were selected for significant change after 5'-Azacytidine/TSA treatment (p-value < 0.05) and a log factor change of > 0.3 to generate a list of 2758 probes with probability of false positives of less than 5% representing 2245 unique genes. **Illumina HumanMethylation27 BeadChip:** Sodium Bisulfite converted DNA was applied to a MIDI plate and analyzed by Infinium HumanMethylation27 bead chips (Illumina) allowing to survey genome-wide methylation including 27'578 CpG sites at single site resolution. Chip analysis was performed using background subtraction by Bead studio software (Illumina). Methylation status of every CpG site analyzed is expressed as relative level of methylation (β), and is calculated as the ratio of methylated-probe signal to total locus signal intensity in Beadstudio **(Beta value)**. 1701 probes fulfilled the criteria of unmethylated in blood (beta-value < 0.25) and ~10% higher methylation in cancer tissue compared to normal mucosa in both patients representing 1203 unique genes.

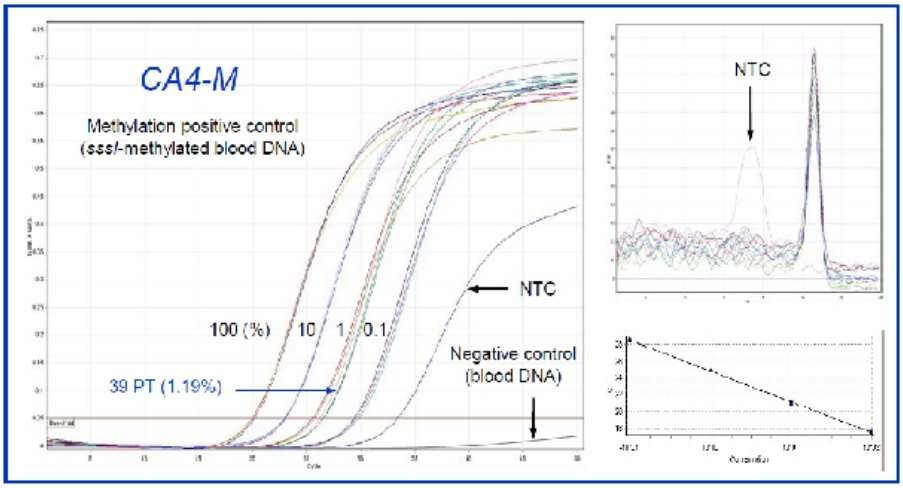

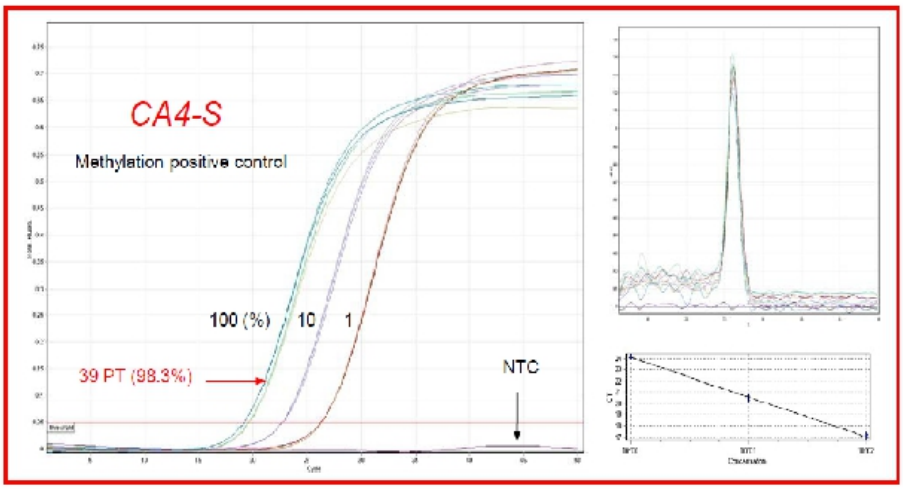

Example for calculation of the percentage of methylated alleles (PMA) in tumor DNA (39 PT):

M-primer amplification level % / S-primer amplification level % X 100 %

↓

1.19% / 98.3% X 100% = 1.21%

Drug treatment: The human microsatellite-instable CRC cell line SW48 was used for demethylating drug treatment with 5'-Aza-cytidine (DNA methyltransferase inhibitor) and/or Trichostatin A (Histone deacetylase inhibitor). After 24 h of culture the DMEM was replaced with medium containing 1 µM 5´-Aza-C or 0.5 µM TSA and incubated for five and two days, respectively. The medium was renewed every 24 h. For the double treatment, cells were initially treated with 5-Aza-cytidine followed by Trichostatin A treatment. The cells were harvested and the genomic DNA and total RNA were extracted with TRI REAGENT (Sigma).
Biological samples: Specimens from colorectal cancer patients and healthy subject were obtained from the Department of Surgery of the Kantonsspital Aarau, Switzerland. All patients gave their informed consent for the use of their tissue specimens for research purposes. Samples from 106 colorectal cancer patients were randomly collected on the occasion of the surgical therapy. From each patient two biopsies were taken, one from the primary tumor (CRC) and the other 7 cm proximal to the primary tumor from the adjacent macroscopically normal mucosa (= cancer-associated mucosa = CAM). Specimens from 31 healthy individuals were randomly collected in the context of a colonoscopy screening program in the cantonal hospital of Uri, Switzerland.
DNA extraction and bisulfite conversion: Genomic DNA from colorectal tissue as well as from human colorectal cancer cell lines was extracted with the QIAamp DNA mini kit (Qiagen). An RNAse A treatment was included in the protocol according to the manufacturer's protocol. Genomic DNA from blood samples was extracted with the NucleoSpin Blood L Kit (Macherey-Nagel). For methy-lation analysis 2 µg of the extracted DNA was sodium bisulfite converted using the EZ DNA Methylation Kit (Zymo).
Locus-normalized quantitative me-thylation specific PCR (In-qMSP): A standardizer primer set in proximity to the studied CpG site was introduced in order to normalize for DNA input after bisulfite conversion and for the investigated locus, thereby excluding ploidy aberration bias. For methylation quantification standard curves were generated by real time amplification of serial 1:10 dilutions (from 100 to 0.1% = Dynamic range) of M.sssI methylase and sodium bisulfite treated blood DNA with methylation-specific-(M) and the standardizer (S)-primers. The tester DNA was amplified by two separate real-time PCR runs with the M- and the S-primer set. The percentage of methylated alleles (PMA) was calculated by the ratio between the values of the amplification with the M- and the S-primer set **(see picture below)**.

Results

1. Experiment

Downregulated early in carcinogenesis

Affymetrix Human Genome U133 Plus 2.0: Transcriptome of 32 matched colorectal adenoma and normal mucosa tissues *
Criteria for targets:
Expression level < 91% of corresponding normal tissue in ≥ 30 adenomas (corresponding to change factor < -0.1)

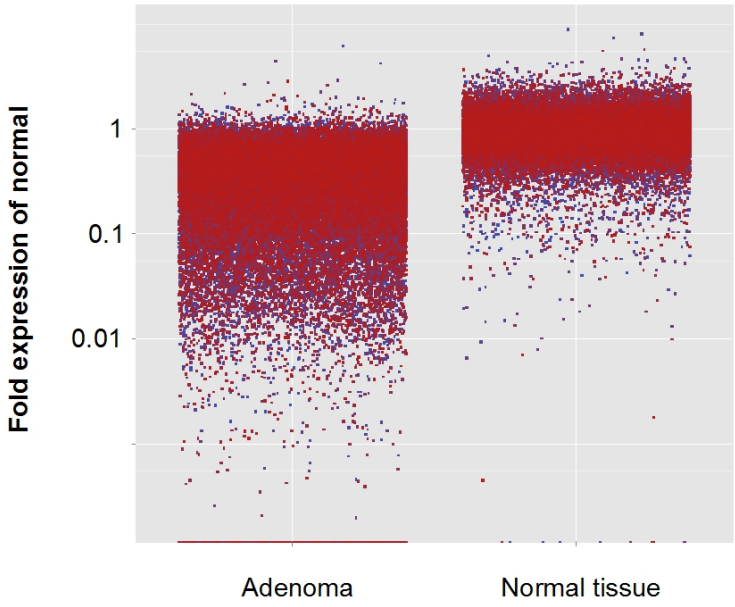

*Scatterplot of the probes of all 32 tissue pairs meeting the above criteria. * Sabates-Bellver, J. et al. (2007) Transcriptome profile of human colorectal adenomas. Mol Cancer Res, 5, 1263-1275.*

2. Experiment

DNA methylation dependent gene expression

Illumina HumanWG-6 v3 Expression BeadChip : Transcriptome of the SW48 colorectal cancer cell line displaying wide-spread DNA methylation before and after demethylating 5'-Azacytidine and/or Trichostatin A treatment
Criteria for targets:
Higher expression after treatment (p-value <0.05, Fdr adjusted, moderate t-test, and log factor change > 0.3)

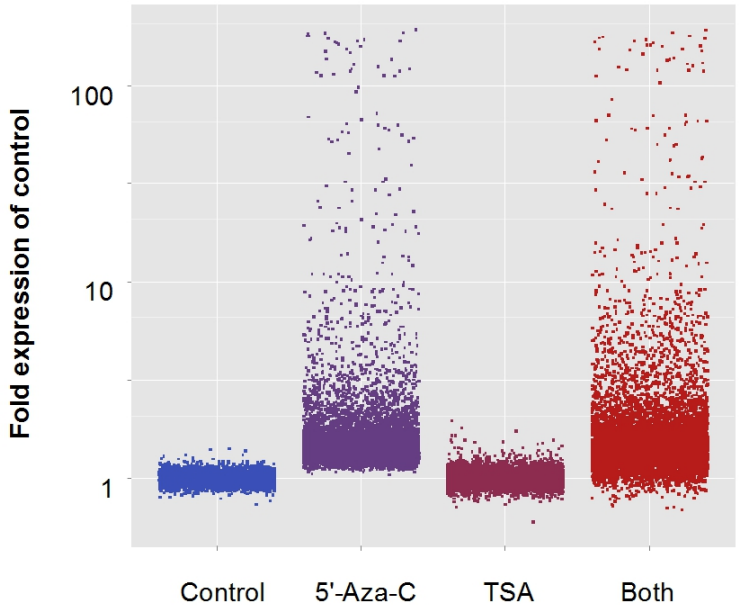

Scatterplot of the probes meeting the above criterium. 5'-Aza-C: 5'-Azacytidine; TSA: Trichostatin A; Fdr: false discovery rate.

3. Experiment

Hypermethylated in the primary cancer

Illumina HumanMethylation27 BeadChip:
Methylome of the matched colorectal cancer tissue (CRC), cancer-associated mucosa (CAM) and blood (B) from two patients
Criteria for targets:
Beta-value * < 0.25 in blood **and**
Beta-value > 0.1 higher in CRC than in CAM **and**
criteria must be fulfilled in both patients

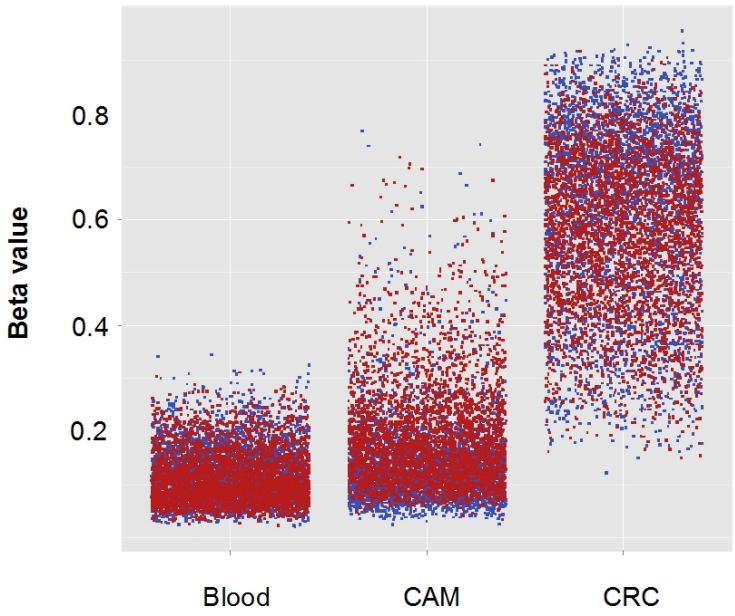

*Scatterplot of the probes meeting the above criteria. * Beta-value = Relative level of methylation (β), is calculated as the ratio of methylated-probe signal to total locus signal intensity (see methods).*

Integration of the three transcriptome and methylome experiments

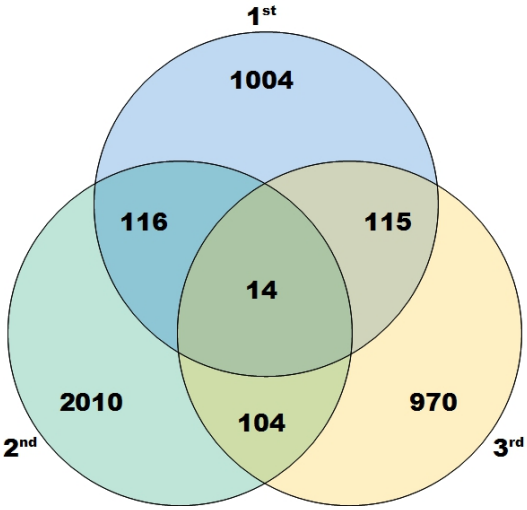

VENN Diagram of the resulting candidate genes. Numbers indicate "unique" genes after converting probes to genes.

Seven marker panel is sensitive in early colorectal neoplasia

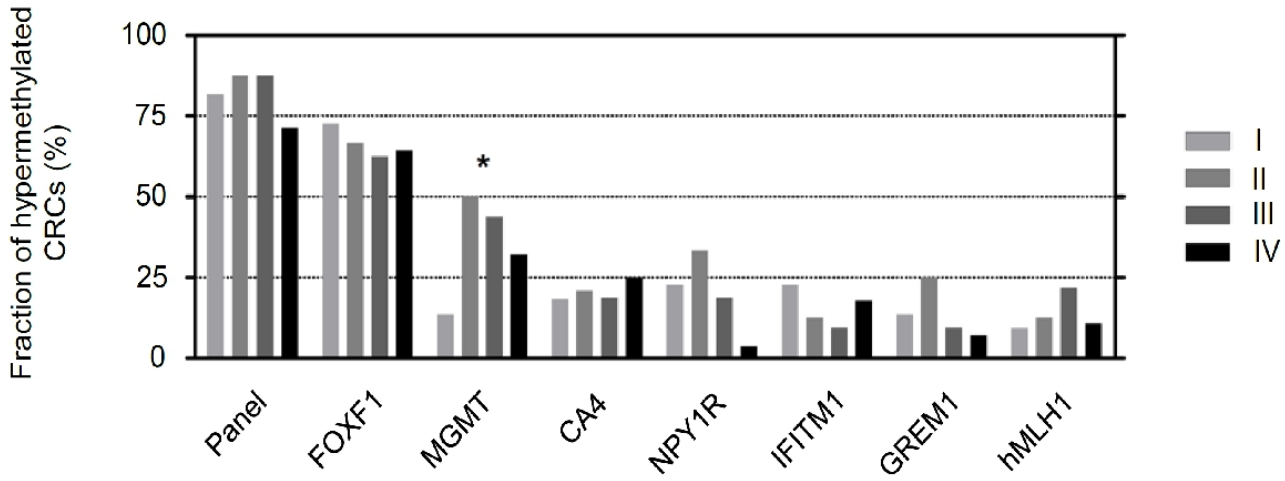

*Cancer sensitivity (frequency) of panel and targets in tumors of different stages of the disease (AJCC/UICC). Early stage I tumors are hypermethylated at the following frequencies: Panel 82%, FOXF1 73%. I: n=22; II: n = 24; III: n = 32; IV: n = 28. * p-value < 0.05 (Chi square-test).*

Resulting targets display low level methylation in normal colorectal tissue

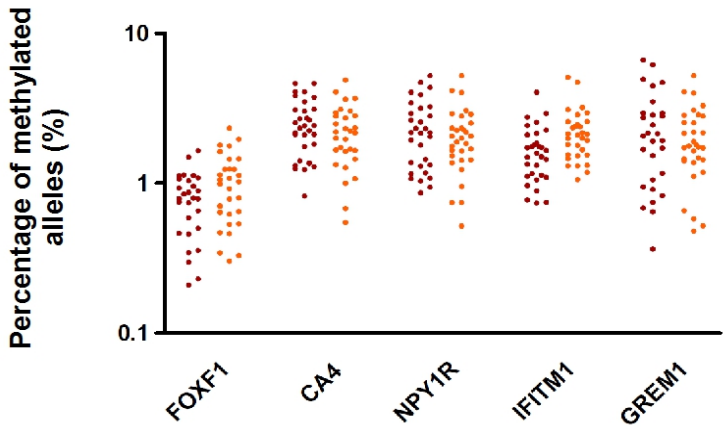

Scatterplot of the In-qMSP analyses of normal colorectal tissues from 31 healthy subjects taken from the right- and the left colonic side. Average target-specific tissue methylation ranges from 0.7 (FOXF1) to 2.8% (CA4).

Resulting targets are specifically hypermethylated in cancer

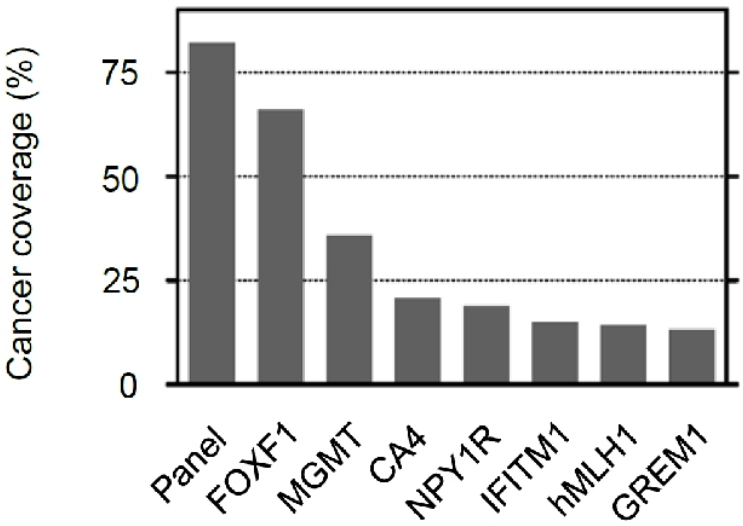

Cancer sensitivity (coverage) of panel and targets. 106 colorectal cancer tissues were hypermethylated at the following frequencies: Panel 82%, FOXF1 67%, MGMT 36%. n=106 cancer tissues.

Seven marker panel covers 82% of colorectal cancers

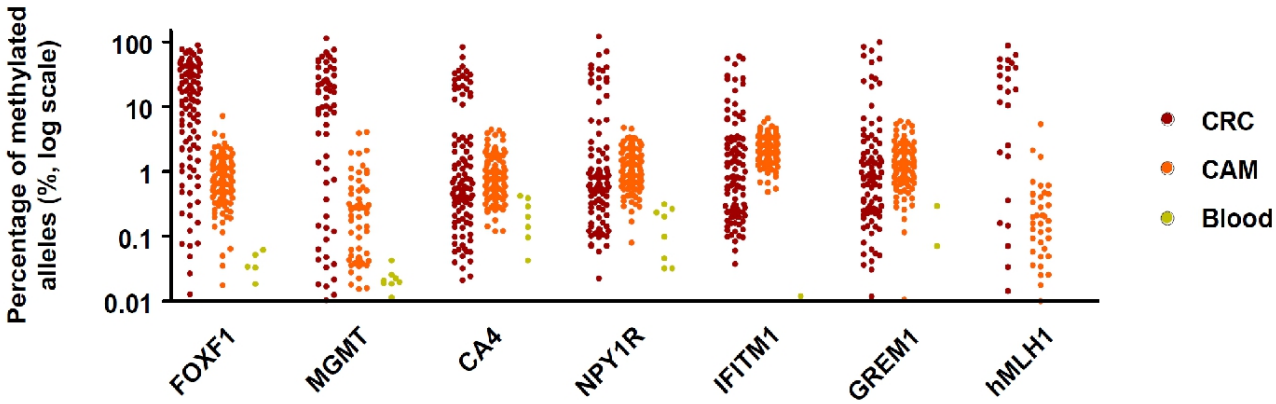

In-qMSP analyses of the colorectal cancer (CRC), cancer-associated mucosa tissue (CAM) and blood from 106 patients (n). The following cancer- and target-specific methylation cut-offs were defined at the 99% specificity level: FOXF1 4%, MGMT 5%, CA4 5%, NPY1R 5%, IFITM1 7%, GREM1 6.5%, hMLH1 6% (gray bar). Samples displaying methylation above these cut-offs were defined hypermethylated for the respective target.

Seven marker panel and FOXF1 are highly sensitive in right sided cancers

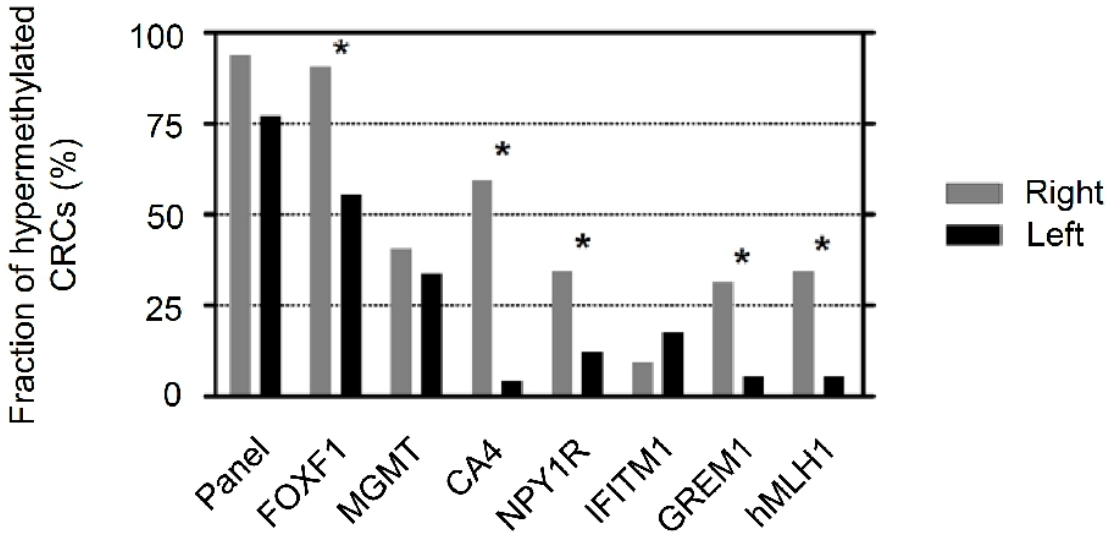

*Cancer sensitivity (frequency) of panel and targets in right- (n=32) and left-sided (n=74) colorectal cancer tissues. Right-sided tumors were hypermethylated at the following frequencies: Panel 94%, FOXF1 91%. *p-value < 0.05 (Fisher's exact test).*

Conclusions

The combination of genome-wide analyses of gene expression and DNA methylation in strategically matched samples is a powerful approach to identify DNA hypermethylation targets. In our case, this strategy led to the discovery of a panel of novel and potent markers of colorectal carcinogenesis. A diagnostic panel consisting of the five markers FOXF1, CA4, NPY1R, GREM1, IFITM1 and the well-known methylation targets MGMT and hMLH1 specifically detected 82% of all and 94% of right-sided colorectal cancers. All of the five targets identified by this comprehensive genome-wide approach displayed a low-level methylation (0.7-2.8% of alleles) in normal colorectal tissue from healthy subjects. Thus, cancer-specific DNA methylation is determined by levels rather than presence or absence.

Interferon-alpha induces reversible DNA demethylation of the IFITM3 core promoter in human melanoma cells

Rachel Scott[a], Fredy Siegrist[a], Stefan Foser[b] and Ulrich Certa[a]*

[a]*Department Non-clinical Safety, F. Hoffmann-La Roche AG, 4070 Basel (Switzerland)*

[b]*Clinical Biomarkers, F. Hoffmann-La Roche AG, 4070 Basel (Switzerland)*

Abbreviations: IFNα, interferon-alpha; TGFβ, tumor growth factor beta; IFITM3, interferon induced transmembrane protein 3; S100A2, small calcium protein S100A2; IGFBP3, insulin-like growth factor binding protein 3; DAC, 5'-aza-2'deoxycytidine

* corresponding author: Prof. Dr. Ulrich Certa, F. Hoffmann-La Roche Ltd., Postfach, CH-4070 Basel, Switzerland. Tel.: +41 61 687 53 40; fax +41 61 688 1448.
E-mail address: ulrich.certa@roche.com

Abstract

The IFNα response gene IFITM3 has antiproliferative properties in a number of biological systems. In the human melanoma cell line D10 IFITM3 is constitutively expressed and we show that the core promoter is significantly hypomethylated compared to ME15 cells where IFITM3 is tightly controlled. We demonstrate that treatment of ME15 cells with the demethylating agent 5'-aza-2'deoxycytidine (DAC) enhances IFITM3 expression following IFNα treatment. In a time course experiment, we show that IFNα induces demethylation of specific CpG sites of the IFITM3 core promoter 6 hours after stimulation and promoter methylation is precisely re-set to the naïve state 24 hours after stimulation. This cyclable modification of methylation requires co-stimulation with TGFβ or expression of the calcium binding protein S100A2 which are known co-factors for enhancement of antiproliferative activity in ME15 cells. Thus, the transcriptional response to IFNα can be enhanced by promoter demethylation of a subset of inducible genes such as IFITM3. This epigenetic modulation might be crucial to augment the immune response under critical conditions *in vivo*.

Key words. Interferon signaling, cytokine inducible DNA demethylation, cell proliferation

1. Introduction

Interferon was discovered 50 years ago as a host derived interference activity induced by heat inactivated viral particles (Isaacs and Lindenmann 1957). The advent of a novel technique termed “high performance liquid chromatography” enabled purification of interferon from virus infected leukocytes 20 years after its discovery (Rubinstein and others 1978). Cloning and recombinant expression of IFNα paved the way for the first protein based medicine (Maeda and others 1980). Since then, several additional interferons were discovered that are involved either in antiviral responses (type I) or play a role in immune defense (type II) (Stark and others 1998).

A hallmark of interferon type I activity is the induction of antiproliferative activity coupled to transcriptional activation of target genes. IFNα inducible genes are divided into primary and secondary response genes (PRG’s and SRG’s) according to their activation mode. PRG’s are induced early after cytokine stimulation and contain single or tandem interferon stimulated regulatory elements (ISRE’s) in the core promoter region whilst SRG’s lack such motifs and show delayed induction by an unknown mechanism. Microarray experiments have revealed, that IFNα resistance is associated with reduced but not defective transcriptional activity in human melanoma cell lines (Certa and others 2003). The exact mechanism of resistance in clinical settings like hepatitis C virus infections is still unclear and dependent on host and pathogen factors (Gale and Foy 2005; Mbow and Sarisky 2004).

We have shown, that co-stimulation of human melanoma cell lines with IFNα and TGFβ results in significant enhancement of anti-proliferative activity. In the resistant cell line D10, restoration of antiproliferative activity is associated with cooperative up-regulation of 28 genes (Foser and others 2006). In particular the small calcium binding protein S100A2 and the insulin-like growth factor binding protein 3 (IGFBP3) are important for cell cycle control as shown in stably transfected cell lines and the molecular mechanism is unknown. In IFNα sensitive cells like ME15, expression of IFITM3, a gene with antiproliferative activity is tightly controlled, and further up-regulation by TGFβ or S100A2 would provide a plausible explanation for increased antiproliferative activity. In D10 melanoma cells IFITM3 is constitutively expressed and further upregulated by IFNα treatment. The IFITM3 core promoter sequence in D10 and ME15 cells is identical and it was proposed that epigenetic DNA hypomethylation might be related to loss of control (Brem and others 2003).

Several studies link DNA methylation and IFNα signaling, e.g. senescence can be induced in the immortalized Li-Fraumeni syndrome cells by treatment with the DNA demethylating and DNA methyltransferase (DNMT) inhibitory agent 5’-aza-2’deoxycytidine (DAC) and interestingly IFNα treatment induces a similar effect in these cells (Fridman and others 2007). In mice, suppression of endogenous IFNs enhances development of metastases (Reid and others 1981) and microarray studies with DAC treated immortalized human cells revealed deregulation of a significant number of IFN pathway genes (Kulaeva and others 2003).

To study a possible role of DNA methylation as part of the promoter control system in IFNα signaling, we used ME15 and D10 cells and IFITM3 as model. We show that the methylation inhibiting agent 5- aza-2’-deoxycytidine (DAC) modifies IFITM3 expression levels in ME15 cells following IFNα stimulation whilst such a response is undetectable in D10 cells. In contrast to ME15 cells, the IFITM3 promoter is hypomethylated in D10 cells under naïve conditions. In a time course experiment we show that IFNα induces hypomethylation of the IFITM3 promoter in ME15 cells 6 hours after stimulation in the presence of the co-factors TGFβ or S100A2 and remarkably the system is re-set to the

naïve state 24 hours after stimulation. Microarray based mRNA profiling shows that only a small number of IFNα response genes are up-regulated like IFITM3 by co-stimulation in ME15 cells and gene expression in D10 cells is apparently not affected.

2. Material and Methods

2.1. Cell lines

The primary human melanoma cell lines D10 and ME15 were kindly supplied by Prof. Giulio Spagnioli (University of Basel) and have been described elsewhere (Luscher and others 1994; Pansky and others 2000). The S100A2 transgenic cell lines D10-5 and ME15-3 have been described by Foser et. al. (Brem and others 2003; Foser and others 2006; Luscher and others 1994; Pansky and others 2000).

2.2. Antibodies, cytokines and reagents

Antibody against IFITM3 (1-8U) has been described previously (Brem and others 2003). IFNα (IFNα2a, Roferon®-A) and its monopegylated isomer K134 ($IFN\alpha^{K134}$ (Foser and others 2006)) were provided by F. Hoffmann-La Roche Ltd. (Basel, Switzerland). TGFβ was purchased from Calobiochem (Germany) and 5- aza-2'-deoxycytidine (DAC) from Sigma (Basel, Switzerland).

2.3. Cell culture

All cell lines were cultured at 37°C in a 5% CO_2 atmosphere in RPMI 1640 medium (GIBCO Life Sciences, Paisley, U.K.) supplemented with 10% fetal bovine serum (FBS), L-glutamine (2 mM), sodium pyruvate (1 mM), nonessential amino acids, antibiotics, and 10 mM HEPES buffer (Certa and others 2003).

2.4. Cell treatments

For genome wide demethylation the cell lines were treated with 5- aza-2'-deoxycytidine (DAC) (2 μg/ml) or a control along with IFNα (1000 U/ml), TGFβ (1 ng/ml) or a combination of both cytokines with incubation times depicted in the figures 1 and 2. For the IFITM3 promoter methylation analysis D10, ME15, D10-5 and ME15-3 cells were stimulated with IFNα (1000 U/ml), TGFβ (2 ng/ml) or a combination of both cytokines with incubation times depicted in the figures 1 and 2. For oligonucleotide array analysis D10, ME15, D10-5 and ME15-3 melanoma cell lines were grown in triplicate cultures for 2 days stimulated with either $IFN\alpha^{K134}$ (1000 U/ml), TGFβ (2 ng/ml) or a combination of both cytokines (Fig. 3).

2.5. Oligonucleotide array analysis

Total RNA was isolated, processed and hybridized to Affymetrix U95Av2 human microarrays according to the manufacturer's instructions (for details see (Foser and others 2006)). After intensities were recorded by laser scanning normalized data was analyzed for differential expression using RACE-A software as described (Certa and others 2003). Genes with a standard deviation smaller than the absolute change in signal intensity as well as a signal intensity of a minimum of 50 RFUs were considered only with the absolute change factor (CHF) threshold set to 2 (Certa and others 2003). Expression data from untreated cells (D10, ME15, D10-5 and ME15-3) were used as baseline to calculate the change factor values. The raw data are available on request.

2.6. Immunoblotting

Total calibrated protein extracts, were separated by SDS PAGE and electroblotted

onto nitrocellulose membranes, which were blocked in commercial blocking buffer. Proteins were detected using 1st antibodies against IFITM3 at a dilution of 1:2000 and a horse-radish-peroxidase (HRP)-conjugated 2nd antibody diluted 1:5000 for detection with a chemiluminescent substrate (BCA Assay; SuperBlock® Blocking Buffer; SuperSignal West Pico Chemiluminescent; Pierce Chemical Co., Thermo Fisher Scientific Inc., Rockford, IL, USA; XCell SureLock™ System; Invitrogen, Basel, Switzerland).

2.7. DNA wide demethylation by 5- aza-2'-deoxycytidine (DAC) treatment

Approximately 10'000 ME15 cells and 20'000 D10, D10-5 and ME15-3 cells were seeded in 6-well plates. Cells were grown for three days following stimulation with TGFβ (1 ng/ml), IFNα (1000 U/ml) or a combination of both cytokines, in the presence or absence of DAC (2 μg/ml). After 6,12, 24 and 51 hours cells were washed twice with PBS, resuspended in standard lysis buffer and the whole protein extract was thereafter used for immunoblot analysis (Fig. 1A and 2A).

2.8. Promoter methylation analysis

D10, ME15 and ME15-3 melanoma cell lines were treated with IFNα (1000 U/ml) for 1, 6 and 24 hours. Cells were also pretreated with TGFβ (2 ng/ml) for 2 days. Isolated genomic DNA was bisulfite treated using the Zymo EZ DNA Methylation™ Kit (Orange, CA, USA) according to the manufactures protocol with 2μg of DNA input. The bottom strand of the IFITM3 promoter was amplified to yield an 820 bp fragment using bisulfite adjusted primers designed to cover 19 CpG sites adjacent to the translation initiation site (ATG). Note that ME15 cells have a SNP at site 422, therefore the analysis for the ME15 and ME15-3 cell lines covers 18 CpG sites. (forward primer (Chromosome 11: 311612) 5'-ATA ATC CAA CTA CCT AAA CAC CATA and backward primer (Chromosome 11: 310821) 5'- AT TTG TGG TAG TTA GTG TGA TAG GTT TGG) with the PCR program consisting of following parameters: initial incubation time of 10 minutes at 95°C, 40 cycles with 1 minute at 94°C, 1 minute at 58°C and 1 minute at 72°C and an additional 10 minutes at 72°C for final elongation. Amplified fragments were cloned into the pCR®2.1-TOPO® vector (Invitrogen, Basel, Switzerland) and transformed into XL1-blue (Stratagene, La Jolla, CA, USA) or TOP10 (Invitrogen, Basel, Switzerland) competent cells and plated on IPTG/ X-gal containing agar plates. Plasmids from white colonies were isolated and sequenced using an ABI 3730xl DNA analyzer instrument and generic vector based primers using standard procedures. Following computer assisted alignment with the clustalw GCG-program the methylation state of CpG sites was determined.

3. Results

3.1. Methylation state of the IFITM3 core promoter in D10 and ME15 cells

The interferon inducible transmembrane protein IFITM3 has antiproliferative activity in several biological system (Siegrist and others 2010). We have previously shown that the IFNα-resistant human melanoma cell line D10 expresses IFITM3 in the absence of IFNα stimulation whilst expression is tightly controlled in the responder line ME15. The IFITM3 core promoter sequences are identical in D10 and ME15 cells which led to the proposal that hypomethylation of the IFITM3 core promoter in D10 cells accounts for loss of interferon control (Brem and others 2003). Microarray studies with DAC treated cells show enhanced expression of several IFNα target genes suggesting that promoter methylation occurs in IFNα response genes (Kulaeva and others 2003). Resistance to interferon in renal carcinoma as well as melanoma cells can be overcome either by DAC therapy or by knock-down of the DNA methylase DNMT1 using antisense transfection (Reu and others

2006).

To analyze the methylation status of the IFITM3 promoter, we compared the induction of the IFITM3 protein in D10 and ME15 cells by IFNα or TGFβ or the combination of both in the presence or absence of the cytosine analog DAC as a generic DNA methylation inhibitor. Following treatment, cell lysates were analyzed by immunoblotting using polyclonal rabbit serum against IFITM3 as probe (Brem and others 2003). In D10 cells, neither DAC treatment nor incubation with TGFβ had a significant effect on IFITM3 expression but IFNα treatment upregulated the expression level as expected (Fig. 1A). In ME15 cells, DAC treatment extended the IFITM3 expression period to at least 51 hours and even unstimulated cells express low levels of IFITM3 at this time point (Fig. 1A; indicated by the asterix). Co-stimulation with TGFβ results in earlier onset of IFITM3 expression independent of DAC co-treatment (Fig. 1A). The insensitivity of the IFITM3 promoter to DAC treatment in D10 cells supports the proposal, that constitutive expression of IFITM3 in this cell line is indeed due to hypomethylation of the core promoter. Along the same lines, the increase of IFITM3 expression in the presence of DAC in ME15 cells suggests core promoter methylation in ME15 under naïve conditions. This model is strongly supported by bisulfite sequencing analysis of the IFITM3 core promoter in untreated ME15 and D10 cells (Frommer and others 1992). Genomic DNA was extracted from bisulfite treated cells and the core promoter was amplified by PCR followed by subcloning and sequencing of individual clones. Consistent with our model, the IFITM3 core promoter is clearly hypomethylated in D10 cells compared to ME15 cells in the native state in particular at residues close to the ATG codon (Fig. 1B). The fully hypomethylated CpG residue 107 next to the ISRE site is part of a consensus binding motif for the generic transcription factor Sp1 which allows IFNα independent transcription. To conclude, the data above strongly support the view that native hypomethylation of the IFITM3 promoter in D10 cells causes leakiness and constitutive expression. In ME15 cells, DAC treatment results in an increase of IFITM3 protein expression consistent with the demethylation of key residues.

3.2. Cyclable methylation of the IFITM3 core promoter in ME15 and ME15-3 cells

We next address the question, whether modulation of the IFITM3 core promoter methylation occurs *in vivo* in response to IFNα. It is expected that IFITM3 levels above the IFNα inducible threshold would further enhance the antiproliferative activity in ME15 cells which has been shown following co-stimulation with TGFβ (Foser and others 2006). Presuming a methylation based mechanism of IFITM3 up-regulation, we would expect that modification of the IFITM3 core promoter requires TGFβ stimulation as co-factor. ME15 cells were stimulated for 1, 6 and 24 hours with IFNα either with or without TGFβ co-stimulation. Following DNA extraction and bisulfite treatment the PCR amplicons were subcloned and the methylation status of individual clones was assessed by DNA sequencing with untreated cells as reference for the naive state (Fig. 2; top panel). The methylation pattern of the core promoter in the absence of TGFβ remains virtually stable. We noted minor demethylation of the IFITM3 core promoter at four CpG sites (392, 418, 425 and 427; Fig. 2). When TGFβ is present, significant hypomethylation across all CpG sites occurs specifically at the 6 hour time point which coincides with protein expression upon co-stimulation with both cytokines (Fig. 1A). After 24 hours the promoter is precisely set-back to the native state.

Interestingly enough, Foser and others (Foser and others 2006) have shown that stable expression of the TGFβ inducible calcium binding protein S100A2 is sufficient to enhance the antiproliferative activity of IFNα in ME15 cells. We stimulated the S100A2

stably transfected cell line ME15-3 with IFNα in the presence or absence of TGFβ in a time course experiment as above and determined the methylation state of the IFITM3 core-promoter. S100A2 as co-factor was indeed sufficient to induce cyclable changes in DNA methylation in response to IFNα in the absence of TGFβ with a very similar kinetic. Interestingly, the activity of TGFβ on promoter methylation at the 6 hour time point was suppressed presumably by S100A2 expression in ME15-3 cells. Treatment of D10 cells with DAC had no impact on the protein levels of IFITM3 (Fig. 1A) and we anticipated that IFNα stimulation would not affect the methylation pattern. We incubated D10 cells under the same conditions as above and examined the methylation pattern at each time point by sequencing (Fig. 2). In contrast to ME15 cells, we did not find any significant alterations in the methylation pattern of the IFITM3 promoter in D10 cells upon cytokine stimulation and the core promoter is not re-methylated after 24 hours in culture either. We conclude that IFNα can induce cyclable methylation of a target gene promoter.

3.3. Transcriptional responses to IFNα in the presence of S100A2

Having shown reversible demethylation of the IFITM3 promoter, we asked whether additional IFNα response genes are upregulated in ME15 cells expressing the co-factor S100A2 (ME15-3; (Foser and others 2006)). ME15 and ME15-3 cells were treated with pegylated IFNα (K134), TGFβ and the combination of both cytokines for 2 days followed by transcript profiling using Affymetrix U95Av2 microarrays. Untreated sample data were used to calculate treatment induced changes in gene expression (Fig. 3). This analysis revealed two clusters of IFNα response genes. Cluster 1 (CL1) contains genes with unaltered expression in ME15 and ME15-3 cells while genes in cluster 2 (CL2) are further upregulated beyond maximal IFNα inducible levels in ME15-3 cells including IFITM3 as expected. For clarity, the names and the calculated change factors for these genes are summarized in table 1 and the majority of these genes are bona fide IFNα response genes. As control, we also profiled D10 cells and a S100A2 overexpressing clone of this line (D10-5; (Foser and others 2006)) under the same experimental conditions. In contrast to ME15-3 we were not able to identify genes showing significant up-regulation in D10-5 (data not shown). We conclude that overexpression of the methylation co-factor S100A2 affects only a subset of interferon inducible genes suggesting functional significance.

4. Discussion

We have shown that expression of the IFNα inducible gene IFITM3 is controlled by DNA methylation of key residues in the core promoter. Constitutive expression of IFITM3 in D10 cells is most likely associated with extensive hypo-methylation of CpG sites close to the transcriptional start site (Fig. 1B). Interestingly this region contains a consensus binding motif for the transcription factor Sp1 which binds to promoter regions given their binding sites are demethylated (Zhu and others 2003). The insulin-like growth factor binding protein 3 (IGFBP3) for example inhibits the growth of non-small-cell lung cancer (NSCLC) cells by inducing apoptosis and expression is frequently abolished in cancers. It was shown, that IGFBP3 expression is controlled by CpG site methylation which inhibits binding of the transcription factor Sp1 (Chang and others 2004). Additional binding of the methyl CpG binding protein 2 (MeCP2) to the core promoter further suppresses Sp1 mediated transcription (Kudo 1998). Liu et al. showed that the Sp1 site in the IFITM3 core promoter region (Fig. 1B and 2, 5' CpG position # 107) is functional because removal by mutagenesis diminishes IFITM3 expression to about 50% (Liu and others 2002). Thus, the hypomethylation of CpG residue 107 in D10 cells apparently enables binding of Sp1 to the target sequence which provides a plausible explanation for constitutive IFITM3 expression in this cell line. We show in figure 1A that treatment of ME15 cells with the demethylating agent DAC augments IFITM3 expression following IFNα stimulation. We show by bisulfite sequencing that IFNα induces hypomethylation of the IFITM3 core promoter in the presence of TGFβ stimulation or expression of S100A2 as co-factor. This includes the Sp1 CpG site which is now accessible for Sp1 binding resulting in upregulation of IFITM3 transcription. 24 hours after stimulation the promoter is silenced and the methylation pattern is precisely reset to the naive state.

Mechanisms of dynamic, inducible CpG methylation have been shown previously. The trefoil factor 1 (TFF1) is a protein that is known to be under estrogen control and its promoter undergoes cyclical demethylation upon estrogen stimulation by recruitment of the *de novo* DNA methyltransferase 3a and 3b (DNMT3a and DNMT3b), thymine DNA glycosylase (TDG) and base excision repair (BER) proteins in a cell cycle independent manner (Kangaspeska and others 2008; Metivier and others 2008). The promoter of the inflammatory cytokine IL2 undergoes demethylation upon stimulation with PMA (phorbol 12-myristate 13-acetate) (Murayama and others 2006). The mechanism in this case involves intracellular calcium release, which results in translocation of the T-cell transcription factor NFAT from the cytoplasm to the nucleus and binding to the IL2 core promoter where a single CpG site of the promoter is hypomethylated. This leads to transition of the "naive state" to the "active state" and facilitates transcription by OCT1 1 hour after PMA stimulation. In contrast to IL2, the IFITM3 is inducible even in the presence of DNA methylation suggesting an open, accessible configuration of the ISRE for ISGF3 binding. It is interesting to note that evidence is arising that DNA repair enzymes as well as glycosylases might function as active demethylating agents in mammals as suggested for the GADD45 protein which is induced in our experimental system following IFNα and TGFβ stimulation (Foser and others 2006; Ma and others 2009a; Schmitz and others 2009).

We have shown previously, that IFNα induces significant and fast intracellular calcium release (Foser and others 2006). In neuronal cells it has been shown, that GADD45β promoted calcium sensitive demethylation of specific genes like BDNF or FGF (Ma and others 2009b). Interestingly, GADD45β is induced in hepatocellular carcinoma cells through promoter hypomethylation following growth arrest which resembles the state of our experimental system (Qiu and others 2004). Thus, it is possible that calcium

activated GADFD45β is involved in the demethylation of the IFITM3 core promoter. After 24 hours, the IFNα signaling has ceased and normal growth conditions may lead to faithful DNA methylation of the target CpG sites in the IFITM3 core promoter. This model can now be validated experimentally by siRNA knock-down of GADFD45β in IFNα induced ME15-3 cells. Further, resistance to IFNα in renal carcinoma as well as melanoma cells can be overcome either by DAC treatment or DNA methyltransferase (DNMT1) depletion by transfection of antisense oligonucleotides (Reu and others 2006). IFNα resistant HCV replicon harboring cells become sensitive to IFNα upon treatment with DAC (Naka and others 2006). Thus, modification of IFNα target gene expression through promoter methylation might be a natural mechanism to adapt the responses to pathogen challenge. The analysis of additional cell lines, target genes and model organisms is now granted for validation of cyclable IFNα mediated promoter methylation as an additional layer of gene expression control.

We have shown by microarray profiling of cytokine treated ME15 and ME15-3 cells, that only a small subset of *bona fide* IFNα inducible genes are further induced in ME15-3 cells (Fig. 3, cluster 2; table 1). Genes of the IFITM-family for instance control cell proliferation (for review see (Siegrist and others 2010)) and oligoadenylate synthase 1 and 2 are associated with antiviral responses (Table 1). Thus, further upregulation of such genes under critical conditions would augment the potency of IFNα defense responses. At this point we can only speculate whether upregulation of genes is related to promoter hypomethylation as shown for IFITM3. Expression of genes in cluster 1 is unaffected by TGFβ or S100A2 as co-factors and they show no obvious functional relation to host defense.

The functional significance of TGFβ signaling and S100A2 as co-factors for cyclable DNA methylation is unknown. We have previously shown that S100A2 and TGFβ signaling have marked impact on the proliferation of ME15 cells and the microarray analysis showed indeed overexpression of genes with antiproliferative properties such as IFITM3. The catalytic function of S100A2 and of the majority of calcium binding protein family members is unknown (Eckert and others 2004). In addition, S100A2 is located in the cytoplasm of ME15 cells, which eliminates to a large extent a direct role in transcription (R. Scott; unpublished data).

In conclusion, dynamic promoter methylation adds an additional layer of complexity to the IFNα signaling pathways and tight control of IFNα key response genes like IFITM3 might be required for comprehensive control of the IFNα response.

Acknowledgement

We are especially grateful to Dr. M. Browner and Dr. L. Burleigh for critical reading and editing of the manuscript prior to submission. Thanks go to all members of the Certa laboratory for support and stimulating discussions.

Author Disclosure Statement

No competing financial interests exist.

Literature

Brem R, Oraszlan-Szovik K, Foser S, Bohrmann B, Certa U. 2003. Inhibition of proliferation by 1-8U in interferon-alpha-responsive and non-responsive cell lines. Cell Mol Life Sci 60(6):1235-48.

Certa U, Wilhelm-Seiler M, Foser S, Broger C, Neeb M. 2003. Expression modes of interferon-alpha inducible genes in sensitive and resistant human melanoma cells stimulated with regular and pegylated interferon-alpha. Gene 315:79-86.

Chang YS, Wang L, Suh YA, Mao L, Karpen SJ, Khuri FR, Hong WK, Lee HY. 2004. Mechanisms underlying lack of insulin-like growth factor-binding protein-3 expression in non-small-cell lung cancer. Oncogene 23(39):6569-80.

Eckert RL, Broome AM, Ruse M, Robinson N, Ryan D, Lee K. 2004. S100 proteins in the epidermis. J Invest Dermatol 123(1):23-33.

Foser S, Redwanz I, Ebeling M, Heizmann CW, Certa U. 2006. Interferon-alpha and transforming growth factor-beta co-induce growth inhibition of human tumor cells. Cell Mol Life Sci 63(19-20):2387-96.

Fridman AL, Rosati R, Li Q, Tainsky MA. 2007. Epigenetic and functional analysis of IGFBP3 and IGFBPrP1 in cellular immortalization. Biochem Biophys Res Commun 357(3):785-91.

Frommer M, McDonald LE, Millar DS, Collis CM, Watt F, Grigg GW, Molloy PL, Paul CL. 1992. A genomic sequencing protocol that yields a positive display of 5-methylcytosine residues in individual DNA strands. Proc Natl Acad Sci U S A 89(5):1827-31.

Gale M, Jr., Foy EM. 2005. Evasion of intracellular host defence by hepatitis C virus. Nature 436(7053):939-45.

Isaacs A, Lindenmann J. 1957. Virus interference. I. The interferon. Proc R Soc Lond B Biol Sci 147(927):258-67.

Kangaspeska S, Stride B, Metivier R, Polycarpou-Schwarz M, Ibberson D, Carmouche RP, Benes V, Gannon F, Reid G. 2008. Transient cyclical methylation of promoter DNA. Nature 452(7183):112-5.

Kudo S. 1998. Methyl-CpG-binding protein MeCP2 represses Sp1-activated transcription of the human leukosialin gene when the promoter is methylated. Mol Cell Biol 18(9):5492-9.

Kulaeva OI, Draghici S, Tang L, Kraniak JM, Land SJ, Tainsky MA. 2003. Epigenetic silencing of multiple interferon pathway genes after cellular immortalization. Oncogene 22(26):4118-27.

Liu H, Kang H, Liu R, Chen X, Zhao K. 2002. Maximal induction of a subset of interferon target genes requires the chromatin-remodeling activity of the BAF complex. Mol Cell Biol 22(18):6471-9.

Luscher U, Filgueira L, Juretic A, Zuber M, Luscher NJ, Heberer M, Spagnoli GC. 1994. The pattern of cytokine gene expression in freshly excised human metastatic melanoma suggests a state of reversible anergy of tumor-infiltrating lymphocytes. Int J Cancer 57(4):612-9.

Ma DK, Guo JU, Ming GL, Song H. 2009a. DNA excision repair proteins and Gadd45 as molecular players for active DNA demethylation. Cell Cycle 8(10):1526-31.

Ma DK, Jang MH, Guo JU, Kitabatake Y, Chang ML, Pow-Anpongkul N, Flavell RA, Lu B, Ming GL, Song H. 2009b. Neuronal activity-induced Gadd45b promotes epigenetic DNA demethylation and adult neurogenesis. Science 323(5917):1074-7.

Maeda S, McCandliss R, Gross M, Sloma A, Familletti PC, Tabor JM, Evinger M, Levy WP, Pestka S. 1980. Construction and identification of bacterial plasmids containing

nucleotide sequence for human leukocyte interferon. Proc Natl Acad Sci U S A 77(12):7010-3.
Mbow ML, Sarisky RT. 2004. What is disrupting IFN-alpha's antiviral activity? Trends Biotechnol 22(8):395-9.
Metivier R, Gallais R, Tiffoche C, Le Peron C, Jurkowska RZ, Carmouche RP, Ibberson D, Barath P, Demay F, Reid G and others. 2008. Cyclical DNA methylation of a transcriptionally active promoter. Nature 452(7183):45-50.
Murayama A, Sakura K, Nakama M, Yasuzawa-Tanaka K, Fujita E, Tateishi Y, Wang Y, Ushijima T, Baba T, Shibuya K and others. 2006. A specific CpG site demethylation in the human interleukin 2 gene promoter is an epigenetic memory. Embo J 25(5):1081-92.
Naka K, Abe K, Takemoto K, Dansako H, Ikeda M, Shimotohno K, Kato N. 2006. Epigenetic silencing of interferon-inducible genes is implicated in interferon resistance of hepatitis C virus replicon-harboring cells. J Hepatol 44(5):869-78.
Pansky A, Hildebrand P, Fasler-Kan E, Baselgia L, Ketterer S, Beglinger C, Heim MH. 2000. Defective Jak-STAT signal transduction pathway in melanoma cells resistant to growth inhibition by interferon-alpha. Int J Cancer 85(5):720-5.
Qiu W, Zhou B, Zou H, Liu X, Chu PG, Lopez R, Shih J, Chung C, Yen Y. 2004. Hypermethylation of growth arrest DNA damage-inducible gene 45 beta promoter in human hepatocellular carcinoma. Am J Pathol 165(5):1689-99.
Reid LM, Minato N, Gresser I, Holland J, Kadish A, Bloom BR. 1981. Influence of anti-mouse interferon serum on the growth and metastasis of tumor cells persistently infected with virus and of human prostatic tumors in athymic nude mice. Proc Natl Acad Sci U S A 78(2):1171-5.
Reu FJ, Bae SI, Cherkassky L, Leaman DW, Lindner D, Beaulieu N, MacLeod AR, Borden EC. 2006. Overcoming resistance to interferon-induced apoptosis of renal carcinoma and melanoma cells by DNA demethylation. J Clin Oncol 24(23):3771-9.
Rubinstein M, Rubinstein S, Familletti PC, Gross MS, Miller RS, Waldman AA, Pestka S. 1978. Human leukocyte interferon purified to homogeneity. Science 202(4374):1289-90.
Schmitz KM, Schmitt N, Hoffmann-Rohrer U, Schafer A, Grummt I, Mayer C. 2009. TAF12 recruits Gadd45a and the nucleotide excision repair complex to the promoter of rRNA genes leading to active DNA demethylation. Mol Cell 33(3):344-53.
Siegrist F, Ebeling M, Certa U. 2010. The Small Interferon-Induced Transmembrane Genes and Proteins. J Interferon Cytokine Res.
Stark GR, Kerr IM, Williams BR, Silverman RH, Schreiber RD. 1998. How cells respond to interferons. Annu Rev Biochem 67:227-64.
Zhu WG, Srinivasan K, Dai Z, Duan W, Druhan LJ, Ding H, Yee L, Villalona-Calero MA, Plass C, Otterson GA. 2003. Methylation of adjacent CpG sites affects Sp1/Sp3 binding and activity in the p21(Cip1) promoter. Mol Cell Biol 23(12):4056-65.

Figure legends

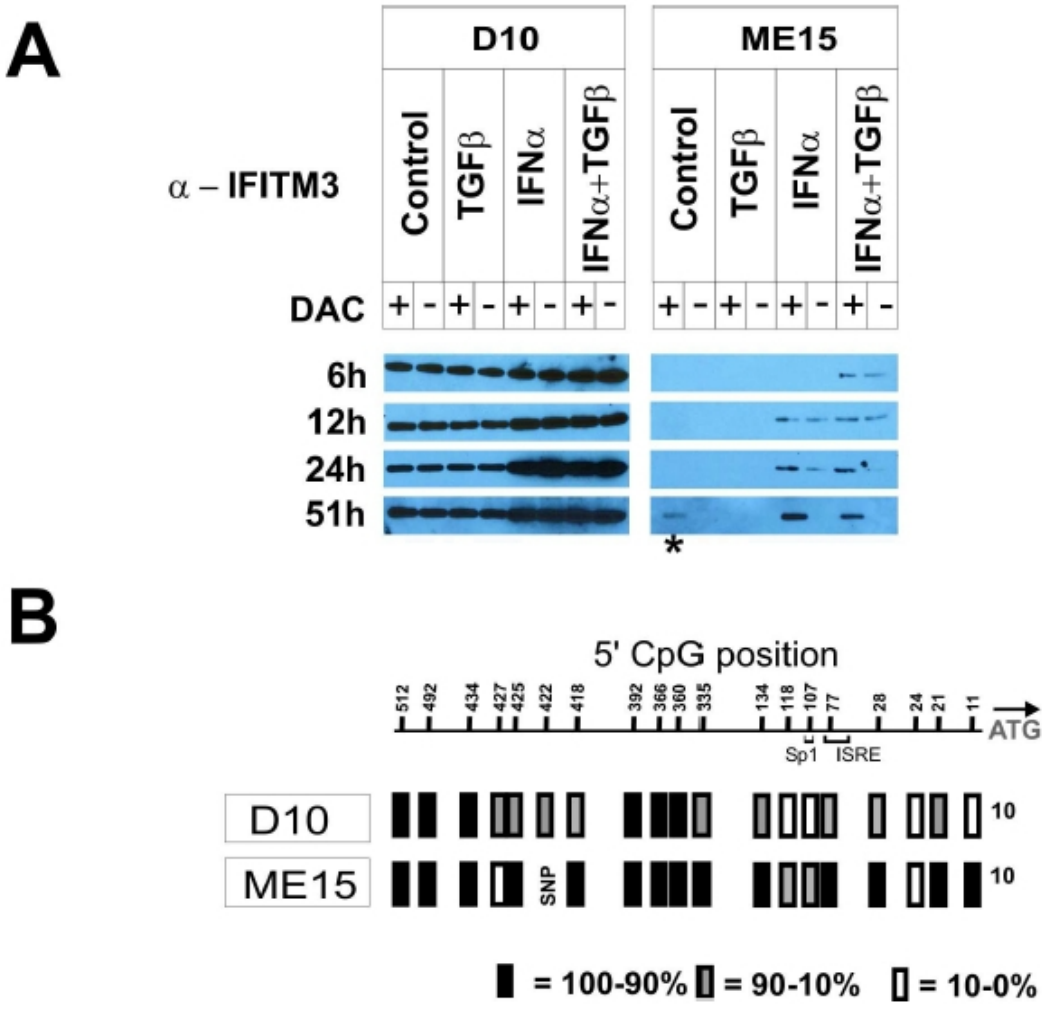

FIG. 1. IFNα-induced dynamic and reversible methylation of the IFITM3 core promoter. Impact of DAC (5'-aza-2'-deoxycytidine) treatment on the expression of IFITM3 in D10 and ME15 cell lines (*A)* treated with cytokines for 6, 12, 24 or 51 hours as indicated in the presence (DAC +) or absence (DAC -) of DAC. Detection of IFITM3 protein in DAC treated D10 and ME15 cells by immunoblotting. Cell lysates were electroblotted for each condition and probed with anti-IFITM3. D10 cells are not affected by DAC treatment. DAC treatment affects the IFITM3 levels in ME15 cells and low-level expression occurs 51 hours after DAC treatment without IFNα stimulation in ME15 (highlighted by a white asterisk in the left data panel).
IFITM3 core promoter methylation analysis (*B*). Total genomic DNA from D10 and ME15 cells was isolated, bisulfite treated and the IFITM3 core promoter was amplified using a bisulfite converted DNA adapted PCR protocol (for details see materials and methods). The amplicons were subcloned and sequenced from both ends using vector born primers. The number of clones sequenced per time point and treatment conditions is indicated on the right to the methylation status of individual CpG sites displayed as boxes. White filling indicates bisulfite conversion of individual CpG sites in at least nine out of ten clones (0-10% methylation). Grey indicates conversion of single CpG sites in two to eight per ten sequence reads(11-89% methylation) and black indicates conversion in one out of ten sequence reads (90-100% methylation). The nucleotide positions of the CpG sites upstream of the ATG start codon are indicated and the position of the ISRE consensus binding site as well as the Sp1 binding site is depicted. The CpG site 422 is a known SNP which is altered in our cell line ME15 (C→ T), therefore eliminating one methylation site from our investigation resulting in 18 CpG sites.

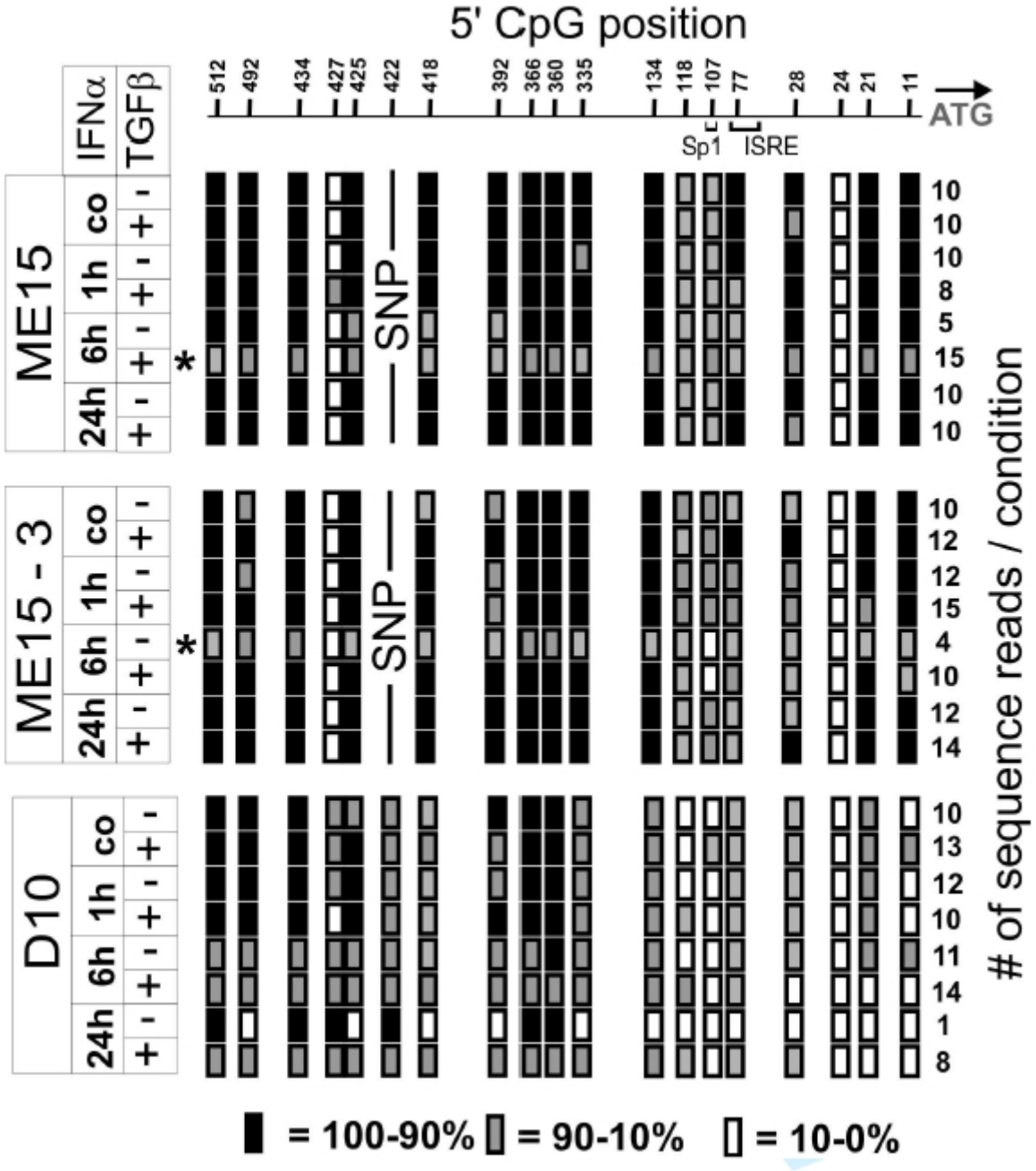

FIG. 2. IFNα-induced dynamic and reversible methylation of the IFITM3 core promoter. D10, ME15 and ME15-3 cells were cultured in the absence or presence of TGFβ. All cell lines were analyzed 0, 1, 6 and 24 hours after IFNα stimulus. Total genomic DNA from each culture was isolated, bisulfite treated and the IFITM3 core promoter was amplified using a bisulfite converted DNA adapted PCR protocol (for details see materials and methods). The amplicons were subcloned and sequenced from both ends using vector born primers. The number of clones sequenced per time point and treatment conditions is indicated on the right to the methylation status of individual CpG sites displayed as boxes. White filling indicates bisulfite conversion of individual CpG sites in at least nine out of ten clones (0-10% methylation). Grey indicates conversion of single CpG sites in two to eight per ten sequence reads(11-89% methylation) and black indicates conversion in one out of ten sequence reads (90-100% methylation). The nucleotide positions of the CpG sites upstream of the ATG start codon are indicated and the position of the ISRE consensus binding site as well as the Sp1 binding site is depicted.

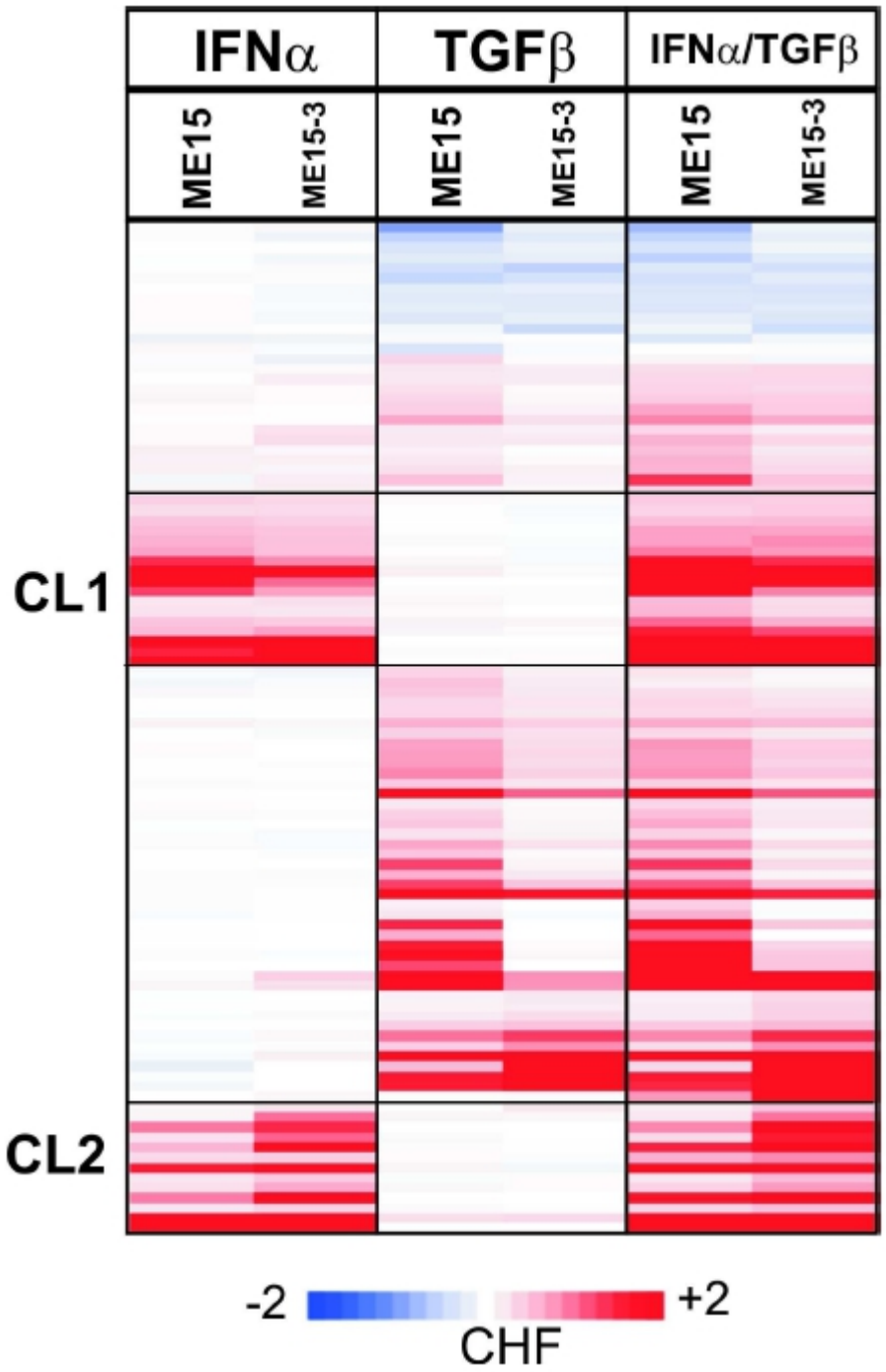

FIG. 3. S100A2 modulates expression efficiency of IFNα-inducible genes in ME15 cells. S100A2 modulates the transcription of selected IFNα target genes in ME15 cells (*A*). ME15 *wt* and ME15 recombinant *S100A2* (ME15-3) cell cultures were treated with $IFN\alpha^{K134}$, TGFβ or both cytokines for two days followed by RNA extraction and processing of the samples for microarray analysis and data processing. Downregulated genes are shown in blue and induced genes in red and maximum color intensity corresponds to a 2-fold change (CHF). IFNα-inducible genes with a common S100A2-dependent expression mode after IFNα induction in ME15 cells are boxed (cluster 2, CL2) and IFNα-inducible genes with no apparent S100A2 dependency appear in cluster 1 (CL1).

Table 1. Change factors of genes in clusters 1 and 2 (Fig. 3)

DESCRIPTION	SYMBOL	CHGF ME15 *wt*	CHGF ME15-3 *S100A2*
cluster 1			
beta-2-microglobulin	B2M	3.3	2.94
interferon-induced protein 35	IFI35	1.83	1.98
beta-2-microglobulin	B2M	2.93	2.51
beta-2-microglobulin	B2M	2.38	2.1
signal transducer and activator of transcription 1, 91kda	STAT1	3.72	3.07
signal transducer and activator of transcription 1, 91kda	STAT1	4.28	3.1
interferon-induced protein with tetratricopeptide repeats 1	IFIT1	11.78	6.35
signal transducer and activator of transcription 1, 91kda	STAT1	16.79	11.77
interferon-induced protein with tetratricopeptide repeats 1	IFIT1	8.59	5.27
ubiquitin-conjugating enzyme e2l 6	UBE2L6	7.78	4.42
lectin, galactoside-binding, soluble, 3 binding protein	LGALS3	1.4	1.71
major histocompatibility complex, class i, f	HLA-F	1.55	1.4
major histocompatibility complex, class i, f	HLA-F	2.96	2.57
major histocompatibility complex, class i, b	HLA-B	3.35	4.37
isg15 ubiquitin-like modifier	ISG15	14.84	14.17
interferon, alpha-inducible protein 6	IFI6	9.09	13.12
isg15 ubiquitin-like modifier	ISG15	18.43	22.7
cluster 2			
small proline-rich protein 2d	SPRR2D	0.5	1.37
dehydrogenase/reductase (sdr family) member 2	DHRS2	0.64	6.22
interferon-induced protein 44-like	IFI44L	5.89	8.86
interferon induced transmembrane protein 3 (1-8u)	IFITM3	1.6	6.52
interferon induced transmembrane protein 1 (9-27)	IFITM1	9.73	27.19
proteasome (prosome, macropain) subunit, beta type, 9	PSMB9	1.97	2.46
interferon induced transmembrane protein 1 (9-27)	IFITM1	3.62	19.79
interferon-induced protein 35	IFI35	1.43	2.69
interferon-stimulated transcription factor 3, gamma 48kda	IRF9	1.71	4.07
2`,5`-oligoadenylate synthetase 1, 40/46kda	OAS1	5.75	13.62
2`-5`-oligoadenylate synthetase 2, 69/71kda	OAS2	1.42	2.19
bone marrow stromal cell antigen 2	BST2	41.07	62.6
interferon, alpha-inducible protein 27	IFI27	65.94	111.36

Table 1. The calculated change factors for the interferon-induced genes in clusters 1 and 2 of figure 3 are shown together with the annotation and the official gene symbol. Change factors (CHF) were calculated as described in material and methodIntegrating transcriptome and epigenome analyses to identify DNA methylation changes associated with colorectal carcinogenesiss (section 2.5). ME15 *wt* refers to native cells and ME15-3 are cells stably transfected with S100A2 cDNA.

Embryonic Lethal Phenotype Reveals a Function of TDG in Maintaining Epigenetic Stability

Daniel Cortázar[1*], Christophe Kunz[1*], Jim Selfridge[2], Teresa Lettieri[3#**], Yusuke Saito[1**], Eilidh MacDougall[2], Annika Wirz[1], David Schuermann[1], Angelika Jacobs[1], Fredy Siegrist[4], Roland Steinacher[1##], Josef Jiricny[3], Adrian Bird[2] & Primo Schär[1§]

[1] Institute of Biochemistry and Genetics, Department of Biomedicine, University of Basel, Basel, Switzerland; [2] The Wellcome Trust Centre for Cell Biology, University of Edinburgh, Edinburgh, United Kingdom; [3] Institute of Molecular Cancer Research, University of Zürich, Zürich, Switzerland; [4] Pharmaceutical Research, Global Preclinical Safety, F. Hoffmann-La Roche Ltd., Basel, Switzerland

, These authors contributed equally to this work*

[§] Corresponding author: Primo Schär, Institute of Biochemistry and Genetics, Department of Biomedicine, University of Basel, Mattenstrasse 28, CH-4058 Basel, Switzerland. Phone: +41 61 267 0767; Fax: +41 61 267 3666; Mail: primo.schaer@unibas.ch

[#] Present address: European Commission, Joint Research Centre, Institute for Environment and Sustainability, Ispra, Italy

[##] Present address: Department of Biochemistry, University of Oxford, United Kingdom

TDG is a member of the uracil DNA glycosylase superfamily of DNA repair enzymes. Owing to its ability to excise thymine when mispaired with guanine, it was proposed to act against the mutability of 5-methylcytosine (5-mC) deamination in mammalian DNA [1]. However, TDG was also found to interact with transcription factors [2,3], histone actetyltransferases [4], and *de novo* DNA methyltransferases [5,6], and it has been associated with DNA demethylation in gene promoters following activation of transcription [7–9], altogether implicating an engagement in gene regulation rather than DNA repair. We pursued a mouse genetic approach to determine the biological function of this multifaceted DNA repair enzyme. We found that, unlike other DNA glycosylases, TDG is essential for embryonic development, and that this phenotype is associated with epigenetic aberrations affecting the expression of developmental genes. Fibroblasts derived from *Tgd* null embryos (MEFs) show impaired gene regulation, coincident with imbalanced histone modification and CpG methylation at promoters of affected genes. TDG associates with the promoters of such genes both in fibroblasts and in embryonic stem cells, but epigenetic aberrations only appear upon cell lineage commitment. We show that TDG contributes to the maintenance of active and bivalent chromatin throughout cell differentiation, facilitating a proper assembly of chromatin-modifying complexes and initiating base excision repair to counter aberrant *de novo* methylation. We thus conclude that TDG-dependent DNA repair has evolved to provide epigenetic stability in lineage committed cells.

TDG is one of four enzymes with uracil DNA glycosylase (UDG) activity in mammalian cells, but its biological function has remained enigmatic [10]. We thus set out to generate and phenotypically investigate a *Tdg* knockout mouse (Supplementary Fig. 1a-c). ESC clones carrying the targeted allele gave rise to healthy heterozygous *Tdg* knockout mice but attempts to generate homozygous null mutants failed, indicating that TDG-deficiency may cause embryonic lethality. This was unexpected, given the generally mild phenotype of other DNA glycosylase knockouts [11]. In timed matings, *Tdg* null embryos isolated up to day E10.5 appeared alive and normal, whereas those isolated at E12.5 were dead, and none were detectable at E16.5 (Fig. 1a, Supplementary Fig. 1d). *Tdg* null embryos at E10.5 produced viable fibroblasts (MEFs) but only a third of E11.5 embryos did so, suggesting that by this stage the majority of them was dead. We thus concluded that lethality in *Tdg* null embryos occurs around E11.5. With regard to the actual cause of lethality, closer examination of the *Tdg* null embryos at E10.5 indicated internal haemorrhage, and evidence for haemorrhagic necrosis (data not shown), but did not reveal an informative pathology otherwise.

We then explored the essential function of TDG in MEFs and ESCs, first addressing a potential DNA repair defect by classical genotoxicity and mutator analyses. The TDG status did not affect cell survival following ionizing radiation or H_2O_2 exposure, both of which induce DNA base lesions processed by TDG *in vitro* [10], nor did it affect mutation frequencies in a Big Blue® transgenic mutation assay (Supplementary Fig. 2). We therefore concluded that the role of TDG in the repair of canonical base damage is minor and therefore unlikely to account for its essential function in mouse embryogenesis.

We next investigated a possible involvement of TDG in gene regulation by expression profiling of TDG proficient and deficient MEFs. To limit potential clonal biases, we compared the transcriptomes of early passages of litter-matched populations of SV40 immortalized MEFs. This identified 461 differentially transcribed genes ($p \leq 0.05$, $FC \geq 1.5$, Fig. 1b), comprising many transcription factors and, thus, likely reflecting both direct and indirect consequences of TDG loss. Global pathway analyses revealed gene networks associated with embryogenesis and development as being most significantly misregulated in the absence of TDG (Supplementary Fig. 3a). Four out of six target genes analyzed showed TDG-dependent differential expression also in independently isolated primary MEF (Supplementary Fig. 3b).

Considering its putative involvement in DNA demethylation [7–9], we next investigated a possible occurrence of aberrant promoter methylation in TDG deficient cells. We examined the CpG islands (CGIs) in the promoters of *Hoxa10, Hoxd13*, *Sfrp2, Twist2,* and *Rarb,* all of which were downregulated in TDG deficient MEFs (Fig. 1b, Supplementary Fig. 3a). These genes are developmentally regulated by the polycomb repressive system [12] and their promoter CGIs are unmethylated in most normal tissues but subject to aberrant *de novo* methylated in human cancers [13,14]. Na-bisulfite sequencing of the respective CGIs revealed an increased occurrence of *de novo* methylation in the TDG deficient MEFs (Fig. 1c, Supplementary Fig. 4, 5a). The patterns and frequency of these methylation events indicated that the loss of TDG generates hotspots of *de novo* methylation in certain gene promoters. We then used chromatin-immunoprecipitation (ChIP) to examine a possible association of TDG with the promoters of these and additional differentially expressed genes. Compared to a randomly chosen intergenic sequence or the silent promoters of *Oct4* and *Tuba3*, DNA fragments surrounding the promoters of all genes examined were significantly enriched in the TDG-precipitates (Fig. 1d). This indicated that TDG is targeted to specific gene promoters, possibly to protect them from acquiring aberrant CpG methylation and eventual epigenetic silencing. Consistently, further examination of the chromatin status revealed a general loss of activating (H3K4me2) and a concomitant increase of repressive histone marks (H3K27me3, H3K9me3) in TDG deficient cells with

promoter-specific scenarios (Fig. 1e): A complete loss of H3K4 dimethylation was accompanied by a strong increase of H3K27 and/or H3K9 trimethylation at the *Hoxd13* and *Hoxa10* promoters; a partial reduction of H3K4me2 coincided with an enrichment of H3K27me3 but not H3K9me3 at the *Sfrp2* and *Twist2* promoters; and reduction of H3K4me2 was coupled with an increase in H3K9me3 but not H3K27me3 at the *Rarb* promoter. Thus, promoter *de novo* methylation in TDG deficient cells is associated with a loss of H3K4 dimethylation and a concomitant increase in trimethylation of H3K27 more than H3K9.

Stable expression of a *Tdg* encoding cDNA in *Tdg*$^{-/-}$ MEFs (Supplementary Fig. 1f) restored activity to the *Sfrp2 and Twist2* genes (Fig. 2a). This correlated with a loss of H3K27 trimethylation in their promoters and an increase in H3K4 dimethylation in the case of *Twist2* (Fig. 3b). Expression of *Hoxd13* and *Hoxa10*, however, was not restored although a partial reduction of H3K27 trimethylation also occurred. This indicated that, once H3K4 methylation is lost (*Hoxd13, Hoxa10*), the repressive chromatin maintained by H3K9 and H3K27 methylation and aberrant CpG methylation cannot be reversed to an active state by re-expression of *Tdg*. If residual H3K4 methylation is present, however, promoter reactivation is possible, and this requires the catalytic function of TDG [15] as shown for *Sfrp2* and *Twist2* (Fig. 2a).

To address the origin of the epigenetic aberrations in *Tdg* null MEFs, we investigated gene expression and chromatin states in TDG proficient and deficient ESCs before and after retinoic acid (RA) induced *in vitro* differentiation to neuronal progenitor cells (NPs) [16] (Supplementary Fig. 6a). Strikingly, gene expression differences were minor in ESCs (16 genes, $p \leq 0.05$, FC ≥ 1.5) but increased significantly upon differentiation to NPs (297 genes, $p \leq 0.05$, FC ≥ 1.5) (Fig. 3a). This was not due to an inability of TDG deficient ESCs to transcriptionally respond to RA (Supplementary Fig. 6b), although they showed somewhat faster kinetics of silencing pluripotency genes (*Oct4*, *Nanog*) and activating developmental genes (e.g. *Gata6, Pax6*) (Supplementary Fig. 6c). Similar to the situation in MEFs, the genes most significantly misregulated in TDG deficient NPs control developmental functions, most of them having CGIs in their promoters and being targets of the polycomb repressive system (Supplementary Fig. 7a). Using ChIP, we confirmed an enrichment of TDG at the promoters of differentially expressed genes both in ESCs and in NPs (Fig. 3b). This also revealed that TDG associates with the promoters of *Oct4* and *Nanog* in ESCs but not in NPs and MEFs (Fig. 3b, Supplementary Fig. 6d), suggesting that its interaction is lost upon heterochromatinization of these promoters. Notably, the inability to associate with heterochromatized promoters may explain why re-expression of TDG in *Tdg* null MEFs failed to restore *Hoxd13 and Hoxa10* transcription (Fig. 2).

Next, we examined the status of CpG methylation in gene promoters down-regulated in TDG deficient NPs, making use of Na-bisulfite (pyro)sequencing and methylated DNA-immunoprecipitation (MeDIP). While MeDIP only detected trends for methylation differences at specific promoters (Supplementary Fig.7b, unpublished data), pyrosequencing revealed significantly increased DNA methylation in *Tdg* null NPs at three out of five gene promoters tested (*Hoxa10*, *Pax6*, *Tgfb2)*. Notably, these methylation differences were not present in ESCs nor in freshly dissociated embryonic bodies, they arose within 48 hours of cultivation of the NPs in progenitor medium (Fig 3c, Supplementary Fig. 7c), and the phenotype was complemented by ectopic expression of *Tdg* during NP differentiation. Similarly, histone methylation marks were not different between TDG proficient and deficient ESCs but arose in NPs with an enrichment of H3K27me3 at the promoters of *Hoxd13, Hoxa10* (Supplementary Fig. 8) and *Pdgfra* (unpublished data). Thus, differences in DNA methylation and histone modifications became apparent at the NP stage but were not as pronounced as in MEFs, indicating an epigenetic phenotype that may progress upon further differentiation and/or cultivation.

Consistently, attempts to differentiate TDG deficient NPs to terminal neurons failed because of a rapid loss of cell viability in neuronal rich medium.

We then wondered whether this epigenetic function of TDG involves active DNA repair as implicated by the inability of a catalytic-dead TDG (N151A) to complement the loss of *Sfrp2* and *Twist2* expression in *Tdg* null MEFs (Fig. 2). To monitor a possible engagement of downstream base excision repair (BER), we first performed ChIP for XRCC1 [17]. This revealed a specific, TDG-dependent enrichment of this critical BER protein at the *Hoxd13*, *Hoxa10*, *Sfrp2* and *Twist2* promoters in MEFs but not in ESCs (Fig. 4a, Supplementary Fig. 5b). Hence, in MEFs, where TDG helps maintain these promoters in an active state, its presence correlates with an enrichment of XRCC1. In ESCs, however, where TDG also associates with these promoters but does not affect their chromatin status, XRCC1 enrichment is not observed. Besides XRCC1, we also found APE1, another component of BER, to associate with these promoters in a TDG dependent manner in MEFs (Fig. 4a). Moreover, RA treatment of ESCs for 8 hours increased the number of chromatin-associated XRCC1 foci in the presence but not in the absence of TDG (Supplementary Fig. 9), and TDG proficient cells were significantly more sensitive to PARP inhibition than TDG deficient cells upon RA-induced differentiation (Supplementary Fig. 10). These observations strongly suggest that cell differentiation-induced TDG activity feeds into PARP and XRCC1-dependent DNA single-strand break repair [18].

Addressing the phenotype on histone modifications, we then found by ChIP that the absence of TDG also compromises the association of the H3K4-specific methyl-transferase MLL1 with the promoters of *Hoxd13, Hoxa10, Sfrp2*, and *Twist2* (Fig. 4b). This was apparent in TDG deficient MEFs but not in ESCs, with the former indeed showing a loss of H3K4 methylation and an occurrence of aberrant CpG methylation at gene promoters reminiscent of the phenotype of MLL defects [19–21]. Similar to MLL, the binding of CBP/p300 to these promoters was significantly reduced in the *Tdg* null MEFs (Fig. 4b). CBP/p300 is a transcription activating histone acetyl transferase known to interact with TDG [4] and, notably, its association with gene promoters has been reported to protect from polycomb mediated H3K27 trimethylation [22].

Taken together, our data suggest structural and catalytic functions of TDG in epigenetic maintenance (Fig. 4c). As a structural component, TDG complexes with activating histone modifiers (e.g. MLL, CBP/p300) to maintain states of active (H3K4me2) and bivalent (H3K4me2, H3K27me3) chromatin during cell differentiation. In the absence of TDG, the assembly and function of such complexes is distorted and, consequently, chromatin modifications imbalanced towards repressive states. TDG also provides DNA repair capacity to locally erase CpG methylation. Aberrant methylation arises at GC-rich promoters in TDG deficient cells following lineage commitment, and the frequencies and patterns of these events indicate an underlying stochastic process of *de novo* methylation. Hence, TDG keeps *de novo* DNMT activities in check to avoid erroneous methylation, and the engagement of XRCC1 and APE1 suggests that it operates through BER. A number of previous studies have implicated TDG in active DNA demethylation [8,9,23]. Mechanistically, it may do so on its own acting as a 5-mC DNA glycosylase [23], or it may cooperate with a 5-mC deaminase (e.g. AID/Apobec [24,25] or DNMTs [8]), or a 5-mC hydroxylase (e.g. TET1 [26,27]) that would convert 5-mC into a favourable substrate for TDG. Numerous efforts to reproduce 5-mC glycosylase activity for mouse and human TDG have failed (Supplementary Fig. 11, unpublished data). We therefore consider a deamination or hydroxylation-mediated, TDG-dependent repair process a preferable scenario for active cytosine demethylation. The mouse *Tdg* knockout phenotype shows that such an epigenetic control system has evolved to protect critical DNA sequences from *de novo* methylation and heterochromatinization during development.

Methods Summary

***Tdg* knockout mouse and cell lines**. The *Tdg*-targeting construct (Supplementary Fig. 1) was generated by replacement of a *Nar*I – *Pac*I fragment enclosing Exons 6 and 7 by a neomycin resistance cassette in a cloned fragment spanning Exons 5 to 10 of the *Tdg* locus. This construct was used to target the *Tdg* allele in 129 mouse ESCs, which were then used to generate chimera and, ultimately, $Tdg^{+/-}$ heterozygotes by backcrossing to C57BL/6. The generation and establishment of MEF's and $Tdg^{-/-}$ ESCs was previously described [28].

In vitro differentiation. *In vitro* differentiation of ESCs was performed essentially according to the protocol published in ref. 16. RNA isolation for transcriptome analysis of MEF's or ESCs and NPs was performed using the RNeasy Mini Kit (Qiagen) or the Trizol reagent (Invitrogen), respectively. Antibodies and sequences of oligonucleotides used for RT-PCR, bisulfite sequencing and ChIP analysis are listed in Supplementary Tables 1-4.

Full methods and associated references are available in the online version of the paper at www.nature.com/nature

1. Gallinari, P. & Jiricny, J. A new class of uracil-DNA glycosylases related to human thymine-DNA glycosylase. Nature 383, 735-738 (1996).
2. Um, S. et al. Retinoic acid receptors interact physically and functionally with the T:G mismatch-specific thymine-DNA glycosylase. J. Biol. Chem. 273, 20728-20736 (1998).
3. Chen, D. et al. T:G mismatch-specific thymine-DNA glycosylase potentiates transcription of estrogen-regulated genes through direct interaction with estrogen receptor alpha. J. Biol. Chem. 278, 38586-38592 (2003).
4. Tini, M. et al. Association of CBP/p300 acetylase and thymine DNA glycosylase links DNA repair and transcription. Mol Cell 9, 265-277 (2002).
5. Li, Y. Q., Zhou, P. Z., Zheng, X. D., Walsh, C. P. & Xu, G. L. Association of Dnmt3a and thymine DNA glycosylase links DNA methylation with base-excision repair. Nucleic Acids Res. 35, 390-400 (2007).
6. Gallais, R. et al. Deoxyribonucleic acid methyl transferases 3a and 3b associate with the nuclear orphan receptor COUP-TFI during gene activation. Mol. Endocrinol. 21, 2085-2098 (2007).
7. Zhu, B. et al. Overexpression of 5-methylcytosine DNA glycosylase in human embryonic kidney cells EcR293 demethylates the promoter of a hormone-regulated reporter gene. Proc. Natl. Acad. Sci. U. S. A. 98, 5031-506. (2001).
8. Metivier, R. et al. Cyclical DNA methylation of a transcriptionally active promoter. Nature 452, 45-50 (2008).
9. Kangaspeska, S. et al. Transient cyclical methylation of promoter DNA. Nature 452, 112-115 (2008).
10. Cortazar, D., Kunz, C., Saito, Y., Steinacher, R. & Schär, P. The enigmatic thymine DNA glycosylase. DNA Repair (Amst) 6, 489-504 (2007).
11. Robertson, A. B., Klungland, A., Rognes, T. & Leiros, I. DNA repair in mammalian cells: Base excision repair: the long and short of it. Cell Mol Life Sci 66, 981-993 (2009).
12. Boyer, L. A. et al. Polycomb complexes repress developmental regulators in murine embryonic stem cells. Nature 441, 349-353 (2006).
13. Furuta, J. et al. Silencing of Peroxiredoxin 2 and aberrant methylation of 33 CpG islands in putative promoter regions in human malignant melanomas. Cancer Res. 66, 6080-6086 (2006).
14. Cheng, Y. Y. et al. Frequent epigenetic inactivation of secreted frizzled-related protein 2 (SFRP2) by promoter methylation in human gastric cancer. Br. J. Cancer 97, 895-901 (2007).
15. Hardeland, U., Bentele, M., Jiricny, J. & Schär, P. Separating substrate recognition from base hydrolysis in human thymine DNA glycosylase by mutational analysis. J. Biol. Chem. 275, 33449-33456 (2000).
16. Bibel, M., Richter, J., Lacroix, E. & Barde, Y. A. Generation of a defined and uniform population of CNS progenitors and neurons from mouse embryonic stem cells. Nat Protoc 2, 1034-1043 (2007).
17. Caldecott, K. W. XRCC1 and DNA strand break repair. DNA Repair (Amst) 2, 955-969 (2003).
18. Bryant, H. E. et al. Specific killing of BRCA2-deficient tumours with inhibitors of poly(ADP-ribose) polymerase. Nature 434, 913-917 (2005).
19. Yu, B. D., Hanson, R. D., Hess, J. L., Horning, S. E. & Korsmeyer, S. J. MLL, a mammalian trithorax-group gene, functions as a transcriptional maintenance factor in morphogenesis. Proc. Natl. Acad. Sci. U. S. A. 95, 10632-10636 (1998).
20. Erfurth, F. E. et al. MLL protects CpG clusters from methylation within the Hoxa9 gene, maintaining transcript expression. Proc. Natl. Acad. Sci. U. S. A. 105, 7517-7522 (2008).

21. Wang, P. et al. Global analysis of H3K4 methylation defines MLL family member targets and points to a role for MLL1-mediated H3K4 methylation in the regulation of transcriptional initiation by RNA polymerase II. Mol. Cell. Biol. 29, 6074-6085 (2009).
22. Pasini, D. et al. Characterization of an antagonistic switch between histone H3 lysine 27 methylation and acetylation in the transcriptional regulation of Polycomb group target genes. Nucleic Acids Res. (2010).
23. Zhu, B. et al. 5-methylcytosine-DNA glycosylase activity is present in a cloned G/T mismatch DNA glycosylase associated with the chicken embryo DNA demethylation complex. Proc. Natl. Acad. Sci. U. S. A. 97, 5135-5139 (2000).
24. Morgan, H. D., Dean, W., Coker, H. A., Reik, W. & Petersen-Mahrt, S. K. Activation-induced cytidine deaminase deaminates 5-methylcytosine in DNA and is expressed in pluripotent tissues: implications for epigenetic reprogramming. J. Biol. Chem. 279, 52353-52360 (2004).
25. Rai, K. et al. DNA demethylation in zebrafish involves the coupling of a deaminase, a glycosylase, and gadd45. Cell 135, 1201-1212 (2008).
26. Tahiliani, M. et al. Conversion of 5-methylcytosine to 5-hydroxymethylcytosine in mammalian DNA by MLL partner TET1. Science 324, 930-935 (2009).
27. Ito, S. et al. Role of Tet proteins in 5mC to 5hmC conversion, ES-cell self-renewal and inner cell mass specification. Nature (2010).
28. Kunz, C. et al. Base excision by thymine DNA glycosylase mediates DNA-directed cytotoxicity of 5-fluorouracil. PLoS Biol 7, e91 (2009).

Supplementary Information accompanies the paper on **www.nature.com/nature**.'

Acknowledgements We wish to thank Daniela Klewe-Nebenius for preparations of mouse primary fibroblast, and Fabio Mohn and Dirk Schübeler for helpful discussions and assistance in the setup and evaluation of the ChIP experiments. The work was supported by project grants from the Swiss National Science Foundation (SNF, 3100A0-108436; 3100A0-122574/) and the Association For International Cancer Research (AICR, 01-330)

Author Contributions D.C. established and performed the ChIP and MeDIP analyses and the *in vitro* differentiation experiments and contributed to paper writing; C.K. established and characterized MEF lines, designed and performed gene expression and DNA methylation analyses and contributed to paper writing; J.S. did blastocyst injections, established the first heterozygous *Tdg* knockout mice, characterized the lethal phenotype of the *Tdg* null embryos and provided SV40 immortalized MEFs; T.L. and Y.S. generated *Tdg* targeting constructs and established heterozygous and homozygous *Tdg* knockout ES cell lines, YS established *in vitro* differentiation protocols; E.MD. performed the Big Blue® mutation assays; A.W. performed ChIP experiments; D.S. isolated primary MEFs and performed RT-PCR validations of gene expression differences and the PARP inhibitor experiments; A.J. established and performed immunofluorescence experiments including XRCC1 foci analyses; F.S. performed bioinformatic analyses of gene expression array data; R.S. affinity-purified anti-TDG antibodies for ChIP; J.J. contributed genomic *Tdg* clones and supervised initial work of T.L.; A.B. was involved in study design (mutation analyses) and supervised the work of J.S. and E.MD.; P.S. designed and coordinated and supervised the study, analysed the data and wrote the paper. D.C. and C.K. as well as T.L. and Y.S contributed equally to the study. All authors discussed the results and commented on the paper.

Author Information All gene expression array data discussed in this publication have been deposited in NCBI's Gene Expression Omnibus and are accessible through GEO Series accession number GSE20693 (http://www.ncbi.nlm.nih.gov/geo/query/acc.cgi?acc=GSE20693). The authors declare no competing financial interests. Correspondence and requests for materials should be addressed to P.S. (e-mail: primo.schaer@unibas,ch).

Legends to Figures

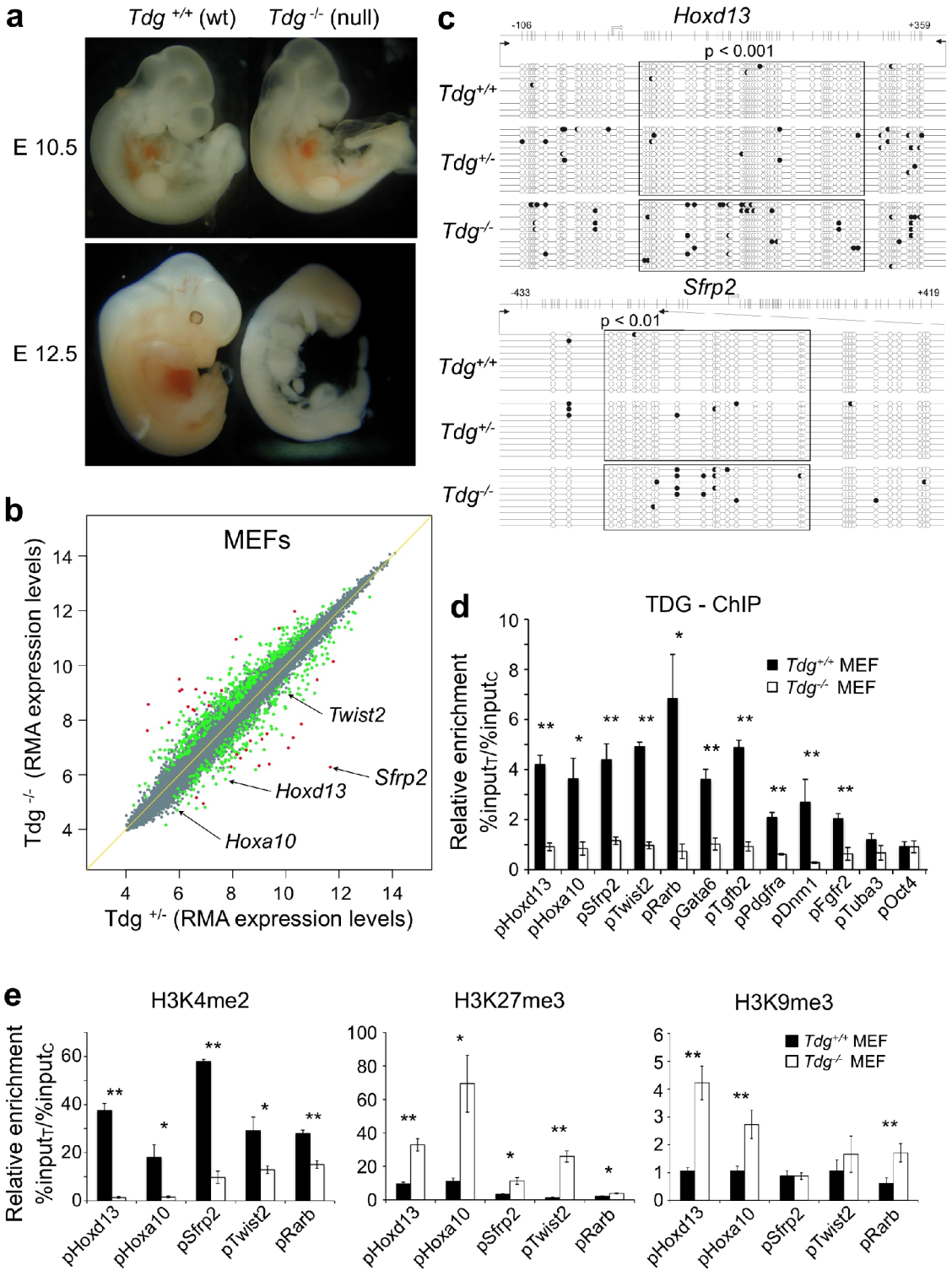

Figure 1 | Embryonic essential function of *Tdg* in epigenetic gene regulation. a, Whole-mount images of typical examples of *Tdg*$^{+/+}$ and *Tdg*$^{-/-}$ littermate embryos taken at E10.5 and E12.5. **b,** Scatter plot comparing gene expression levels of matched *Tdg*$^{+/-}$ and *Tdg*$^{-/-}$ MEFs. Differentially expressed genes at p<0.05 and p<0.01 are indicated by green and red dots, respectively, and examples of developmental genes affected are denoted. **c,** Na-bisulfite sequencing of the *Hoxd13* and *Sfrp2* promoters in *Tdg*$^{+/+}$, *Tdg*$^{+/-}$ and *Tdg*$^{-/-}$ MEFs. White and black circles indicate unmethylated and methylated CpGs, respectively. p-values indicate statistical difference of methylation frequencies as determined by

contingency tables and Chi-square test. **d,** ChIP-qPCR analysis of TDG association with the promoters of the genes indicated in chromatin from *Tdg*$^{+/+}$ and *Tdg*$^{-/-}$ MEFs. Shown are relative enrichments of TDG at these promoters normalized to a randomly chosen intergenic control region (means±s.e.m.; n≥3; *, p<0.05; **, p<0.01, unpaired Students t-test). **e,** ChIP-qPCR analyses in *Tdg*$^{+/+}$ and *Tdg*$^{-/-}$ MEFs to assess the presence of activating (H3K4me2) and repressive (H3K9me3, H3K27me3) histone modifications at the promoter regions indicated. Shown are relative enrichments relative to appropriate negative controls; intracisternal A-particle (*Iap*) transposon for active chromatin marks and the *Hprt* promoter for silencing marks (means±s.e.m.; n≥3; *, p<0.05; **, p<0.01; unpaired Student's t-test). $_{T}$, target region; $_{C}$, control region.

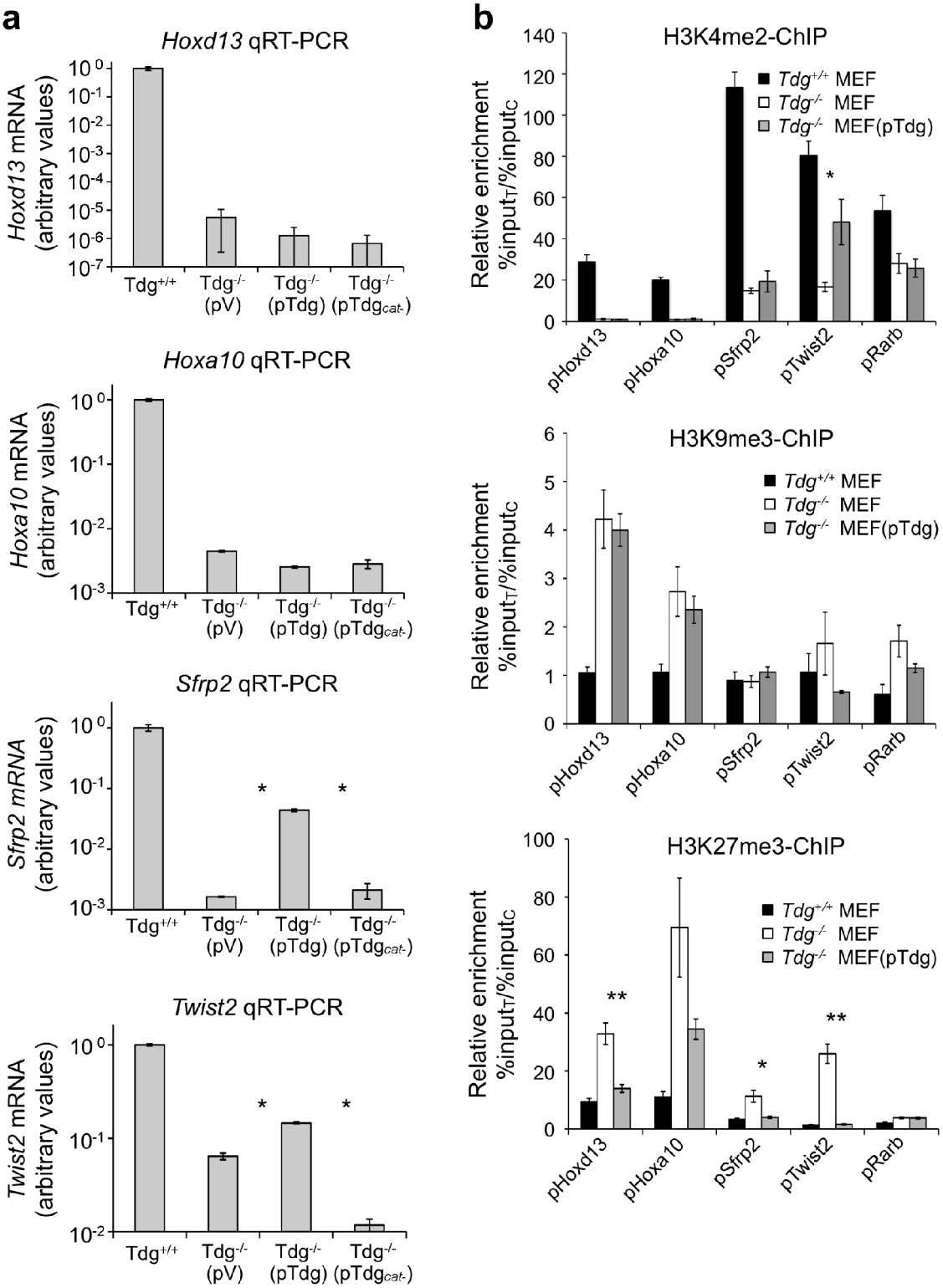

Figure 2 | Complementation of the loss of gene expression depends on the chromatin state of the promoter. a, *Hoxd13, Hoxa10*, *Sfrp2*, and *Twist2* expression in *Tdg*$^{+/+}$ and *Tdg*$^{-/-}$ MEFs complemented with vectors expressing either a wildtype (pTdg) or a catalytically deficient *Tdg* (pTdg$_{cat-}$, N151A), or a vector control (pV). Target-specific mRNA levels were assessed by qRT-PCR and normalized to *Gapdh* mRNA; values represent arbitrary units (means±s.d.; n≥3; *, p<0.05, unpaired Student's t-test). **b,** ChIP-qPCR analyses to detect H3K27me3 and H3K4me2 marks at the gene promoters indicated in chromatin of *Tdg*$^{+/+}$, *Tdg*$^{-/-}$ and *Tdg*$^{-/-}$ MEFs complemented with a wildtype *Tdg* cDNA. *IAP* and the *Hprt* promoter were used as normalizers for active and repressive

chromatin marks, respectively (means±s.e.m.; n=3; *, p<0.05; **, p<0.01; unpaired Student's t-test). T, target region; C, control region.

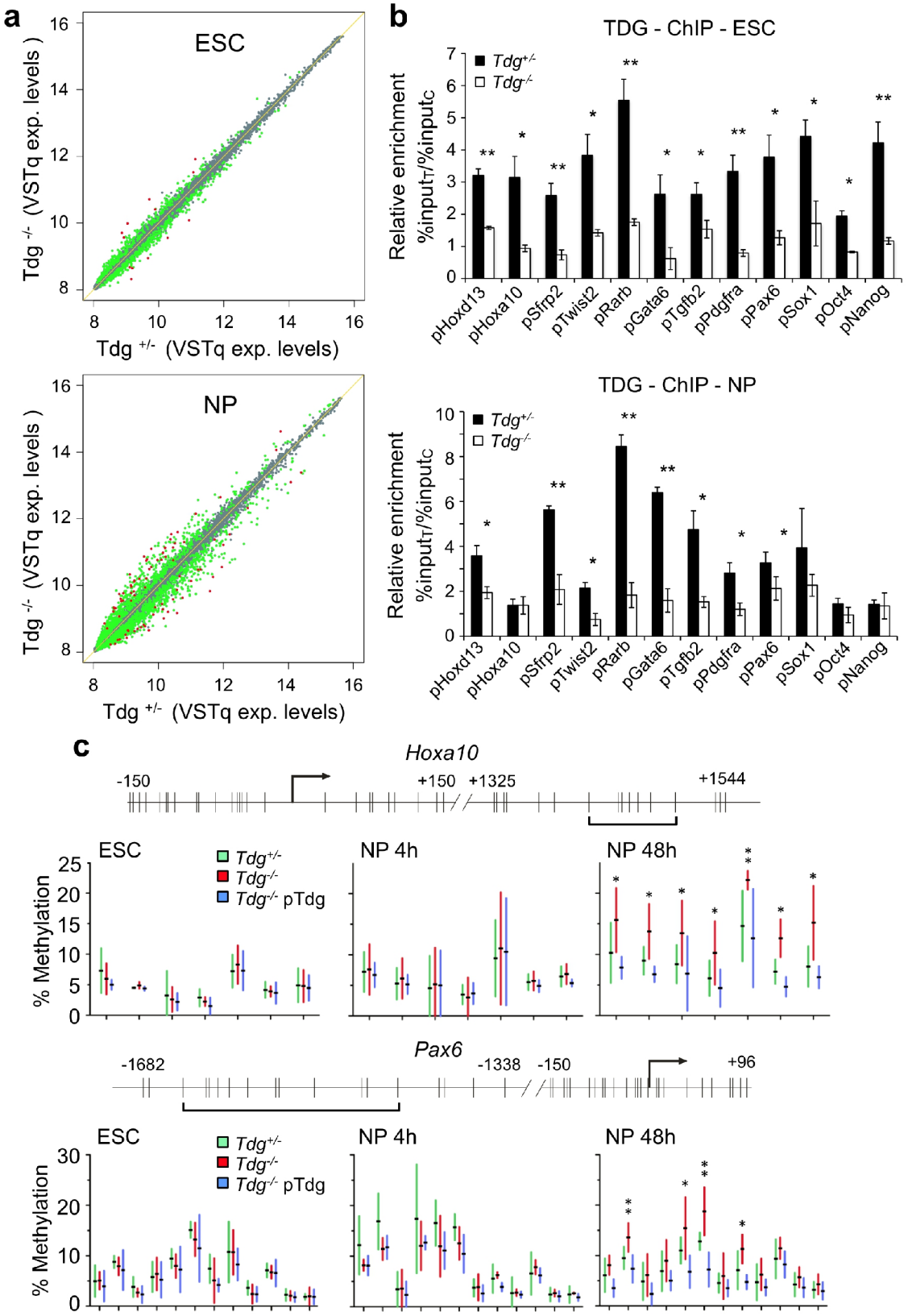

Figure 3 | TDG-dependent differences in gene expression and chromatin status arise during cell differentiation. a, Scatter plots comparing gene expression profiles of

Tdg$^{+/-}$ and *Tdg*$^{-/-}$ embryonic stem cells (ESCs) or *in vitro* differentiated neuronal progenitors (NPs). Green and red dots indicate differentially expressed genes at p<0.05 and p<0.01, respectively. **b,** ChIP-qPCR analysis of TDG association with the gene promoters indicated in chromatin from *Tdg*$^{+/-}$ and *Tdg*$^{-/-}$ ESCs and NPs. Shown is the relative enrichment of TDG at these promoters normalized to a randomly chosen intergenic control region (means±s.e.m.; ESCs, n=3; NPs, n=3; *, p<0.05, **, p<0.01; unpaired Student's t-test). $_{T}$, target region; $_{C}$, control region. **c,** DNA methylation states at the *Hoxa10* and *Pax6* promoters in TDG deficient ESCs and NPs analyzed by bisulfite-Pyrosequencing. Promoter regions are depicted schematically at the top. Vertical tick marks indicate CpG sites, bent arrows transcription start sites, and horizontal brackets the CpGs for which methylation data is presented in the graphs. Methylation levels are given as percentage of methylated cytosines at each CpG analyzed. Shown are means with the 95% confidence intervals (bars) as obtained from three differentiation experiments. *, p<0.05; **, p<0.01; unpaired Student's t-test.

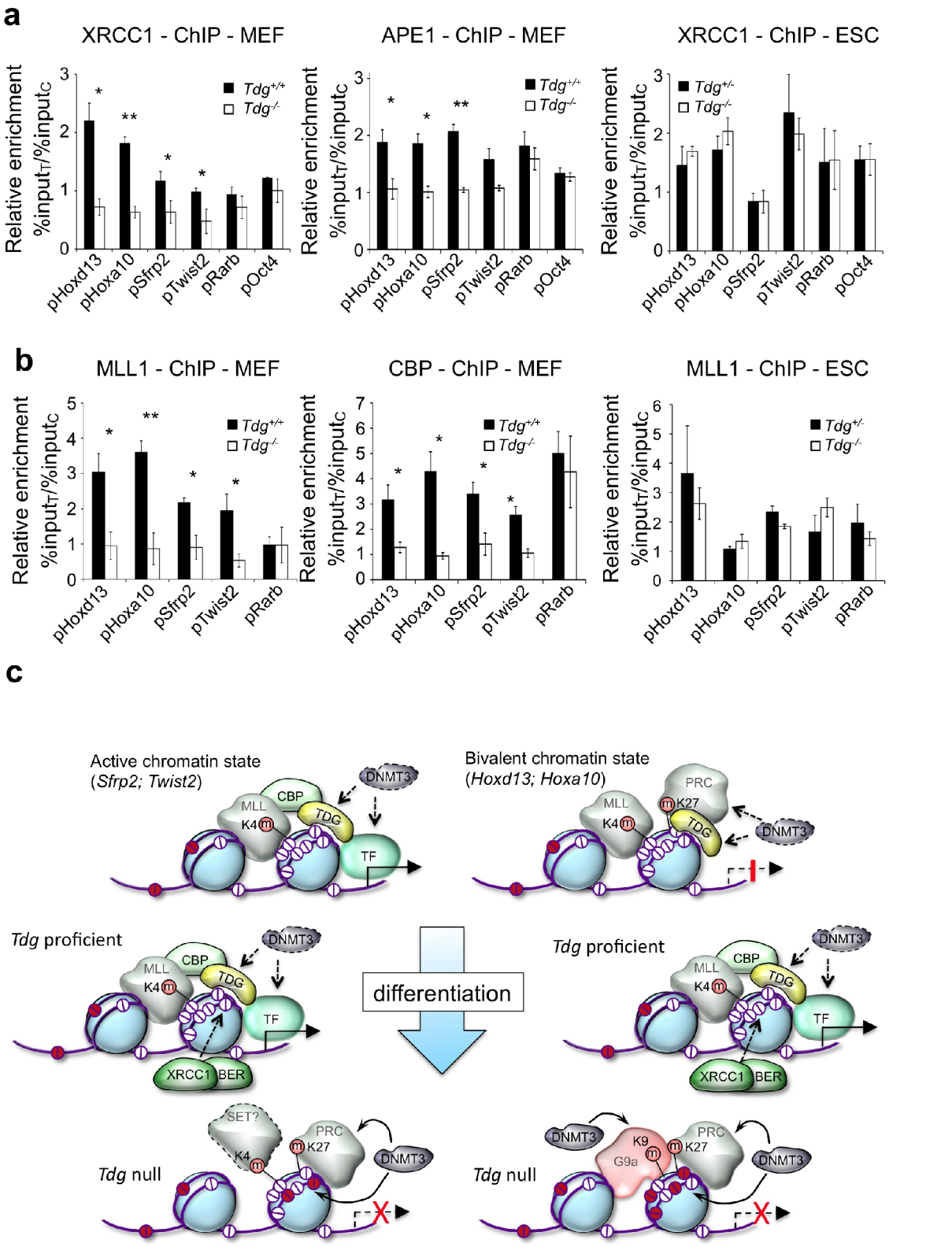

Figure 4 | Structural and catalytic functions of TDG in epigenetic maintenance. a, ChIP-qPCR analysis of XRCC1 and APE1 association with the gene promoters indicated in chromatin of TDG proficient and deficient MEFs and ESCs. Shown are relative enrichments of XRCC1 and APE1 at these promoters normalized to a randomly chosen intergenic control region (means±s.e.m.; n≥3; *, p<0.05; **, p<0.01, unpaired Student's t-test). **b,** ChIP-qPCR analysis of MLL1 and CBP/p300 association with the gene promoters indicated in chromatin of TDG proficient and deficient MEFs and ESCs. Shown are relative enrichments of MLL1 and CBP/p200 at these promoters normalized to a randomly chosen

intergenic control region (means±s.e.m.; n≥3; *, p<0.05; **, p<0.01, unpaired Student's t-test). $_T$, target region; $_C$, control region. **c,** Model summarizing epigenetic aberrations and implicated functions observed in the absence of TDG. In ESCs TDG associates with gene promoters in an active "open" (H3K4me2, e.g. *Sfrp2, Twist2,* left side) or transiently silent "bivalent" chromatin conformation (H3K4me2 and H3K27me3, e.g. *Hoxd13* and *Hoxa10,* right side). In active chromatin, the lack of TDG results in a partial loss of H3K4 dimethylation and a gain of H3K27 trimethylation as well as in sporadic DNA hypermethylation (red balls) upon cell differentiation. Differentiation associated activation of promoters in "bivalent" chromatin involves the demethylation of H3K27me3 and transcription factor binding. The absence of TDG results in an aberrant loss of H3K4 dimethylation accompanied by a gain in repressive H3K9 and H3K27 trimethylation and in DNA methylation, eventually directing irreversible transcriptional silencing. In both cases, the loss of active and the gain in repressive histone marks can be accounted for by a failure of TDG deficient cells to target MLL and CBP to these promoters. We propose that TDG, as part of transcription regulatory complexes, assures the establishment and the maintenance of proper epigenetic states at developmentally regulated gene promoters. As a DNA glycosylase, it protects these regions from aberrant CpG methylation in a process that engages XRCC1 and APE1, factors essential for downstream BER.

Methods

Cell culture and ES cell differentiation. SV40 immortalized MEF cell lines were previously described [29] and cultivated in growth medium (DMEM, 10% FCS, 2 mM L-glutamine) at 37°C in a humidified atmosphere containing 5% CO_2. For growth of cell lines complemented with Tdg expressing vectors the growth medium was additionally supplemented with 1 µg/ml puromycin.

For isolation of primary MEFs, 10.5 dpc embryos were dissected, homogenized and cells dissociated in 0.05% Trypsin-EDTA for 5 min before plating in modified ES cell medium without LIF (DMEM, 10% FCS seraplus, 1x nonessential amino acids, 1 mM sodium pyruvate, 2 mM L-glutamine and 50 µM β-mercaptoethanol, 1x penicillin/streptomycin) and cultivation for 10 days.

ES cells (ESC) were grown in the presence of feeder cells at 37°C in ES cell medium (ECM: DMEM, 15% heat inactivated FCS, LIF (1,000 U/ml), 1x nonessential amino acids, 1 mM Na-pyruvate, 2 mM L-glutamine and 90 µM β-mercaptoethanol) in a humidified atmosphere containing 5% CO_2.

Before differentiation experiments for neuronal differentiation, time-course, PARP inhibitor and immunofluorescence experiments, ESC were grown in the absence of feeder cells for two passages. For embryoid body formation during neuronal differentiation 4 x 10^6 $Tdg^{+/-}$ or $Tdg^{-/-}$ ESC were plated into nonadherent bacterial dishes (Greiner Bio-one, Germany) in differentiation medium (ECM without LIF and with 10% FCS) and grown at 37°C with a medium exchange after two days. After four days, 5 µM all-trans retinoic acid (RA) was added and cells were further incubated for four days with a medium exchange after two days. Embryoid bodies were washed twice with 1x PBS and dissociated with freshly prepared trypsin solution (0.05% TPCK-treated trypsin in 0.05% EDTA/1x PBS) at 37°C for 3 min. Dissociated embryoid bodies were resuspended in 10 ml differentiation medium and collected by centrifugation at 700g for 5 min at room temperature (RT). The pellet was resuspended in N2 medium (DMEM-F12 nutrient mixture 1:1, 1x N2 supplement) and the cell suspension filtered through a 40 µm nylon cell strainer (BD, USA). Filtered cells were immediately plated onto poly-L-lysine (PLL) and laminin-coated dishes at a density of 5 x 10^6 cells/60 mm dish or 1.5 x 10^7 cells/100 mm dish. The N2 medium was exchanged after 2 and 24 hours after plating and cells were harvested after 4 and 48 hours for further analysis.

RA induced differentiation of ESC for time-course, PARP inhibitor and immunofluorescence experiments was induced in ECM without LIF in the presence of 1 or 5 µM RA. The RA containing medium was exchanged every 24 hours and cells were harvested at the indicated time points. For immunofluorescence experiments, 10^5 ESC were seeded onto gelatin-coated cover slips one day prior to differentiation. For the analysis of PARP inhibition on cell survival during differentiation, 10^5 ESC were seeded into gelatin-coated 12-well dishes, one day before the addition of 5 µM RA or further cultivation in ECM. After 24 hours, increasing concentrations of the PARP inhibitor AG-014699 (a generous gift of SelleckChem) were added and cell numbers determined 24 hours later with the CASYcell counter. The 50% lethal dose (LD_{50}) of the inhibitor and statistical differences between Tdg proficient and deficient cells were calculated on triplicate experiments by linear regression with 95% confidence interval using the GraphPad PRISM software.

Microarray gene expression analysis. For the analysis of differential gene expression among $Tdg^{+/-}$ and $Tdg^{-/-}$ MEF's, total RNA was isolated form three independent cultures of each cell line using the RNeasy Mini Kit (Qiagen, Germany), cDNA synthesized from 13 µg RNA with the SuperScript double-Stranded cDNA Synthesis kit (Invitrogen) followed by *in vitro* transcription reactions using the MEGA Script T7 Kit (Ambion, USA) supplemented with 1.5 mM Bio-11-CTP and Bio-16-UTP (Enzo Life Sciences, USA). cDNAs and cRNAs were purified using the GeneChip® Sample Cleanup Module (Qiagen, Germany). 15 µg of cRNA were fragmented and hybridized to GeneChip Mouse Expression Arrays 430A (Affymetrix, USA). Hybridized arrays were stained and washed according to the manufacturers' protocol and scanned with the Affymetrix Scanner 3000 7G. Scanned images were processed with the Microarray Suite software and obtained 'cel'-files used for further data analysis.

For gene expression analysis of ESC and *in vitro* differentiated NP cells, total RNA was extracted from independent triplicates using the Trizol reagent (Invitrogen, USA). RNA was quantified using the Quant-iT™ RiboGreen® RNA Assay (Invitrogen, USA) and 500 ng of total RNA subjected to cDNA synthesis and subsequent *in vitro* transcription to biotiylated cRNA using the Illumina® TotalPrep RNA Amplification Kit (Ambion, USA). 1.5 µg of cRNA was hybridized to MouseWG-6v2 slides (Illumina, USA) according to the manufacturer's protocol. Bead arrays were washed and stained using FluoroLink Cy3 Streptavidin (GE Healthcare, USA). Fluorescent signals were imaged using the iScan system (Illumina, USA). Scanner images files were processed to probe intensity files by the manufacturers' software and further processed with the genome studio software (Illumina, USA.) without normalization and background correction.

Affymetrix data and Illumina probe intensity data were either processed by robust multi-array average (RMA) or variance stabilization transformation (VST), respectively using the R/Bioconductor software and "affy" or "lumi" libraries, followed by quantile normalization. Significance of effects for probes (Illumina) or probe-sets (Affymetrix) was tested in R/Bioconductor ("limma" library) using a moderated t-test and the false discovery rate (FDR = 5%) method by Benjamini and Hochberg for multiple testing correction. No unspecific filter was applied and multiple probe-sets per gene or probe-sets with ambiguous genomic target were retained.

Methylation analyses. Genomic DNA from MEF, ESC, and NP cells was isolated with the QIAamp DNA Mini Kit (Qiagen, Germany). 2 µg of DNA were subjected to bisulfite conversion using the EZ DNA Methylation Kit (ZYMO RESEARCH, USA). Respective target regions were amplified from bisulfite treated DNA with TrueStart Taq polymerase (New England Biolabs, USA). For conventional bisulfite sequencing, *Hoxd13* or *Sfrp2* promoter regions were amplified from converted DNA and cloned into the *Xho*I and *Bam*HI restrictions sites of pBluescript SK- before sequencing of individual clones. For

Pyrosequencing, potential regions of hypermethylation were first identified by COBRA. Pyrosequencing primers (Supplementary Table 1) were designed using the PyroMark Assays Design Software (v. 2.0.1.15, Qiagen, Germany). Primer pairs included either one biotinylated primer or one primer containing a universal region. In the latter case products were subjected to a second amplification using a biotinylated universal primer and Phusion Hot Start High-Fidelity DNA Polymerase (Finnzymes, Finland). PCR products were purified using the QIAquick PCR Purification Kit (Qiagen, Germany), quantified and 300 to 500 ng were used for pyrosequencing in a PyroMark Q24 (Qiagen, Germany). Reactions were analysed using the PyroMark Q24 Software (v. 2.0.6, Qiagen, Germany). Significance of methylation differences between different Tdg proficient and deficient cell lines at individual CpG sites was evaluated by unpaired, two-tailed *t*-tests.

Chromatin immunoprecipitations (ChIP). To crosslink protein bound DNA, MEFs, ESC and NPs were incubated in freshly prepared crosslinking solution (PBS pH 7.4, 1% formaldehyde) at RT. The reaction was quenched after 10 min by addition of glycine to a final concentration of 125 mM. After washing twice with cold PBS cells were collected using a cell scraper and subsequent centrifugation at 600g and 4°C. Nuclei were isolated by incubation in 200 µl of cold ChIP Buffer I (10 mM HEPES [pH 6.5], 10 mM EDTA, 0.5 mM EGTA, 0.25% Triton X-100) for 5 min on ice followed by two incubations of 5 min on ice in 200 µl cold ChIP buffer II (10 mM HEPES pH 6.5, 1 mM EDTA, 0.5 mM EGTA, 200 mM NaCl). Pelleted nuclei were lysed in 400 µl ChIP buffer III (50 mM Tris-HCl pH 8.0, 1 mM EDTA, 0.5% Triton X-100, 1% SDS, 1 mM PMSF) for 10 min on ice followed by sonication for 15 min (15 seconds ON, 30 seconds OFF, power HIGH) using a BIORUPTOR sonicator (Diagenode, UK) to produce random chromatin fragments ranging from 300 to 1'000 bp. The solution was cleared by centrifugation at 14'000g and 4°C for 10 min and the concentration of chromatin was estimated by OD_{260} absorption. For ChIP of TDG, MLL and APE1 100-150 µg of chromatin were diluted 10 times in ChIP dilution buffer I (50 mM Tris-HCl pH 8.0, 1 mM EDTA, 150 mM NaCl, 0.1% Triton X-100, 1 mM PMSF). For Histone ChIPs, 25-75 µg of chromatin were diluted in ChIP dilution Buffer II (16.7 mM Tris-HCl pH 8.0, 1.2 mM EDTA, 167 mM NaCl, 1.1% Triton X-100, 0.01% SDS, 1 mM PMSF). Diluted chromatin was precleared at 4°C for 1 hour with 40 µl of a 50% slurry of magnetic Protein G beads (Invitrogen, USA) preblocked with 1 mg/ml BSA and 1 mg/ml tRNA (TDG, XRCC1, APE1, and MLL-ChIPs) or salmon sperm ssDNA (histone ChIPs). Precleared chromatin was incubated with 2-5 µg of the respective antibody (Supplementary table 2) overnight at 4°C under slow rotation. Immuno-complexes were precipitated with 40 µl of a 50% slurry of blocked Protein G beads and further incubation at 4°C for 2 hours. Beads were then serially washed with 500 µl ChIP wash buffer I (20 mM Tris-HCl pH 8.0, 2 mM EDTA, 150 mM NaCl, 0.1% SDS, 1% Triton X-100), 500 µl ChIP wash buffer II (20 mM Tris-HCl pH 8.0, 2 mM EDTA, 500 mM NaCl, 0.1% SDS, 1% Triton X-100) and 500 µl ChIP wash buffer III (10 mM Tris-HCl pH 8.0, 1 mM EDTA, 250 mM LiCl, 1% sodium deoxycholate, 1% NP-40). In case of TDG, APE1 and MLL ChIPs, beads were washed once with 500 µl ChIP wash buffer I and twice with 500 µl ChIP wash buffer II. After two additional washes with 500 µl TE (10 mM Tris-HCl pH 8.0, 1 mM EDTA), bound complexes were eluted by two sequential incubations with 150 µl elution buffer (1% SDS, 0.1 M $NaHCO_3$) at 65°C for 10 min. Crosslink reversal of eluates and respective input samples (1% of chromatin used for ChIP) was done in the presence of 200 mM NaCl at 65°C for 4 hours followed by Proteinase K digestion (50 µg/ml) in the presence of 10 mM EDTA at 45°C for one hour. DNA was purified by phenol/chloroform extraction and Na-acetate/ethanol precipitation and resuspended in 10 mM Tris-HCl pH 8.0. qPCR analysis with target specific primers (Supplementary Table 3) was performed using Quantitect SYBR Green (Qiagen, Germany) with a Rotor-Gene 3000 thermocycler (Qiagen, Germany). The significance of different ChIP efficiencies among Tdg proficient

and deficient cell lines was evaluated from triplicate experiments by non-paired, two-tailed *t*-tests.

Methylated DNA Immunoprecipitation (MeDIP). MeDIP assays were performed as described in ref. 30. Shortly, genomic DNA was prepared from 5 x 10^6 cells by incubation in lysis buffer (20 mM Tris-HCl pH 8.0, 4 mM EDTA, 20 mM NaCl, 1% SDS and 1 mg/ml Proteinase K) at 55°C for 5 hours and subsequent phenol/chloroform extraction and Na-acetate/ethanol precipitation. DNA pellets were resuspended in TE containing 20 µg/ml RNase. DNA was sonicated as described for ChIP followed by NaCl(400 mM)/EtOH precipitation in the presence of glycogen-carrier. 4 µg of fragmented DNA in 450 µl TE were denatured at 95°C for 10 min and immediately chilled on ice. After addition of 10x IP buffer (100 mM sodium phosphate pH 7.0, 1.4 M NaCl, 0.5% Triton X-100) the DNA was incubated with 10 µg of a monoclonal anti 5-methylcytidine antibody (clone 33D2, Eurogentec, Belgium) at 4°C for 2 hours. Immuno-complexes were precipitated by the addition of 40 µl M-280 sheep anti mouse IgG antibody coupled Dynabeads (Invitrogen, USA) and incubation at 4°C for 2 hours followed by three washes in 700 µl IP buffer. Bound material was treated with 250 µl Proteinase K digestion buffer (50 mM Tris-HCl pH 8.0, 10 mM EDTA, 0.5% SDS and 0.25 mg/ml Proteinase K) at 50°C for 3 hours. Immunoprecipitated methylated DNA was purified by phenol/chloroform extraction followed by Na-acetate/ethanol precipitation and resuspended in TE. qPCR analysis of sonicated genomic input DNA and MeDIP DNA with target specific primers (Supplementary table 3) was performed as described for ChIP and significance of MeDIP efficiencies tested by non-paired, two-tailed *t*-tests.

Quantitative RT-PCR analyses. 2-4 µg of total RNA extracted by RNeasy Mini Kit or by Trizol methods were reverse transcribed with the RevertAid™ H Minus M-MuLV Kit (Fermetas, Germany) according to the manufacturers' protocol. qPCR with target specific primers (Supplementary table 4) was performed using Power SYBR Green Master Mix (Applied Biosystems, USA) with a Rotor-Gene 3000 thermocycler. Conditions for each target were validated by standard and melting curve analyses. Target specific amplifications were normalized to a GAPDH control and data of at least three independent experiments were analyzed by unpaired, two-tailed *t*-tests. *Tdg* genotype-specific target gene expression in primary MEFs were analyzed by the non-parametric Kruskal-Wallis test and post-hoc Dunn's multiple comparison.

Western blot analyses. Whole cell extracts were prepared by cell lysis in lysis buffer (50 mM Na-phosphate pH 8.0, 125 mM NaCl, 1% NP-40, 0.5 mM EDTA, 1 mM PMSF, 1 mM DTT, 1x Complete protease inhibitor, 2x phosphatase inhibitor cocktail 1 and 2) on ice for 30 min and clarification by centrifugation (15 min, 20,000g, 4°C). Chromatin extracts were isolated as described for ChIP assays. 50 µg of soluble proteins were separated on 7% or 10% SDS-polyacrylamide gels and transferred to a nitrocellulose membrane (Millipore, USA). Membranes were washed once with TBS-T (100 mM Tris-HCl pH 8.0, 150 mM NaCl, 0.1% Tween-20), blocked with blocking buffer (TBS-T, 5% dry milk) at RT for 1 hour and incubated with the primary antibody at 33°C (anti-mTDG) or RT (anti-DNMT1, anti-DNMT3a, anti-XRCC1, anti-APE1, anti-MLL, anti–β-actin) for 1 hour in blocking buffer. Dilutions were: 1:10'000 for the rabbit anti-mTDG, the mouse anti-β-actin and the anti-DNMT1 antibodies; 1:1'000 for the anti-DNMT3a and anti-XRCC1 antibodies; 1:500 for the anti-APE1 and anti-MLL antibodies. Washing steps after hybridization were: once at 33°C and twice at RT for 15 min for anti-mTDG or three times at RT for 10 min for all other antibodies. Membranes were incubated with secondary HRP–conjugated antibodies diluted 1:5'000 in blocking buffer and at RT for 1 hour. After three washing steps of 10 min at RT, detection of the signals was carried out using the Immobilon Western Chemiluminescent HRP Substrate (Millipore, USA).

Cytotoxicity assays. For measurement of γ-ray sensitivity, MEF single cell suspensions

at a cell density of 2 x 10^5 cells/ml in PBS were irradiated with the indicated doses in a Gammacell 40 irradiator using ^{137}Cs as a radioactive source. Irradiated cells were plated in 96-well microtiter plates at a density of 1000 cells/well in growth medium and survival was measured after 3 days using the cell counting kit 8 (Dojindo, Japan). Alternatively, survival was determined by clonogenic growth by plating 500 to 2000 cells in triplicate in 10 cm dishes containing growth medium and counting of Giemsa stained colonies after 10 days. For measurement of sensitivity to H_2O_2 cells were plated at 2500 cells/well in 96-well plates. After 24 hours cells were treated for 15 min with the indicated concentrations of H_2O_2, washed with PBS and incubated in fresh growth medium for further 24 hours before measurement of survival with the cell counting kit 8. Survival was determined as percent of mock treated cells.

Base release assay. For base release assays, 25 to 50 µg of ESC whole cell extracts were incubated with 0.5 pmol of a fluorescein-labelled GC/TG, GCm/CG or GCm/mCG DNA substrate in reaction buffer (50 mM Tris-HCl [pH 8.0], 1 mM EDTA, 1 mM DTT, 1 mg/ml BSA) at 37°C for 1 hour (GC/TG) or overnight (methylated substrates). Resulting AP-sites were cleaved by the addition of NaOH to a final concentration of 100 mM and heating to 95°C for 10 min. Subsequently, DNA was ethanol precipitated overnight at −20 °C in the presence of 0.3 M Na-acetate pH 5.2 and 0.4 mg/ml carrier t-RNA. DNA was collected by centrifugation (20 min, 20'000g, 4°C) and washed with 80% ethanol. Air-dried pellets were resuspended in loading buffer (1x TBE, 90% formamide), heated at 95°C for 5 min and immediately chilled on ice. Reaction products were separated on denaturing 8 M urea/15% polyacrylamide gels in 1x TBE. The fluorescein-labelled DNA was visualized with a Typhoon 9400 and quantified using the ImageQuant TL software (GE Healthcare, USA).

Immunofluorescence. For detection of XRCC1 foci during RA stimulation, cells were fixed in ice-cold methanol for 5 min, then permeated in 0.2% Triton X-100/PBS pH 7.4 and 0.2% Triton X-100/0.2% $NaBH_4$/PBS pH 7.4 on ice for 5 min each. The induceability of XRCC1 foci formation in ESC was tested by incubation with H_2O_2 (50µM in PBS) or PBS for 15 min at 37°C and additional 5 min in ECM with LIF before further processing. Coverslips were blocked in blocking buffer (BF:1% BSA/0.05% Tween20/PBS pH 7.4), stained with rabbit anti-XRCC1 antibody (1:100 in BF) at RT for 1 hour, washed 3 times for 10 min with BF before labelling with goat anti-rabbit Alexa594 (1:200 in BF) for 30-60 min. After two washes of 10 min with BF, cells were again fixed in -20°C cold methanol, incubated in BF for 1 hour and stained with a mouse monoclonal anti-PCNA antibody (1:100 dilution) in BF overnight at 4°C. Slides were counterstained for DNA with 50ng/ml DAPI and mounted in VectaShield mounting medium (Vector Lab, USA). Slides were randomized and blinded before z-stacks were acquired on a Leica SP5 with the 405 nm diode, Argon 488 nm and He-Ne 594 nm laser lines. XRCC1 foci-number for individual cells were determined by visual inspection of the 3D stacks. 150 (RA stimulation) or 50 (H_2O_2) cells per sample were analyzed. For co-staining of PAR and XRCC1 during RA differentiation, cells were fixed with 2% formaldehyde/PBS at RT for 30 min, permeabilized with PBS/0.2% Triton-X100 for 30 min. Antigene detection was done with a 1:250 diluted monoclonal α-PAR antibody 10H (Enzo Life Sciences) and a polyclonal α-XRCC1 as described above but using 1:250 diluted anti-rabbit AlexaFluor-594 and anti-mouse AlexaFluor-488 secondary antibodies (Invitrogen). Pictures were acquired with a Nikon Diaphot 300 epifluorescence microscope using identical settings for all slides.

29. Kunz, C. et al. Base excision by thymine DNA glycosylase mediates DNA-directed cytotoxicity of 5-fluorouracil. PLoS Biol 7, e91 (2009).
30. Weber, M. et al. Chromosome-wide and promoter-specific analyses identify sites of differential DNA methylation in normal and transformed human cells. Nat Genet 37, 853-862 (2005).

CURRICULUM VITAE

PERSONAL DATA

Title	PhD
Name	Fredy Siegrist
Place, date of birth	Berne, 11.06.1978
Nationality	Swiss (Menziken AG)
Marital status	single
Children	-
Private address	Schoenbergweg 11, 3006 Berne, Switzerland
Email	sieg (at) gmx.ch
Languages	German (native), English (proficient), French (working knowledge) and Spanish (basics)

PRESENT POSITION

Research Fellow 2011-2013, Department of genetic and laboratory medicine, Laboratory of virology, University Hospitals of Geneva. Nominal percentage distribution: 100% research.

DIPLOMAS, GRADUATE AND UNDERGRATUATE TRAINING

2011, Apr 13	PhD in Cell Biology, University of Basel, Switzerland. Title: - 'Transcriptional responses of tumor cell lines to interferon-alpha'
2005 – 2011	PhD studies in Cell Biology, University of Basel.
2003, Oct 24	University of Berne, Master Degree in Biochemistry. Title: ‘Construction and analysis of a cis-acting Ribonucleasemimic’ (orig. title: ‘Auf der Spur eines artifiziellen, selbstspaltenden RNA-Moleküls’)
2001, Nov 15	University of Berne, 2nd year diploma in Biochemistry
2000, Aug 4	University of Berne, 1st year diploma in Chemistry
1999 – 2003	Master studies, University of Berne

TRAINING AND EDUCATION SINCE SECONDARY SCHOOL

1999, June 17	Matura typus C, Gymnasium Kirchenfeld, Berne, Switzerland.

PROFESSIONAL ACTIVITIES (POST-GRADUATE)

2011 – 2013	Post-doctoral position Laboratory of virology, University of Geneva, Switzerland.
2006 – 2010	PhD thesis Molecular Medicine and Toxicology, Roche, Basel, Switzerland.
2004 – 2005	Trainee Functional Genomics, Novartis, Basel, Switzerland.

PROFESSIONAL ACTIVITIES (MISCELLANEOUS)

2010 – 2010 Informatics, Compucorp AG, Bowil, Switzerland

TEACHING

2008 – 2010 Modular course in Clinical Medicine for bachelor students (University of Basel)

'Tracking down genes' modern genetics in clinical research (orig. title: „Den Genen Auf der Spur" Moderne Genetik in Klinik und Forschung)

ADMINISTRATION

2001 – 2004 Committee Bernese Environmental Research Award (student representative)

2000 – 2002 Students Council, Berne (elected representative)

PROFESSIONAL SOCIETIES

2008 - International Society for Interferon & Cytokine Research

OFFICIAL POSTS

2010 - Administrative Board Member, Moosbad Immobilien AG, Emmenmatt

1999 – 2008 Meteorological support in the Swiss Air Force command support training unit

TECHNICAL AND SCIENTIFIC ROLES

Served as referee for:

- BMC Research Notes (BioMed Central)
- International Journal of Interferon, Cytokine and Mediator Research (Dove Press)

DATE AND SIGNATURE

Basel, 11.04.2013

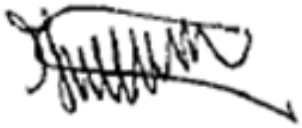

PUBLICATION LIST

Original articles published or accepted in peer reviewed journals (IF 2011)

Scott R, Siegrist F, Foser S, Certa U. Interferon-alpha induces reversible DNA demethylation of the IFITM3 core promoter in human melanoma cells. J Interferon Cytokine Res 2011 Aug 11; 31(8):601-8. IF: 3.1

Cortázar D, Kunz C, Selfridge J, Lettieri T, Saito Y, MacDougall E, Wirz A, Schuermann D, Jacobs A, Siegrist F, Steinacher R, Jiricny J, Bird A, Schär P. Embryonic Lethal Phenotype Reveals a Function of TDG in Maintaining Epigenetic Stability. Nature 2011 Feb 17; 470 (7334): 419-423. IF: 36.3

Siegrist F, Singer T, Certa U. MicroRNA Expression Profiling by Bead Array Technology in Human Tumor Cell Lines Treated with Interferon-Alpha-2a. Biol Proced Online 2009 Dec; 11 (1): 113-29. IF: 1.3

Hallen LC, Burki Y, Ebeling M, Broger C, Siegrist F, Oroszlan-Szovik K, Bohrmann B, Certa U, Foser S. Antiproliferative Activity of the Human IFN-alpha-Inducible Protein IFI44. J Interferon Cytokine Res 2007 Aug; 27 (8): 675-80. IF: 3.1

Reviews published or accepted in peer reviewed journals (IF 2011)

Tapparel C, Siegrist F, Petty TJ, Kaiser L. Picornavirus and enterovirus diversity with associated human diseases. Infect Genet Evol. 2013; 14: 282-293. IF: 3.1

Siegrist F, Ebeling M, Certa U. The small interferon induced transmembrane genes and proteins. J Interferon Cytokine Res 2011 Jan; 31 (1): 183-97. IF: 3.1

Original articles, reviews, editorials, letters, published or accepted in non-peer reviewed journals

Siegrist F, Certa U. Micro RNA Induction by Interferon Alpha and a Potential Role to Interfere with SOCS. In 7th Joint Conference – Montréal, Québec, Canada, October 12-16, 2008 Editor: John Hiscott. Medimont International Proceedings 2008: 93-97.

Thesis

Siegrist F. Transcriptional responses of tumor cell lines to interferon-alpha. PhD Thesis, cell biology, University of Basel 2011.

Siegrist F. Auf der Spur eines artifiziellen, selbstspaltenden RNA-Moleküls. Diplomathesis, Master of Biochemistry, University of Berne 2003.

Abstracts presented at international and national meetings

Siegrist F, Otten-Hernandez P, Thomas Y, Farinelli L, Kaiser L & Tapparel C. Viral genome sequencing and small RNA detection by next generation sequencing. Cytokines2012 Sep ; 59(3) : 565.

Siegrist F, Otten P, Thomas Y, Farinelli L, Kaiser L & Tapparel C. Viral genome sequencing and small RNA detection by next generation sequencing. 3rd Swiss Funtamental Virology Workshop 2011 Aug.

Urfer PM, Siegrist F, Noreen F, Weis S, Certa U, Truninger K, Schär P. Integrating transcriptome and epigenome analyses to identify DNA methylation changes associated with colorectal carcinogenesis. BioValley Science Day 2010 Sep.

Cortazar D, Kunz C, Selfridge J, Lettieri T, Wirz A, Schürmann D, Jacobs A, Siegrist F, Jiricny J, Bird A, Schär P. Embryonic lethality of TDG-deficient mice reveals a function of TDG in the maintenance of epigenetic stability. BioValley Science Day 2010 Sep.

Siegrist F, Certa U. Suppression of interferon alpha mediated gene expression by SOCS1 and SOCS3. FEBS-Special Meeting: Jak-Stat Signalling: from Basics to Disease 2010 Feb.

Siegrist F, Ebeling M, Certa U. Phylogenetic analysis of interferon inducible transmembrane gene family and functional aspects of IFITM3. Cytokine 2009 Oct-Nov; 48 (1-2): 87.

Siegrist F, Certa U. Micro RNA induction by interferon alpha and their potential role to interfere in the negative feedback pathway. Cytokine, 2008 Sep; 43 (3): 284-285.

Scott RW, Siegrist F, Burki Y, Foser S, Certa U. Methylation Status' Influence On Interferon-alpha Sensitivity In Human Melanoma Cells. 3rd Swiss Meeting on Genome Stability „DNA Dynamics and Epigenetics". 2007 Oct.

h index (26.07.2012)

3

DATE AND SIGNATURE

Basel, 11.04.2013